

https://dspace.org/

Neutron activation analysis of samples from the Kimberley Reef Conglomerate

Rasmussen, Stephen Eric

2015
http://hdl.handle.net/10539/18147

Downloaded from a DSpace repository. https://dspace.org/

NEUTRON ACTIVATION ANALYSIS OF SAMPLES FROM THE KIMBERLEY REEF CONGLOMERATE

Stephen Eric Rasmussen

A Dissertation Submitted to the Faculty of Science
University of the Witwatersrand, Johannesburg
in part fulfilment of the requirements for the
Degree of Master of Science

Johannesburg 1973

ABSTRACT

The technique of instrumental neutron activation analysis as applied to the analysis of geological material has been studied with particular emphasis on methods of reducing or eliminating analytical errors.

The neutron flux gradients in the reactor irradiation facilities used were found to introduce errors of up to 20%. The use of iron foils to monitor both the thermal and fast neutron flux received by individual samples has been shown to reduce irradiation errors to approximately 1%. The contribution of epithermal neutron resonances to (n, γ) reaction cross sections has been recognised. Estimated epithermal neutron flux factors have been shown to reduce the associated errors by as much as 7%.

Methods of optimising experimental parameters for the use of I.N.A.A. as a multi-element analytical technique are presented. In particular, decay times have been optimised for minimum error in the determination of peak areas. An analysis has shown that the errors due to counting statistics are in general equal to all other errors combined.

The accuracy of the methods developed has been estimated from the analysis of standard reference materials. The analysis of four U.S.G.S. multi-element rock standards for 23 elements has shown that an accuracy of 6% can be expected for determinations at the 10 parts per million level.

The analytical technique developed has been applied to a problem of interest to the gold mining industry in South Africa, namely the identification of sedimentary strata within a known succession. At present the strata are distinguished using qualitative methods based on known mineralogical differences between strata. A quantitative method based on trace element patterns has been investigated and found to be successful.

A series of conglomerate and quartzite samples from the Kimberley Reef Conglomerates at the Durban Roodepoort Deep Mine have been analysed by I.N.A.A. and up to 28 trace and minor elements determined. Multivariate statistical techniques have been used to determine trace element patterns, characteristic of each stratum. Six strata have been investigated and 100% accuracy of separation achieved using homogeneous powdered samples. It has been shown that whole rock conglomerate chip samples can be classified with 87% confidence and quartzite chip samples with 100% confidence.

DECLARATION

The work presented in this dissertation is my own and has not previously been submitted for a degree at any university.



S.E. RASMUSSEN

JUNE 1973

ACKNOWLEDGEMENTS

This investigation was undertaken at the Activation Analysis Research Group, a joint group of the National Institute for Metallurgy and the University of the Witwatersrand, Johannesburg.

The project was made possible by the sponsorship of Rand Mines Ltd. The financial support of Rand Mines Ltd., the National Institute for Metallurgy and the University of the Witwatersrand is gratefully acknowledged.

The Atomic Energy Board is thanked for the use of irradiation facilities in the reactor Safari I, and the University of the Witwatersrand Computer Centre for making available the necessary computer time.

The author wishes to express his sincere thanks to the following people:

Dr R.E. Robinson, director-general of the National Institute for Metallurgy, and Prof J.P.F. Sellschop, director of the Nuclear Physics Research Unit, without whose able assistance this project would not have been possible.

Prof J.P.F. Sellschop and Mr H.W. Fesq for their guidance throughout the period of this investigation. In particular I would like to thank Prof J.P.F. Sellschop for his encouragement through often difficult times, and Mr H.W. Fesq for many helpful discussions on analytical problems in general, and geochemical problems in particular.

Mr A. Kriek and Mr V. Werdmuller of Rand Mines Ltd., for their active co-operation in the collection of suitable samples.

Prof D.M. Hawkins for his interest and participation in the statistical analysis of the data, and for his permission to use certain computer programmes.

The members of the Activation Analysis Research Group for their assistance which enabled this work to be brought to a successful conclusion. In particular I would like to thank Mr J.I.W. Watterson and Dr D.M. Bibby for many helpful and stimulating discussions of various problems.

Finally I wish to thank my wife Heather, for her understanding and encouragement over the past two years, and for the many hours she has spent on the preparation of this manuscript

CONTENTS

		PAGE
ABSTRACT ..	.. ..	ii
DECLARATION	.. ..	iii
ACKNOWLEDGEMENTS	.. ..	iv
CONTENTS	.. ..	v
LIST OF TABLES	.. ..	viii
LIST OF FIGURES	.. ..	ix
1 INTRODUCTION	.. ..	1
2 GEOLOGY OF THE SAMPLING AREA	.. .. ..	4
3 SAMPLING	.. ..	7
3.1 Sampling Site	.. ..	7
3.2 Sampling Technique	.. .. ..	9
3.2.1 Chip Samples	.. .. ..	10
3.2.2 Powdered Samples	.. .. ..	11
4 I.N.A.A. - THEORETICAL CONSIDERATIONS	.. ..	15
4.1 Neutron Induced Reactions	.. .. ..	15
4.2 Neutron Sources	.. ..	18
4.3 Cross Sections	.. ..	20
4.4 Growth and Decay of Radioactive Nuclei	.. ..	23
4.5 Electromagnetic Interactions with Matter	..	24
4.6 Gamma Ray Detectors	.. .. ..	26
4.7 Discussion	.. ..	29
5 EQUIPMENT	.. ..	31
5.1 Reactor	.. ..	31
5.1.1 Neutron Flux Gradients	.. ..	33
5.1.2 Neutron Flux Monitoring	.. ..	34
5.1.3 Epithermal Flux Corrections	.. ..	36
5.2 Gamma Spectroscopy System	.. .. ..	39
5.2.1 Detector Characterisation	.. ..	39
5.2.2 Count Rate Effects	.. .. ..	43
5.2.3 System Parameters	.. .. ..	47
5.3 Discussion	.. ..	52

6 EXPERIMENTAL PARAMETERS 52
6.1 Irradiation 52
6.1.1 Chip Samples 52
6.1.2 Powdered Samples 52
6.2 Gamma Counting 54
6.2.1 Counting Distance 54
6.2.2 Counting Period 54
6.2.3 Optimum Decay Time 55
6.2.4 Peak Identification 58
6.2.5 Peak Interferences 60
6.2.6 Reaction Interferences 64
6.3 Discussion 67

7 ERRORS ASSOCIATED WITH I.N.A.A. 69
7.1 Sampling 69
7.1.1 Representative Sampling 69
7.1.2 Sample Preparation 69
7.2 Irradiation 70
7.3 Gamma Counting 71
7.3.1 Geometry Errors 71
7.3.2 Distance Correction 73
7.3.3 Dead Time Correction 74
7.3.4 Spectrum Analysis 74
7.3.5 Decay Correction 75
7.4 Standardisation 77
7.5 Experimental Precision 78
7.6 Discussion 81

8 STANDARDS 82
8.1 Absolute Method 82
8.2 Comparitor Method 83
8.3 Discussion 86

9 COMPUTER REDUCTION OF DATA 91
9.1 Mathematical Models 91
9.2 Gamma Spectra Analysis 91
9.3 Peak Data Processing 92
9.4 Data Analysis 94
9.5 Data Presentation 94
9.6 Discussion 94

10 ANALYTICAL RESULTS 95
10.1 Preliminary Survey Samples 95
10.2 Chip Samples 97
10.3 Powdered Samples 99

11 STATISTICAL ANALYSIS 104
11.1 Discriminant Analysis 105
11.1.1 Two Dimensional Model 107
11.1.2 Accuracy of Classification 109
11.1.3 Graphical Representation 110
11.1.4 Relative Importance of the Elements .. 110
11.2 Statistical Analysis of Chip Samples 111
11.3 Statistical Analysis of Powdered Samples .. 115
11.4 Discussion 119

12 GEOCHEMISTRY 121
12.1 Mineralogy 121
12.2 Element Interrelationships 123
12.3 Uranium 132
12.4 Gold 135
12.5 Summary 138

13 SUMMARY AND CONCLUSIONS 139

APPENDIX 1 - STANDARDS 143
APPENDIX 2 - RESULTS FOR 19 ELEMENTS DETERMINED IN CHIP SAMPLES 150
APPENDIX 3 - RESULTS FOR 28 ELEMENTS DETERMINED IN POWDERED SAMPLES 155
APPENDIX 4 - FORMULATION OF THE STATISTICAL ANALYSIS .. 175
APPENDIX 5 - STATISTICAL ANALYSIS OF CHIP SAMPLES .. 203
APPENDIX 6 - STATISTICAL ANALYSIS OF POWDERED SAMPLES .. 222

REFERENCES 236

LIST OF TABLES

		PAGE
2.1	WITWATERSRAND SYSTEM : STRATIGRAPHIC SUCCESSION ...	4
4.1	NEUTRON REACTION CROSS SECTIONS FOR Fe, Co, Cd, Au and U	22
4.2	COMPARISON OF TYPICAL NaI(Tl) AND Ge(Li) DETECTORS ..	27
5.1	SPECIFICATIONS OF REACTOR	31
5.2	REACTOR IRRADIATION FACILITIES	32
5.3	NEUTRON FLUX GRADIENTS	34
5.4	GAMMA SPECTROSCOPY SYSTEMS	40
6.1	ELEMENT COUNTING SCHEME	59
6.2	PEAK INTERFERENCES CORRECTED USING BRANCHING RATIOS ..	64
6.3	INTERFERING REACTIONS	65
6.4	FISSION INTERFERENCES	66
7.1	ANALYSIS OF CONTAMINATED QUARTZ VIAL	70
7.2	FREQUENCY GROUPING OF PEAK DETERMINATIONS AT DIFFERENT DECAY TIMES	75
7.3	RANGE OF ELEMENT DETERMINATIONS FOR FOUR U.S.G.S. STANDARDS	77
7.4	MEASURED AND ESTIMATED ANALYTICAL PRECISION ..	79
8.1	DESCRIPTION OF STANDARDS ANALYSED	84
8.2	RESULTS FOR SELECTED ELEMENTS DETERMINED IN BCR-1 ..	88
9.1	SUMMARY OF COMPUTER PROGRAMMES	93
10.1	RESULTS FOR THE ANALYSIS OF PRELIMINARY SAMPLES ..	96
10.2	CHIP SAMPLES - MEANS AND C.O.V.	98
10.3	POWDERED SAMPLES - MEANS AND C.O.V.	101
10.4	AVERAGE LEVEL, ERROR AND DETECTION LIMIT FOR CONGLOMERATE AND QUARTZITE SAMPLES	102
11.1	SUMMARY OF THE STATISTICAL ANALYSIS OF CHIP SAMPLES ..	114
11.2	SUMMARY OF RELATIVE IMPORTANCE OF ELEMENTS FOR CHIP SAMPLES	115
11.3	SUMMARY OF THE STATISTICAL ANALYSIS OF POWDERED SAMPLES	117
11.4	SUMMARY OF RELATIVE IMPORTANCE OF ELEMENTS FOR POWDERED SAMPLES	118
12.1	MINERALS GENERALLY PRESENT IN THE WITWATERSRAND SEDIMENTS	122
12.2	ELEMENT CORRELATION COEFFICIENTS	124
12.3	RARE EARTH VALUES FOR AVERAGE ROCK TYPES	125

LIST OF FIGURES

		PAGE
3.1	DESCRIPTIVE GEOLOGICAL CROSS SECTION OF AREA SAMPLED	8
3.2	FLOW DIAGRAM FOR POWDERED SAMPLE PREPARATION ..	13
4.1	TYPICAL REACTOR NEUTRON FLUX DISTRIBUTION	19
4.2	NEUTRON EXCITATION FUNCTIONS	21
4.3	COMPARISON OF NaI(Tl) AND Ge(Li) DETECTORS ..	28
5.1	NEUTRON FLUX DISTRIBUTION MEASURED USING IRON FOIL MONITORS	37
5.2	MEASURED DETECTOR EFFICIENCY CURVES	42
5.3	EFFECTIVE INTERACTION DEPTH FOR THREE DETECTORS ..	42
5.4	COUNT RATE PERFORMANCE OF SYSTEM A	45
5.5	COUNT RATE PERFORMANCE OF SYSTEMS B AND E	46
5.6	PEAK DEGREDATION AT HIGH COUNT RATES	48
5.7	PILE-UP REJECTION USING THE ELSCINT CAV-N-3 AMPLIFIER	48
5.8	DIFFERENTIAL LINEARITY OF SYSTEM C	49
5.9	DEAD TIME CORRECTION BY PULSER PEAK NORMALISATION ..	50
6.1	TOTAL ACTIVITY DECAY CURVE OF REPRESENTATIVE SAMPLES	53
6.2	ACTIVITY AND ERROR DECAY CURVES	56
6.3	OPTIMUM DECAY TIMES	57
6.4	COMPARISON OF NORMAL AND HIGH RESOLUTION COUNTING SYSTEMS	61
6.5	PEAK INTERFERENCES IDENTIFIED USING A HIGH RESOLUTION DETECTOR	62
7.1	SAMPLE DISPLACEMENT ERRORS	72
7.2	ERROR IN HALF-LIFE CORRECTION FACTOR	76
7.3	FREQUENCY DISTRIBUTION OF ELEMENT CONCENTRATIONS AND ERRORS FOR QUARTZITE SAMPLES	80
8.1	CALIBRATION CURVES FOR IRON AND EUROPIUM	85
8.2	FREQUENCY DISTRIBUTION OF RELATIVE ERRORS FOR THE DETERMINATION OF 23 ELEMENTS IN FOUR U.S.G.S. STANDARDS	87
11.1	DISCRIMINATION IN TWO DIMENSIONAL SPACE	108
12.1	RARE EARTH PATTERNS OF EACH ZONE RELATIVE TO CHONDRITES	126
12.2	RARE EARTH PATTERNS OF AVERAGE ROCK TYPES RELATIVE TO CHONDRITES	126
12.3	DISTRIBUTION OF RARE EARTH ELEMENTS IN SOME RARE EARTH MINERALS	127
12.4	DISTRIBUTION OF MONAZITES FROM DIFFERENT PARAGENESES	127

PAGE

12.5 SCATTER DIAGRAM OF THORIUM AND CERIUM 128
12.6 SCATTER DIAGRAM OF ZIRCONIUM AND CERIUM 129
12.7 SCATTER DIAGRAM OF ZIRCONIUM AND TANTALUM .. 131
12.8 SCATTER DIAGRAM OF ZIRCONIUM AND CHROMIUM .. 131
12.9 SCATTER DIAGRAM OF URANIUM AND TANTALUM 133
12.10 SCATTER DIAGRAM OF URANIUM AND ARSENIC 133
12.11 SCATTER DIAGRAM OF GOLD AND URANIUM 136
12.12 SCATTER DIAGRAM OF GOLD AND IRON 136

1 INTRODUCTION

The technique of Neutron Activation Analysis was first proposed by Hevesy and Levi, who in 1936 used it to determine dysprosium impurities in yttrium. During the 1940's Neutron Activation Analysis was regarded as a curiosity until the advent of the first nuclear reactors showed that it could be used as a highly sensitive analytical technique. Today it is applied in many different fields of research and technology to determine elements ranging in concentration from below parts per million to percent levels.

In the field of earth science Instrumental Neutron Activation Analysis can be used to analyse rock samples for many trace elements, but cannot always be used to accurately determine every element that might be of interest to a geochemist, for example. It should therefore be considered as complementary to the many other analytical techniques available.

Some of the advantages and disadvantages of Instrumental Neutron Activation Analysis (I.N.A.A.) as compared to other instrumental analytical techniques can be seen from the following discussion and from Smales' review of the analytical techniques applied in the geosciences. (Sm71) Samples ranging in mass from less than a microgram to more than 10 grams can be analysed nondestructively by I.N.A.A. In addition, no special sample preparation is necessary as geological material is virtually transparent to both neutrons and gamma rays. Of the other instrumental techniques, only X-ray Fluorescence is considered to be nondestructive, however, samples must be specially prepared for analysis.

Together with I.N.A.A., Emission Spectrography and Spark Source Mass Spectroscopy are generally considered to be multi-element analytical techniques. As such they all suffer from interference problems which can sometimes be resolved instrumentally but may often require a chemical

separation of the interfering element. In this respect Neutron Activation Analysis (N.A.A.) has the advantage that any contamination introduced during a post-irradiation separation of the interfering element will not affect the analysis.

The accuracy obtainable with an analytical technique is closely related to the sensitivity of the technique. For example, it is often difficult to obtain accurate results when determining an element near the detection limit. X-ray Fluorescence has been developed to the stage at which elements can in general be accurately determined as long as certain procedures are followed. In the case of I.N.A.A. and Spark Source Mass Spectroscopy, routine analytical methods have yet to be developed.

Recently, techniques based on the analysis of short-lived isotopes have shown that I.N.A.A. can be an extremely rapid analytical technique. Unfortunately this increase in speed results in a proportionate decrease in the number of elements which can be simultaneously determined. Perhaps the most serious disadvantage of I.N.A.A. is the high initial capital cost of a suitable neutron source (generally a nuclear reactor) and gamma spectroscopy system.

One of the objectives of this investigation was to study and develop the technique of I.N.A.A. as currently employed for the analysis of geological material. A problem of interest to the gold mining industry in South Africa has been chosen to stimulate this development.

The major economic deposits of gold in this country occur in the conglomerates of the Witwatersrand System. Although gold is found disseminated throughout the conglomerates, it is generally only enriched to economic levels in narrow 'pay bands'. The problem which faces the mine geologist is to locate these pay bands in areas which are often

extensively deformed. Once the sedimentary sequence has been established, the pay band is identified by detailed sampling and subsequent gold assay. At present the sedimentary succession is determined using qualitative methods based on a detailed knowledge of the mineralogical features of individual strata. The identification of an individual layer is often complicated by the fact that some of the sedimentary strata are visually indistinguishable.

A series of strata from the Kimberley Reef Conglomerates have been sampled at the Durban Roodepoort Deep Mine. Instrumental Neutron Activation Analysis has been used to determine as many as 28 elements in conglomerate and quartzite samples from these strata, and statistical techniques have been developed to quantitatively characterise strata according to their trace element geochemistry.

2 GEOLOGY OF THE SAMPLING AREA

The first discovery of gold-bearing conglomerates was made on the farm Langlaagte near Johannesburg in the early part of 1886. These conglomerates form only a small portion of the total sedimentary succession known as the Witwatersrand System.

This system consists of a succession of quartzites and conglomerates, interspersed with shales and volcanic rocks. It is subdivided into five series as shown in Table 2.1.

Table 2.1 WITWATERSRAND SYSTEM : STRATIGRAPHIC SUCCESSION

Upper Division	Kimberley - Elsburg Series	2000 m
	Main - Bird Series	1100 m
Lower Division	Jeppestown Series	1200 m
	Government Reef Series	2000 m
	Hospital Hill Series	1600 m

According to a review of the geology of the Witwatersrand System by Brock and Pretorius, Br64, the sediments forming the system were deposited over an extended period, approximately 2600 million years ago, in an inland basin some 300 km in diameter. This basin was subjected to periodic tectonic activity in which the rim of Archean granite suffered uplift and erosion complimentary to the subsidence of the basin floor.

Fine grained shales were deposited during deep water phases and quartzites during phases of shallow water. The conglomerates are believed to be the result of the action of floods over extensive delta plains.

The basin was fed with alluvial material from rivers eroding the surrounding granites. In many areas, particularly in the West Rand, definite erosion channels have been identified.

Although there were undoubtedly many such rivers entering the basin, four main entry points have been identified.

(a) Orange Free State Entry Point - South of Welkom

(b) Far West Rand Entry Point - Northwest of Klerksdorp

(c) West Rand Entry Point - Northwest of Krugersdorp

(d) East Rand Entry Point - North of Benoni

The distribution of the conglomerates in the Witwatersrand System has been extensively investigated. In the Central Rand they form some 8% of the total succession, decreasing to about 1% in the Vredefort dome area. This is in agreement with the overall decrease in grain size from the Central Rand towards the south east, indicating predominantly northern source entry points to the basin.

The material entering the basin was deposited as deltaic plains which were reworked by the currents within the basin which appear to have circulated in a clockwise direction parallel to the shore.

The gold, present predominantly in the conglomerates of the Witwatersrand System, is believed to have been contained in the Archean schists, which filled synclines within the 'Old Granites', and which were eroded together with the granites. Examples of such gold bearing schists exist in the gold fields of Rhodesia and in the Barberton area.

In periods of flooding, gold and other heavy minerals were able to settle quicker than the lighter alluvial material. Thus the gold is concentrated together with the heavy minerals, in the conglomerates, or so-called bankets. A limited reworking by hydrothermal solutions of this detrital gold could have occurred. This would also account for the presence of minerals coexisting with gold, such as arsenopyrite, which are believed to be of hydrothermal origin in the sediments of the Witwatersrand System. (Hi68a)

The Kimberley - Elsburg Series of the Witwatersrand System can be subdivided into four groups.

(a)	The Elsburg Reef group	550 m
(b)	The Kimberley Quartzites	900 m
(c)	The Kimberley Reef group	320 m
(d)	The Kimberley Shales	200 m

The Kimberley Reef group, consisting of a succession of conglomerates and quartzites, is fairly extensively developed in the East Rand area, but decreases in thickness towards the Far West Rand. In the vicinity of the Durban Roodepoort Deep Mine, the Kimberley Reef is approximately 200 m thick.

3 SAMPLING

3.1 Sampling Site

The Kimberley Reef conglomerates were sampled at the Durban Roodepoort Deep Gold Mine (D.R.D.), one of the Rand Mines Group, which is situated on the West Rand some 30 km from Johannesburg.

Four major gold bearing reefs are found in this area : the Main Reef, South Reef, Main Reef Leader and the Kimberley Reef, all belonging to the Upper division of the Witwatersrand System. Mining at D.R.D. is carried out to depths greater than 3.000 m.

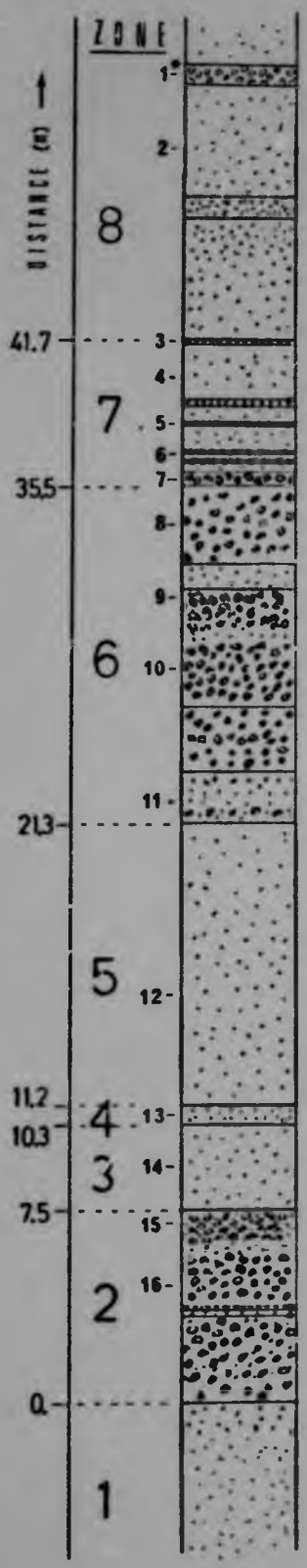
The mine covers an area of extreme folding and faulting and can be conveniently subdivided into three sections : East, West and Central. Sampling was undertaken only in the Central section.

The samples were taken from the Kimberley Reef from 30 level crosscut, 1500 m below surface, leading off Number 6 Shaft. The section sampled consisted of eight sedimentary units, including the 'pay band' which is mined for gold.

A description of the section, as logged by the mine geologist, is given in Figure 3.1. For convenience the sedimentary units have been labelled Zones 1 - 8, and all future references will be made to this numbering system.

Zones 2, 6 and 7 are conglomerate zones and 1, 3, 4, 5 and 8 are quartzite zones. Zones 1 and 8 were not representatively sampled in all cases and have been excluded from the final analysis.

Although detailed mineralogical investigations are necessary for underground gold exploration and may serve to distinguish zones, the methods are qualitative and cumbersome. The purpose of this investigation was therefore to develop a quantitative method of distinguishing the conglomerate zones 2, 6 and 7 and the quartzite zones 3, 4 and 5.



Mod-dev. Poorly mineralised ¼" white pebble congl. Numerous coloureds

Quartzite, numerous coloureds

Poorly dev. to mod. dev. small pebble congl. numerous shale

Yellow grey subglassy med. grained quartzite, occasional thin argillaceous stringers

TOP CONTACT 9 BAND
Yellow medium coarse grained subglassy quartzite
Well developed and well mineralised grey pebble conglomerate, some shale and light green chert
PAY BAND
7 BAND Moderately developed, slightly mineralised white and grey pebble conglomerate in slightly argillaceous subglassy to dull matrix
Yellow medium coarse grained quartzite with pyrite stringers

7 BAND well developed and poorly mineralised white pebble conglomerate in clear glassy matrix

7 BAND Poor-Mod. devel. and poorly min. white and grey pebbled conglomerate in clear matrix
BOTTOM 7 BAND Yellow grey coarse grained slightly argillaceous subglassy quartzite

Laminated quartzite
Yellow coarse grained
Slightly argillaceous

HARD BAR Grey fine grained glassy quartzite
Grey subglassy quartzite plus numerous blue, grey and some coloured grit

6 BAND Well developed and poorly mineralised <¼" white and grey pebble conglomerate in dark glassy matrix

6 BAND Well developed and poorly mineralised ¼" - 1¼" white pebble conglomerate in a clear glassy matrix

Grey medium-grained, subglassy quartzite

Figure 3.1 DESCRIPTIVE GEOLOGICAL CROSS SECTION OF AREA SAMPLED

* Preliminary Sample Positions

The sedimentary strata at D.R.D. have a near vertical dip and it is therefore possible to sample the succession at intervals along a single horizontal level. This fact was one of the prime motivations for initiating this investigation at the D.R.D. mine.

3.2 Sampling Technique

The first sampling was undertaken along 30 level crosscut, ex 6 shaft. A series of hand specimens, with a mass of approx. 5 kg each, was broken from the rock face using a heavy hammer. A suite of 16 samples was taken in this manner across the section of interest. The actual sampling positions are shown in Figure 3.1.

These samples were prepared for analysis by I.N.A.A. using two different techniques.

(i) Small chips with a mass of approx. 2g each were removed from the parent specimen using a hammer and steel chisel. Care was taken at all times to remove samples from a fresh surface, and to avoid excessive contamination from the chisel.

(ii) The remaining rock specimen was then crushed using a jaw crusher, a small cone crusher and a stellite bowl swing-mill crusher, to produce a powdered sample.

The analysis of these samples had a two-fold purpose.

(i) To make a rapid initial analysis of conglomerate and quartzitic material using I.N.A.A.

(ii) To compare results obtained from pulverised samples with those obtained from chip samples.

Although chip sampling had been used successfully in the analysis of granitic material, Uk69, it had not been investigated previously on such heterogeneous material as conglomerates.

Before an analysis of the chip samples was undertaken, however, the sampling procedure was improved, and a new suite of samples obtained. The improved sampling method instituted consisted of drilling through the region of interest with a diamond core drill and then sampling the core at the points required. This technique has a number of important advantages over the previous method of manual removal of specimens from the rock wall.

(i) The exact sampling position is known and can be reproduced easily.

(ii) Sampling can be undertaken under controlled conditions. Thus although contamination occurs, suitable cleaning methods can be devised to overcome this problem.

(iii)The core is available for reference purposes, enabling a far more detailed study of the sampled section to be made than is possible underground.

A series of three AX size (32mm diameter) boreholes, laterally displaced by approx. 2 metres, was drilled through the region of interest. They were designated 30/U1, 30/U2 and 30/U3. The first core, 30/U1, was sampled initially using the modified chip sampling technique. All three cores were later split longitudinally into two sections. One half of each was stored for reference purposes, and the other pulverised to produce a powdered sample less than 100 mesh.

3.2.1 Chip Samples

The improved chip sampling technique was implemented as follows. Using a water cooled diamond saw, a 7mm thick slice was cut from the 32mm diameter core at a point at which a sample was required. The centre of this slice was then removed using a water cooled diamond coring drill. This resulted in a 'tablet' sample 7mm thick and 17mm in diameter, with

a mass of approx. 5g. The dimensions of this tablet were chosen to fit the irradiation containers which are 2[illegible] in diameter.

This technique retains all the advantages of hand specimen sampling as well as having the additional advantage that contamination of the sample to be analysed can be kept under laboratory control. A generous flow of water over the cutting surface resulted in minimum contamination.

Borehole core 30/U1 was sampled according to the following scheme: Chip samples were taken from five levels or sampling points within each zone; one at each zone contact and another equally spaced between the contacts. This resulted in 1 x 5 x 3 = 15 samples for each quartzite zone (3, 4 and 5).

Each conglomerate zone (2, 6 and 7) was sampled by taking five samples, immediately adjacent to one another, at each sampling point, resulting in 5 x 5 x 3 = 75 conglomerate samples. Altogether 90 chip tablet samples were prepared in this fashion.

3.2.2. Powdered Samples

The preliminary analysis of the powdered samples prepared from the hand specimens showed definite indications of contamination from the grinding procedure. For this reason the source of the contamination was investigated.

A sample of pure quartz (SiO_2) was pulverised using the stellite bowl. Samples were taken at each stage of the crushing and pulverising procedure and then analysed by I.N.A.A.

The following samples were taken:

(i) A chip sample was taken from the quartz hand specimen. This was assumed to be the least contaminated and was used as the basis of comparison.

(ii) The sample was then passed through a jew crusher and small chips were taken from the crushed material.

(iii) The jaw crushed material was then pulverised using a stellite bowl for periods of 1 minute, 2 minutes and 5 minutes. The resulting powder was sampled in replicate.

(iv) A similar series of samples was taken after pulverising the jaw crushed material in an agate bowl.

All equipment was cleaned by washing and wiping out with a cloth before use. The results obtained were as follows:

* No contamination was detected in the jaw crushings.

* The powder produced in the stellite bowl, initially white, became dark grey as the grinding period increased. This contamination was found to be from iron, tungsten, nickel, and surprisingly lanthanum.

* There is reason to suspect that the lanthanum contamination is from inadequate cleaning of the bowl.

* No contamination was detected in the powder produced in the agate bowl.

The agate bowl was therefore used to pulverise all samples used in the following investigations. The results from the stellite bowl test emphasised the importance of proper cleaning techniques. Therefore, before subsequent sample preparation, a waste sample, as similar in composition to the actual sample as possible, was crushed in the agate bowl. This waste sample served to clean the bowl.

Samples from each zone of each of the three borehole cores (30/U1, 30/U2 and 30/U3) were pulverised according to the scheme shown in Figure 3.2, and produced final samples, each of 300g, with 99% of the material smaller than 100 mesh (150 μm). This resulted in 18 powdered samples, one from each of the six zones from three borehole cores.

The three sample preparation techniques which have been used, can be compared with respect to amount of information obtained, preparation time, cost etc. No single method is superior on all criteria, but each

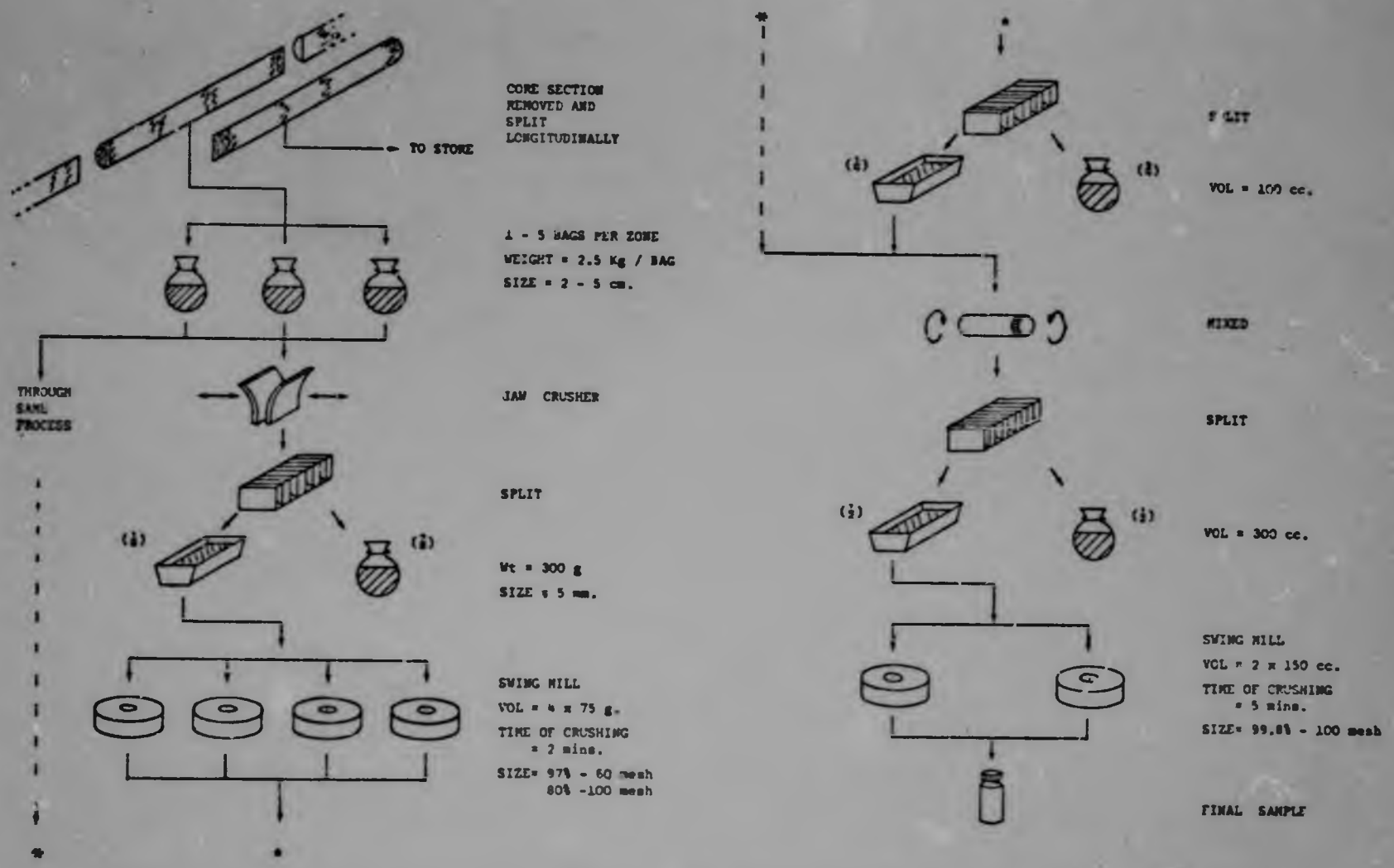


Figure 3.2 FLOW DIAGRAM FOR POWDERED SAMPLE PREPARATION

has advantages and disadvantages.

Hand specimen collection and preparation is easy, rapid and cheap.

Borehole tablet sampling retains detailed information on the sampling locality and is still reasonably rapid.

Crushed samples produce a representative sample of each sedimentary stratum. Thus an average value of each zone is obtained which is difficult to obtain with other sampling techniques.

4 I.N.A.A. - THEORETICAL CONSIDERATIONS

Before applying a technique such as Neutron Activation Analysis it is necessary to understand the physical processes on which the technique is based.

4.1 Neutron Induced Reactions

Neutrons can interact with stable isotopes through a number of different reactions.

(a) Elastic Scattering

When particles collide with one another, kinetic energy is exchanged between them according to the laws of conservation of energy and momentum. If, during the interaction, kinetic energy is conserved, the interaction is referred to as elastic scattering, which can be represented by: $X + n \longrightarrow X + n$

(b) Inelastic Scattering

If, during the interaction, kinetic energy is not conserved, i.e. one of the particles increases in potential energy, the process is referred to as inelastic scattering, and can be represented by:

$$X + n \longrightarrow X^{*} + n' + Q$$

where X^{*} refers to an excited state of the nucleus X, and Q denotes the kinetic energy released in the process.

(c) Inelastic Reactions

The interaction of a neutron with a stable isotope can be written in general as:

$$X + n \longrightarrow Y_1 + b_1 + Q_1$$
$$\longrightarrow Y_2 + b_2 + Q_2$$

where $Y_1 + b_1$, $Y_2 + b_2$, ... are reaction channels, and the system $X + n$ defines the incident channel.

The Q value for the reaction is calculable from the masses of X, n, Y and b and is given by:

$$Q = [(M_x + M_n) - (M_Y + M_b)] \times 931 \text{ MeV}$$

If Q is positive the reaction is exothermic and in principle the reaction will proceed even if the incident channel energy, E_n, is zero. If Q is negative the reaction is endothermic and there is a threshold E_T, below which the reaction will not proceed. The value of the reaction threshold is given by:

$$E_T = - \frac{M_x + M_n}{M_x} \times Q$$

(d) Reaction Mechanism

When the incident neutron is captured by the stable nucleus, a compound nucleus is formed which has a relatively long lifetime, typically $10^{-14} - 10^{-15}$ sec. The compound nucleus, having gained the binding energy and the kinetic energy of the neutron, is in a highly excited state. This excited state of the compound nucleus is bound if the energy level is lower than the binding energy of the most weakly bound nucleon. A bound state of an excited nucleus must de-excite by emission of one or more photons (prompt gamma decay). This reaction can be represented by:

$$X + n \longrightarrow C^* \longrightarrow C + \gamma + Q$$

which is generally denoted $X(n, \gamma)C$.

When a compound nucleus is formed in an excited state above the binding energy of the weakest bound nucleon, the nucleus can de-excite from this virtual level by emission of photons or nucleons or both. Even if, for example, the emission of a proton is the most probable method of decay, there is still a finite probability for emission of a photon or other nucleons.

Proton decay is represented by:

$$X + n \longrightarrow C^{*} \longrightarrow C + p + Q \text{ , denoted } X(n, p)C .$$

An important consideration is that the breakup of the compound nucleus into various reaction channels is independent of the incident channel.

(e) Fission Reactions

Most neutron induced reactions can be readily explained on the basis of the compound nucleus model. Although fission also proceeds via a compound nucleus, the mechanism is best explained in terms of the liquid drop model of the nucleus.

The stability of a nucleus against fission depends critically on the relative effects of the short-range attractive nuclear forces and the long-range repulsive Coulomb forces. In the case of a very heavy nucleus (say, A = 300), the Coulomb force is the more important, and the nucleus, once formed, will break up into two fragments almost instantaneously.

According to the Bohr-Wheeler theory of fission, the critical energy for fission E_f , which must be supplied by the incident particle in the case of induced fission, depends in the quantity Z^2/A of the compound nucleus. A nucleus would be instantaneously fissile if $Z^2/A \geq 47.8$. For values of Z^2/A less than this limiting value there is a lower probability of fission, which is reflected in a long half-life for spontaneous fission.

In the case of the induced fission reaction

$$^{235}U + n \longrightarrow {}^{236}U^{*} \dashrightarrow A + B + xn + Q$$

the value of Z^2/A for ^{236}U is only 35.1 so that energy must be supplied by the incident channel. The critical energy for fission of ^{236}U is about 5 MeV, and since this is less than the neutron

separation energy (6.4 MeV) it is made available by absorption by ^{235}U of a neutron of even zero energy.

The exit channels carry off an average 200 MeV of energy divided amongst: the fission fragments A and B, the on average x = 2.5 neutrons, the gamma radiation, and the beta decay particles.

4.2 Neutron Sources

Neutrons must be produced by some primary nuclear reaction.

(a) Isotopic sources

Reactions such as $^{9}Be + \gamma \longrightarrow {}^{8}Be + n - 1.67$ MeV

and $^{9}Be + \alpha \longrightarrow {}^{12}C + n + 5.70$ MeV

are used as a source of neutrons in isotopic sources, where beryllium is combined with a gamma source, e.g. ^{124}Sb or an alpha source, e.g. ^{241}Am, respectively.

(b) Accelerator sources

When an accelerator is available, a wide variety of reactions can be used to produce neutrons of various energies. Using an electron acceleration to produce bremsstrahlung, photon reactions such as

$$^{2}H + \gamma \longrightarrow {}^{1}H + n - 2.23 \text{ MeV}$$

can be used to produce neutrons.

Particle accelerators can be used, employing reactions such as

$$^{7}Li + p \longrightarrow {}^{7}Be + n - 1.64 \text{ MeV}$$

or $$^{2}H + {}^{2}H \longrightarrow {}^{3}He + n + 3.27 \text{ MeV}$$

As a neutron source for activation analysis, the '(d-T)' reaction namely $^{2}H + {}^{3}H \longrightarrow {}^{4}He + n + 17.58$ MeV is often employed using a small (150 KV) accelerator. This reaction is used as a convenient source of 14 MeV ('fast') neutrons.

(c) Nuclear Reactors

By far the most commonly used source of neutrons for activation analysis is the nuclear reactor. A reactor employs the nuclear fission reaction as a source of neutrons, with ^{235}U commonly used as the fissile material. This reaction produces neutrons of about 1 MeV but requires neutrons of about 0.02 eV for the reaction to proceed with high probability. For the reaction to be self-sustaining it is therefore necessary to reduce the average neutron energy to about 0.02 eV with a minimum loss of neutron flux. This is achieved by elastically scattering the neutrons off a 'moderator' such as D_2O or graphite. A typical reactor neutron energy spectrum is given in Figure 4.1.

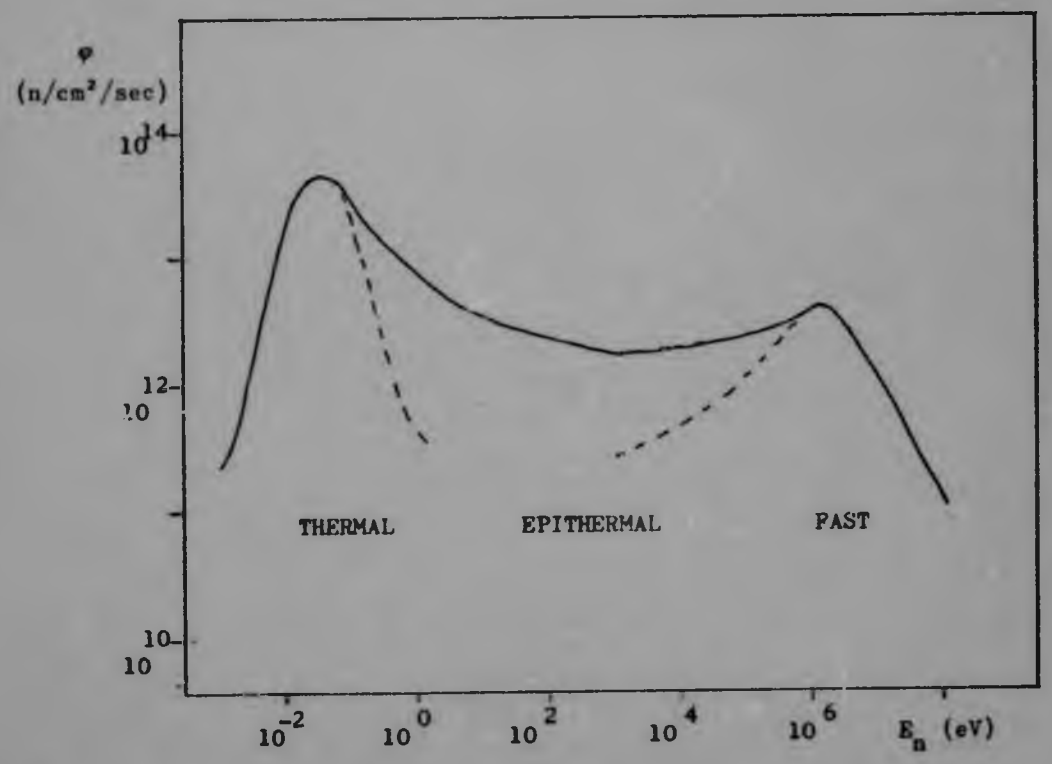


Figure 4.1 TYPICAL REACTOR NEUTRON FLUX DISTRIBUTION

The neutrons range in energy from the fission or fast neutrons (about 1 MeV) to the well-moderated thermal neutrons (about 0.025 eV). The neutrons with an energy in the range $1 - 10^5$ eV are referred to as epithermal or resonance neutrons.

4.3 Cross Sections

Consider a neutron beam of flux φ $\left[\text{neutrons cm}^{-2} \text{ sec}^{-1}\right]$ incident on a target containing N $\left[\text{nuclei cm}^{-3}\right]$ scattering or absorption centres. The probability P $\left[\text{probability cm}^{-3} \text{ sec}^{-1}\right]$ of an interaction between the neutrons and the target nuclei is given by:

$$P = \sigma N \varphi$$

where σ $\left[\text{cm}^2\right]$ is known as the cross section for the reaction, and can be considered as an effective area based on each scattering centre. The cross section is usually expressed in units of barns. ($1 \text{ b} = 10^{-24} \text{ cm}^2$)

The interaction of neutrons with a nucleus can proceed through a number of possible reactions. There is a different cross section for each of these reactions, e.g.

σ_s : cross section for scattering

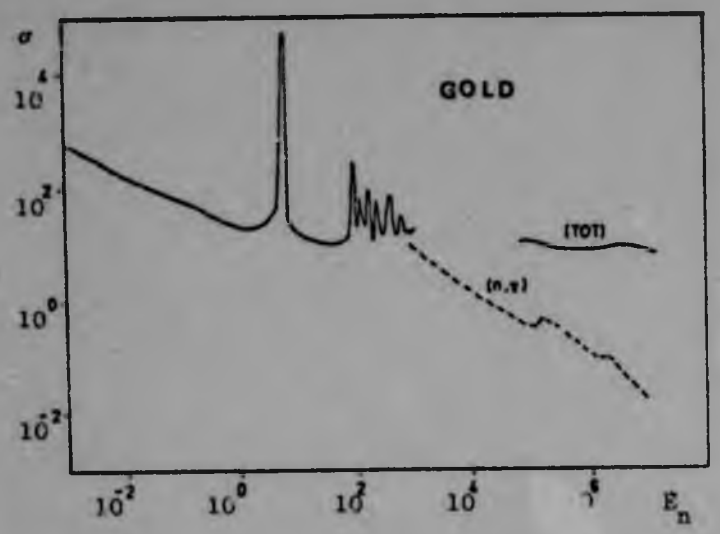
σ_{abs} : cross section for neutron absorption

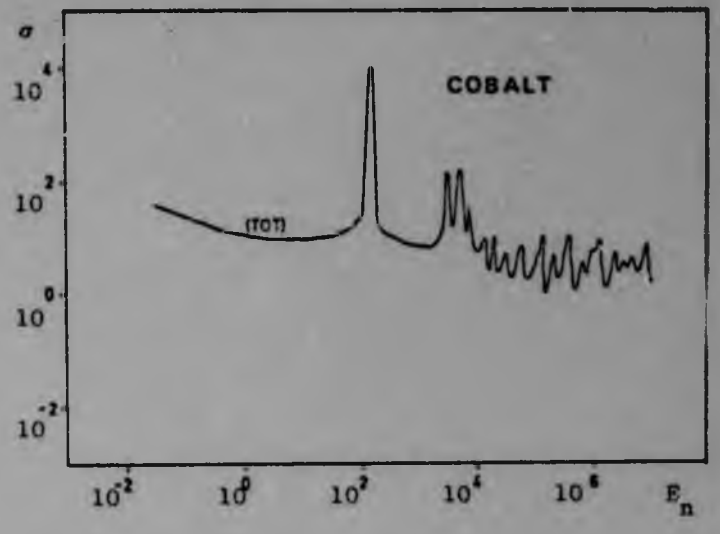
σ_{tot} : total absorption neutron cross section $= \sigma_s + \sigma_{abs}$

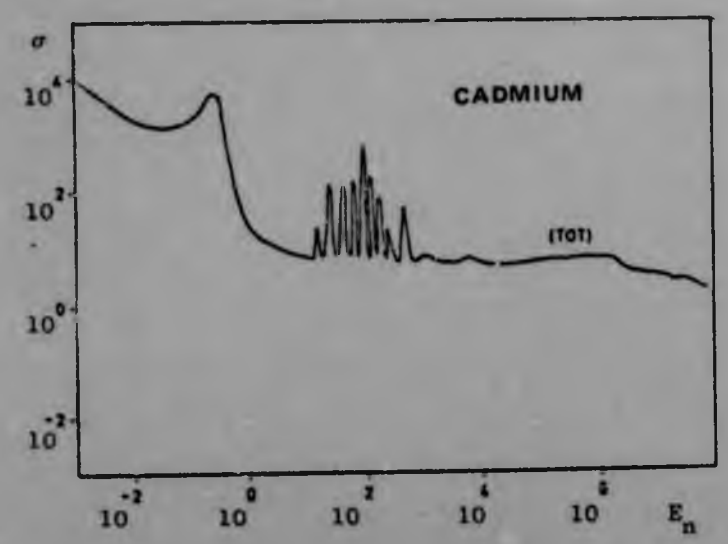
Cross sections can also be defined for particular reactions e.g.

$\sigma_{(n, \gamma)}$: cross section for the (n, γ) reaction.

The probability for any reaction is also a function of the neutron energy, e.g. the total absorption cross sections for Au, Co, Cd and Fe are shown as a function of the neutron energy in Figure 4.2. The reaction cross section for neutrons of a particular energy (or range







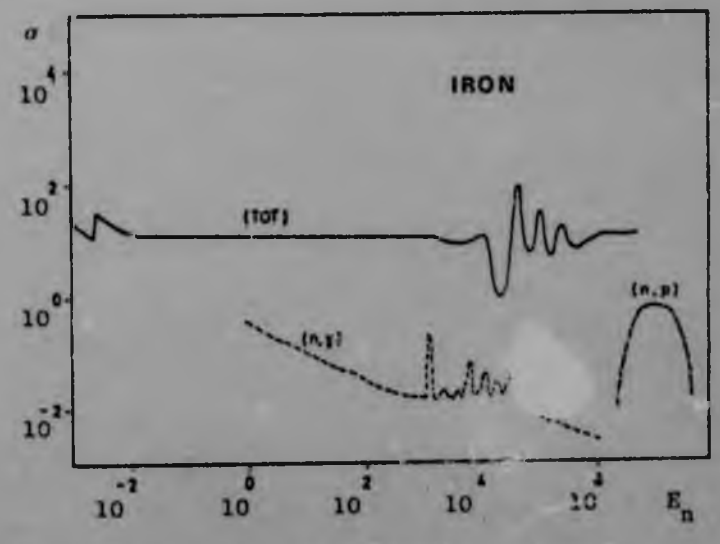


Figure 4.2 NEUTRON EXCITATION FUNCTIONS (ref. St64)

of energies) can be denoted:

σ_{th} : cross section for reaction with thermal neutrons

I_{res} : integrated resonance cross section for reaction with epithermal neutrons

The cross sections for a few reactions of interest are given in Table 4.1.

Table 4.1 NEUTRON REACTION CROSS SECTIONS FOR Fe, Co, Cd, Au and U

REACTION	CROSS SECTIONS				I_{res}/σ_{th}
$^{58}Fe\ (n,\gamma)\ ^{59}Fe$	σ_{th}	= 1.21 b	I_{res}	= 1.15 b	0.95
$^{54}Fe\ (n,p)\ ^{54}Mn$	σ_{8MeV}	= 0.55 b			
$^{59}Co\ (n,\gamma)\ ^{60}Co$	σ_{th}	= 37 b	I_{res}	= 70 b	1.9
$^{113}Cd + n$	σ_{abs}	= 20000 b			
$^{197}Au\ (n,\gamma)\ ^{198}Au$	σ_{th}	= 99 b	I_{res}	= 1550 b	15.6
$^{238}U\ (n,\gamma,\beta^-)\ ^{239}Np$	σ_{th}	= 2.7 b	I_{res}	= 280 b	104

The Bohr model of the compound nucleus predicts that the cross section for the scattering of slow neutrons is approximately constant, i.e. $\sigma_{(n,n)} \approx$ constant, whereas the (n, γ) cross section is inversely proportional to the neutron velocity i.e. $\sigma_{(n,\gamma)} \approx {}^{1}/_{v}$

The constant scattering cross section and the ${}^{1}/_{v}$ law for (n, γ) reactions is well illustrated by the reaction with iron, see Figure 4.2. The cross section for neutron reactions with cadmium, see Figure 4.2, shows a high probability for absorption of slow neutrons but a much lower absorption of epithermal and fast neutrons. This property of cadmium can be put to good use as a thermal neutron shield, i.e to effectively enhance the epithermal and fast neutron flux as seen by nuclei within the shield.

The ratio of the measured activity for irradiation without and with a cadmium shield is defined as the cadmium ratio.

$$R_{Cd} = \frac{\sigma_{th}\,\varphi_{th} + I_{res}\,\varphi_{res}}{I_{res}\,\varphi_{res}}$$

Thus for any given reaction, e.g. $^{197}Au\ (n, \gamma)\ ^{198}Au$, a high cadmium ratio ($R_{Cd}$ = 100, say) implies a well thermalised flux, whereas a low figure (R_{Cd} = 5, say) implies a poorly thermalised flux.

4.4 Growth and Decay of Radioactive Nuclei

Consider the case of a nuclide (1) which is activated and the radioactive nuclide (2) formed. This nuclide (2) then decays to a stable nuclide (3). The rate of decay of nuclide (2) is proportional to the number of nuclei, N_2, present at any time, i.e.

$$\frac{dN_2}{dt} \propto N_2 = -\lambda_2 N_2$$

where λ_2 = decay constant of nuclide (2)

$$\therefore \quad N_2(t) = N_2(0)e^{-\lambda t}$$

where $N_2(t)$ = number of nuclei (2) present at time t

$$\text{or} \quad N_2(t) = N_2(0)e^{-0.693t/T_{\frac{1}{2}}}$$

where $T_{\frac{1}{2}}$ = half-life of nuclide (2)

During the irradiation of nuclide (1), the growth of nuclide (2) is proportional to the cross section σ, the neutron flux φ, and the number of nuclei (1) present. Although the number of nuclei (1) remains approximately constant, i.e. $N_1(t) \approx N_1(0)$, nuclide (2) is decaying at a rate proportional to λ_2. The rate of formation of nuclide (2) is therefore given by:

$$\frac{dN_2}{dt} = \varphi\sigma N_1 - \lambda_2 N_2$$

This equation can be solved giving

$$N_2(T_i) = \frac{N_1(0)\,\varphi\,\sigma\,S}{\lambda}$$

where $S = (1 - e^{-\lambda T_i})$ is the 'saturation factor' and T_i the period of irradiation. This can be simplified to the well known equation:

$$D = N\,\varphi\,\sigma\,S$$

where D is the disintegration rate.

4,5 Electromagnetic Interactions with Matter

Neutron Activation Analysis is normally applied by detecting the gamma radiation from radioactive isotopes. In the interaction of gamma rays with matter, three separate processes are important.

(a) Photoelectric Effect

A photon can interact with a bound electron and eject the electron from the atom. This photo-electron will have an energy $E_e = E_\gamma - E_K$, where E_γ is the energy of the incident photon and E_K is the binding energy of the (usually K shell) electron.

For non-relativistic photoelectrons, the cross section is proportional to $z^4\ \lambda^3$, so that the highest probability is for the interaction of low energy photons with high z absorbers.

(b) Compton Scattering

The Compton effect arises when a photon collides with an electron, and transfers all or part of its energy. From the laws of conservation of energy and momentum the energy of the scattered photon is given by:

$$E_\gamma = E_o / (1 + E_o/m_o c^2) (1 - \cos\theta)$$

where E_o is the incident photon energy, $m_o c^2$ is the rest mass of an electron, and θ is the scattering angle. The energy of the scattered electron is given by:

$$E_e = E_o - E_\gamma$$

Since E_γ is angle dependent, E_e can vary from zero to E_{max} given by:

$$E_{max} = E_o / (1 + m_o c^2/2E_o)$$

Thus for a given incident photon energy, Compton scattering produces a range of electron energies whereas the photoelectric effect produces monoenergetic electrons.

(c) Pair production

Dirac's relativistic wave equation, which describes the electronic structure of an atom, predicts the existance of negative electrons or positrons from the relativistic energy-mass, momentum relationship,

$$E^2 = (T + mc^2)$$

$$\text{i.e.} \quad E = \pm\sqrt{T + mc^2}$$

The interaction of a photon with the external field of a nucleus can give rise to a free electron and a positron (or 'electron hole'). The energy supplied must be sufficient to create the electron-positron pair, i.e. have an energy greater than $2m_o c^2 = 1.022$ MeV.

If the incident photon forming the electron-positron pair has energy greater than 1.022 MeV, the excess energy is equally divided as kinetic energy between the electron and positron. The electron and positron lose energy by elastic scattering. When the positron comes to rest, it annihilates with any available electron, liberating two 0.511 MeV photons in opposite directions. These photons can then interact by the photoelectric effect to deposit the full 1.022 MeV. It may happen that one or both of these photons may escape from the absorbing material, in which case only $E_\gamma - m_o c^2$ or $E_\gamma - 2m_o c^2$ will be deposited in the absorber.

4.6 Gamma Ray Detectors

Of the many types of gamma detectors, scintillation detectors and semiconductor detectors are used for gamma ray spectroscopy.

(a) Scintillation detectors

Gamma photons can interact with the electrons in the crystal lattice structure by ionisation and excitation. Luminescent radiation is produced when an excited electron de-excites by emitting a light photon. These light photons can then be collected and amplified by a photomultiplier tube.

By the use of certain impurities or activators, luminescent centres can be produced which have emissions at wavelengths suitable for detection by photomultiplier tubes.

A scintillator should be of high density and be transparent to its own luminescent radiation. The most commonly used scintillator is a thallium activated sodium iodide crystal, NaI(Tl).

(b) Semiconductor detectors

Gamma radiation incident on an absorber can liberate electrons and produce a series of electron-hole pairs. The purpose of a gamma ray detector is to act as a fast and efficient collector of these electron-hole pairs.

Consider a cylinder of germanium into which lithium ions have been drifted. Germanium is a p-type material, i.e. it has an excess of electron holes, while the n-type i.e. electron-rich, lithium is introduced to compensate for the excess p-type impurities originally present in the germanium. The fully compensated region between the p-type core and the n-type surface is known as the i-type or intrinsic region.

If a reverse bias is applied between the n-type and p-type material, i.e. across the p.i.n. junction, all free electrons and electron holes are rapidly carried to the positive and negative potentials respectively, resulting in conduction.

The collection of the electron-hole pairs produced in intrinsic material by the interaction of gamma rays with matter gives rise to an output signal which is proportional to the amount of energy absorbed. The quality of a gamma detector can be judged in terms of its resolution and efficiency. Data for typical NaI(Tl) and Ge(Li) detectors is given in Table 4.2 and comparative spectra in Figure 4.3.

Table 4.2 COMPARISON OF TYPICAL NaI(Tl) AND Ge(Li) DETECTORS

PARAMETER	DEFINITION	TYPICAL VALUES	
		NaI(Tl)	Ge(Li)
SIZE	Dimensions of the cylindrical crystal in cm (diameter x height)	7.5 x 7.5	-
VOLUME	Volume of the intrinsic region	-	45 cm³
RES^{n} (FWHM)	Resolution - Full width at half maximum peak height ($H_p/2$)	80 KeV	2.5 KeV
FW$\frac{1}{10}$M	Full width at one tenth maximum peak height ($H_p/10$)	-	5.0 KeV
P:C	Ratio of peak height to Compton continuum ($H_p:H_C$)	4:1	30:1
EFF.	Efficiency - Normalised peak area counts for point source at 25 cm, relative to 7.5 x 7.5 NaI	100 %	10 %
Notes:	The symbols are defined in Figure 4.3 Values are given for the 1.33 MeV peak of ^{60}Co		

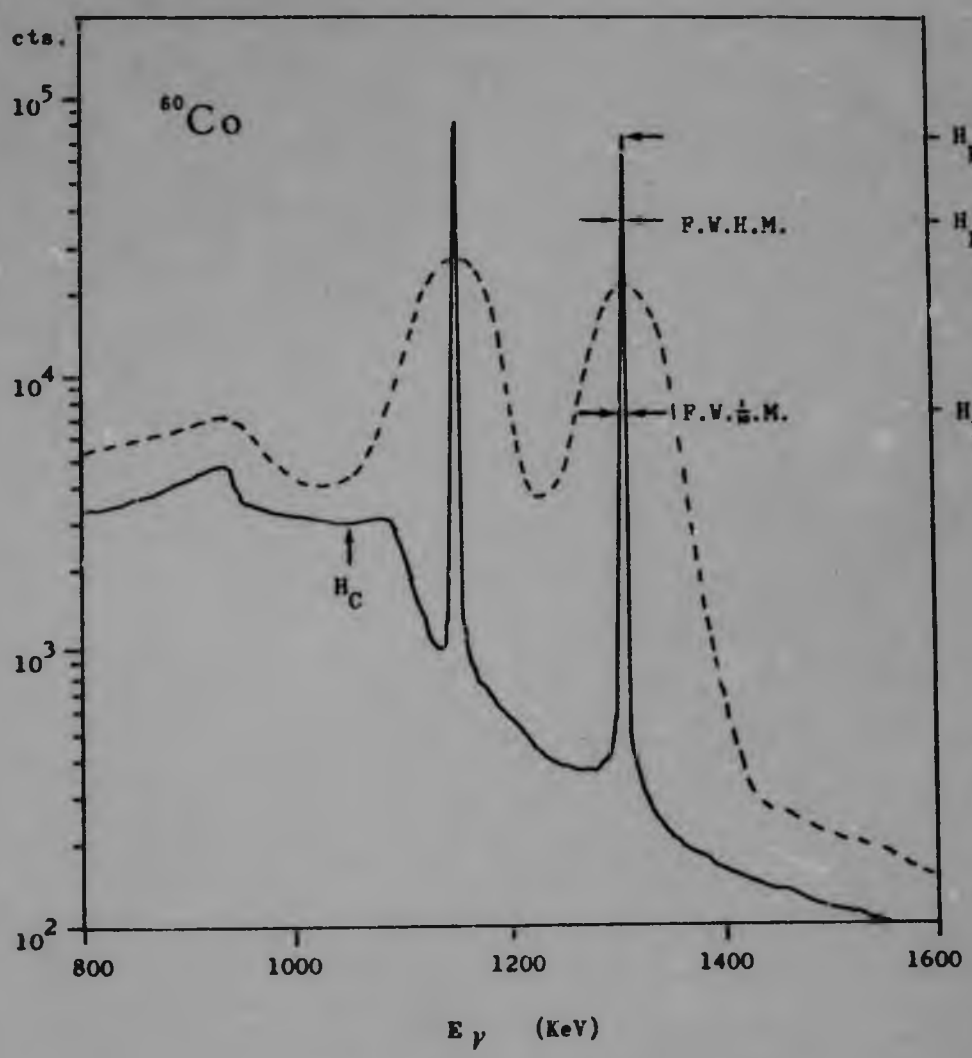


Figure 4.3 COMPARISON OF NaI(Tl) AND Ge(Li) DETECTORS

Note: ----- NaI(Tl) 7.5 x 7.5 cm

——— Ge(Li) 45 cm³

Source distance 25 cm

Equal counting times

4.7 Discussion

A number of different neutron induced reactions have been discussed, all of which have certain advantages and disadvantages when used for analytical purposes. The type of reaction used in any particular application is generally dependent on the source of neutrons available.

(a) Fast neutron activation analysis

The most commonly used source of fast neutrons is a neutron generator. This is usually a small 150 KV deuteron accelerator which uses the '(d,T)' reaction to produce 14 MeV neutrons.

Isotopic sources are used for 'on-line' analyses and for in-situ geochemical analyses.

Although in general not as sensitive as (n, γ) reactions, fast neutron induced threshold reactions can be used to determine a number of elements. For example, elements such as O, Si, P, Fe, Y and Pb can in fact be determined more sensitively by fast neutron activation analysis than by thermal neutron activation. (DS72)

For the determination of single elements, activation by fast neutrons is often chosen in preference to thermal neutron activation. This is because the many thermal neutron induced reactions often introduce serious interferences in multi-element samples.

(b) Thermal neutron activation analysis

Although any source of fast neutrons can in principle be used as a source of thermal neutrons, only nuclear reactors have a sufficiently high neutron flux to produce usable amounts of thermal neutrons. Reactors have an added advantage in that the fission neutrons can also be used for fast neutron activation analysis. Generally, 'in-core' irradiation positions have a high percentage of fast neutrons whereas positions outside the core have a low percentage of fast neutrons.

Thus a reactor can be used for both thermal and fast neutron activation analysis by the judicious positioning of irradiation facilities.

Thermal neutron activation analysis is a very sensitive analytical technique. Under interference-free conditions, some 75 elements can be determined with a median sensitivity of 10^{-9}g. (Gu72)

The multi-element analysis capability of thermal neutron activation analysis arises from the fact that many elements of similar induced activity can be determined from relatively long lived isotopes ($T_{\frac{1}{2}} \geq 1$ day). Thus a single measurement at a reasonably long decay time can be used to determine a number of isotopes.

The gamma activity of a single isotope can be measured using a scintillation detector and very simple electronic equipment. As the number of isotopes to be determined from a single measurement is increased, accurate gamma energy measurements must be made to identify individual isotopes.

In this investigation, reactor thermal neutron activation analysis has been employed. and the induced activities have been measured using a Ge(Li) gamma spectroscopy system.

5 EQUIPMENT

5.1 Reactor

All irradiations were carried out in Safari 1, an Oak Ridge type reactor situated at Pelindaba, the National Nuclear Research Centre of the South African Atomic Energy Board. Specifications of the reactor are given in Table 5.1

Table 5.1 SPECIFICATIONS OF REACTOR

SAFARI 1	South African Fundamental Atomic Research Installation.
TYPE :	ORR (Oak Ridge Reactor) Tank type, light water moderated, beryllium reflected.
SUPPLIER :	Allis-Chalmers Manufacturing Company, USA.
RATED OUTPUT :	10 MW (raised to 20 MW, 1973)
REACTOR VESSEL :	Aluminium tank 1 5 m x 4.3 m
FUEL ELEMENTS :	MTR Plate type 62 cm x 7.4 cm 19 plates per element 7 g ^{235}U per plate 90 % enriched uranium 2 % uranium in aluminium alloy 27 fuel elements 17 beryllium reflector elements 17 aluminium filler elements 5 control rods approx. 4 kg ^{235}U
MODERATOR :	High purity light water also serving as coolant.

Ref : Brochure - SAFARI 1, issued by the S.A. Atomic Energy Board Liasion and Information Division.

This type of reactor is designed for materials testing for which high flux densities are required. Although the high flux is an advantage in I.N.A.A., the reactor suffers from several disadvantages:

(i) Poor neutron thermalisation. The high neutron flux positions, see Table 5.2, have a cadmium ratio of 6 - 7, whereas the low flux positions have a cadmium ratio of about 20. A well-thermalised flux would have a ratio of about 100.

(ii) Very steep neutron flux gradients exist across irradiation positions, and there is at present no rotational facility or 'Lazy-Susan', such as is used in TRIGA reactors. It is hoped that a rotational facility will be installed in the near future, but this will be in a low flux position. Details of the facilities presently available are given in Table 5.2.

Table 5.2 REACTOR IRRADIATION FACILITIES

POSITION		NEUTRON FLUX $\times 10^6$ n/cm^2/watt	CADMIUM RATIO FOR GOLD	IRRADIATION CONTAINERS
Hydraulic	West	5.1	6.0	Aluminium cans
	East	5.0	7.0	Aluminium cans
Poolside	A	1.1 - 4.2	9.7 - 7.6	Aluminium cans
	B	1.0 - 3.7	13 - 11	Aluminium cans
	C	0.8 - 2.1	16 - 15	Aluminium cans
Pneumatic		1.1	21	Polythene and epoxy rabbits

(iii) It is impossible to irradiate a large batch of samples at one time at similar fluxes, due to the lack of a lazy-Susan facility.

(iv) The reactor is used simultaneously by many people for widely different purposes such as materials testing and isotope production, thus long, and indeed even short-term stability cannot be assumed.

5.1.1 Neutron Flux Gradients

The neutron flux gradients across the hydraulic facility were measured as follows. Six 5 cm lengths of Co-Al wire (N.B.S. Ref. Mat. SM395) were placed about the internal circumference of an irradiation container. After irradiation for a period of one hour, each length was cut into three sections, and the total activity of each section was measured using a NaI detector.

The results showed that the flux gradients in the east and west hydraulic facilities were slightly different. There was an 8 % - 10 % horizontal flux gradient i.e. across the can, and an 8 % vertical flux gradient, i.e. along the axis of the can.

An alternative method was developed to determine flux differences between individual samples in one container, and to measure both thermal and fast neutron flux differences.

Lengths of iron foil were made to sleeve quartz vials. Six foils were placed in a can and irradiated. The (n,γ) reaction on iron was used to determine thermal flux differences and the (n,p) reaction for fast flux differences.

The results of this experiment agreed fairly well with those of the preliminary Co-Al measurements, indicating that the thermal neutron flux received by samples diagonally opposite each other could differ by as much as 6 % - 8 %. The difference in the fast neutron flux could be as high as 18 % - 25 %.

The neutron flux gradients in the pneumatic facility were also measured using iron foils. A stack of 3 x 3 = 9 samples was irradiated, each sleeved with iron foil. The results showed a 12 % horizontal gradient and a 6 % vertical gradient between samples. The fast neutron flux in this facility was too low to obtain accurate results for the fast flux gradient, but estimated values showed results similar to those obtained in the hydraulic facility.

Measurements of the neutron flux gradients are summarised in Table 5.3.

Table 5.3 NEUTRON FLUX GRADIENTS

MONITOR	Co-Al WIRE		IRON FOIL		IRON FOIL
NEUTRON ENERGY	thermal		thermal		fast
FACILITY	VERTICAL	HORIZONTAL	VERTICAL	HORIZONTAL	HORIZONTAL
PNEUMATIC	-	-	1.3 % cm^{-1}	10 % cm^{-1}	-
HYDRAULIC (EAST)	-	3.5 % cm^{-1}	-	4 % cm^{-1}	15 % cm^{-1}
HYDRAULIC (WEST)	1.7 % cm^{-1}	4.5 % cm^{-1}	-	5 % cm^{-1}	20 % cm^{-1}

Note: Vertical implies along the axis, and Horizontal across the axis of the irradiation can.

5.1.2 Neutron Flux Monitoring

The results obtained for the measurements of the neutron flux gradients indicated the need for adequate monitoring of individual samples.

Initially a single length of Co-Al wire was randomly placed in each irradiation container. This method is obviously unsatisfactory if accurate results are required.

From a study of the nuclear properties of the elements, and of their commercial availability it was decided to investigate the use of iron as a possible neutron flux monitor, (Bi72). The iron was obtained as 0.05 mm thick foil, nominally 99 % pure.

By tightly rolling the foil it could be made to sleeve the sample vial externally with an adequate mechanical hold. The advantages of the use of iron foils as neutron flux monitors can be seen as follows:

(i) Each sample can be individually monitored.

(ii) A true average dosage is measured, as the monitor completely surrounds the sample.

(iii) The ^{58}Fe (n , γ) ^{59}Fe reaction can be used to measure the thermal flux and the ^{54}Fe (n , p) ^{54}Mn reaction to monitor the fast neutron flux. Thus two neutron energies are simultaneously monitored.

(iv) There are no homogeneity problems as compared to metal alloys, since a pure metal is used.

(v) The thickness of the foil used can be varied to obtain a suitable level of activity from the neutron dosage required for the sample. If too great a thickness is used, resonance shielding could become a problem. The 0.05 mm foil is suitable for irradiation dosages up to 10^{18} n/cm^2.

(vi) A relatively large mass of iron can be irradiated because of the low reaction cross section, namely 1.2 b. A typical mass of 0.2 g allows the weight of the monitor to be accurately and rapidly determined.

In practice, the following technique is applied.
Sample vials are always filled to the same height, 2.5 cm, and sleeved with a 2.5 cm high iron foil monitor. The samples are placed in known positions about the circumference of the irradiation container.

After irradiation, the foils are removed and the ^{59}Fe and ^{54}Mn activity determined. The values obtained are compared to that of a

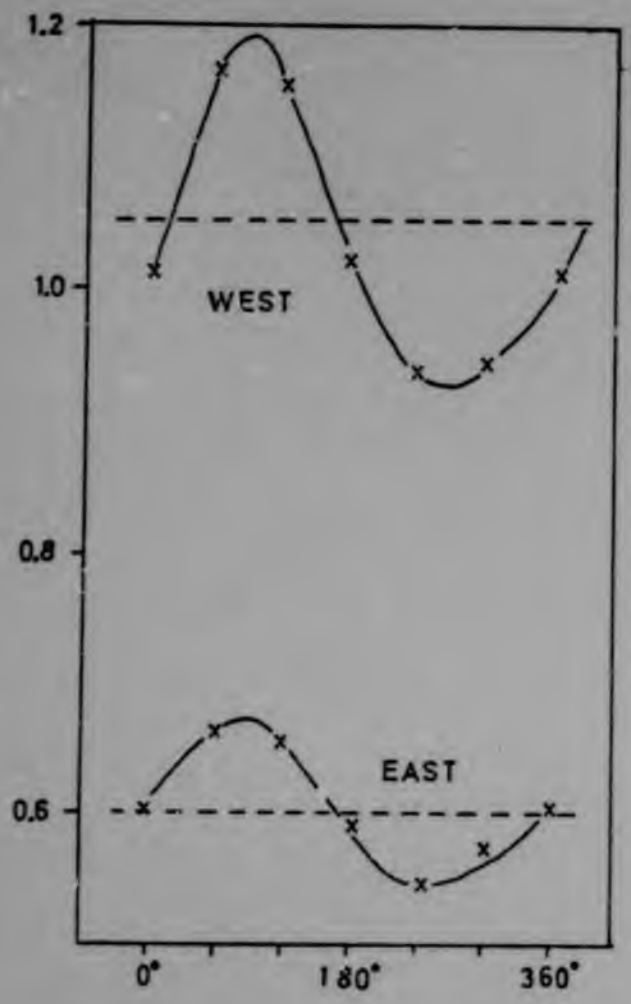
standard calibrated source, and the 'flux factor' for each sample is determined in units of μCi/g. The absolute neutron flux can then be calculated directly if required. The flux factor is plotted against sample position to check for any spurious values. Examples of typical plots obtained for samples irradiated in the two hydraulic facilities, are given in Figure 5.1.

5.1.3 Epithermal Flux Corrections

Neutron reaction cross sections are a function of the neutron energy, see Figure 4.2. In the case of iron, the excitation function follows the $^{1}/v$ law and so iron is acting purely as a thermal neutron flux monitor.

A detailed analysis of the single comparator method of neutron flux monitoring has been given by Girardi et al, Gi65, who point out the importance of the epithermal neutron contribution to reaction cross sections. The thermal and epithermal neutron flux magnitudes and their ratio can be determined using a triple comparator method, as suggested by De Corte et al, DC69. An alternative approach is offered by Maenhaut et al, Ma71, who suggest the use of two tin isotopes for the simultaneous determinations of these factors.

The importance of the epithermal reaction contribution can be estimated for a given neutron flux spectrum, from the cadmium ratio for gold, R_{Cd} (Au), and the ratio of the thermal cross section to resonance integral, σ_{Th} / I_{res}, of the reaction of interest. In the hydraulic facility, R_{Cd} (Au) $\simeq$ 6, and the use of a purely thermal flux monitor such as iron may introduce a maximum error of 10 % for those reactions for which σ_{Th} / I_{res} is greater than 20. (Gi65).



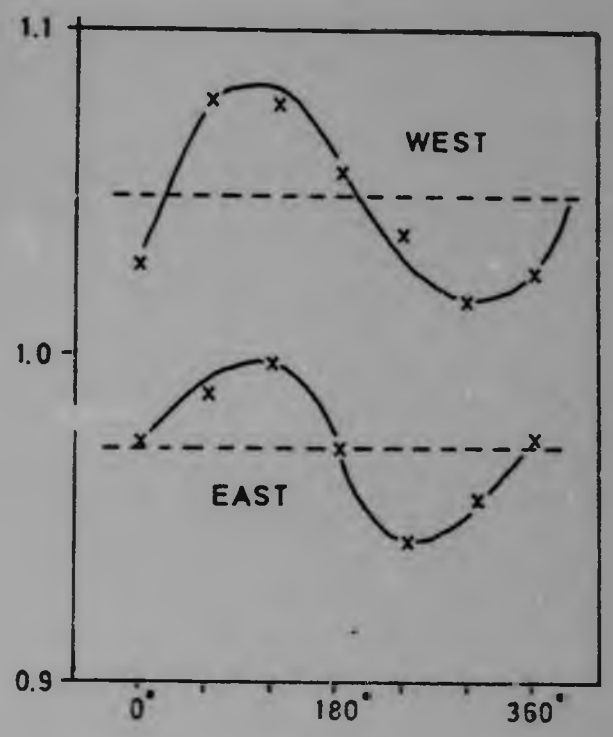


Figure 5.1 NEUTRON FLUX DISTRIBUTION MEASURED USING IRON FOIL MONITORS

Note: Hydraulic Facility
Left: Fast neutron flux distribution
Right: Thermal neutron flux distribution
Scale in arbitrary units

Of the elements of interest in this investigation, only four have a σ_{Th} / I_{res} ratio larger than 20.

Target nuclide	σ_{Th} / I_{res}
^{130}Ba	25
^{181}Ta	34
^{123}Sb	54
^{238}U	104

To investigate the severity of this effect, samples containing uranium and sleeved with an iron foil monitor were irradiated in the east and west hydraulic facilities. The results showed that the neutron flux as seen by uranium (the uranium neutron flux), differed from both the thermal and fast flux as seen by iron. The magnitude of the uranium flux lay somewhere between the thermal and fast flux extremes. This suggested that an 'epithermal flux factor' (EFF) could be derived from a linear sum of the thermal (TFF) and fast (FFF) flux factors. The following function was obtained for the hydraulic facility:

$$EFF = 0.70 \times TFF + 0.23 \times FFF$$

(The coefficients of the linear sum used to define the epithermal flux factor must be determined for each irradiation facility, and will of course differ for individual reactions.)

The use of the epithermal flux factor was demonstrated by irradiating 23 replicate quartzite samples in both the east and west hydraulic facilities. The uranium determinations were corrected for flux variations and the C.O.V. for the 23 samples calculated. The following results were obtained.

Results corrected for:	Measured C.O.V.
No correction	12 %
Fast flux	20 %
Thermal flux	8.6 %
Epithermal flux	5.0 %

Therefore in the case of the uranium reaction, the epithermal flux factor can remove $(8.6^2 - 5.0^2)^{\frac{1}{2}} = 7\ \%$ of the error not accounted for when using a thermal flux factor. In this investigation, only the uranium determinations have been corrected for epithermal reaction contributions.

5.2 Gamma Spectroscopy System

The gamma ray spectroscopy system used consisted of a Ge(Li) detector coupled to a 4000 channel analyser. A sequence of four coaxial Ge(Li) detectors, obtained from Princeton Gamma-Tech, have been used, as well as one thin window planar Ge(Li) detector, manufactured by Nuclear Enterprises. The detectors were coupled to Intertechnique DIDAC 4000 multichannel analysers. Output was obtained on punched paper tape at first, but later Ampex magnetic tape units were added to the system. Table 5.4 describes a series of six systems, which have been used at one time or another. Each system follows the one above it in chronological order, and in general shows improved performance.

5.2.1 Detector Characterisation

(a) Efficiency

A series of efficiency versus energy measurements have been taken for each of the coaxial Ge(Li) detectors. The absolute photo peak efficiency and the efficiency relative to a 7.5 x 7.5 cm NaI crystal is given in Figure 5.2 for a 25 cm source to detector distance.

(b) Distance Corrections

A number of efficiency measurements were made at various source to detector distances. Although gamma radiation follows an inverse square law, i.e. the activity, A is proportional to $1/r^2$, the true distance r cannot be measured since the distance from the front of the detector container to the centre of the crystal is unknown.

Table 5.4 GAMMA SPECTROSCOPY SYSTEMS

SYSTEM	Ge (Li) DETECTOR					PREAMP	PULSER	AMP.	B.L.R.	ANALYSER DIDAC 4000			OUTPUT UNITS			
	NO.	VOLUME	EFF.	RES^{n} (KeV)	P:C	MODEL	MODEL	MODEL	MODEL	A.D.C.	RATE (MHz)	DIGISTAB	PRINTER	PLOTTER	PAPER TAPE	MAGN. TAPE
A	PGT 312	30 cm³	4 %	4.0	15:1	ORTEC 118A		INT C 42		INT C 42	25		*		*	
B	PGT 494	40 cm³	7.1%	2.5	30:1	CANB 1408 C		CANB 1417		INT C 42	25		*		*	
C	PGT 515	45 cm³	9.4%	2.4	26:1	CANB 1408 C	CANB 1501	CANB 1417	CANB 1464	INT C44B	100	A 18B	*	*	*	
D	N.E. GDX	100 mm² x 3 mm	600 eV @ 60 KeV		-	N.E.		CANB 1417 b		INT C 42	25		*	*	*	
B'	PGT 494	38 cm³	6.3%	2.5	23:1	CANB 1408 C	CANB 1501	CANB 1417	CANB 1464	INT C44B	100	A 18B	*	*		*
E	PGT 511	60 cm³	9.5%	2.3	30:1	PGT RG-11	CANB 1501	CANB 1417	CANB 1464	INT C44B	100	A 18B	*	*		*

NOTES:

MANUFACTURERS

ORTEC : Ortec
PGT : Princeton Gamma-Tech
CANB : Canberra Industries
N.E. : Nuclear Enterprises
INT : Intertechnique

SYMBOLS

EFF. : Efficiency relative to a 7.5 x 7.5 cm NaI crystal for 1.33 MeV photopeak of ^{60}Co
RES^{n} : Resolution (FWHM) at 1.33 MeV
P:C : Peak to Compton Ratio for 1.33 MeV
B.L.R. : Base line restoration unit
A.D.C. : Analogue to Digital converter
DIGISTAB : Digital stabiliser unit

In an attempt to determine the position of the crystal centre, an equation of the form $A \propto {}^{1}/(R + \Delta R)^2$ was proposed, where R is the source to detector face distance and ΔR is the distance to the crystal centre. The value of ΔR can be obtained from the intercept of a graph of ${}^{1}/\sqrt{A}$ vs R.

The measured value of ΔR was found to approximate a straight line function of $\log E_\gamma$ for $E_\gamma \geq 100$ KeV, see Figure 5.3. Similar results have been obtained by Chrisler, Cr71, who refers to ΔR as the effective interaction distance.

This modified form of the inverse square law, $A \propto {}^{1}/(R + \Delta R(E))^2$, was used to correct all subsequent measurements to a counting distance of 10 cm.

(c) Geometry Effects

A small displacement of the sample at a close distance can introduce a large error in the measured activity because of the inverse square law. For this reason, the following sample location system was developed.

The detector, mounted in the arm of the chicken feed dewar, was bolted via a rubber mount to a wooden bench. A standard optical bench was rigidly mounted on the bench, beneath and in line with the arm of the dewar. Samples were placed in special holders machined from perspex to hold a variety of sample geometries. Standard optical bench saddles were used to locate the sample holders to the optical bench. In practice, the samples can be located very accurately using saddles incorporating vertical and horizontal vernier scales if so desired.

A special holder was designed to rotate the sample during counting to ensure that on average the sample is accurately centred, and to allow inhomogeneous samples to be more accurately counted. (Bi73).

An automatic sample changer was taken into use after several prototypes had been tested, Za73. This accepts samples in polythene

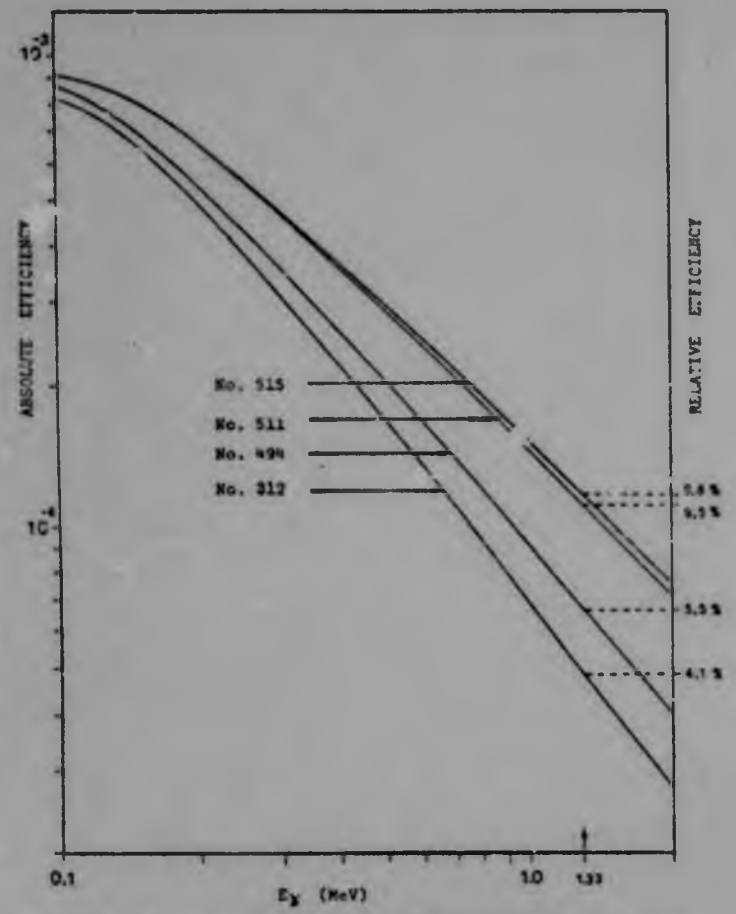


Figure 5.2 MEASURED DETECTOR EFFICIENCY CURVES

Note: Source to detector distance = 25 cm.
Relative efficiency given for 1.33 MeV
compared to 7.5 x 7.5 cm NaI(Tl) detector

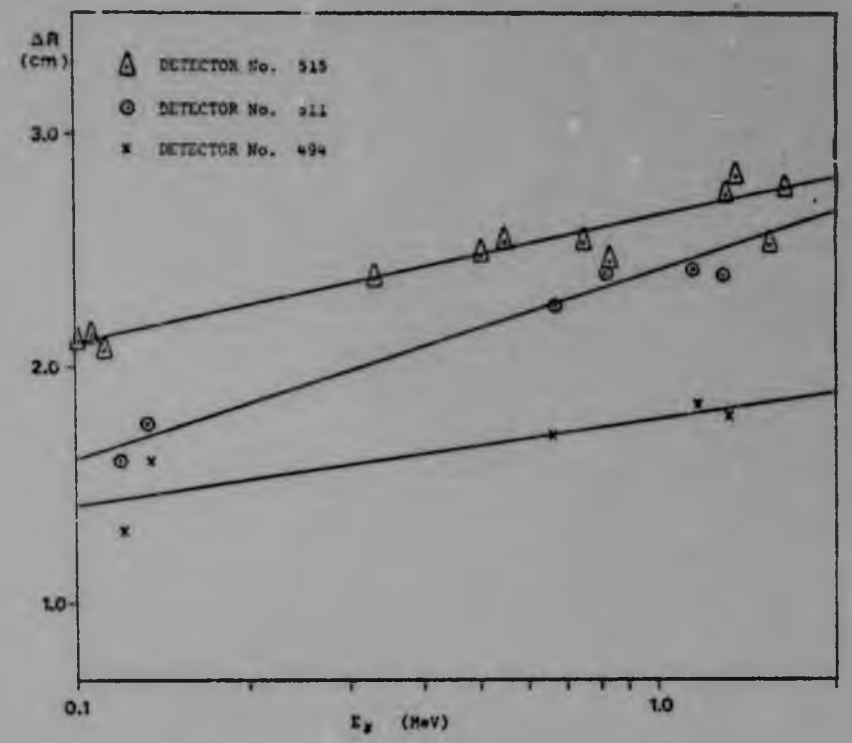


Figure 5.3 EFFECTIVE INTERACTION DEPTH FOR THREE DETECTORS

vials which are moved from a cartridge by compressed air to a counting head mounted on the optical bench. The counting head consists of a perspex receiving tube which is rotated, and simulteneously causes the sample to vibrate, thus compacting powdered material and ensuring a constant sample height. The changing of samples is controlled by signals from the multichannel analyser. On termination of the count, the sample is returned to a store and another sample loaded. A single transfer line is used with a set of points to select the despatch station or waste store.

5.2.2 Count Rate Effects

As the count rate handled by a gamma spectroscopy system is increased, the quality of the measured spectrum decreases. In general the parameters affected are as follows.

(i) The resolution (FWHM) is degraded. which means that closely spaced peaks are no longer resolved.

(ii) The peak to Compton ratio (P : C) decreases, resulting in a higher detection limit for low energy peaks which are lost in the Compton continuum.

(iii) The peak shape often becomes asymmetrical, showing high or low energy tailing. This makes the determination of the peak boundaries difficult, resulting in erroneous peak area determinations.

The effect of increased count rate on certain of these parameters has been investigated for the gamma spectroscopy systems used.

(a) System A

Spectroscopy system A, see Table 5.4, consisted of a 30 cm^3 Ge(Li) detector coupled to a multichannel analyser via an Intertechnique C42 amplifier. The count rate capability of this first system was such

that frequencies over 2000 cts/sec could not be tolerated.

The poor quality of this system was demonstrated by comparing results obtained with the C42 amplifier with those of an Ortec 410 amplifier, see Figure 5.4.

(b) System B

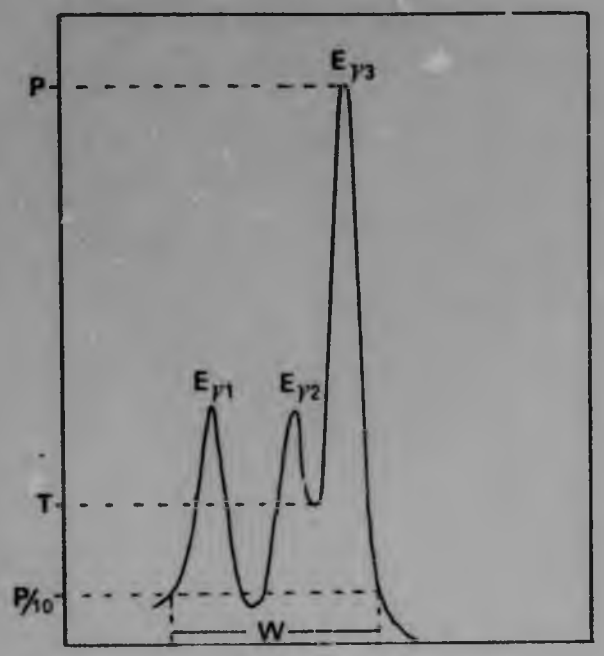
System A was replaced by System B, which consisted of a 40 cm^3 Ge(Li) detector coupled to the analyser via a Canberra 1408c preamplifier and Canberra 1417 amplifier. This system was a considerable improvement on System A in that count rates as high as 5000 cts/sec could be used, with only 0.5 KeV increase in resolution.

(c) Systems C and E

System C and System E differed in that 45 cm^3 and 60 cm^3 Ge(Li) detectors were used respectively and System E incorporated an improved preamplifier. A significant improvement on System B was that a Canberra 1464 base line restoration unit was included. The use of this unit enabled much higher count rates to be handled while retaining good resolution. The improved performance of System E, shown in Fig. 5.5(a) indicates that with this system the analysed count rate can be taken up to 15000 cts/sec before the resolution is seriously degraded.

(d) Dead Time

A distinction should be made between input count rate and analysed count rate. Because of the finite resolving time of the analyser, it is not possible to accept every pulse for analysis. This 'dead time' is a function of the pulse length and of the resolving time of the analyser. For example, for an input count rate of 45 000 cts/sec, only 30 % of the pulses would be analysed, while for an input rate of 100 000 cts/sec, only 16 % would be analysed.



Resolution of the ^{192}Ir triplet

$E_{\gamma 1}$ = 295.8 KeV

$E_{\gamma 2}$ = 308.4 KeV

$E_{\gamma 3}$ = 316.5 KeV

P = Peak height of $E_{\gamma 3}$

T = Height of $E_{\gamma 2} - E_{\gamma 3}$ trough

W = Width of triplet at $P/_{10}$

AMPLIFIER	INTERTECHNIQUE C42			ORTEC 410		
DEAD TIME	10 %	20 %	50 %	10 %	20 %	50 %
FWHM $E_{\gamma 3}$	4.8	7	NR*	5.2	NM**	5.5
P/T	3.1	1.85	NR*	4.0	NM**	3.2
W	32	44	70	30	NM**	33

* NR : Not Resolved

** NM : Not Measured

Figure 5.4 COUNT RATE PERFORMANCE OF SYSTEM A

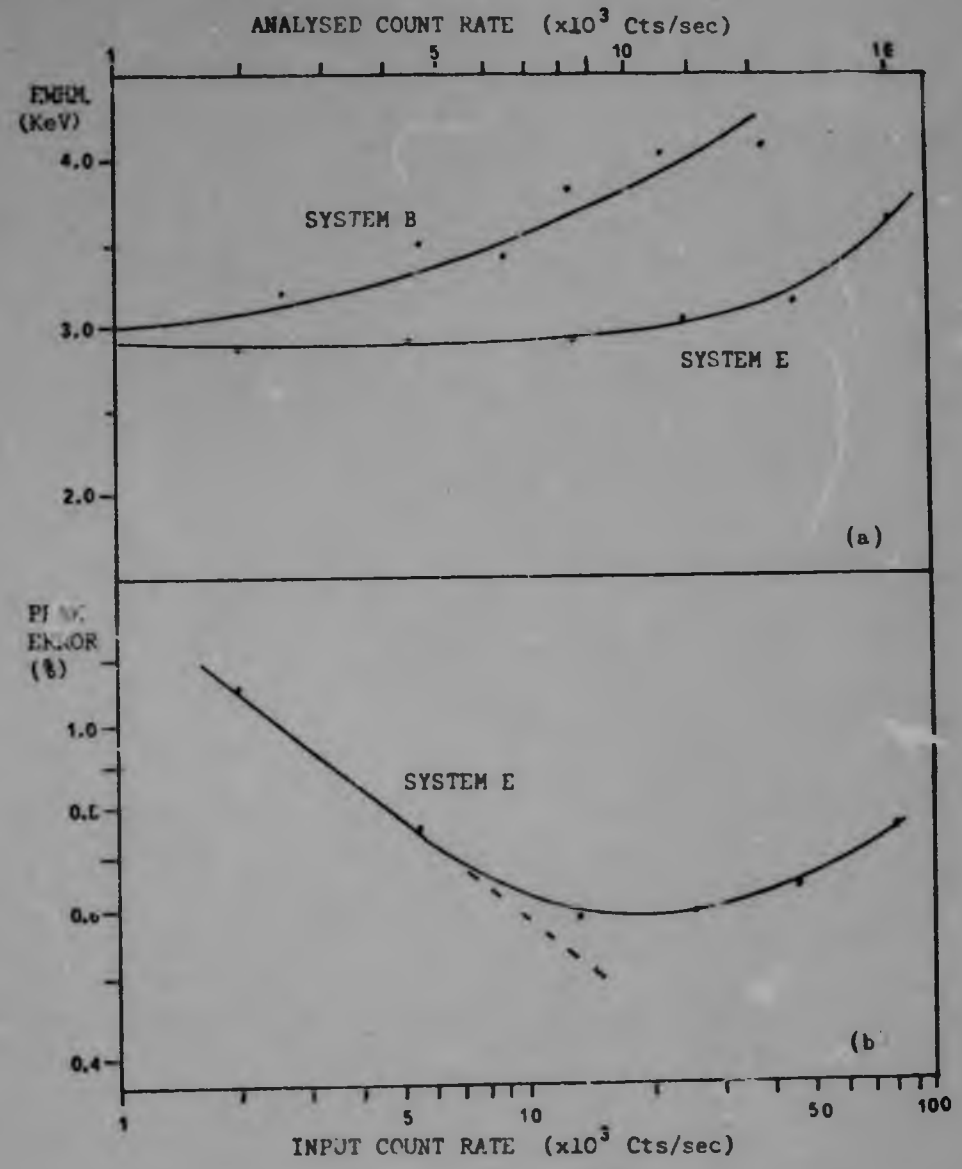


Figure 5.5 COUNT RATE PERFORMANCE OF SYSTEMS B AND E

Note: Details are given for the 1.33 MeV peak of ^{60}Co. Input count rate was measured at 2000 cts/sec and calculated as the source was moved to closer distances.
Analysed count rate was obtained by integrating the analysed spectrum.

(e) Pulse Pile-up

As the count rate increases, the probability that two pulses will coincide and add together is also increased. Therefore at high pulse rates, counts are lost from the peak into the background. This pulse pile-up often negates any improvement that might be obtained from increased count rates.

The purpose of counting at high count rates is to obtain the lowest peak determination error for a given counting period. The effect of pulse pile-up on the determination of the 1.33 MeV peak of ^{60}Co is demonstrated in Figure 5.5 (b). These results show that there is no advantage in increasing the input count rate beyond 20000 cts/sec, as the peak error in fact increases at higher count rates.

Pulse pile-up is also a function of the duration of the pulse. If the pulse length is decreased, the pile up will decrease proportionally, however, other parameters may be adversely affected. Often a choice between pile-up and resolution must be made. The effect of pulse shaping on the resolution is shown in Figure 5.6.

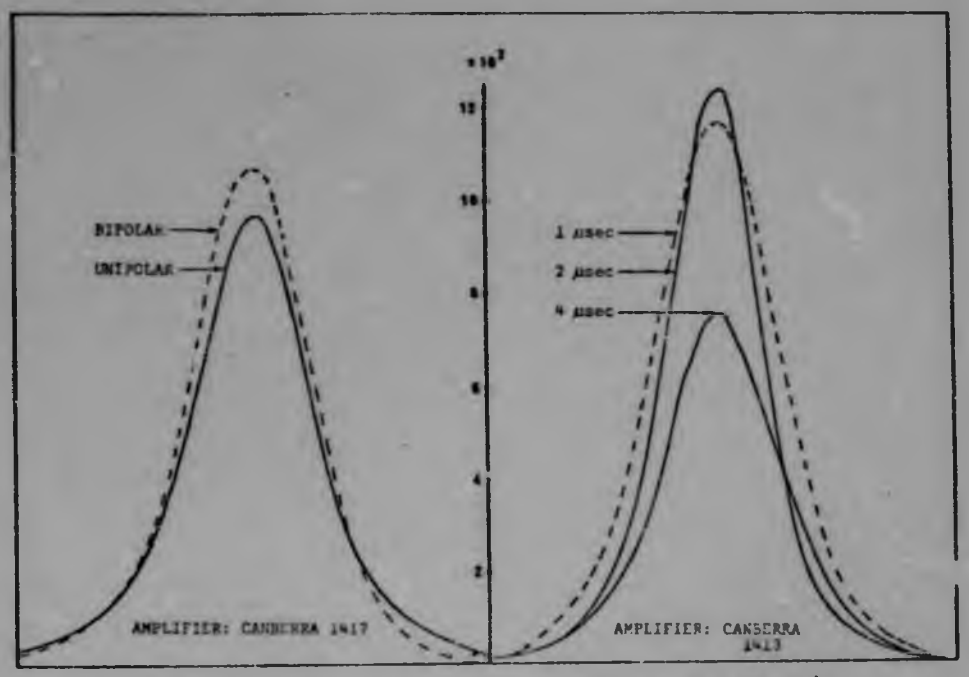
Piled-up pulses are distorted, and can thus be detected and rejected. A system using a pile-up inspection signal, being the sum of a Gaussian pulse and a fraction of its second differential, Sa7l, is used in the Elscint CAV-N-3 amplifier-rejector. Spectra obtained using this unit are given in Figure 5.7.

Although pile-up rejection can be used to 'clean up' spectra, the problem of accurate live timing prohibits the routine application in quantitative gamma spectroscopy.

5.2.3 System Parameters

(a) Linearity

The gamma ray detector and amplifier serve to convert a gamma energy E_γ into a voltage pulse, V where V is proportional to E_γ .



MODE	FWHM	FWθM
Unipolar	3.1	7.2
Bipolar	3.2	6.4

TIME CONSTANT	FWHM	FWθM
1 μsec	3.2	6.3
2 μsec	2.6	5.0
4 μsec	3.2	6.7

Figure 5.6 Peak Degradation at High Count Rates

Notes: Input count rate 40 000 cts./sec.

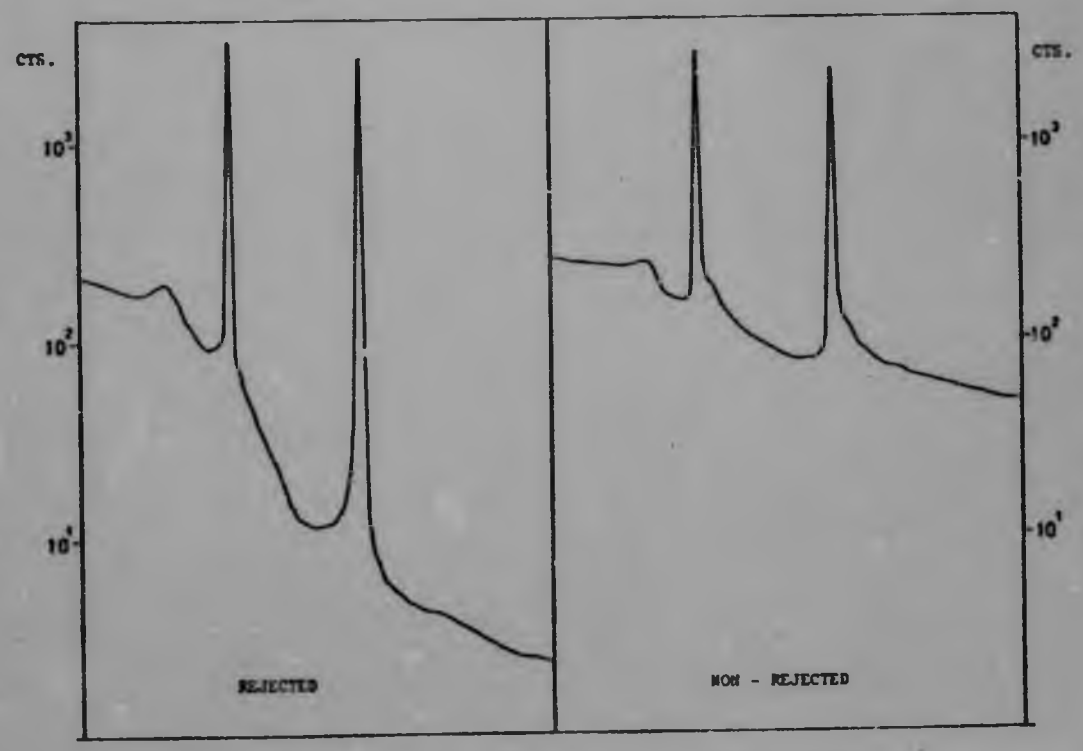


Figure 5.7 Pile-up Rejection Using The Elscint CAV-N-3 Amplifier

Notes: Input count rate 100 000 cts./sec.
Amplifier coupled to system E

The analog to digital converter (A.D.C.) converts the voltage pulse into a digital channel number, C. If the system is perfectly linear, then the channel number will be proportional to the energy, i.e. $C \propto E_\gamma$.

The system linearity can be measured using a series of gamma rays of accurately known energy. The differential linearity of System C is given in Figure 5.8.

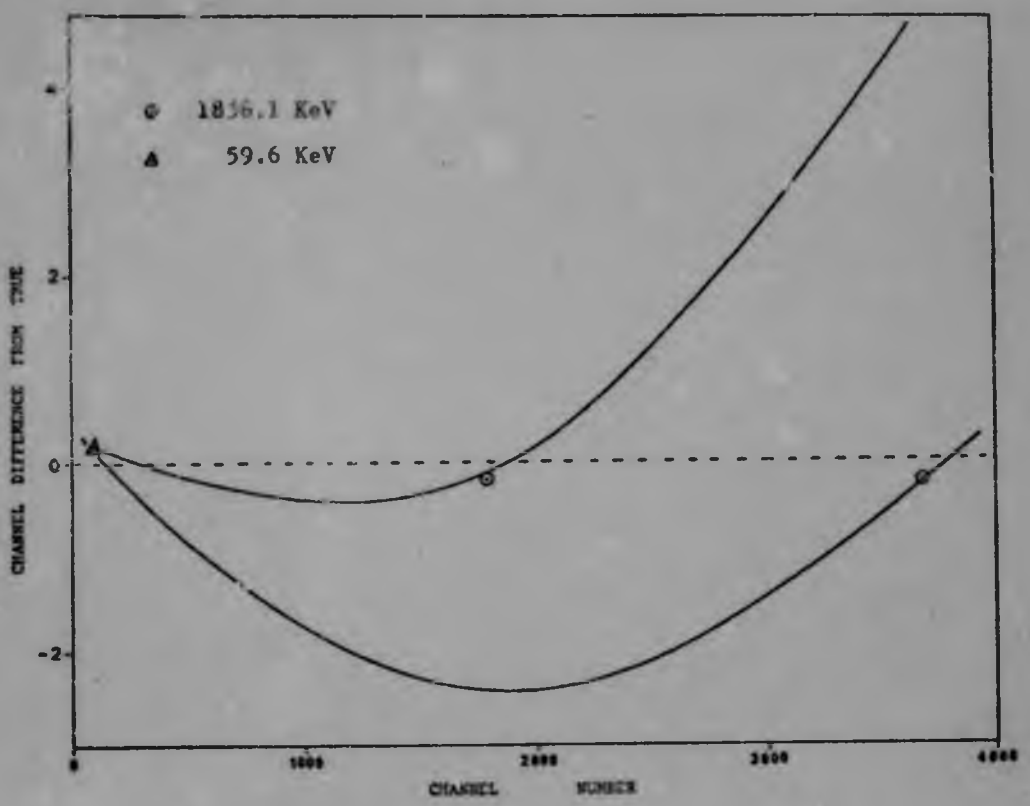


Figure 5.8 DIFFERENTIAL LINEARITY OF SYSTEM C

If the first 2000 channels are used to represent 0 - 2 MeV, the system is correct within this range, to better than 0.5 KeV, but is out by 5 KeV at 4 MeV.

(b) System Dead Time

The system dead time is considered to include any effect which will decrease the peak counts from the true value.

The A.D.C. dead time can be corrected for by using a live timing circuit, but the effect of pulse pile-up is not so easily corrected. A solution could be to inject a pulser of known frequency into the preamplifier. Assuming that the pulser pulses are treated no differently to detector pulses, losses in the pulser peak can be used to correct other gamma peaks, An69 and Bo70.

This method was tested as follows. A ^{137}Cs source was kept at a constant distance from the detector, and the input count rate and hence the pile-up, increased by moving a ^{60}Co source closer to the detector. The pulser 'energy' was kept constant at about 1.8 MeV. The caesium peak counts were found to drop rapidly with increased count rate, but the pulser peak dropped in the same proportion. Thus the ratio of the caesium peak to the pulser peak was constant, and since the number of pulses injected into the system was known, the caesium peak could be accurately corrected, see Figure 5.9.

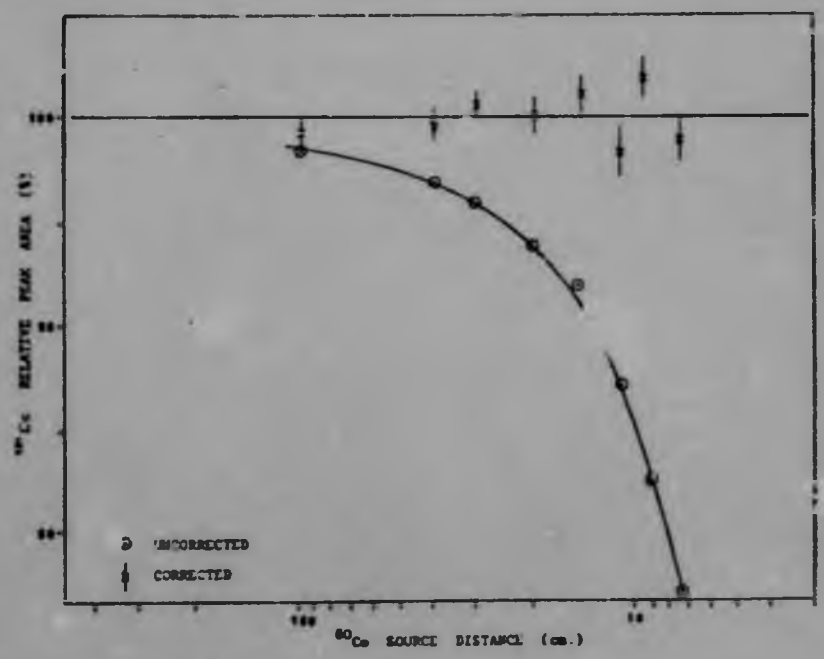


Figure 5.9 DEAD TIME CORRECTION BY PULSER PEAK NORMALISATION

The experiment was repeated, keeping the ^{60}Co source at a fixed distance and varying the ^{137}Cs source. Again, within experimental error, a fixed gamma peak to pulser ratio was obtained.

In order to correct for gain shifts, digital stabilisers were used with systems B', C and E, see Table 5.4. The system is stabilised by a feedback circuit which alters the conversion gain of the A.D.C. to maintain a reference peak in a given channel. The reference peak used is generated by a Canberra 1501 Stabilisation pulser. The peak generated by this 50 Hz pulser is also used to determine the Pulser Peak Correction Factor (P.P.C.F.) used for system dead time correction.

5.3 Discussion

The problems associated with the irradiation of samples are to some extent local in that the reactor used was not designed for Neutron Activation Analysis. Nevertheless, the results obtained and the methods developed are generally applicable.

The geometry errors which arise from the positioning of samples have been largely overcome. The improvements are such that it is now possible to use an automated counting system even at close sample to detector counting distances.

The count rate capability of Ge(Li) detectors is constantly improving. With the increasing availability of fast electronics, the implementation of effective pile-up rejection systems which introduces further problems of system dead time correction, becomes ever more important. It should be noted that the live timing problems of short lived isotope counting have not been investigated. In this respect a system based on Harm's Dead Time Correction Method, Ha67, shows great promise.

6 EXPERIMENTAL PARAMETERS

A number of parameters pertaining to I.N.A.A. can be adjusted to suit the particular requirements of the samples to be analysed.

6.1 Irradiation

6.1.1 Chip Samples

The quartzite and conglomerate chip samples were sufficiently resistant to handling to make their encapsulation unnecessary. They were placed directly into the irradiation cans and irradiated in the hydraulic facility for one hour.

6.1.2 Powdered Samples

Approximately 0.5 g of powdered sample was sealed in a 4 mm internal diameter quartz vial for irradiation purposes. Representative quartzite and conglomerate samples were irradiated for one hour in the hydraulic facility. After irradiation these samples were counted at decay periods ranging from 0.2 days to 60 days. The measured total activity decay curve, normalised to a counting distance of 10 cm, is given in Figure 6.1. From this curve it is possible to predict the irradiation period required to give a suitable level of activity at any decay time.

From an analysis of the optimum decay times for the determination of elements detected in quartzites and conglomerates, it was decided that these samples should be counted for the first time at 4 days decay. Since the handling of samples with an activity greater than 1 r/h on contact introduces radiation hazards, the irradiation period was chosen to produce an induced activity lower than this level at a decay time of 4 days. All the powdered quartzite and conglomerate

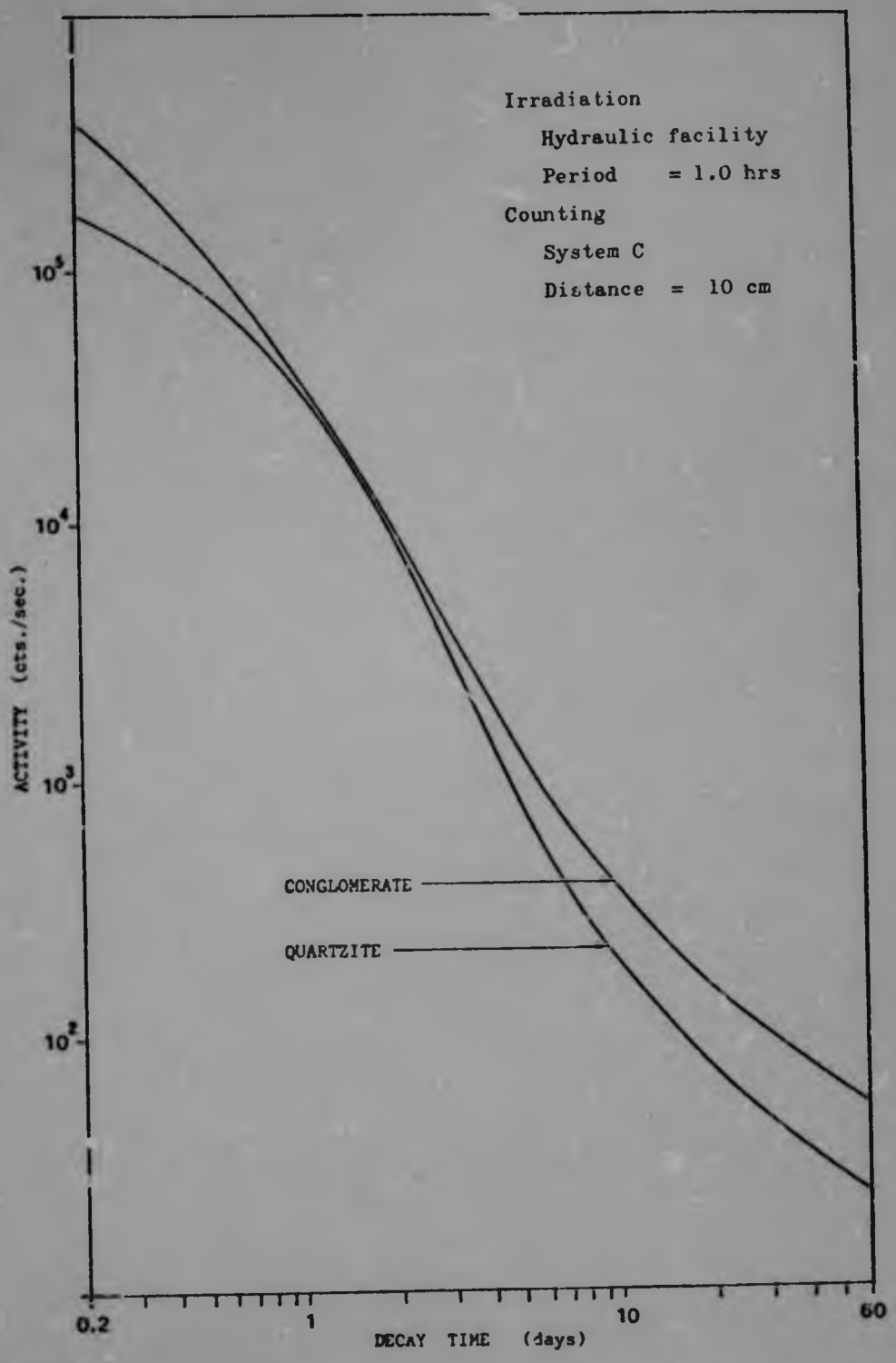


Figure 6.1 TOTAL ACTIVITY DECAY CURVE OF REPRESENTATIVE SAMPLES

samples were therefore irradiated for a period of 5 hours in the hydraulic facility.

6.2 Gamma Counting

The analysis of the chip samples was kept as simple as possible. For this reason the samples were counted only once. A decay time of 10 days was chosen so that both long and some short lived isotopes could be measured. The elements determined and the choice of analytical peaks was based on the information obtained from the preliminary survey samples. The analytical conditions for the analysis of the powdered samples were optimised as follows.

6.2.1 Counting Distance

The sample to detector distance was adjusted in order to obtain a count rate of approximately 5000 cts/sec. At short decay times the samples were counted at 25 cm, while at longer decay times this count rate could not be attained even by placing the sample against the detector face. The error due to sample displacement increases as the sample to detector counting distance in decreased. At 1.5 cm, a typical displacement of 0.3 mm introduces a 2 % error. It was decided that an error greater than 2 % could not be tolerated and the minimum counting distance was therefore limited to 1.5 cm.

6.2.2 Counting Period

The error in the peak area determination is a function of the number of counts in the peak and in the background. In general, if the counting period is increased by a factor of 4, the error in the peak area determination will be halved. Thus the counting period should be as long as possible, but is generally limited by the

necessity of having to count a number of samples within a given period. For this reason the quartzite and conglomerate samples were counted for half hour periods.

6.2.3 Optimum Decay Time

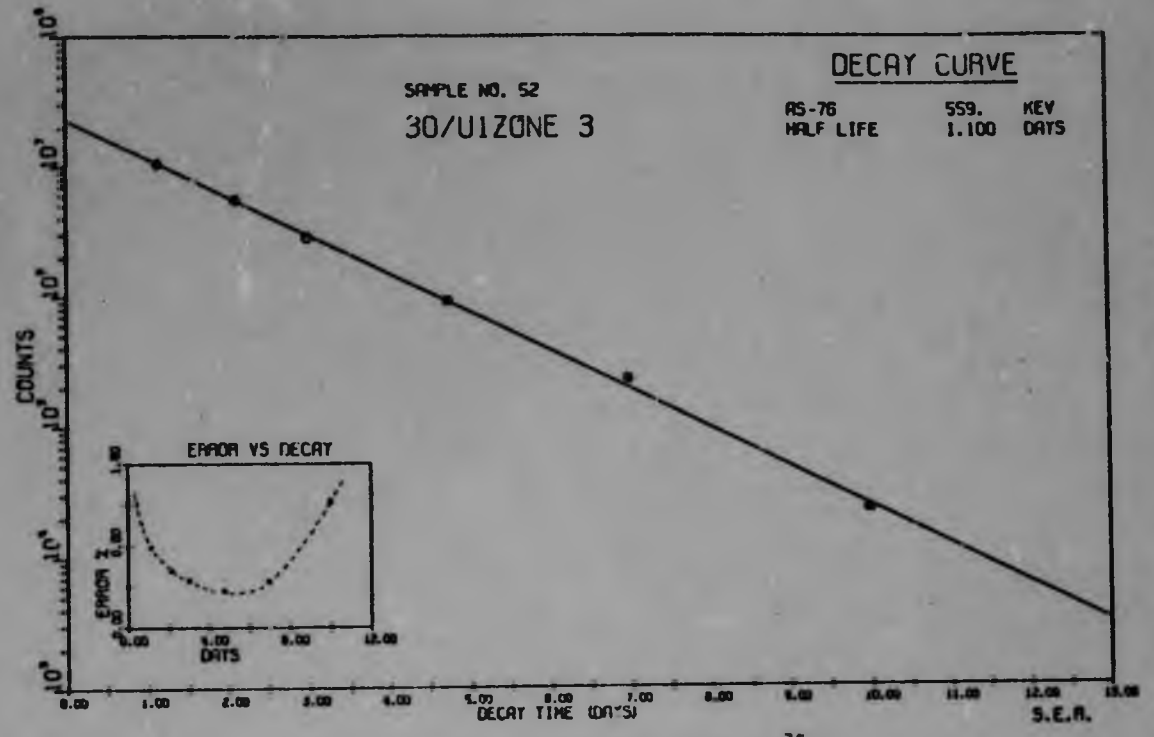
There is no direct method of deciding upon the optimum decay times for the determination of individual elements in multi-element samples. Although computer simulations can be of some help, it was decided to determine the optimum decay times empirically.

Representative quartzite and conglomerate samples were irradiated and then counted at various decay times. The spectra were analysed and peak areas and the errors for the peak area determinations were calculated. The error, normalised for counting period, was then plotted against decay period for selected peaks. Two examples are shown as inserts to Figure 6.2.

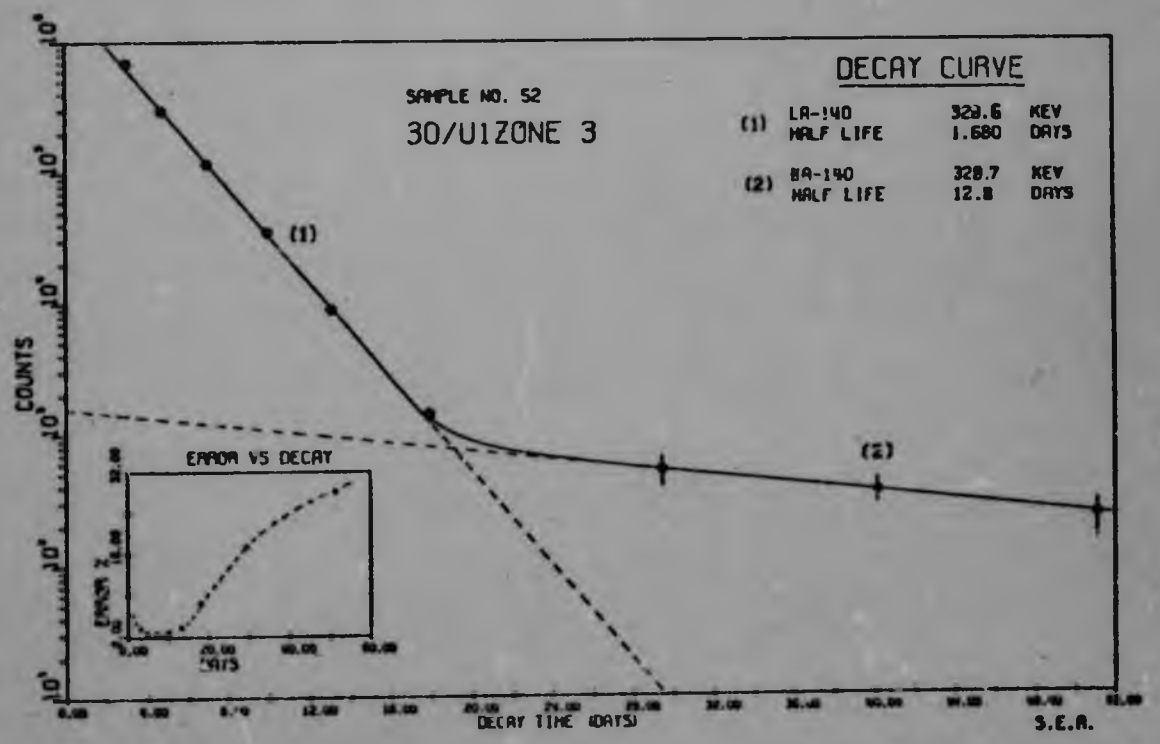
Both of these curves show the same characteristic shape, i.e. a large error which decreases to a fairly broad minimum and then increases. For short lived isotopes, the left side of the curve is truncated because samples were not counted at less than 4 hours decay time. For long lived isotopes, the right side is truncated, and the error remains almost constant with increasing decay time.

The periods for the optimum determination of the isotopes of interest plotted against half-life are shown in Figure 6.3. Short lived isotopes should be determined after decay times of 2 to 4 half-lives, whereas long lived isotopes can be determined at any time after 20 days decay.

In this investigation as many elements as possible had to be accurately determined. Inspection of Figure 6.3 showed that most of the elements could be determined by counting at decay times of



(a) Decay Curve of 559 KeV Peak of ^{76}As



(b) Decay Curve of 328 Kev Peak Showing Interference

Figure 6.2 ACTIVITY AND ERROR DECAY CURVES

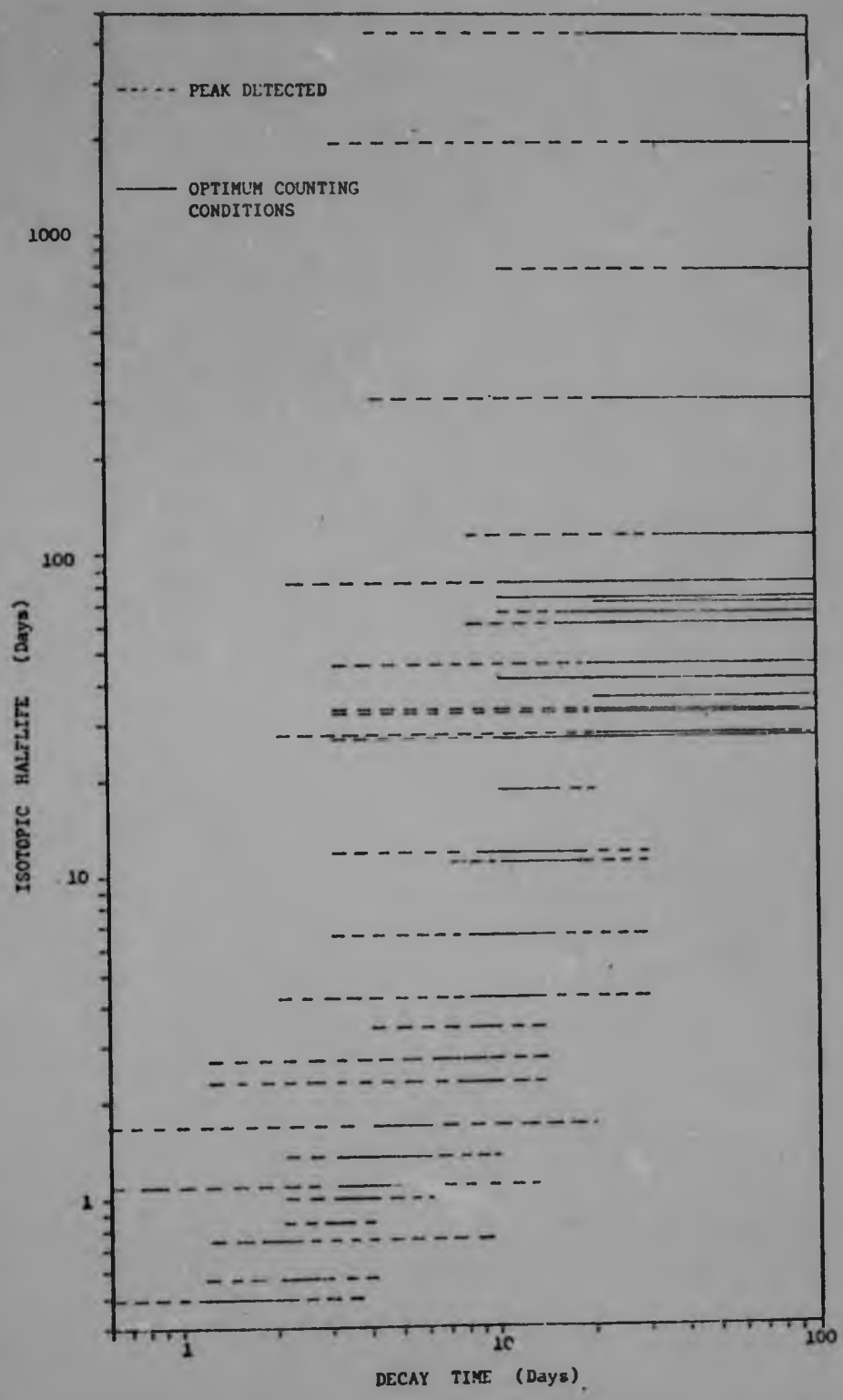


Figure 6.3 OPTIMUM DECAY TIMES

4 days and 30 days. To improve the accuracy of determination of some elements it was decided to make two further measurements, and counting was therefore undertaken at decay times of 4, 10, 20 and 40 days.

6.2.4 Peak Identification

Isotopes can be identified by their half-life and by their characteristic gamma radiation. Generally a number of gamma rays may be emitted with varying probability by a decaying isotope. For example the gamma rays emitted by ^{60}Co and ^{59}Fe are given below together with their branching ratio, viz. the number of gamma rays emitted per disintegration.

ISOTOPE	ENERGY (Branching Ratio) KeV
^{60}Co	1173 (1.0) 1332 (1.0)
^{59}Fe	1098 (0.50) 1292 (0.44) 193 (0.025)
	143 (0.008) 335 (0.003)

A preliminary isotope assignment was made for each peak on the basis of known gamma energies from published data, Da68. These assignments were checked by confirming the presence of all the major peaks from a particular isotope, and verifying that the peak ratios agreed with the published values of the branching ratios. As a final check, decay curves of selected peaks were plotted, and their half-lives calculated, see Figure 6.2. A list of isotopes, analytical peaks, and the decay times at which the peaks were measured is given in Table 6.1.

Table 6.1 ELEMENT COUNTING SCHEME

ISOTOPE	HALF-LIFE Days	E_γ KeV	DETERMINED AT: 4 Days	10 Days	20 Days	40 Days
^{42}K	0.51	1525	*			
^{72}Ga	0.60	834, 630	*			
^{24}Na	0.63	1732, 1368	*			
^{187}W	1.0	686	*			
^{76}As	1.1	657, 559	*			
^{143}Ce	1.38	293	*			
^{140}La	1.68	1596, 329	*			
^{239}Np	2.35	278, 228	*			
^{198}Au	2.7	412	*			
^{47}Sc	3.4	160		*		
^{175}Yb	4.2	396		*		
^{177}Lu	6.7	208		*		
^{131}Ba	11.3	496		*		
^{147}Nd	11.0	531			*	
^{86}Rb	18.7	1078			*	*
^{233}Pa	27.0	312, 300			*	*
^{51}Cr	27.8	320			*	*
^{169}Yb	32.0	198, 177			*	*
^{141}Ce	32.5	145			*	*
^{181}Hf	42.1	482, 133			*	*
^{59}Fe	45.1	1292, 1099			*	*
^{124}Sb	60.9	1691			*	*
^{95}Zr	65.0	756, 724			*	*
^{58}Co	71.3	810			*	*
^{160}Tb	72.1	879			*	*
^{46}Sc	83.9	1120, 889			*	*
^{182}Ta	115.1	1222			*	*
^{54}Mn	303	835			*	*
^{134}Cs	748	796			*	*
^{60}Co	1920	1332, 1173			*	*
^{152}Eu	4453	1408			*	*

6.2.5 Peak Interferences

Gamma spectra of multi-element samples are often so complex that there may be more than 100 peaks in the range 0.1 - 2.0 MeV. Instrumental N.A.A. approaches the problem of complex spectra by using high resolution detectors and mathematically correcting for overlapping peaks that cannot be fully resolved.

(a) High resolution detectors

When radiochemical separations are employed, NaI(Tl) detectors can often be satisfactorily used, but for I.N.A.A. it is usually necessary to utilise the improved resolution offered by Ge(Li) detectors, see Section 4.6.

In certain applications a small volume planar Ge(Li) detector can be used. This type of detector offers a considerable improvement in resolution over that of a large volume coaxial type detector. (The resolution at 122 KeV would be typically 600 eV as compared to 1800 eV.) Unfortunately, small volume planar detectors are only of use in the low energy region, say < 200 KeV, because of the steep efficiency-energy curve of Ge(Li) detectors, see Figure 5.2.

Spectra of a quartzite sample measured using a 40 cm^3 coaxial detector (System E in Table 5.4) and a 1 cm^3 planar detector (System D) are shown in Figure 6.4. Some interferences are resolved, but the region below 120 KeV is still too complicated to obtain quantitative results.

The peaks in this energy range are from X-rays as well as gamma rays. X-rays are produced when an isotope decays by electron capture and the outer electron configuration is re-arranged to suit the new nucleus. In addition, the X-rays are produced by X-ray fluorescence which occurs whenever there are any strong gamma

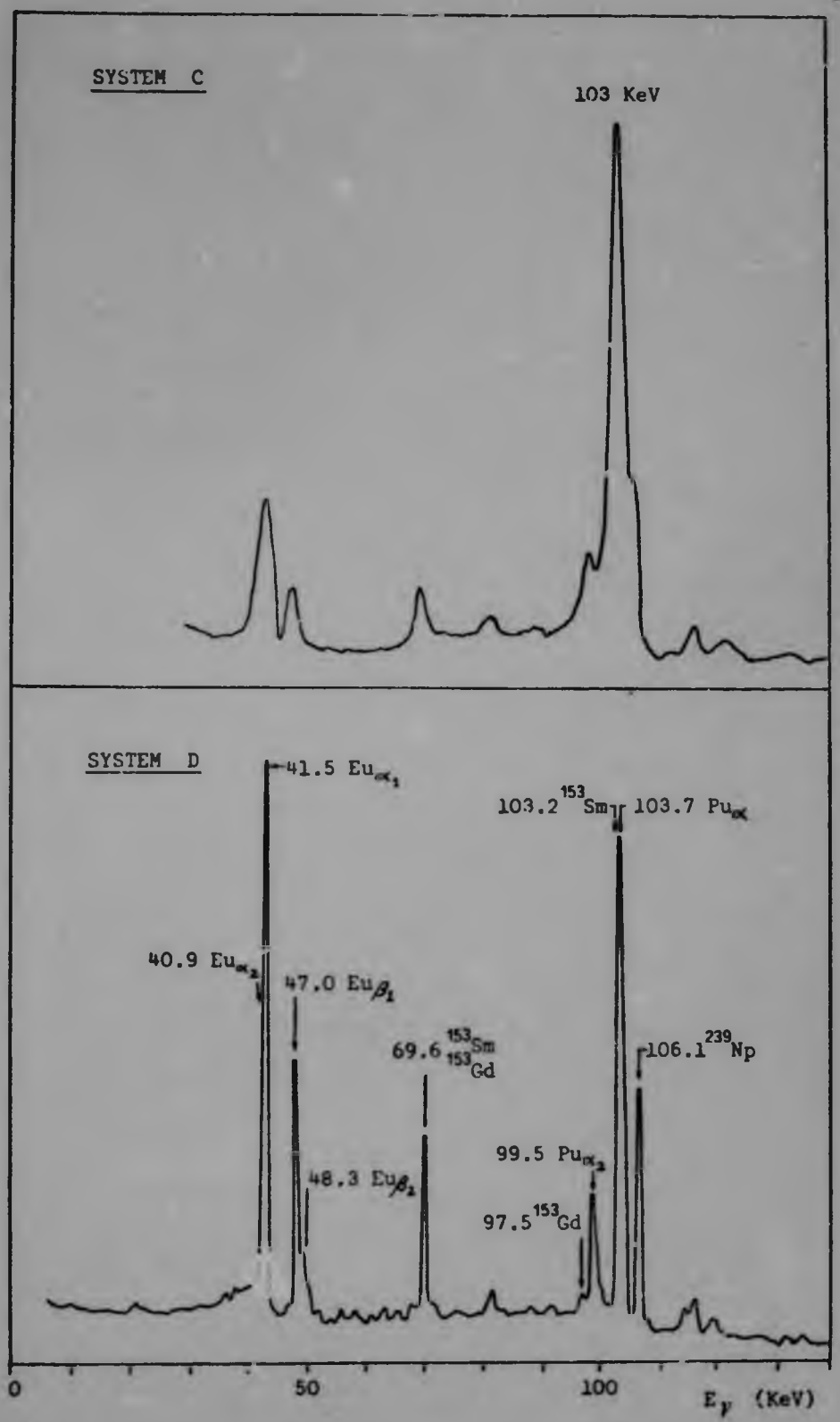
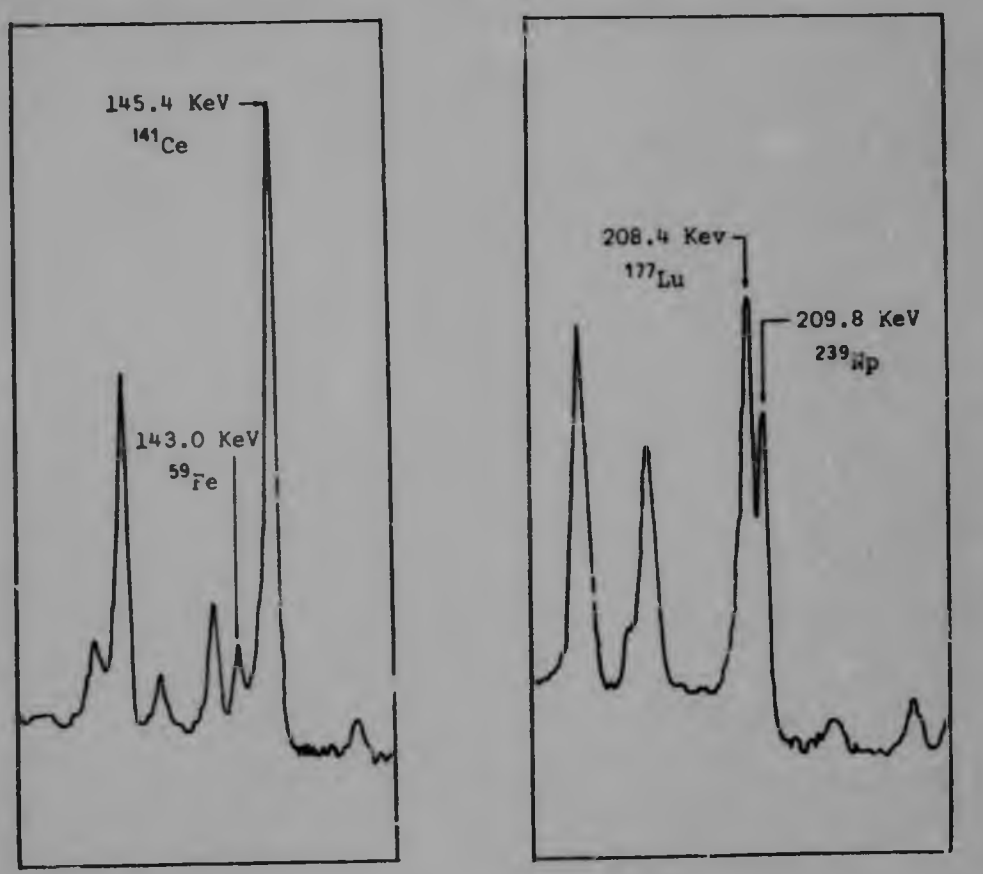


Figure 6.4 COMPARISON OF NORMAL AND HIGH RESOLUTION COUNTING SYSTEMS

lines near an absorption edge, which is unfortunately a frequent occurrence. Even with all these problems, X-ray spectroscopy has been applied in Activation Analysis with some success by Mantel and Amiel, Mn72, and Pillay and Miller, Pi68.

Although interferences can often be resolved using a high resolution detector, as in Figure 6.5 (a), some interferences can still not be resolved, such as the Np-Lu doublet at 209 KeV, as in Figure 6.5 (b).



(a) Cerium - Iron Interference (b) Lutetium - Uranium Interference

Figure 6.5 PEAK INTERFERENCES IDENTIFIED USING A HIGH RESOLUTION DETECTOR

(b) Decay curve analysis

When the interfering isotope has a half-life which differs by at least a factor of two from that of the isotope of interest, the level of interference can be determined quantitatively from a decay curve analysis.

An example of the interference of ^{140}La ($T_{\frac{1}{2}}$ = 1.68 days) with the longer lived ^{140}Ba ($T_{\frac{1}{2}}$ = 12.8 days) is given in Figure 6.2 (b). From this curve it is estimated that ^{140}La can be determined on or before 7 days decay with less than 1 % interference from ^{140}Ba. Similarly ^{140}Ba can be determined after 30 days decay with less than 1 % interference from ^{140}La.

The ^{54}Mn ($T_{\frac{1}{2}}$ = 303 d) interference on ^{72}Ga ($T_{\frac{1}{2}}$ = 0.59 d) has been corrected for by subtracting the ^{54}Mn contribution at a decay time of 4 days by back extrapolation from the determination of ^{54}Mn at 20 and 40 days.

(c) Peak fitting

If peak areas are determined by least squares fitting of suitable peak shapes, then the presence of interferences can often be detected from inspection of the residuals. By fitting two or more components, the interference can be quantitatively determined. Although this method is computationally slow, it is considered to be the most accurate method of correcting peak interferences.

(d) Branching Ratio corrections

Once an interference has been identified, corrections can be applied if the interfering isotope has another peak which can be accurately determined. The magnitude of the interference is estimated from the non-interfered peak and a knowledge of the branching ratios.

In practice the peak ratios were determined from pure element spectra, and so both the branching ratio and the relative detector efficiency could be determined simultaneously. The interferences corrected for using this method are listed in Table 6.2.

Table 6.2 PEAK INTERFERENCES CORRECTED USING BRANCHING RATIOS

PEAK DETERMINED			INTERFERENCE			
ISOTOPE	HALF-LIFE (days)	ENERGY (KeV)	ISOTOPE	HALF-LIFE (days)	ENERGY (KeV)	NON-INTERFERED PEAK ENERGY (KeV)
^{177}Lu	6.8	208	^{239}Np	2.4	210	228
^{233}Pa	27	300	^{160}Tb	72	299	879
^{141}Ce	33	145	^{59}Fe	45	143	1099
^{46}Sc	84	1120	^{182}Ta	115	1121	1222

6.2.6 Reaction Interferences

(a) (n , p) and (n , α) Reactions

Most reactor activation reactions are (n , γ) reactions on isotope ^{m-1}Z which produce the isotope ^{m}Z. This same isotope can be produced by $^{m}Z + 1$ (n , p) ^{m}Z or by $^{m+3}Z + 2$ (n , α) ^{m}Z. Thus the presence of elements of atomic number $Z + 1$ and $Z + 2$ can interfere with the determination of element of atomic number Z.

The level of interference is a function of the relative concentrations of the target nuclei, the fast to thermal neutron flux ratio, and the ratio of the reaction cross sections. In general the magnitudes of these reaction cross sections are as follows:

$$\sigma(n,\gamma) \gg \sigma(n,p) > \sigma(n,\alpha)$$

Thus fast neutron reactions will only cause serious interferences when the concentration of element of atomic number Z is considerably less than that of either $Z + 1$ or $Z + 2$.

A short list of possible interfering reactions is given in Table 6.3.

Table 6.3 INTERFERING REACTIONS

ELEMENT	PRIMARY REACTION	INTERFERING REACTION
Sodium	^{23}Na (n , γ) ^{24}Na	^{24}Mg (n , p) ^{24}Na
Potassium	^{41}K (n , γ) ^{42}K	^{42}Ca (n , p) ^{42}K
Scandium	^{45}Sc (n , γ) ^{46}Sc	^{46}Ti (n , p) ^{46}Sc
Titanium	^{47}Ti (n , p) ^{47}Sc	^{46}Ca (n , γ , β^-) ^{47}Sc
Chromium	^{50}Cr (n , γ) ^{51}Cr	^{54}Fe (n , α) ^{51}Cr
Cobalt	^{59}Co (n , γ) ^{60}Co	^{60}Ni (n , p) ^{60}Co
Gallium	^{71}Ga (n , γ) ^{72}Ga	^{72}Ge (n , p) ^{72}Ga

The interference from magnesium on the determination of sodium has been detected in ultra basic rocks such as the U.S.S.R. standard DTS-1. The sodium content was determined at 0.030 % instead of the reference value of 0.007 %. In this rock type, a dunite, the magnesium content is 28.8 %, which is 4000 times the sodium level.

The production of ^{47}Sc is somewhat anomalous in that the (n , p) reaction on titanium is more sensitive than the (n , γ , β^-) reaction on calcium. The main reason for this is the extremely low abundance of the ^{46}Ca isotope, namely 0.0033 %, compared to that of ^{47}Ti , 7.3 %.

The parent isotope of ^{47}Sc can be identified by inspection of the decay curve. ^{47}Ca (n , γ) ^{47}Ca (β^-) ^{47}Sc is a typical mother-daughter reaction in which the ^{47}Sc activity shows a maximum at 5.6 days. The titanium (n , p) reaction decay curve, on the other hand, is linear with log activity. Inspection of the ^{47}Sc decay curve from the conglomerates and quartzites showed ^{47}Ti to be the parent isotope in these samples.

(b) Fission reaction

Even small amounts of fissionable material can cause significant and often unexpected errors. In geological material, particularly the uranium-rich sediments of the Witwatersrand System, the presence of fissionable material can introduce errors in the determination of elements with masses ranging from 90 to 160.

The ratio of the activity induced by fission to that by the corresponding (n , γ) reaction for equal masses of uranium and element x is given by: (DS72)

$$\frac{I_x(n,f)}{I_x(n,\gamma)} = \frac{A_x \quad Y_x \quad 4.18}{238 \quad \theta_x \quad \sigma(n,\gamma)}$$

where:

A_x = Atomic mass of isotope x
θ_x = Isotopic abundance of x
Y_x = Fission yield of x
σ = Cross section for (n , γ) reaction

This ratio is tabulated in Table 6.4 for all isotopes determined within the uranium fission mass region.

Table 6.4 FISSION INTERFERENCES

ISOTOPE	RATIO	ISOTOPE	RATIO
^{86}Rb	0.59	^{134}Cs	0.0065
^{95}Zr	8.4	^{140}La	0.016
^{99}Mo	3.2	^{143}Ce	1.4
^{103}Ru	0.14	^{149}Nd	0.18
$^{131}Ba^{\dagger}$	7.2	^{153}Sm	0.0001
^{124}Sb	0.0003	^{160}Tb	0.00003

† ^{131}Ba is not a uranium fission product but has an interference from the fission product ^{103}Ru at 496 KeV. The ratio given is for ^{103}Ru

fission production to $^{130}Ba\ (n, \gamma)\ ^{131}Ba$ production.

Fission product interference was found to be important for the following elements: Zr, Mo, Ru - Ba (see † above) and Ce.

The equivalent concentration yield of each of these elements was determined from the irradiation of pure uranium samples, and suitable corrections were applied to each element. The interferences were most severe in powdered conglomerate samples from Zone 2, which contained approximately 100 ppm uranium. All the molybdenum and a large fraction of the zirconium determined in samples from this zone were found to be of fission origin.

6.3 Discussion

The reactor used for all the irradiations is situated some 70 km from the laboratory in which this work was undertaken. It was therefore not possible to undertake analyses of short lived isotopes.

The samples were counted at decay times ranging from a few hours to 60 days, during which the total activity was found to decrease by four orders of magnitude. It would be sensible to undertake multiple irradiations and optimise irradiation conditions for elements of similar half-life, if samples could be more conveniently irradiated. For example, an irradiation period of 50 to 100 hours would be suitable for the determination of the long lived isotopes such as Sb, Co, Eu etc., while for short lived isotopes such as K and Ga, an irradiation of 1 hour would have been sufficient.

Peak interferences have in general been corrected by applying knowledge of the gamma branching ratios. The technique of multi-component peak fitting is regarded as superior, but rapid methods of least squares fitting are required before this technique can be routinely applied.

The improvement in the resolution of Ge(Li) detectors offers some hope of separating peak interferences, particularly in the low energy region.

The severity of fast neutron reaction interferences can be solved by irradiating samples in a well thermalised flux. In this respect there may be some advantage in using special graphite irradiation containers. In some cases the thermal neutron reactions interfere with fast neutron reactions. This problem can be alleviated by using in-core irradiation positions and cadmium shielded containers. For samples containing fairly large quantities of uranium, these measures may still be insufficient, and a pre-irradiation separation of the uranium may be necessary.

7 ERRORS ASSOCIATED WITH I.N.A.A.

I.N.A.A. is still a relatively new technique and should perhaps be considered more a research technique than a standard laboratory method. As such it is important to know what errors can arise in the technique and how to minimise their effects.

7.1 Sampling

7.1.1 Representative Sampling

Errors due to sampling are not confined to I.N.A.A. alone. The problem arises when, for example, a complete rock cannot be analysed but only a small homogenised portion. Such a sample may or may not be representative of the whole. The problems of sampling have been discussed extensively by Griffiths, Gr71. Nicholls, Ni71, shows that for a 1 mg subsample taken from powdered material of average homogeneity, a sampling error of 5 % could be expected, for an element present at the 1 % level.

The powdered samples used in these experiments weighed from 0.2 g to 0.8 g. For this sample size, sampling errors will only be apparent for extremely inhomogeneously distributed elements. Such an error is detectable in the case of gold, which is known to be very inhomogeneous in its distribution.

7.1.2 Sample Preparation

Errors can arise from sample contamination during pulverisation. The precautions adopted to avoid contamination of the samples have been discussed in Section 3.2.

The sample weight is obtained by weighing the quartz vial before and after filling with powdered sample. Weighing errors are estimated at 0.01 % (i.e. 0.x0000 $\pm$ 0.0000x).

A more significant error can occur when the vials are heat-sealed, which may result in the loss of some of the more volatile elements, e.g. Sb.

The vial itself contains impurities and a blank should be included in each analytical run. The quartz vials used for these experiments showed some impurities, but at very low levels.

An analysis of a quartz vial, contaminated with reactor pool water during irradiation is given in Table 7.1.

Table 7.1 ANALYSIS OF CONTAMINATED QUARTZ VIAL

Au	0.001	Zr	2.7
Th	0.025	Fe	16
Na	2	Sc	0.001
La	0.012	Cr	0.1
Eu	0.007	Co	0.01
Yb	0.01	As	1.6
		Sb	0.035

Note: All determinations are expressed in ppm.

These values can be considered as an upper limit since in practice all samples were washed in DECON 75 before counting, to remove any possible contamination.

7.2 Irradiation

The major error associated with the irradiation is still the accurate monitoring of the neutron flux received by each sample. This fact has been realised by other workers, for example Bruninx, Bx72.

As discussed earlier, iron foil monitors provide an accurate estimate of the average neutron flux received by each sample, but only at the two neutron energies monitored by iron. Iron flux factors are a very accurate method for correcting the iron values determined in each sample, but are not necessarily accurate for all other elements. Different elements have different excitation functions, see Figure 4.2, and in principle require different monitors. To be strictly accurate, only the element to be determined should be used as a neutron flux monitor. This problem has been recognised by Girardi Gi65, who proposed the use of a 'k value' determined for each irradiation position.

The error in the determination of the neutron flux factor using iron foil monitors is estimated at less than 0.7 %.

7.3 Gamma Counting

7.3.1 Geometry Errors

The error in accurately and reproducibly positioning the sample in front of the detector can be surprisingly large. For example, at a distance of 10 cm, a displacement error of 1 mm horizontally, along the axis of the detector, introduces a 2 % error, while at 1.0 cm, the corresponding error would be 7 %, see Figure 7.1 (a).

The displacement error associated with hand-positioning a sample in a machined perspex holder was estimated at 0.3 mm. This was deduced from a measured error of 1.2 % for repeated counting of an iron foil sample positioned 3 cm from the detector.

In addition to the horizontal displacement error, a displacement of the sample vertical to the axis of the detector will also introduce an error. The magnitude of the error will vary with sample size and distance, but observations taken using a 2.5 cm high source at a distance of 1.5 cm showed a 1 % error for a 4 mm vertical displacement, which increased to 4 % for an 8 mm displacement, see Figure 7.1 (b).

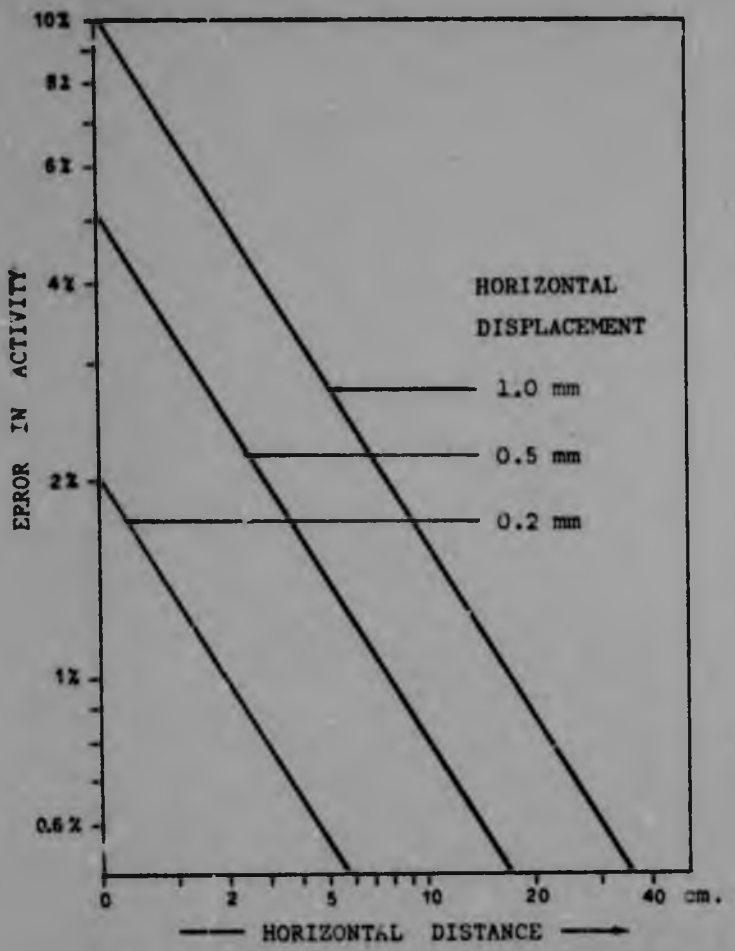


Figure 7.1 (a) Horizontal Displacement

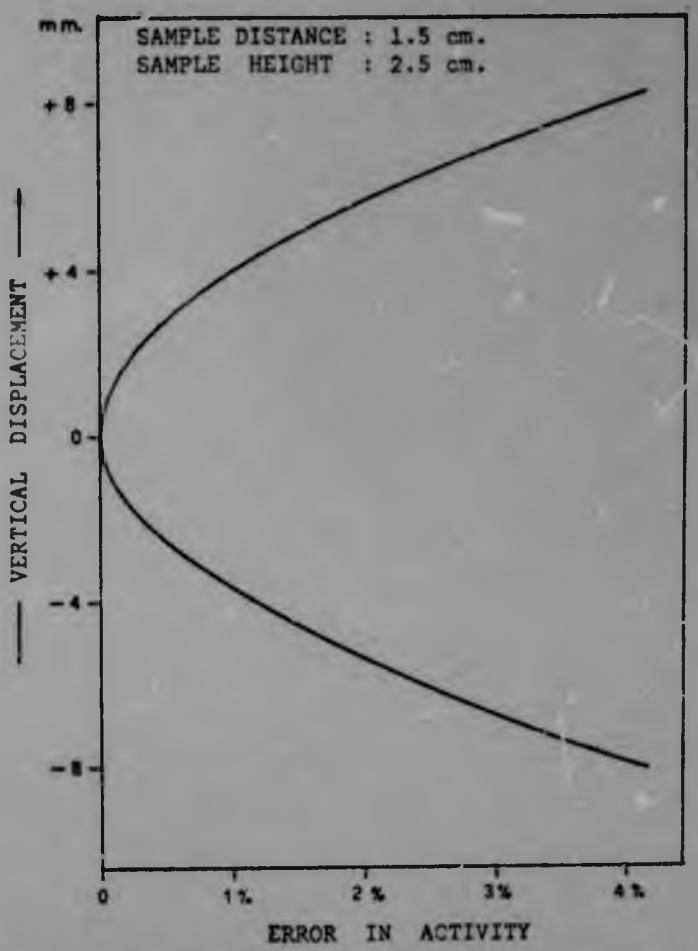


Figure 7.1 (b) Vertical Displacement

Figure 7.1 SAMPLE DISPLACEMENT ERRORS

When counting powdered sample material, the vertical displacement error can become significant. Care should always be taken to ensure that all the powdered material is settled at the bottom of the vial in order to maintain a constant sample height.

To minimise both the horizontal and vertical displacement errors, a special sample holder was designed to both rotate and agitate the sample during counting. The reduction in geometry errors using this sample holder was measured by repeated counting of a single powdered sample. At a counting distance of 1.5 cm, the error was reduced from 1.0 % to 0.5 % (Bi73). This residual error corresponds to a horizontal displacement error of less than 0.1 mm, or a vertical displacement error of 2 mm.

The major advantage of this type of sample holder is that it is operator-independent. The design of the holder nas been very successfully incorporated in an automatic sample changer, Za73.

Rotating an inhomogeneous sample during counting can considerably reduce the analytical error. An extremely low activity diamond sample, containing an active mineral inclusion, was repeatedly counted at a distance of 1.3 cm from the detector. Random positioning of the sample resulted in a C.O.V. of .8 %. On rotating the sample this error was reduced to 0.6 %.

By the careful positioning, rotation and agitation of powdered samples during counting, the geometry errors can be kept below 1 %, for samples counted at distances up to 1.0 cm from the detector face.

7.3.2 Distance Correction

Samples counted at different distances have been compared by using a modified $1/r^2$ law. The determination of the interaction depth ΔR requires a very accurate experiment. It is estimated that the error in the determination of ΔR is at least 5 %. This produces an error of 3 % for a distance correction from 1.5 cm to 15 cm.

7.3.3 Dead Time Correction

At count rates above 2000 cts/sec the accuracy of gamma counting depends on the accuracy of the system dead time correction. The pulser method used, An69, is considered to be accurate to approximately 1 %, up to count rates of 20 000 cts/sec. Above this count rate the pulser frequency of 50 Hz is too low and inaccuracies arise in the determination of the pulse peak area. If the pulser frequency is fixed at too high a rate, the pulse distribution will no longer be random, and the correction factor no longer valid. An optimum figure would be a pulser rate of from 1 % to 5 % of the total count rate, Wi71.

The correction factor calculated from the pulser peak assumes a known pulser frequency. The Canberra 1501 Pulser used triggers from the a.c. line and thus any variations in the line frequency will cause an error in the P.P.C.F. No shift from 50 Hz has been experimentally detected, to within an accuracy of 1 %.

7.3.4 Spectrum Analysis

The largest errors associated with I.N.A.A. are found to arise in the determination of peak areas by computer analysis. Of the several methods available to locate peak boundaries and to determine peak areas, not one can be used to analyse accurately all possible peak shapes and backgrounds that occur. An analysis of all peaks that were visible in the gamma spectra of a quartzite sample counted at 4, 10, 20 and 40 days, is given in Table 7.2.

Only 6 % of the peaks had errors less than 1 %, while 42 % had errors greater than 15 %. A significant advance in the precision obtainable with multi-element I.N.A.A. will be made only when peak areas can be determined more accurately.

Table 7.2 FREQUENCY GROUPING OF PEAK DETERMINATIONS AT DIFFERENT DECAY TIMES

PEAK ERROR	DECAY TIME			
	4 DAYS	10 DAYS	20 DAYS	40 DAYS
< 0.5 %	0	0	0	1
0.5 % - 1.0 %	4	4	3	4
1.0 % - 5.0 %	10	16	14	14
5.0 % - 15.0 %	18	22	18	19
> 15.0 %	22	31	26	24
TOTAL NUMBER OF PEAKS:	54	73	61	52

Associated with peak area determination is the problem of peak interferences. The best solution at present appears to be that of fitting one or more Gaussian shaped curves to the complex peak. This is computationally slow and thus cannot be routinely applied.

7.3.5 Decay Correction

When counting samples at various decay periods it is often necessary to apply decay corrections. Half-lives of many isotopes are not known to better than 1 %, which can introduce large errors. For example, assuming a 1 % error in the half-life determination of ^{76}As, an error of 6 % arises when correcting between samples analysed at decay periods of 2 days and 8 days.

The error in the correction factor is given as a function of the ratio of decay period to half-life in Figure 7.2, for three values of the error in the half-life.

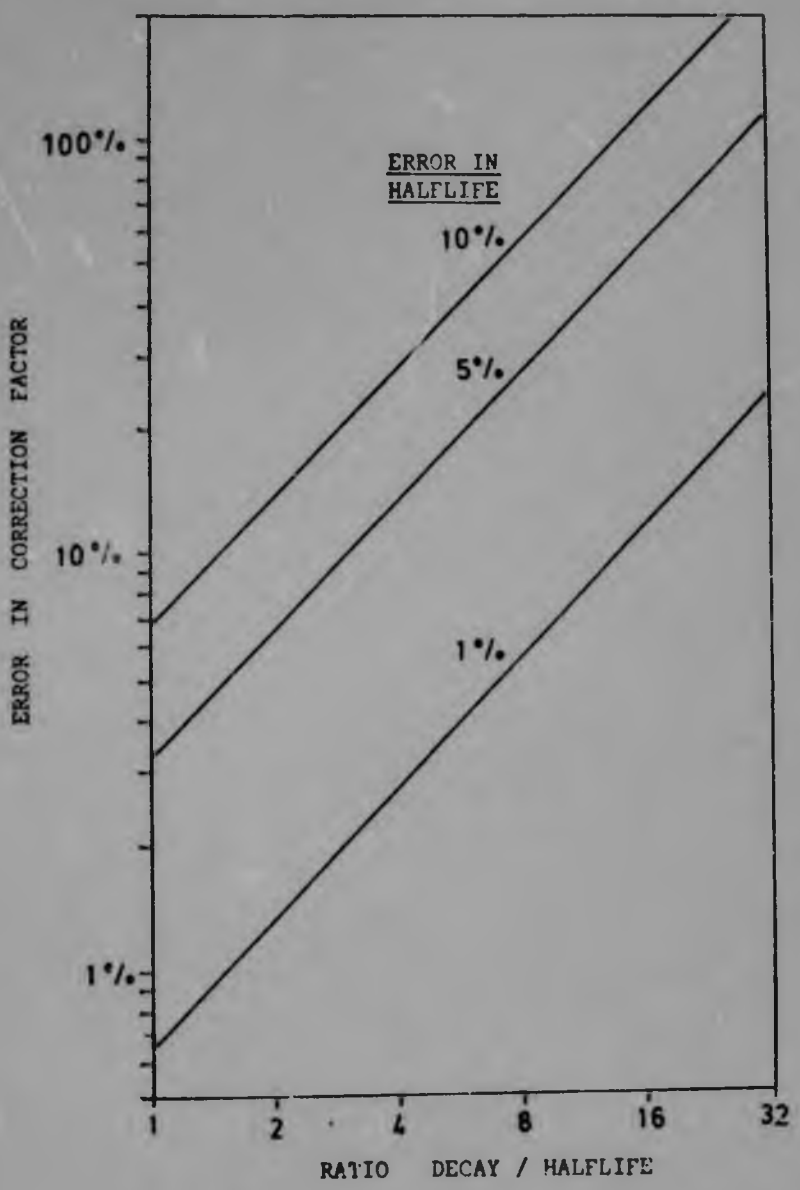


Figure 7.2 ERROR IN HALFLIFE CORRECTION FACTOR

7.4 Standardisation

Virtually all the errors discussed so far will affect the precision obtainable with I.N.A.A. Accuracy, however, depends on the use of well-determined standard reference materials.

The preparation of artificial standards has not proved to be very satisfactory for concentrations in the parts per million range. For this reason, international rock standards are widely used for trace element analyses. Of those available, the U.S.G.S. standards are considered to be the best. The fact that they are the best does not however imply that they are well-determined. Table 7.3 shows the range of determinations for a series of 19 major, minor and trace elements taken from Flanagans compilation. (F168)

Table 7.3 RANGE OF ELEMENT DETERMINATIONS FOR FOUR U.S.G.S. STANDARDS

ELEMENT	G-2	GSP-1	BCR-1	DTS-1
U	1.3 - 3.4	0.2 - 2.7	1.2 - 2.2	0.003 - 0.004
Th	22 - 30	99 - 125	5.5 - 15	-
Na	2.4 - 3.2	1.7 - 2.2	1.5 - 2.5	0.006 - 0.08
K	3.9 - 4.8	2.6 - 5.7	1.4 - 3.2	0.001 - 0.4
Ba	1500 - 3000	855 - 2000	480 - 1230	-
Rb	108 - 513	200 - 690	45 - 150	-
Cs	1.1 - 2.0	0.8 - 3	0.9 - 1.6	0.02 - 0.05
La	76 - 250	160 - 450	22 - 36	-
Ce	144 - 180	350 - 800	40 - 53	-
Yb	0.8 - 1.2	2 - 3	3.0 - 5.5	-
Fe	1.5 - 2.1	2.8 - 3.4	9.0 - 10.0	6.0 - 7.8
Sc	2 - 10	6 - 22	30 - 50	2 - 5.3
Cr	5 - 29	5 - 18	8 - 45	2840 - 5560
Co	5 - 21	3 - 22	29 - 60	96 - 200
Ni	7 - 14	3 - 25	3 - 30	1770 - 3300
Sb	0.015 - 0.06	1.4 - 4.1	0.3 - 0.6	0.4 - 0.5
Ti	0.2 - 0.5	0.4 - 0.5	1.1 - 1.4	0.002 - 0.19
Zr	250 - 400	323 - 685	144 - 275	-
Hf	6.1 - 8.4	9.7 - 15	3.3 - 5.4	-

The relative errors vary from 10 % for iron in BCR-1 to over three orders of magnitude for potassium in DTS-1. Thus the correct value for any particular element is difficult to determine and the choice should be based on experience and knowledge of the techniques involved, and should not simply be a mean value of many determinations. This point has been discussed in detail by Abbey, Ab70.

7.5 Experimental Precision

In order to determine to what level of precision the analytical technique had been developed, a series of 23 replicate quartzite samples was analysed.

These samples were irradiated in two batches. The first 12 samples were irradiated simultaneously for 5 hours, while the remaining 11 samples were irradiated individually for 5 hours each over a period of 2 days.

The neutron flux received by each sample was monitored using an iron foil monitor. The thermal neutron flux measured for each of the 23 replicate samples varied by 20 %, while the fast neutron flux varied by over 80 %.

However, no significant difference in the results for the two batches of samples could be detected after neutron flux corrections had been applied, thus indicating that the precision obtainable on a series of samples irradiated separately is no worse than that obtainable on a similar series irradiated together.

The data on the 23 replicate samples was combined and a mean and C.O.V. calculated for each of the 28 elements determined. These results are presented in Table 7.4 together with a predicted error estimated from counting statistics, distance correction errors and calibration errors.

TABLE 7.4 MEASURED AND ESTIMATED ANALYTICAL PRECISION

ELEMENT		MEAN	STANDARD DEVIATION	C.O.V.	ESTIMATED ERROR
GOLD	ppm	0.045	0.024	53 %	22 %
URANIUM	ppm	9.2	0.5	5.0 %	7.6 %
THORIUM	ppm	5.5	0.4	6.6 %	3.9 %
SODIUM	%	0.0568	0.0009	1.6 %	2.9 %
POTASSIUM	%	0.113	0.009	7.7 %	15 %
BARIUM	ppm	60.	13.	22 %	27 %
RUBIDIUM	ppm	8.	1.7	21 %	30 %
CAESIUM	ppm	0.52	0.04	7.6 %	12 %
LANTHANUM	ppm	15.0	0.3	2.0 %	2.8 %
CERIUM	ppm	32.	2.	5.2 %	2.5 %
NEODYMIUM	ppm	16.	3.	20 %	29 %
EUROPIUM	ppm	0.50	0.021	4.2 %	4.7 %
TERBIUM	ppm	0.24	0.027	12 %	15 %
YTTERBIUM	ppm	0.98	0.06	6.5 %	6.2 %
LUTETIUM	ppm	0.11	0.03	27 %	25 %
TITANIUM	%	0.11	0.02	18 %	20 %
ZIRCONIUM	ppm	140.	13.	9 %	10 %
HAFNIUM	ppm	3.9	0.3	6.9 %	3.3 %
TANTALUM	ppm	0.47	0.03	7.1 %	5.0 %
TUNGSTEN	ppm	0.8	0.24	30 %	30 %
GALLIUM	ppm	6.2	0.7	12 %	20 %
IRON	%	0.71	0.025	3.5 %	2.0 %
SCANDIUM	ppm	2.7	0.10	3.8 %	2.1 %
CHROMIUM	ppm	130.	10.	7.7 %	3.9 %
COBALT	ppm	19.	1.1	6 %	1.4 %
NICKEL	ppm	44.	6.3	14 %	15 %
ARSENIC	ppm	55.	3.6	6.6 %	2.0 %
ANTIMONY	ppm	0.37	0.023	6.3 %	8.6 %

The results presented in this table have been analysed further and are presented in histogram form in Figure 7.3.

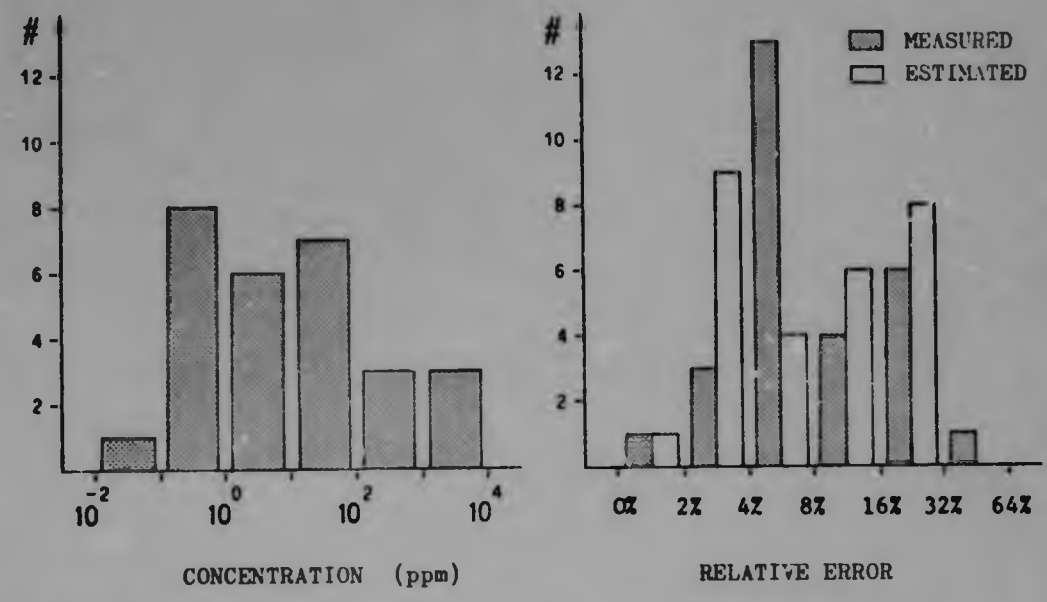


Figure 7.3 FREQUENCY DISTRIBUTION OF ELEMENT CONCENTRATIONS AND ERRORS FOR QUARTZITE SAMPLES

The elements determined ranged in concentration from gold at 0.045 ppm to iron at 7100 ppm, with a median element concentration of about 10 ppm. The measured errors (C.O.V.) of these samples varied from 1.6 % for sodium to 53 % for gold, with a median value of about 6 %. A comparison of the estimated and measured errors shows that in general the low errors have been underestimated and the high values overestimated.

The best determined element, sodium, was measured at a level of 0.05 %, with a precision of 1.6 %. This compares favourably with a precision of 1.2 % obtained by Parker, Pa68, who determined sodium at the 3 % level.

7.6 Discussion

If average errors associated with sampling, preparation, irradiation, counting and distance and decay corrections are combined, an error estimated at 4 % is obtained. The average measured precision for an element is about 6 %. Thus the error due to peak determination is abo.. 4 %, i.e. equal to all the other sources of error combined.

Therefore most of the analytical errors have been successfully reduced to insignificant levels, in comparison to peak area determination errors.

8 STANDARDS

There are two methods for converting isotopic data in cts/hr/g to element concentrations in either ppm or %. These are the Absolute method and the Comparator method.

8.1 Absolute Method

This method requires knowledge of all but one of the parameters in the activation equation:

$$A_s = \phi_\gamma I \varphi \frac{m}{A} N_o \theta \sigma \left(1 - e^{-\lambda T_i}\right) e^{-\lambda T_d} \left(1 - e^{-\lambda T_c}\right)$$

where for any particular isotope:

A_s = Number of counts in the measured gamma peak

ϕ_γ = Detector efficiency at energy E_γ

I = Branching ratio

φ = Neutron flux in $n/cm^2/sec$

A = Atomic mass

m = Element mass

N_o = Avogadro's number

θ = Isotopic abundance

σ = Cross section

λ = Isotope decay constant

T_i = Duration of irradiation

T_d = Duration of decay

T_c = Duration of count

Thus if m, the mass of the isotope contained in the sample, is the only unknown, it can be calculated. This method can introduce large errors since most of the parameters must be determined experimentally.

8.2 Comparator Method

This method is based on a comparison between the unknown sample and a standard sample of known composition, i.e. containing an accurately known quantity of the element of interest. Since the sample and standard can in principle be irradiated and counted under identical conditions, the activation equation can be reduced to the following simple expression:

$$\frac{A_s}{A_u} = \frac{m_s}{m_u} \qquad \text{i.e.} \qquad m_u = m_s \frac{A_u}{A_s}$$

where: A_s = Measured gamma peak area of standard

A_u = Measured gamma peak area of unknown

m_s = Mass of isotope in standard

m_u = Mass of isotope in unknown

Several factors make it difficult to irradiate and count standards and samples under 'identical' conditions. As a result, if slightly different conditions are used, comparison factors are required. An example would be a flux comparison factor between different irradiations, as described in Section 5.1.

A range of standard materials is required if an unknown sample is to be analysed for several elements. Although in this respect multi-element rock standards are useful, no single rock-standard produces satisfactory results for all elements.

In order to standardise the quartzite and conglomerate samples, a number of standards, see Table 8.1, was analysed. An analysis similar to that described in Chapter 6 was used to determine optimum irradiation and decay times, see Table A 1.1 in Appendix 1.

Table 8.1 DESCRIPTION OF STANDARDS ANALYSED

(A)	INTERNATIONAL STANDARDS	(B)	IN-HOUSE STANDARDS	
United States Geological Survey		OK-227	Gabbro Picrite	(U.C.T.)
G-2	Granite	M-38	Shale	(U.C.T.)
GSP-1	Grandiorite	M-39	Shale	(U.C.T.)
BCR-1	Basalt	M-60	Shale	(U.C.T.)
DTS-1	Dunite	M-63	Shale	(U.C.T.)
		5/67	Uranium Ore	(NIM)
National Institute for Metallurgy		61/67	Tungsten	(NIM)
NIM-G	Granite	18/68	Feldspar	(NIM)
NIM-S	Syenite	64/69	Titanium	(NIM)
NIM-L	Lujavrite	107/69	Tantalite Dilution	(NIM)
NIM-N	Gabbro	114/69	Tantalite Dilution	(NIM)
NIM-P	Pyroxene	SG-96	Gold Ore	(NIM)
NIM-D	Dunite	Au-A	Gold Concentrate	(Goldfields)

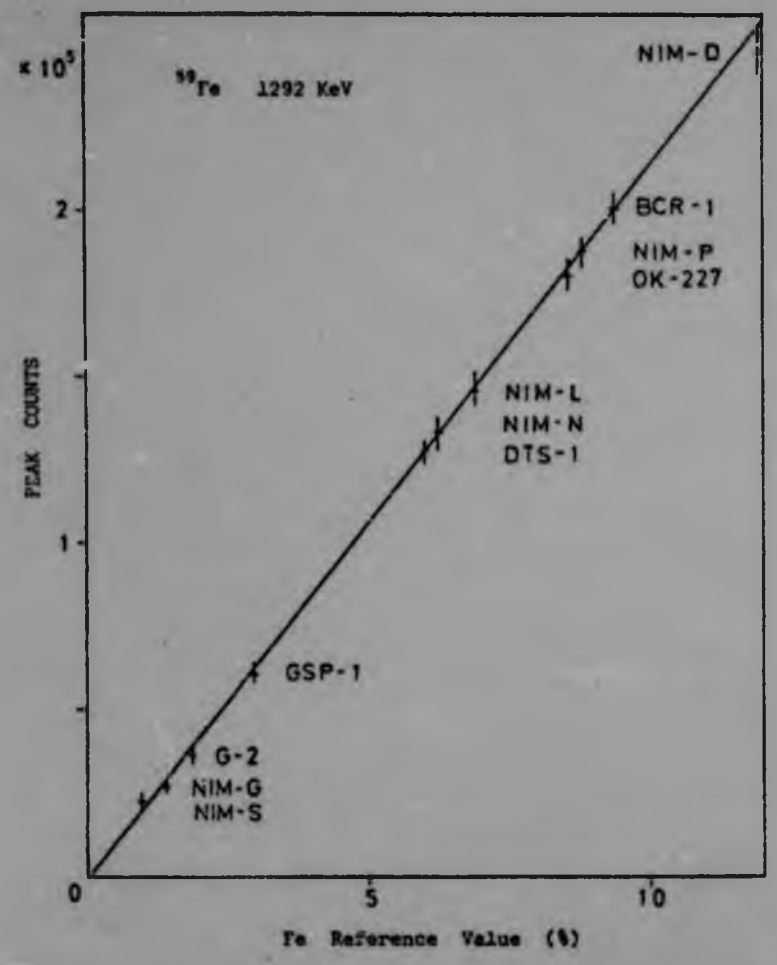
(C) PREPARED SOLUTIONS

Au, U, Ba, Nd, Tb, Yb, Lu, As, Sb, Mo, Zn, Ca

The determination of the activity due to each gamma peak at zero decay was found by fitting a line of correct half-life to the decay curve of the isotope of interest. Thus the resultant error is considerably smaller than that for a single determination.

A calibration curve of cts/hr/g at zero decay vs concentration was drawn for each isotope gamma peak, see Figure 8.1. A straight line through zero was fitted by eye to each set of points. A least squares fit was not done for the following reasons:

(a) As the calibration curve must pass through zero, the point with the highest concentration would receive excessive weight.



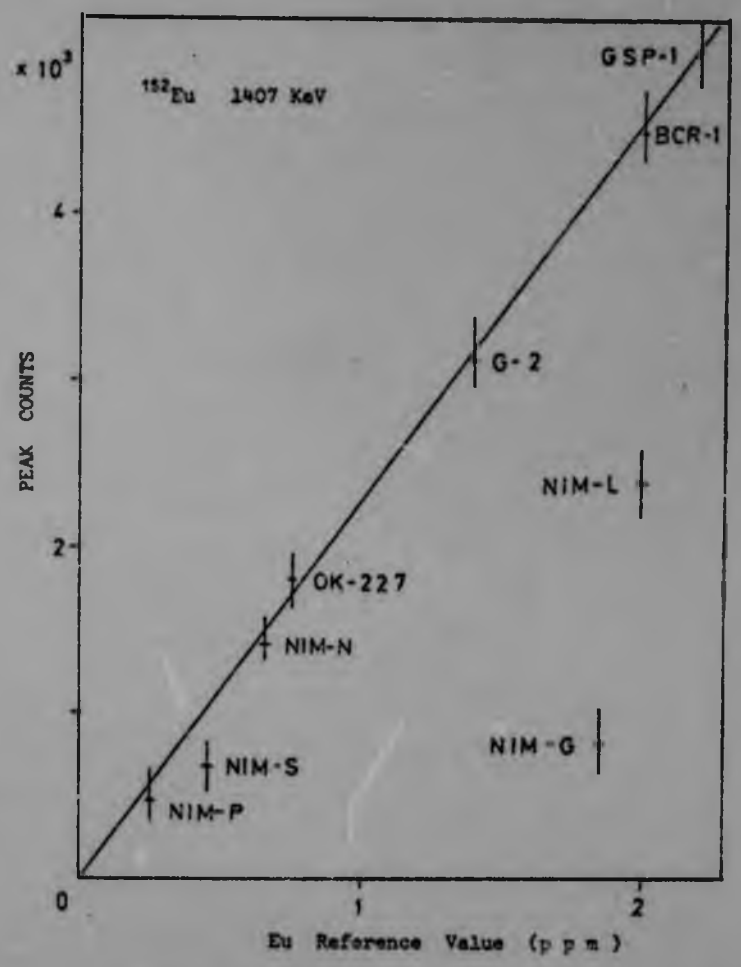


Figure 8.1 CALIBRATION CURVES FOR IRON AND EUROPIUM

(b) The line fit should be weighted to the 'more reliable' standards e.g. the U.S.G.S. standard .

The correct reference values are not well known even for the international standards. For this reason, values were selected from a number of references, which are given in Table A 1.4 in Appendix 1.

It should be noted that for some elements, the standards used were not satisfactory. In particular the gold standard Au-A did not agree with the prepared gold solution standard. In this case Au-A was used as the standard since it could always be restandardised at a later date, whereas the concentration of the solution will not remain constant with time, as the gold is readily absorbed onto the walls of the glass container.

A tabulation of the reference values, measured values and the relative difference for each standard are given in Tables A 1.2 and A 1.3 in Appendix 1.

8.3 Discussion

I.N.A.A. has been used to determine 23 elements in a series of multi-element rock standards, and the results used to standardise analyses of the unknown quartzites and conglomerates.

I.N.A.A. can be used to determine a wide range of elements, some of which can be measured with great sensitivity and accuracy. In this investigation, the maximum number of elements was determined in order to obtain the best possible trace element signature for distinguishing rock types. Analytical conditions were optimised for multi-element determinations. Most if not all of the elements could have been more accurately determined if conditions were optimised for individual elements. Nevertheless, an attempt has been made to determine each element as accurately as possible within the framework of the multi-element analytical technique.

The concentration of the elements determined in the standards range from below 1 ppm to greater than 10 %. The results obtained have been compared to selected reference values and the relative differences calculated. The distribution of these errors for the four U.S.G.S. standards G-2, GSP-1, BCR-1 and DTS-1 is given in Figure 8.2. The results for the NIM multi-element standards have not been included as the reference values for these standards are not yet well known.

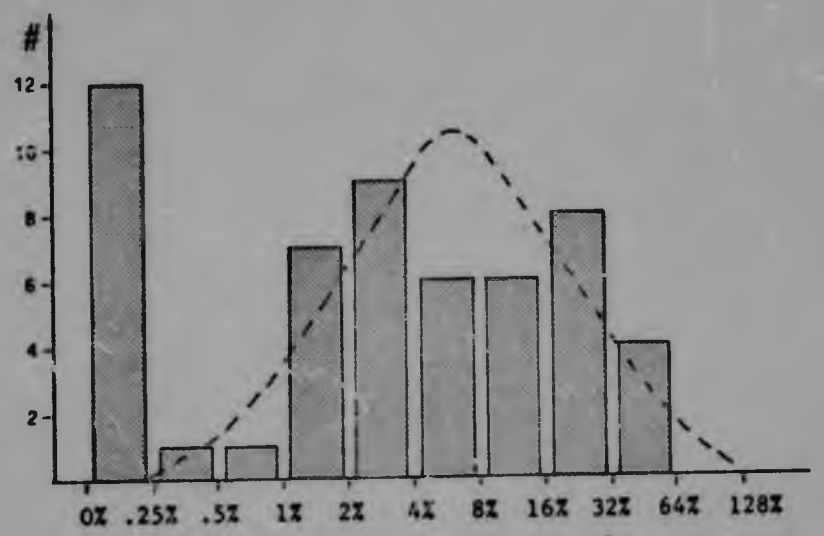


Figure 8.2 FREQUENCY DISTRIBUTION OF RELATIVE ERRORS FOR THE DETERMINATION OF 23 ELEMENTS IN FOUR U.S.G.S. STANDARDS

The distribution shows that a number of determinations had errors below 0.25 %. This preponderence of accurate determinations has two possible explanations.

(i) The reference values quoted have been selected on the basis of knowledge of the analyst and of the techniques employed. N.A.A. results were often chosen, as in some cases the elements cannot be accurately determined by any other method. Results that compare favourably to

these reference values may reflect the fact that similar analytical methods produce similar results, i.e. these 'accurate' results may reflect precision rather than accuracy.

(ii) Another explanation could be attributed to human weakness. The values determined for these standards were obtained from a calibration curve, and there is a tendency for the analyst to try to 'obtain the correct result'. This problem can be partially overcome by the use of a computer to calculate results.

Disregarding the very accurate results, a median value of about 6 % is obtained. Comparison of Figure 8.2 with the precision errors given in Figure 7.3 shows that the level of accuracy obtained is not very much worse than the precision measured in a series of quartzite samples.

Accuracy can also be measured by comparing results with those obtained by other workers on well analysed samples, e.g. U.S.G.S. rock standards,

Two groups actively engaged in the analysis of lunar samples have recently published analyses of the U.S.G.S. standard BCR-1, using N.A.A. and post irradiation separations of chemically related elements. The results obtained using this analytical technique should in general be superior to that of purely instrumental N.A.A.

The accuracy of the data presented in this work will therefore be illustrated by comparing selected results with those of Brunfeldt and Steinnes(Bn71) and Allen et al (A170), summarised in Table 8.2.

Table 8.2 RESULTS FOR SELECTED ELEMENTS DETERMINED IN BCR-1

ELEMENT		THIS WORK	BRUNFELDT (Bn71)	ALLEN (A170)
Fe	%	9.37 ± 0.3	9.38	9.3 ± 0.8
Na	%	2.52 ± 0.1	2.42 ± 0.07	
Ba	ppm	700 ± 50	580 ± 72	656 ± 8
Rb	ppm	62 ± 10	50 ± 2	44.9 ± 4.2
Ce	ppm	50 ± 8	53	54 ± 2
Eu	ppm	2.0 ± 0.1	1.94 ± 0.08	1.93 ± 0.04

The errors quoted for this work are at the 90 % confidence level. Those for Allen et al have been multiplied by a factor of 2 to convert them to the 2 sigma level. The errors given for the results of Brunfeldt and Steinnes have been calculated at the 2 sigma level from the published results.

Of the major elements in rocks, sodium is perhaps the most sensitively determined by I.N.A.A. The value of 2.52 ± 0.1 % obtained for sodium compares favourably with that of 2.42 ± 0.07 % obtained by Brunfeldt. Iron, on the other hand, is one of the least sensitive elements determinable by I.N.A.A., but in rock samples is present at levels that can be readily determined. The value determined was 9.37 ± 0.3 % as compared to 9.38 % (Bn71), and 9.3 ± 0.8 % (A170). The results obtained by I.N.A.A. for these two major elements show that for some elements there is no advantage in using radiochemical techniques.

At the other end of the concentration scale, I.N.A.A. can be used to accurately analyse ultra-trace elements such as europium. The value of 2.0 ± 0.1 ppm measured in BCR-1 is within 0.07 ppm of 1.94 ± 0.08 ppm (Bn71) and 1.93 ± 0.04 ppm (A170), although the error quoted is slightly larger.

Other elements that can, under suitable conditions, be accurately determined by I.N.A.A. are K, Cs, La, Tb, Sc, Co and Sb. Some elements can be determined sensitively by I.N.A.A. but may often suffer interference from other elements in geological material, e.g. Ce, Yb, Lu and Ga may have interferences from Fe, Tb, U and Fe respectively.

In BCR-1, the light rare earths are relatively low in concentration, while the iron level is high. Thus the iron interference on cerium is severe. Without any correction factor, a value of 70 ppm was determined. After correcting for the iron interference, a value of 50 ± 8 ppm was obtained, which compares favourably with Brunfeldt, 53 ppm, and Allen, 54 ± 2 ppm. These results demonstrate that reasonable determinations

of 'problem' elements can be obtained by I.N.A.A., as long as corrections are made for possible interferences.

Although a number of elements can be well determined by I.N.A.A., this method cannot be used to analyse all the elements important to the geochemist. Thus although tantalum can be determined at less than 1 ppm in geological material, the geochemically related element niobium cannot in general be determined by I.N.A.A.

The group of geochemically related elements barium, rubidium and caesium can all be determined by I.N.A.A. with varying degrees of success. Caesium can be determined at levels below 1 ppm, which is sufficiently sensitive for most geological material. Barium and rubidium can only be determined at reasonably high levels since the detection limits for both these elements is poor in geological material. Barium was determined at 700 $\pm$ 50 ppm in BCR-1 in comparison with 580 $\pm$ 72 ppm (Bn71) and 656 $\pm$ 8 ppm (Al70). The rubidium values show a similar scatter with a value of 62 $\pm$ 10 ppm as compared to 50 $\pm$ 2 (Bn71) and 44.9 $\pm$ 4.2 (Al70).

9 COMPUTER REDUCTION OF DATA

Activation analysis, as so many other techniques today, relies heavily on the use of large, fast computers to handle the large amounts of data produced.

9.1 Mathematical Models

The irradiation and decay of complex samples can be simulated by computer programmes based on mathematical models. A programme has been developed by Isenhour and Morrison, Is64, to optimise irradiation and decay times. This programme has however not been used extensively as it requires previous knowledge of the composition of the sample. Charyula and Horn, Ch68, developed a programme to simulate gamma spectra obtained from in situ neutron activation borehole logging under varying irradiation and detection conditions.

9.2 Gamma Spectra Analysis

The analysis of gamma spectra consists primarily of the location of peaks and the calculation of peak areas. A more complete analysis would include the determination of peak centroids, F.W.H.M., F.W.$\frac{1}{10}$.M. and the error in peak area. Spectral analysis by least squares methods has been used by Blackburn, Bl65, and Routti and Prüssin, Ro69. The effect of spectral smoothing has been investigated by Yule, Yu67, Yu72, and Tominaga et al, To72.

Methods for calculating peak areas have been suggested by Covell, Co59, Yule, Yu68, and Quittner, Qu69. Zimmerman, Zi61, has given a simple method of determining the F.W.H.M. of gaussian shaped peaks. Complete spectral analysis programmes have been discussed by Barnes, B-68, Routti and Prüssin, Ro69 and Op de Beeck, Op72. Many of these

publications also discuss peak interferences. A recent review of computer data reduction methods has been given by Yule, Yu71.

The programme used for these experiments is an amended version of 'Hevesy', a programme developed by H.P. Yule (Yu67, Yu68). The programme uses a five point quadratic convolution of the data and locates peaks using the first derivative method. The amended version identifies peaks using a library of known peak energies of various isotopes and applies certain correction factors, e.g. P.P.C.F. The programme output is also written onto magnetic tape for further analysis. This 'processed data tape' is used as input to the programme SERHLF, which plots decay and error curves for any peak of interest, and is also used as input to the peak data conversion programmes.

9.3 Peak Data Processing

Considerable attention has been given to the conversion of peak data information into concentrations of the elements determined. When only one or two elements are to be determined from a spectrum, it is a relatively simple matter to process a series of spectra from a suite of similar samples. A single computer programme can be used to convert the peak data directly to absolute element concentrations. However, when several elements must be determined from a spectrum, there are generally a number of correction factors, e.g. interference correction factors, which must be applied to different peaks. Furthermore, each sample is often counted more than once, and so data from parallel analyses must be combined.

When the data reduction problems reach this level of sophistication, the use of a single general purpose computer programme becomes too complicated. Therefore the problem of data reduction in this investigation was approached via a suite of programmes, each designed to handle a distinct phase of the data reduction.

This method allows the analyst to intervene at each phase of the data reduction, and to make decisions based on experience and knowledge of the samples. A list of these programmes and their functions is given in Table 9.1.

Table 9.1 SUMMARY OF COMPUTER PROGRAMMES

PROGRAMME	
TUBORG	Gamma spectra analysis and peak identification. Output is copied onto a processed data (PD) magnetic tape,
SERHLF	Selects data from PD tape for decay curve, minimum error and interference analysis.
SERWIT	Selects data from PD tape, applies correction factors and converts peak data to element concentrations with error estimates. Creates master disk file.
SERINT	Corrects peaks for interferences by subtracting a given fraction of another peak.
SERMIX	Combines data from parallel analytical runs.
SERCOM	Merges data on different peaks for a single sample.
SERFC	Corrects data for fast or epithermal neutron flux differences.
SERMOD	Combines data on several peaks to produce element concentrations.
SERLIM	Replaces missing data with an estimate of the detection limit.
SERT	Sorts data files into the required sample sequence.
SERPR	Tabulates results with errors.
SERHST	Produces histograms of selected elements.
SERSCT	Produces scatter diagrams of selected element pairs.

9.4 Data Analysis

Once the data was in the required element concentration form, computer programmes were used to calculate means, standard deviations, covariance and correlation coefficients. Sophisticated statistical analyses of large amounts of data can in general only be handled by the computer. Programmes for multivariate analysis of variance, stepwise multiple regression analysis and principal component analysis (Hw72) were applied.

9.5 Data Presentation

A series of programmes was developed to handle the time-consuming task of data presentation, e.g. data tabulation, histogram plotting and scatter diagram plotting. Good, accurate presentation can help considerably with the interpretation of the data.

9.6 Discussion

The computer analysis of gamma spectra is still a major problem. Although the use of high resolution Ge(Li) detectors has made I.N.A.A. a viable technique, it has also introduced problems which were not readily apparent using NaI detectors. In particular, the many gamma rays emitted by most isotopes often overlap and introduce interference problems.

Although extensive investigations into resolving peak interferences have been undertaken by many workers, no single method has as yet been found that is generally applicable and computationally fast enough to be routinely applied.

An alternative approach to the stepwise reduction of data developed for this investigation would be a fully automated analytical system based on a small dedicated computer. This method has been successfully implemented for relatively simple analyses, but the application of automated systems for the routine analysis of geological material should be considered as something of the future.

10 ANALYTICAL RESULTS

Results are presented for three suites of conglomerate and quartzite samples taken from the Kimberley Reef Conglomerates at the Lurban Roodepoort Deep Mine.

10.1 Preliminary Survey Samples

These samples consisted of a suite of 16 hand specimens taken along 30 level crosscut, see Figure 3.1

(a) Analysis

Preparation: The hand specimens were crushed in a swing-mill using a stellite bowl.

Irradiation: The samples were irradiated in duplicate together with the multi-element standards GSP-1, DTS-1, NIM G and NIM D. Co-Al wire was used as a neutron flux monitor for the 30 minute irradiation in the hydraulic facility.

Counting: Samples and standards were counted for 20 minutes each, using System A, see Table 5.4, at decay times of 7 and 14 days.

(b) Results

Quantitative results were obtained using the standards simultaneously irradiated, and were subsequently updated from the analysis of standard samples, see Chapter 8.

Four elements, Au, Na, La and Yb were determined at a decay time of 7 days and a further 8 elements, Cs, Eu, Hf, Ta, Fe, Sc, Co and Sb, at 14 days decay, see Table 10.1.

Table 10.1 RESULTS FOR THE ANALYSIS OF PRELIMINARY SAMPLES

	SAMPLE NO	Au ppm	Na %	Ce ppm	La ppm	Eu ppm	Yb ppm	Hf ppm	Ta ppm	Fe %	Sc ppm	Co ppm	Sb ppm
	1	0.15	0.054	0.27	21	0.44	0.63	1.6	0.36	0.96	1.7	27	0.10
ZONE 8	2	0.25	0.054	-	23	0.26	0.29	1.9	0.37	0.13	2.3	5	-
	3	0.92	0.037	-	24	0.46	0.44	3.1	0.92	2.3	2.6	63	0.30
	4	0.09	0.078	-	16	0.31	0.38	2.0	-	0.35	1.2	4	-
ZONE 7	5	0.24	0.052	0.69	21	0.43	0.42	2.6	0.38	1.2	1.6	27	-
	6	18	0.047	-	27	0.49	-	3.8	0.79	2.2	4.3	39	0.45
	7	0.09	0.060	-	19	0.51	0.55	1.8	0.43	0.97	4.6	24	-
	8	2.3	0.040	-	24	0.76	0.32	2.6	0.46	2.9	5.4	49	0.48
	9	0.62	0.049	-	25	0.69	0.59	3.3	0.67	1.1	4.0	31	0.33
ZONE 6	10	0.53	0.040	-	12	0.38	0.32	1.2	-	1.0	2.4	38	0.19
	11	0.07	0.15	1.3	47	1.1	1.4	5.0	-	1.4	8.3	34	0.54
ZONE 5	12	0.08	0.14	2.3	83	1.8	1.6	7.7	0.75	0.23	9.5	11	0.50
ZONE 4	13	0.06	0.17	-	26	0.72	0.69	3.1	-	0.34	3.0	11	0.58
ZONE 3	14	0.08	0.072	-	16	0.31	0.33	2.4	0.37	1.0	1.9	28	0.34
	15	0.32	-	2.9	13	0.10	0.18	15	8.4	3.8	5.0	230	-
ZONE 2	16	0.59	0.042	-	22	0.11	0.42	3.5	1.4	2.5	3.8	67	0.27

(c) Discussion

The results were plotted as a series of histograms based on the sampling positions, see Figure 3.1. The following observations were made.

(i) Sample Number 6 from the 'Pay Band' showed a high gold content, (18 ppm). There did not appear to be any correlation with gold by any other element.

(ii) Zone 2 conglomerates are high in Ta, Hf, Co and Fe.

(iii) No differences were visible between conglomerate zones 6 and 7.

(iv) The quartzite zones 3, 4 and 5 are high in Na, Sc, La, Eu and Yb.

These results were encouraging in that they indicated certain zone differences, particularly between quartzites and conglomerates.

10.2 Chip Samples

15 quartzite and 75 conglomerate chip samples were taken from the borehole core 30/U1, which fully intersected the 6 zones of interest.

(a) Analysis

Preparation: The samples were cut from the core in the form of small tablets, using a water cooled diamond saw and drill.

Irradiation: The chip samples were irradiated for a period of one hour, with lengths of Co-Al wire as neutron flux monitors.

Counting: The samples were counted for 30 minutes each, using System B, see Table 5.4, at a decay time of 10 days

(b) Results

Results for the determination of 19 elements in the 90 chip samples are presented in Appendix 2. The mean value and the C.O.V. calculated from the results of the samples from each zone are given in Table 10.2.

Only eleven elements were determined in all 90 samples, viz. Th, La, Eu, Yb, Lu, Hf, Ta, Fe, Sc, Cr and Co. In addition, gold was determined in all 75 conglomerates.

Table 10.2 CHIP SAMPLES - MEANS AND C.O.V.

	ZONE 2		ZONE 3		ZONE 4		ZONE 5		ZONE 6		ZONE 7	
	MEAN	COV	MEAN	COV	MEAN	COV	MEAN	COV	MEAN	COV	MEAN	COV
Au ppm	0.45	105 %	0.07	15 %	0.52	125 %	-	-	1.7	206 %	0.29	165 %
Th ppm	16	121 %	7.9	34 %	2.6	41 %	5.1	31 %	20	76 %	9.9	136 %
Ba ppm	500	168 %	250	88 %	81	17 %	130	19 %	900	75 %	110	95 %
Rb ppm	8.6	20 %	18	68 %	12	7 %	18	44 %	36	41 %	8.3	19 %
Cs ppm	2.0	122 %	0.71	55 %	0.45	32 %	0.76	35 %	1.2	41 %	1.7	240 %
La ppm	110	120 %	37	69 %	23	20 %	50	44 %	150	81 %	69	106 %
Ce ppm	72	105 %	ND		ND		ND		190	58 %	63	100 %
Nd ppm	47	93 %	ND		ND		ND		127	180 %	25	70 %
Sm ppm	0.95	96 %	0.57	33 %	0.59	20 %	0.74	92 %	2.3	60 %	0.91	71 %
Tb ppm	0.79	97 %	-		-		-		2.2	77 %	0.45	72 %
Yb ppm	2.2	92 %	0.96	32 %	0.70	45 %	1.0	32 %	6.0	73 %	1.8	78 %
Lu ppm	0.86	136 %	0.21	125 %	0.10	37 %	0.14	22%	1.0	100 %	0.27	102 %
Hf ppm	4.3	175 %	2.5	20 %	15	187 %	2.9	22 %	6.3	80 %	9.7	134 %
Ta ppm	4.9	177 %	0.41	38 %	0.36	17 %	0.85	82 %	4.7	180 %	5.5	430 %
Fe %	2.0	72 %	0.31	68 %	0.33	180 %	0.15	49 %	7.5	170 %	1.2	107 %
Sc ppm	5.1	59 %	2.2	49 %	2.4	37 %	7.2	30 %	15	60 %	4.9	48 %
Cr ppm	130	126 %	44	63 %	130	80 %	100	49 %	230	82 %	100	90 %
Co ppm	62	112 %	9.4	105 %	12	125 %	3.9	92 %	140	156 %	24	140 %
Sb ppm	0.39	90 %	0.11	49 %	0.10	36 %	0	50 %	0.84	120 %	0.14	73 %

(c) Discussion

Inspection of the results showed that the within-zone variation was similar to the between-zone variation, however, results for the quartzites showed less variation than those for the conglomerates.

The sampling technique employed does not distinguish between pebbles and matrix in the conglomerates, but samples both randomly. Absolute concentrations could be expected to vary, since the silica pebbles act as a diluent. Element ratios tend to remove the effect of this silica dilution.

However, even the element ratios showed considerable variation. Three-quarters of the ratios calculated for the quartzite samples had within-zone variations of greater than 25 % (one standard deviation). Visual inspection of the data did not indicate the presence of any ratio that could act as a possible zone marker.

10.3 Powdered Samples

A series of 18 powdered samples was prepared; one sample from each of the six zones intersected by the three borehole cores 30/U1, 30/U2 and 30/U3.

(a) Analysis

Preparation: The core samples were pulverised in an agate bowl using a swing-mill. The samples were analysed in triplicate with each sample being assigned a three figure code ABC as follows.

A	= Zone number	2 - 7
B	= Core number	1 - 3
C	= Replicate number	1 - 3

Thus sample 312 is replicate 2 from zone 3 of core number 1.

Irradiation: The samples were sealed in quartz vials and irradiated for 5 hours in the hydraulic facility. Each sample was individually monitored using an iron foil neutron flux monitor.

Counting: The samples were counted for 30 minutes using System E, see Table 5.4, at a decay time of 4 days. A fault developed in this system, and the remaining three counts, at decay times of 10, 20 and 40 days, were made using System B'.

(b) Results

The values were calibrated using results obtained from the analysis of a suite of 35 standard reference samples, see Chapter 8. Quantitative results for 28 elements in 54 quartzite and conglomerate powdered samples are presented in Appendix 3.

Nine samples from each zone, viz. triplicate analyses from three borehole cores, have been combined and a mean and C.O.V. calculated, see Table 10.3.

Average values, errors, and detection limits for the determination of the 28 elements in conglomerates and quartzites are presented in Table 10.4.

(c) Discussion

Results for the determination of each element were plotted in a series of histograms, see Appendix 3. Inspection of these results showed that several of the elements e.g. La, Ce, Eu, Yb, Hf, Fe, Sc and Cr have relatively small within-zone variations.

The variation in element concentration within a zone but between the three cores is reflected in the concentrations of elements such as U, Cs, Fe, Sc, Co and As. These variations are in general less than the between-zone variations.

Table 10.3 POWDERED SAMPLES - MEANS AND C.O.V.

		ZONE 2		ZONE 3		ZONE 4		ZONE 5		ZONE 6		ZONE 7	
		MEAN	COV	MEAN	COV	MEAN	COV	MEAN	COV	MEAN	COV	MEAN	COV
Au	ppm	1.1	83 %	0.059	43 %	0.018	30 %	0.019	34 %	1.0	100 %	0.31	60 %
U	ppm	94	18 %	9.6	8.2 %	4.2	13 %	5.4	20 %	8.1	8.9 %	11	18 %
Th	ppm	11	11 %	5.5	5.5 %	1.8	21 %	7.5	9.8 %	4.2	7.5 %	5.3	14 %
Na	%	0.024	14 %	0.060	11 %	0.055	2.3 %	0.031	12 %	0.030	8.8 %	0.047	17 %
K	%	0.033	22 %	0.18	6.5 %	0.097	1? %	0.079	23 %	0.068	9.2 %	0.11	20 %
Ba	ppm	110	64 %	73	8.9 %	49	15 %	50	9.0 %	61	38 %	69	22 %
Rb	ppm	<8		10	31 %	5.0		5.7	35 %	10	31 %	11	18 %
Cs	ppm	0.93	32 %	0.52	11 %	0.31	21 %	0.53	13 %	0.34	14 %	0.58	11 %
La	ppm	16	9.0 %	15	2.0 %	8.1	6.4 %	22	2.1 %	13	3.7 %	19	6.2 %
Ce	ppm	45	13 %	32	2.4 %	16	14 %	44	8.0 %	26	3.9 %	35	12 %
Nd	ppm	22	21 %	15	10 %	8.4	24 %	16	28 %	15	10 %	19	25 %
Eu	ppm	0.45	12 %	0.52	3.3 %	0.37	11 %	0.66	3.5 %	0.51	4.2 %	0.49	7.3 %
Tb	ppm	0.25	16 %	0.25	13 %	0.17	12 %	0.26	15 %	0.21	15 %	0.18	10 %
Yb	ppm	1.37	7.3 %	1.03	8.8 %	0.51	8.2 %	1.26	5.7 %	1.13	4.4 %	1.11	9.1 %
Lu	ppm	0.12	45 %	0.15	8.1 %	0.075	13 %	0.18	7.1 %	0.17	9.0 %	0.15	11.2 %
Ti	%	0.19	60 %	0.124	13 %	0.053	10 %	0.115	10 %	0.20	75 %	0.13	17 %
Zr	ppm	200	25 %	150	7.8 %	7?	12 %	130	9.4 %	109	6.4 %	136	17 %
Hf	ppm	2.6	14 %	4.0	4.3 %	1.9	10 %	3.9	7.6 %	2.8	4.6 %	4.0	15 %
Ta	ppm	1.5	13 %	0.53	12 %	0.15	12.7 %	0.34	9.2 %	0.40	11 %	0.44	20 %
W	ppm	<0.45		0.73	29 %	0.83	8.6 %	0.89	18 %	0.60	16 %	0.56	14 %
Ga	ppm	3.7	56 %	6.1	16 %	4.3	27 %	15	11 %	5.2	9.3 %	7.9	12.4 %
Fe	%	1.7	8.4 %	0.85	13 %	0.18	13 %	0.17	10 %	1.12	5.5 %	0.93	16 %
Sc	ppm	3.8	6.2 %	2.9	4.2 %	1.2	9.3 %	4.1	5.2 %	3.8	4.6 %	3.3	13 %
Cr	ppm	108	8.8 %	149	7.5 %	88	15 %	89	10 %	80	5.8 %	73	13 %
Co	ppm	43	13 %	21	9.4 %	5.8	8.4 %	5.4	7.9 %	19	6.9 %	21	17 %
Ni	ppm	39	21 %	46	19 %	17	23 %	24	14 %	43	12 %	37	24 %
As	ppm	200	22 %	57	7.0 %	19	11.2 %	22	6.3 %	32	7.2 %	31	19 %
Sb	ppm	0.43	17 %	0.37	8.9 %	0.17	19 %	0.17	11 %	0.29	10 %	0.23	16 %

Table 10.4 AVERAGE LEVEL, ERROR AND DETECTION LIMIT FOR CONGLOMERATE AND QUARTZITE SAMPLES

ELEMENT	CONGLOMERATES			QUARTZITES		
	AVERAGE	ERROR	DET. LIMIT	AVERAGE	ERROR	DET. LIMIT
GOLD	1 ppm	14 %	16 ppb	0.03 ppm	20 %	15 ppb
URANIUM	10 ppm	7 %	0.7 ppm	6 ppm	8 %	0.6 ppm
THORIUM	7 ppm	3 %	0.18 ppm	5 ppm	3 %	0.15 ppm
SODIUM	0.04 %	3 %	5 ppm	0.05 %	3 %	5 ppm
POTASSIUM	0.08 %	20 %	0.02 %	0.10 %	15 %	0.02 %
BARIUM	60 ppm	25 %	50 ppm	50 ppm	30 %	40 ppm
RUBIDIUM	10 ppm	30 %	8 ppm	7 ppm	30 %	2.5 ppm
CAESIUM	0.6 ppm	12 %	0.2 ppm	0.45 ppm	12 %	0.1 ppm
LANTHANUM	15 ppm	2.8 %	0.2 ppm	15 ppm	2.8 %	0.2 ppm
CERIUM	35 ppm	1.5 %	0.9 ppm	30 ppm	1.5 %	0.6 ppm
NEODYMIUM	20 ppm	25 %	12 ppm	10 ppm	30 %	7 ppm
EUROPIUM	0.5 ppm	5 %	0.07 ppm	0.5 ppm	4.5 %	0.05 ppm
TERBIUM	0.2 ppm	16 %	0.12 ppm	0.2 ppm	16 %	0.10 ppm
YTTERBIUM	1.2 ppm	6 %	0.2 ppm	1.0 ppm	6 %	0.15 ppm
LUTETIUM	0.15 ppm	15 %	0.02 ppm	0.10 ppm	16 %	0.015 ppm
TITANIUM	0.15 %	20 %	0.05 %	0.08 %	20 %	0.04 %
ZIRCONIUM	160 ppm	12 %	65 ppm	130 ppm	12 %	40 ppm
HAFNIUM	3.5 ppm	3.5 %	0.2 ppm	3.5 ppm	3.5 %	0.2 ppm
TANTALUM	0.5 ppm	5 %	0.06 ppm	0.5 ppm	5 %	0.06 ppm
TUNGSTEN	0.5 %	35 %	0.45 ppm	0.6 %	35 %	0.45 ppm
GALLIUM	5.0 ppm	20 %	1.2 ppm	5.0 ppm	20 %	1.2 ppm
IRON	1.3 %	2 %	0.02 %	0.2 %	2.5 %	0.015 %
SCANDIUM	4 ppm	2 %	0.04 ppm	3 ppm	2 %	0.03 ppm
CHROMIUM	90 ppm	4 %	2.1 ppm	90 ppm	3 %	1.4 ppm
COBALT	30 ppm	1.5 %	0.4 ppm	5.5 ppm	1.5 %	0.2 ppm
NICKEL	45 ppm	30 %	30 ppm	25 ppm	30 %	25 ppm
ARSENIC	30 ppm	2.5 %	0.4 ppm	30 ppm	2.5 %	0.4 ppm
ANTIMONY	0.3 ppm	10 %	0.1 ppm	0.25 ppm	10 %	0.05 ppm

Certain elements such as cerium show a particularly large between-zone separation in comparison to the small within-zone variation.

The choice of elements for discriminating zones is not immediately obvious from a visual inspection of the data. Statistical techniques have therefore been developed to obtain optimum discrimination between zones.

11 STATISTICAL ANALYSIS

At this stage it is appropriate to restate the objective of the geological investigation.

A series of samples was taken from six sedimentary horizons. What we wish to do is to find some quantitative geochemical signature which will serve to identify each horizon.

The first possible signature would be different absolute concentrations of various elements between each zone. Neither the preliminary samples nor the chip samples produced any data that could be used in this way. The data on the powdered core samples, on the other hand, showed some differences in concentration from one zone to another, e.g. the uranium concentration of Zone 2 is ten times that of the concentration of any other zone. Although it is quite possible to check the relative merit of each element by eye, statistical techniques should be used to provide a more accurate indication.

The second possible signature would be the relative concentration of one element against that of another, i.e. element ratios. The use of simple ratios was investigated in the interpretation of the chip data, but with no success. The concept of a simple ratio can be extended to many elements as follows:

Simple ratio : $$R = \frac{C_1}{C_2}$$

i.e. $$R' = \log R = \log C_1 - \log C_2$$

Generalised Ratios: $$R' = \sum_{i=1}^{n} a_i c_i$$

where: C_i = Absolute concentration of element i

c_i = Log of the absolute concentration of i

a = Coefficient n = Number of elements

For simple ratios, $\alpha_i = \pm 1$, but this is in fact an unnecessary constraint. The α_i's can have any value, and can be simply normalised, for convenience, to:

$$\sum_{i=1}^{n} \alpha_i^2 = 1$$

This argument implies that it may be advantageous to consider the log concentrations rather than absolute concentrations, in the development of a signature. In fact it has been suggested by several authors, notably Ahrens, Ah54, that many elements follow a lognormal distribution, particularly in sedimentary rocks.

The preliminary requirement of the statistical technique is that it is able to handle all the data, preferably simultaneously, and show maximal difference between zones. In fact what is required is the technique of discriminant analysis.

11.1 Discriminant Analysis

Discriminant analysis can be considered as a method of classifying multivariate observations into one or more groups by calcul ting linear combinations of the variables that comprise the observations.

It can be approached through two equivalent methods. The first is to use the discriminant function. Given any two populations, a function, known as the discriminant function, can be derived which will vary maximally between the populations. To classify unknown samples, the value of the function is calculated for the sample, which is then assigned to one of the populations depending on the value of the function. When there are more than two populations to consider, say k populations, this involves the calculation of (k - 1) discriminant functions. Unknown samples are initially classified according to each separate discriminant function, i.e. between pairs of populations, and then the results for the classification between all possible pairs of populations are combined.

The technique of discriminant analysis was first applied in the geological field by Emery and Griffiths, Em54, to differentiate barren and oil-bearing sandstones. Since then it has been used by several other workers who have applied it in many different ways. Wood, Wo61, for example, used it to classify refractory and non-refractory quartzites. The basic concept of the technique has been clearly illustrated by Klovan and Billings, Kl67, who used it to distinguish different rock types. A review of the many applications of discriminant analysis is given by Griffiths, Gr66.

The alternative approach to discriminant analysis is the calculation of the so-called generalised distance, also known as the Mahalanobis distance (D^2). This method was first used by Mahalanobis in 1939 to classify ethnic groups in India, Mh49. Since then it has been applied in the paleontological sciences, for example to classify various fossils, Re63. Computer programmes for the calculation of the D^2 statistic have been published by Casetti, Ca64, Davis and Sampson, Dv66, Wolleben et al, Wl68 and Reyment et al, Re69.

Although virtually all the authors point out that this method of discriminant analysis is generally applicable, its use in the geosciences appears to be scant.

In this present analysis, discrimination between zones has been approached by calculating the Mahalanobis distance. It appears that this method is superior to that of the discriminant function analysis, in that it is considerably easier to treat many populations simultaneously. In addition it is possible to obtain a graphical representation of the populations.

The concept of the Mahalanobis distance can best be appreciated from a simple example.

11.1.1 Two Dimensional Model

Consider the two-dimensional scatter diagram given in Figure 11.1. Each point is defined by an observation (x_i , y_i). The points come from two distinct populations 1 and 2, which have means $(\bar{x}_1 , \bar{y}_1)$ and $(\bar{x}_2 , \bar{y}_2)$ respectively.

The line separating the two populations (L_1) is the locus of all points equidistant from both population means. Thus any point lying above the line would be classified to population 1, and points lying below to population 2.

The line perpendicular to this line passing through the mean of each population line (L_2), corresponds to the discriminant function between these two populations. Consider the origin of L_2 as the point of intersection with L_1 and down as the positive direction. If the discriminant function is calculated for any unknown sample, a positive value suggests that it is from population 2, while a negative value suggests that it is from population 1.

Consider an unknown sample which plots at the point (x_u , y_u). The euclidian distance to the mean of each population is calculated, i.e.

$$d_1^2 = (\bar{x}_1 - x_u)^2 + (\bar{y}_1 - y_u)^2$$

similarly:

$$d_2^2 = (\bar{x}_2 - x_u)^2 + (\bar{y}_2 - y_u)^2$$

The unknown sample is assigned to that population to which it is closest, i.e. in this example $d_2^2 << d_1^2$, therefore the unknown is from population 2.

Is it necessary to view the classification in two dimensions? Consider the case of the x observations, i.e. the projection of the two populations onto the X-axis. It is immediately apparent that the two populations cannot be separated by the x values alone. If the unknown

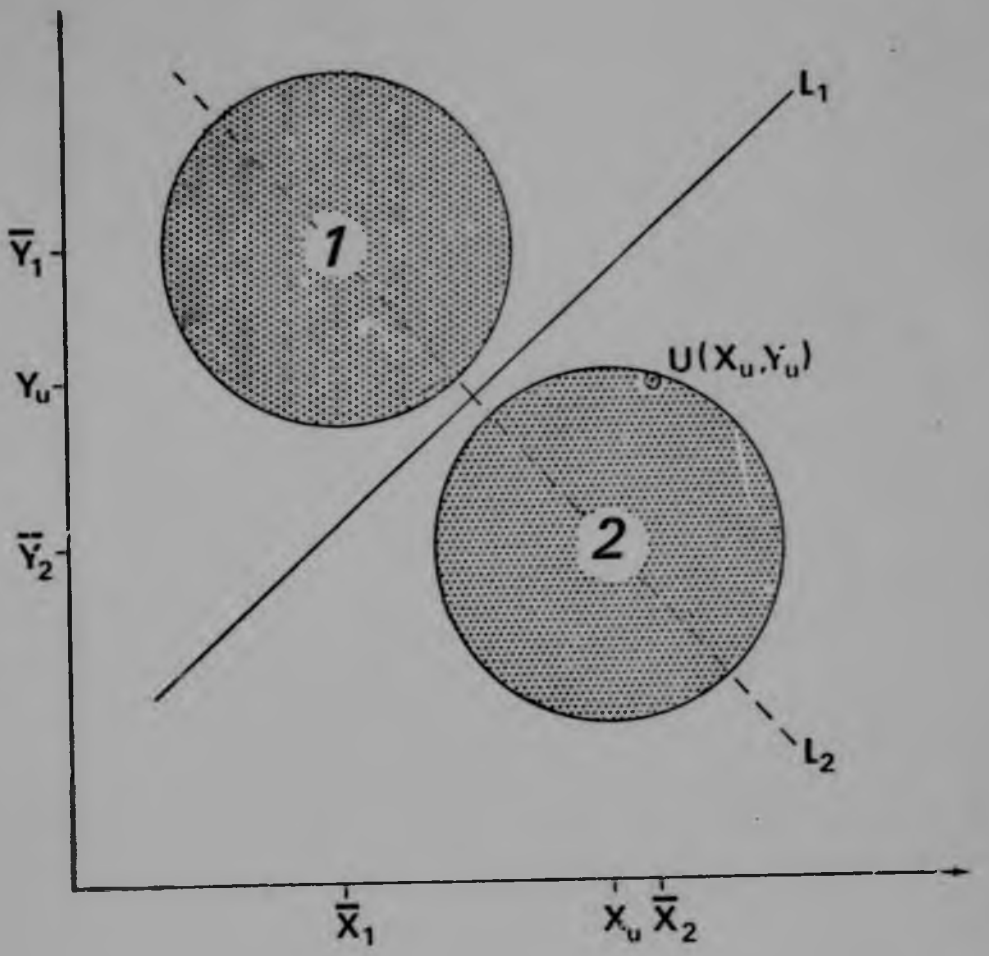


Figure 11.1 DISCRIMINATION IN TWO DIMENSIONAL SPACE

sample is classified using a distance-from-the-mean criterion, then it is co ctly classified as population 2. On the other hand, consideration of only the y observations, which also show no clear population discrimination, leads us to believe that the unknown is from population 1.

Thus each one-dimensional case can lead to no definite conclusion as to the parent population of the unknown, whereas the two-dimensional case leaves us in no doubt that the unk own sample belongs to population 2.

The above example illustrates the fact that the discriminating power will usually increase as the number of dimensions is increased. Discriminant analysis allows one to view populations in multidimensional space.

The distance measure used in this multidimensional space could be a simple euclidian metric, or some other suitable metric. The Mahalanobis Generalised Distance (D^2) can be shown to give optimal discrimination between population groups. The mathematical development of this measure is contained in the reference included as Appendix 4. This reference develops the statistical model in terms of the chip samples, but the powdered core material follows an analogous argument.

11.1.2 Accuracy of Classification

To test the accuracy of classification, a set of known samples was classified according to the following technique.

Each sample was withdrawn from the analysis in turn, and its Mahalanobis distance to each population mean, as defined by all other samples, was calculated. The sample was then assigned to the nearest population, i.e. to which the Mahalanobis distance was the smallest, and the frequency of correct classification was noted. Thus this technique not only assigns unknown samples to one of the known populations, but it can also be used to predict the frequency of correct classification.

11.1.3 Graphical Representation

A graphical representation of the 'discriminant space' can be obtained via a multivariate analysis of variance, see Appendix 4. Such an analysis produces canonical variates Y_i which vary maximally between populations. The two highest values of Y_i are used to define a two-dimensional plane co-ordinate system. This plane can be considered as that plane in multidimensional space upon which the greatest discrimination between populations is obtained. For three populations, this plane will pass through the centroid of each population. If there are more than three populations, the projection onto the plane will be a best approximation to the multidimensional discrimination between the population centroids.

The percentage representation of the populations on the plane can be calculated from the eigen values (λ_i) of the canonical variates (Y_i). The eigen value (λ_i) is the ratio of the variance of Y_i between populations to the variance of Y_i within populations.

11.1.4 Relative Importance of the Elements

Each canonical variate Y_i is in fact a linear sum of the observations x_j.

i.e. $$Y_i = \sum_j \beta_{ij} x_j$$

where β_{ij} is the weight attached to the observation x_j.

Consider all canonical variates, Y_i , which have large eigen values λ_i. (We need not consider those Y_i's which have small λ_i's as these do not markedly contribute to the discrimination.) If the coefficient β_{ij} of the observation x_j is large, then the observation x_j is important to the discrimination. Thus consideration of each β_{ij} from those Y_i showing significant discrimination can lead us to some

estimate of the relative importance of the various elements. Unfortunately, this technique does not offer a complete solution to the problem of the relative importance of the observations.

Frequently an observation, say x_1, shows good separation between groups, but has a high correlation with element x_2, which also shows good separation between groups. A multivariate analysis assigns a high weight to observation x_1 but a low weight to observation x_2. This apparent contradiction can be resolved as follows.

The observation x_2 contains the same 'information' as observation x_1. Therefore if observation x_1 is included in the analysis there is no need to include observation x_2 as well.

Thus for a given set of elements, the relative importance of each of the important elements can be determined. Some idea of the relative importance of the low weight elements could be obtained by repeating the analysis excluding the elements of high weight.

This statistical technique has been developed for the specific purpose of classifying unknown samples to known sedimentary strata. Apart from this specific application, it can be used to classify unknown samples to known populations, when a graphical representation and the relative importance of the observations are of interest.

11.2 Statistical Analysis of Chip Samples

The statistical analysis of the chip sample data was undertaken using the statistical methods described. The methods and computer routines used for all these analyses have been developed by, and were used under the supervision of Prof. D.M. Hawkins, Department of Statistics, University of the Witwatersrand.

The statistical analysis developed cannot be confidently implemented if any data is missing. For this reason only 11 of the 19 elements

determined in the chip samples were used in the statistical analysis, viz. Th, La, Eu, Yb, Lu, Hf, Ta, Fe, Sc, Cr and Co. Gold was included in the analysis involving only conglomerate samples, as it was determined in all these samples.

The full analysis consisted of several 'runs', in which certain parameters were changed from one run to the next. Full details and results of these statistical analyses are given in Appendix 5, which should be consulted for the relevant data and figures referred to in this section.

Run 1 :

This run included all the samples and the data on the determination of the 11 elements. The Mahalanobis distance, D^2, between population means, and between each sample and each mean, was calculated. Although the distances between population means were relatively small, 40% of the samples were correctly classified, using the 'distance-from the-mean' criterion discussed. A multivariate analysis of variance was carried out and a two-dimensional representation of the samples plotted. (Figure A 5.1). Inspection of the classification obtained, Table A 5.1.2, showed that no quartzite samples had been correctly classified. This suggested that improved classification might be obtained if the quartzite and conglomerate samples were treated separately.

Run 2 :

The data on the conglomerate samples was removed and the quartzite data analysed separately. The values of D^2 between population means increased considerably, see Table A 5.2.1. The D^2 values are much larger than the sample to parent population values and so a 100% accuracy of classification was obtained.

Run 3 :

In this run the quartzite samples were removed from the analysis and only the conglomerate data was used. Gold was included in the analysis to increase the number of elements to twelve.

The results showed a definite improvement on those of Run 1, but were not as good as those for the quartzite samples of Run 2. An overall accuracy of classification of 77% was obtained. The two-dimensional representation obtained from the analysis of variance showed that the samples were fairly well clustered but with some overlap between populations, Figure A 5.3.

Inspection of the data suggested that a subdivision of each population might produce interesting results.

Run 4 :

The conglomerate zones had been sampled at five levels equally spaced within each zone. The five samples taken at each of these levels within the three zones were used to define 15 separate populations.

The results of this analysis showed some improvement over previous analyses. Although only 74% of the samples were classified to the correct level within the parent zone, a further 13% were classified to an incorrect level, but to a level within the parent zone. This implies an overall accuracy of classification to the correct zone of 87%.

Inspection of the classifications obtained, see Table A 5.4.2, showed that 4 of the 20 misclassified samples came from a single level within Zone 6. This suggests that a single sample, perhaps a poor analysis, could have shifted the mean of this level sufficiently to cause the misclassification of the other four samples from the level. This effect would be considerably reduced if population sizes were larger, suggesting that the accuracy of classification obtained might be biased low.

Run 5 :

The analysis of Run 4 involved the complete set of 12 elements. Because of the very nature of the observations, i.e. element concentrations, it could be expected that several of the observations are highly correlated. It is of interest to decrease the number of observations and note what accuracy of classification can be obtained. On the basis of the weights assigned to elements on previous runs, a subset of six elements was selected, viz. La, Eu, Fe, Sc, Cr and Th.

Results obtained were very similar to those of Run 4, with 88% classified to the correct parent zone. The major difference being that only 65% of the samples were classified to the correct parent level, whereas the figure was 74% in Run 4.

The results of the statistical analysis of the chip samples are summarised in Table 11.1.

Table 11.1 SUMMARY OF THE STATISTICAL ANALYSIS OF CHIP SAMPLES

RUN	SAMPLES	PARENT POPULATIONS	ELEMENTS	ACCURACY OF CLASSIFICATION
1	Quartzites & Conglomerates	6	11	40 %
2	Quartzites	3	11	100 %
3	Conglomerates	3	all 12	77 %
4	Conglomerates	15	all 12	87 %
5	Conglomerates	15	'best' 6	88 %

The results show that 100% accuracy of classification of quartzite samples can be obtained, and that the determination of only 6 elements is necessary to classify even conglomerate samples with 88% confidence.

The relative importance of each element in each run is summarised in Table 11.2.

Table 11.2 SUMMARY OF RELATIVE IMPORTANCE OF ELEMENTS FOR CHIP SAMPLES

ARBITRARY SCALE*	RUN 1	RUN 2	RUN 3	RUN 4	RUN 5
>8 - 10	Fe, Co	Cr	Eu	Fe, Co	La, Eu
>6 - 8	Eu	Hf	La	Eu	Fe, Th
>4 - 6	La, Sc, Lu	Co, Ta, Yb, Eu	Sc, Cr	Th	Cr, Sc
>2 - 4	Cr, Yb, Ta	Sc, Th, La	Fe, Lu, Ta, Th, Yb, Co	Cr, La, Sc, Hf, Yb, Ta	
0 - 2	Hf, Th	Fe, Lu	Hf, Au	Lu, Au	

* The most important element is assigned a weight of 10

11.3 Statistical Analysis of Powdered Samples

Visual inspection of the analytical results obtained by I.N.A.A. for the powdered samples showed that there would be no problem in classifying unknown samples using the statistical technique developed. A number of elements showed large variations between zones but relatively small variations within zones.

The problem of missing data was overcome by replacing the unknown values with estimates of the detection limits. This affects the following elements: Au, Ba, Rb, Nd, W and Ni.

Thus it was possible to include all 28 elements in the statistical analysis. Full details of the results obtained are given in Appendix 6, which should be consulted for the relevant data and figures referred to in this section.

The statistical analysis was again divided into a series of runs, based on the exclusion of elements and samples.

Run 1 :

This run included all samples and the data on all 28 elements.

The Mahalanobis distances between population means and each sample were calculated and each sample was classified according to a 'distance-from-the-mean' criterion. The distances between means were at least 100 times larger than the distance between individual samples and parent populations, see Table A 6.1.1. There is thus no doubt that 100% accuracy of classification could be expected. The two-dimensional representation of the population means, obtained from the multivariate analysis, serves to emphasise this fact, see Figure A 6.1. The closest distance between any two populations is that between the two conglomerate zones 6 and 7. Even these two zones are at least as well separated as the quartzite chip samples, (Appendix 5).

Run 2 :

The analysis was repeated using the same 11 elements determined in the chip samples. Again 100% accuracy of classification was obtained, although the population separations did however decrease. This analysis demonstrates that these 11 elements are quite sufficient to separate the zones, depending on the sampling techniques employed.

Run 3 :

In this run the conglomerate samples were removed from the analysis, leaving only the quartzite samples. The point of this analysis was to determine which elements were important to discriminate between the quartzite zones.

Run 4 :

This run was the complement of Run 3 for the conglomerate samples.

The results for the statistical analysis of the powdered samples are summarised in Table 11.3

Table 11.3 SUMMARY OF THE STATISTICAL ANALYSIS OF POWDERED SAMPLES

RUN	SAMPLES	PARENT POPULATIONS	ELEMENTS	ACCURACY OF CLASSIFICATION
1	Quartzites & Conglomerates	6	all 28	100 %
2	Quartzites & Conglomerates	6	chip 11 *	100 %
3	Quartzites	3	all 28	100 %
4	Conglomerates	3	all 28	100 %

* 11 elements determined in the chip samples

The relative importance of the elements to the discrimination for each run is summarised in Table 11.4.

Table 11.4 SUMMARY OF RELATIVE IMPORTANCE OF ELEMENTS FOR POWDERED SAMPLES

ARBITRARY SCALE	RUN 1	RUN 2	RUN 3	RUN 4
>8 - 10	Cr, Ce	Cr, La, Ta	Sc	U
>6 - 8	La	Fe	La	Na, W
>4 - 6	U, Fe, Ta	Sc, Tb. Th, Eu	Na, Cr, Ta, Lu, Eu	Zr, La As, K
>3 - 4	Na		As, Zr, Co, Fe	Ta, Hf

All other elements have weights below 3

11.4 Discussion

Although multivariant statistical techniques are not new to the geosciences, it is only with the advent of large, fast computers that their application has become feasible. Apart from discriminant analysis, methods such as factor analysis, trend surface analysis, cluster analysis, pattern recognition and Markov modelling techniques are becoming more widely used. A great deal of work in the application of these techniques in the geosciences has been carried out at the Kansas Geological Survey's school of geostatistics.

The use of multidimensional statistical techniques to handle data produced from a multi-element analytical technique such as neutron activation is very powerful. Initial inspection of the data on the chip samples offered no hope of being able to differentiate zones, but with the application of statistical methods, quartzite zones could be differentiated with 100 % confidence and conglomerate zones with at least 77 % confidence.

The powdered samples showed greater differences between zones than did the chip samples. Inspection of the element concentration histograms, Appendix 3, shows that elements such as U, As and Ce vary considerably between zones, but are fairly constant within zones. Application of discriminant analysis to the data emphasised these zone separations and indicated that zones could be distinguished with 100 % confidence.

The selection of elements to be included in the statistical analysis is obviously important. In the research phase it is wise to include all possible elements, as one does not know which elements will be important in distinguishing particular zones. Once the problem is better understood the number of elements could well be reduced with no loss in the accuracy of classification.

An attempt has been made to compare the relative importance of elements included in this present analysis.

Elements such as Cr, Fe, Co, La, Ce and Eu are important in order to distinguish quartzite from conglomerate zones. Discrimination between quartzite zones relies on Cr, Sc, La, Co and Na, whereas conglomerate zones are differentiated by U, Na, Eu, La, Sc and Zr.

The statistical methods as applied should not be regarded as complete. Considerable work remains to be done on the problem of the relative importance of elements to the statistical analysis. The present method determines only the relative importance of some elements. A method is required to rank all the elements in the correct order of importance and to supply information on the interrelationship between elements supplying similar discriminatory information.

The method of discriminatory analysis developed for this investigation is of general application to problems requiring the classification of unknown samples to known populations, and several applications in the earth sciences can be foreseen. The use of computers in general and the application of statistical techniques in particular seems to offer a solution to many problems in the geosciences.

12 GEOCHEMISTRY

The objective of this investigation was to determine trace element signatures which could be used to distinguish sedimentary horizons. At no stage was there any intention to undertake a detailed mineralogical or geochemical investigation of the sedimentary horizons studied.

Nevertheless a large number of conglomerates and quartzites have been analysed and quantitative data for the two economically important elements, gold and uranium, have been obtained. There is therefore some interest in attempting a geochemical interpretation of the data.

The samples analysed were from the Kimberley Reef conglomerates at Durban Roodepoort Deep Mine. Any conclusions as to the origin of these conglomerates, and more particu' rly of their gold and uranium, refers only to this portion of the Witwatersrand succession, although similar conclusions may be valid for other regions as well.

12.1 Mineralogy

The mineralogy of the samples has not been investigated. Nevertheless some indication of the minerals present in these samples can be obtained from a study of the literature, e.g. Hiemstra's study of the Dominion Reef, Hi68a, and Brock and Pretorius' summary of the geology of the Witwatersrand system, Br64.

The minerals generally present can be subdivided into those that were syngenetic and those that were epigenetic with the formation of the sediments. A summary of a number of possible detrital (i.e. syngenetic) and hydrothermal (i.e. epigenetic) minerals is given in Table 12.1 together with the elements determined by I.N.A.A. which can occur in these minerals.

Table 12.1 MINERALS GENERALLY PRESENT IN THE WITWATERSRAND SEDIMENTS

	SOURCE	MINERAL	ELEMENTS
DETRITAL MINERALS	GRANITIC	Quartz	
		Zircon	Zr
		Monazite	REE, Th
		Tantalite	Ta
		Cassiterite	
		Thorite	Th
	BASIC	Ilmenite	Ti, Fe, Ta
		Rutile	Ti
		Chromite	Cr, Fe
ALTERATION PRODUCTS	GRANITIC	Sericite (clays)	K
	BASIC	Chlorite	Fe
		Leucoxene	Ti, Fe
PROBABLE HYDROTHERMAL	GRANITIC	Uraninite	U, Th
	SULPHIDES	Galena	
		Covellite	Co
		Cobaltite	Co, Ni
		Pyrite	Fe, Sb, Ni, Co
		Chalcopyrite	Fe, Sb, Ni, Co
		Arsenopyrite	As, Fe, Sb, Ni, Co

Minerals such as zircon and tantalite which are extremely resistant to weathering must be included among the syngenetic minerals. The origin of some of the other minerals is subject to dispute, but it is generally agreed that most of the sulphides, and particularly the pyrite, are epigenetic in that they formed from hydrothermal solutions percolating through the conglomerates. Armed with this knowledge, one can assume that elements correlated with, for example Zr, have detrital host minerals, whereas elements correlated with elements such as Co and Sb are probably contained in minerals of hydrothermal origin.

12.2 Element Interrelationships

Statistical analysis of the data for the determination of 28 elements in the powdered samples suggested that on average the elements are lognormally distributed.

Element interrelationships have therefore been investigated by determining the log correlation coefficients between the 28 elements see Table 12.2. Considering the results to represent replicate analyses of only six different samples, a correlation coefficient of 0.73 is significant at the 90 % confidence level.

Analysis of these correlation coefficients has confirmed that there are three groups of elements which are geochemically related.

(a) Rare Earth Elements

Of the 14 rare earth elements (REE), seven have been determined, namely La, Ce, Nd, Eu, Tb, Yb and Lu. The elements that correlate significantly with these REE and should apparently be included with this group are Th, Sc and Cs.

The distribution of the REE has been investigated by comparing the values obtained to those of an average Chondrite. (He70)

Table 12.2 ELEMENT CORRELATION COEFFICIENTS

	Au	U	Th	Na	K	Ba	Rb	Ce	La	Ce	Nd	Eu	Tb	Yb	Lu	Ti	Zr	Hf	Ta	V	Ga	Fe	Sc	Cr	Co	Ni	As	Sb
Au	1	.48	.39	-.47	-.51	.40	-.30	.40	.10	.28	.10	-.09	.04	.51	.15	.66	.48	-.06	.65	-.32	-.42	.88	.50	-.11	.84	.55	.61	.65
U	.48	1	.68	-.50	-.72	.48	-.27	.79	.24	.54	.46	-.13	.33	.56	-.12	.44	.74	-.08	.92	-.22	-.45	.74	.42	.25	.13	.7[illegible]	.95	.74
Th	.39	.68	1	-.57	-.5	.34	-.17	.82	.81	.97	.61	.56	.62	.92	.34	.59	.89	.54	.86	-.03	.18	.49	.84	.32	.54	.46	.67	.55
Na	-.47	-.50	-.57	1	.84	.06	.43	-.35	-.33	-.50	-.25	-.26	-.27	-.59	-.11	-.49	-.35	.09	-.51	.29	.07	-.28	-.64	.21	-.26	-.13	-.39	-.21
K	-.51	-.72	-.50	.84	1	-.09	.40	-.45	-.07	.38	-.27	.05	-.22	-.42	.08	-.32	-.43	.33	-.61	.41	.41	.38	-.37	.09	-.42	-.02	-.64	-.40
Ba	.40	.48	.34	.06	-.09	1	.05	.49	.10	.27	.43	-.03	.28	.26	-.19	.36	.54	.12	.48	.03	-.24	.47	.17	.31	.53	.16	.52	.53
Rb	-.30	-.27	-.17	.43	.40	.05	1	-.19	.03	-.15	-.24	.00	-.03	-.14	.03	-.24	-.09	.15	-.21	.14	.14	-.14	-.21	.06	-.17	-.05	-.25	-.09
Ce	.40	.79	.82	-.35	-.45	.49	-.19	1	.62	.81	.60	.30	.48	.70	.07	.36	.88	.35	.84	.00	.03	.51	.56	.29	.62	.33	.74	.56
La	.10	.24	.81	-.33	-.07	.10	.03	.62	1	.90	.44	.80	.50	.83	.55	.46	.65	.81	.50	.15	.61	.18	.81	.05	.20	.36	.20	.14
Ce	.28	.54	.97	-.50	-.38	.27	-.15	.81	.90	1	.61	.66	.58	.90	.39	.52	.86	.66	.75	.01	.34	.37	.84	.26	.41	.41	.51	.40
Nd	.10	.46	.61	-.25	-.27	.43	-.24	.60	.44	.61	1	.25	.43	.47	.11	.29	.57	.34	.53	.17	.08	.19	.41	.37	.28	.23	.49	.33
Eu	-.09	-.13	.56	-.26	.05	-.03	.00	.30	.80	.66	.25	1	.5[illegible]	.67	.67	.29	.40	.72	.18	.27	.73	-.07	.71	.10	-.12	.24	-.10	-.02
Tb	.04	.33	.62	-.27	-.22	.28	-.03	.48	.50	.58	.43	.53	1	.60	.18	.34	.60	.37	.52	.29	.22	.18	.56	.48	.21	.29	.43	.42
Yb	.51	.56	.92	-.59	-.42	.26	-.14	.70	.83	.90	.47	.67	.60	1	.53	.67	.81	.60	.79	.00	.27	.57	.96	.15	.55	.59	.53	.52
Lu	.15	-.12	.34	-.11	.08	-.19	.03	.07	.55	.39	.11	.67	.18	.53	1	.35	.20	.53	.11	.15	.50	.14	.59	.05	.06	.33	-.11	.00
Ti	.66	.44	.59	-.49	-.32	.36	-.24	.36	.46	.52	.29	.29	.34	.67	.35	1	.49	.31	.61	.00	-.04	.60	.73	.07	.55	.53	.43	.49
Zr	.48	.74	.89	-.35	-.43	.54	-.09	.88	.65	.86	.57	.40	.60	.81	.20	.49	1	.51	.88	-.02	.00	.63	.69	.44	.69	.50	.76	.72
Hf	-.08	-.08	.54	.09	.33	.12	.15	.35	.81	.66	.34	.72	.37	.60	.53	.31	.51	1	.25	.25	.59	.15	.6[illegible]	.25	.12	.47	-.02	.14
Ta	.65	.92	.86	-.51	-.61	.48	-.21	.84	.50	.75	.53	.18	.52	.79	.11	.61	.88	.25	1	-.10	-.23	.78	.68	.38	.84	.58	.92	.82
V	-.32	-.22	-.03	.29	.41	.03	.03	.00	.15	.01	.17	.27	.29	.00	.15	.00	-.02	.25	-.10	1	.31	-.20	.03	.27	-.20	.10	-.16	-.08
Ga	-.42	-.45	.18	[illegible]	.41	-.24	-.24	.03	.61	.34	.08	.73	.22	.27	.50	-.04	.00	.59	-.23	.31	1	-.43	.32	-.17	-.46	.02	-.47	-.41
Fe	.88	.74	.49	-.28	.38	.47	-.14	.51	.18	.37	.19	-.07	.18	.57	.14	.60	.63	.15	.78	-.20	-.43	1	.51	.21	.97	.73	.74	.85
Sc	.50	.42	.84	-.64	-.37	.17	-.21	.56	.81	.84	.41	.71	.36	.96	.59	.73	.69	.61	.68	.03	.32	.51	1	.06	.46	.60	.39	.42
Cr	-.11.	.25	.32	.21	.00	.31	.06	.29	.05	.26	.[illegible]	.10	.48	.15	-.05	.07	.44	.25	.38	.27	-.17	.21	.06	1	.27	.33	.47	.55
Co	.84	.83	.54	-.26	-.42	.53	-.17	.62	.20	.41	.28	-.12	.21	.55	.08	.55	.69	.12	.84	-.20	-.46	.97	.46	.27	1	.68	.85	.86
Ni	.55	.37	.46	-.13	-.02	.16	-.05	.33	.36	.41	.23	.24	.29	.59	.33	.55	.50	.47	.58	.10	.02	.73	.60	.33	.68	1	.44	.66
As	.61	.95	.67	-.40	-.64	.52	-.25	.74	.20	.31	.49	-.10	.43	.53	-.11	.43	.76	-.02	.92	-.16	-.47	.74	.39	.47	.85	.44	1	.7[illegible]
Sb	.65	.74	.55	-.21	-.40	.53	-.09	.56	.14	.40	.33	-.02	.42	.52	.00	.49	.72	.14	.82	-.08	-.41	.85	.42	.55	.86	.66	.85	1

The distribution pattern of each individual zone, see Figure 12.1, shows that all the zones follow a similar pattern. The results have therefore been combined to give an average conglomerate-quartzite sample.

The REE values for this average conglomerate-quartzite, denoted C-Q ave., are given in Table 12.3, together with values for an average chondrite, an average granite and an average basalt.

Table 12.3 RARE EARTH VALUES FOR AVERAGE ROCK TYPES

ELEMENT	CHONDRITES*	BASALTS*	GRANITES*	C-Q ave.**
La ppm	0.32	6.1	55.	15.
Ce ppm	0.94	16.	104.	33.
Pr ppm	0.12	2.7	12.	(3.8)
Nd ppm	0.60	14.	47.	16.
Sm ppm	0.20	4.3	8.	(2.6)
Eu ppm	0.073	1.5	1.1	0.50
Gd ppm	0.31	6.2	7.4	(1.6)
Tb ppm	0.050	1.1	1.1	0.22
Dy ppm	0.31	5.9	6.2	(1.5)
Ho ppm	0.073	1.4	1.5	(0.36)
Er ppm	0.21	3.6	4.2	(1.0)
Tm ppm	0.033	0.60	0.59	(0.17)
Yb ppm	0.19	3.2	4.3	1.07
Lu ppm	0.031	0.55	0.68	0.14

* Values from He70

** Values within parenthesis have been estimated by interpolation of the REE patte given in Figure 12.2

These average rock types are plotted relative to the chondrite average in Figure 12.2. The results show that the C-Q average follows a similar pattern to the average granite except that the REE concentrations are only about 25 % of those of the granite.

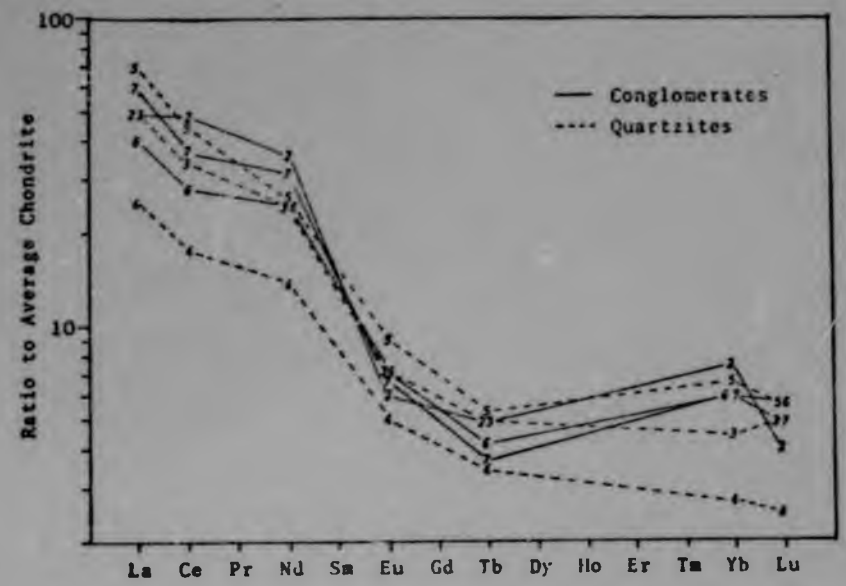


Figure 12.1 RARE EARTH PATTERNS OF EACH ZONE RELATIVE TO CHONDRITES

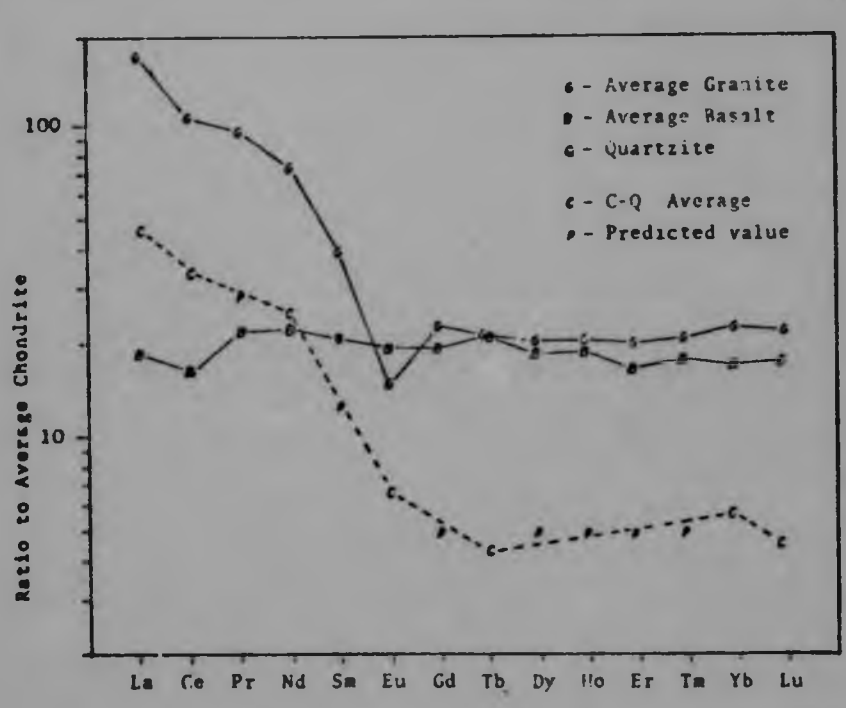


Figure 12.2 RARE EARTH PATTERNS OF AVERAGE ROCK TYPES RELATIVE TO CHONDRITES

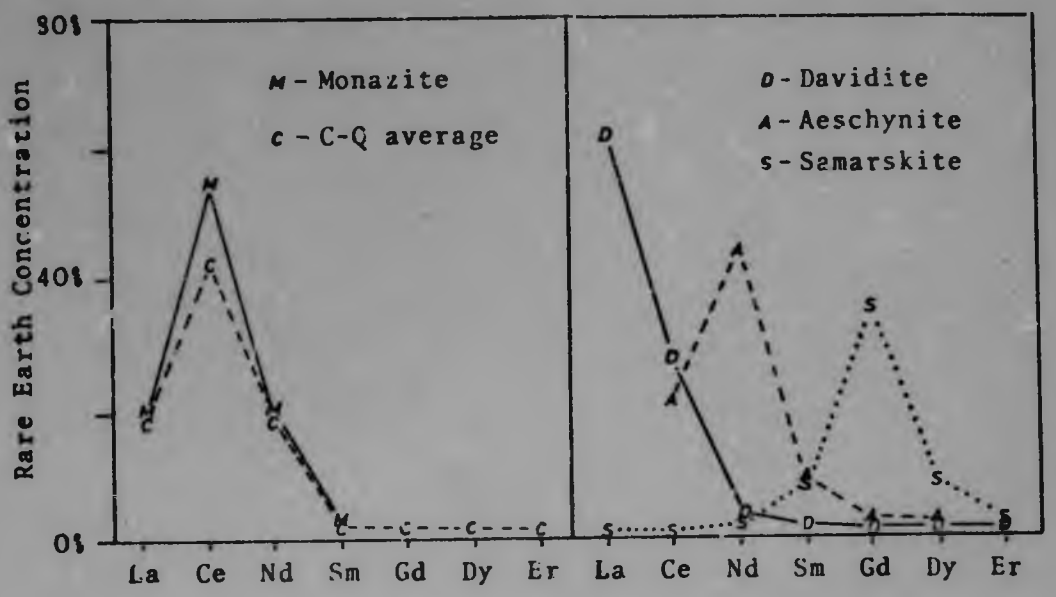


Figure 12.3 DISTRIBUTION OF RARE EARTH ELEMENTS IN SOME RARE EARTH MINERALS (Quoted from He70)

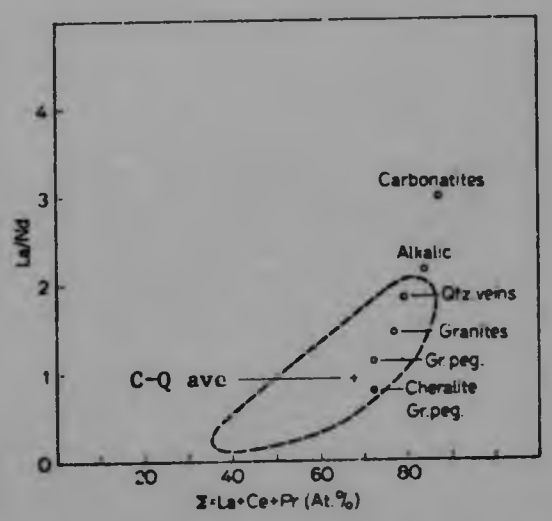


Figure 12.4 DISTRIBUTION OF MONAZITES FROM DIFFERENT PARAGENESES (Quoted from He70)

This suggests that the REE are probably contained in a mineral or minerals from a granitic provenance. The distribution of the REE can also be used to obtain some indication of the REE host mineral. In Figure 12.3, the REE distribution of a number of minerals is plotted together with the C-Q average. This indicates that monazite is the probable host mineral.

Monazite is considered to have a slightly variable REE content, He70. The distribution of monazites from different sources is shown in Figure 12.4. The average conglomerate-quartzite has a composition very similar to that of cheralite, a monazite type mineral from a granite pegmatite which may contain up to 30 % ThO_2. If in fact the REE in the conglomerates are contained in cheralite, it would explain the extremely good correlation of thorium with the REE, see for example the correlation of Th and Ce in Figure 12.5.

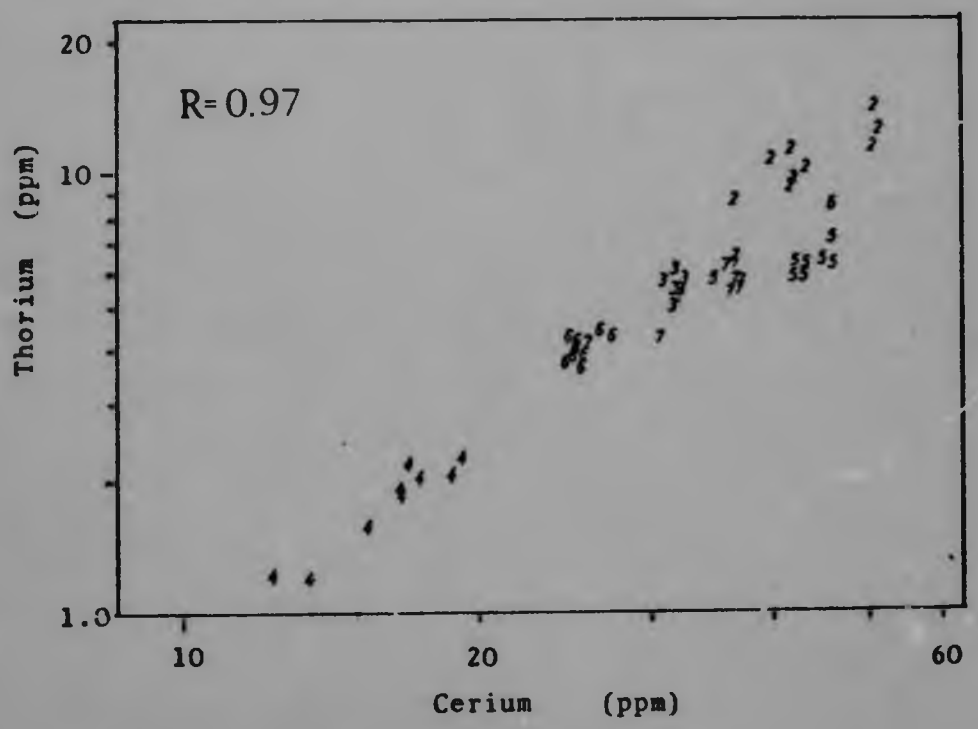


Figure 12.5 SCATTER DIAGRAM OF THORIUM AND CERIUM

Note: The correlation, R, of Th and Ce is 0.97
The symbols used for the plotting of sample points correspond to the parent zone number. This system has been used for all scatter diagrams presented in this chapter.

(b) Detrital minerals

Th detrital minerals are predominantly of granitic origin with some of basic and even ultramafic origin. Granitic source minerals can be characterised by elements such as the REE, Th, Zr and Ta, and the basic minerals by Ti and Cr. The relationship betwee these minerals can be seen from the element correlation coefficients.

	Ce	Yb	Th	Zr	Ta	Ti	Cr
Ce	1	0.90	0.97	0.86	0.75	0.52	0.26
Yb	0.90	1	0.92	0.81	0.79	0.67	0.15
Th	0.97	0.92	1	0.89	0.86	0.59	0.32
Zr	0.86	0.81	0.89	1	0.88	0.49	0.44
Ta	0.75	0.79	0.86	0.88	1	0.61	0.38
Ti	0.52	0.67	0.59	0.49	0.61	1	0.07
Cr	0.26	0.15	0.32	0.44	0.38	0.07	1

The REE patterns have shown that monazite is the most probable REE host mineral, and that it is probably from a granite pegmatite source. There is a strong correlation of the REE with other granitophile elements such as Zr, see Figure 12.6, which tends to confirm the postulated granite source for the REE containing minerals.

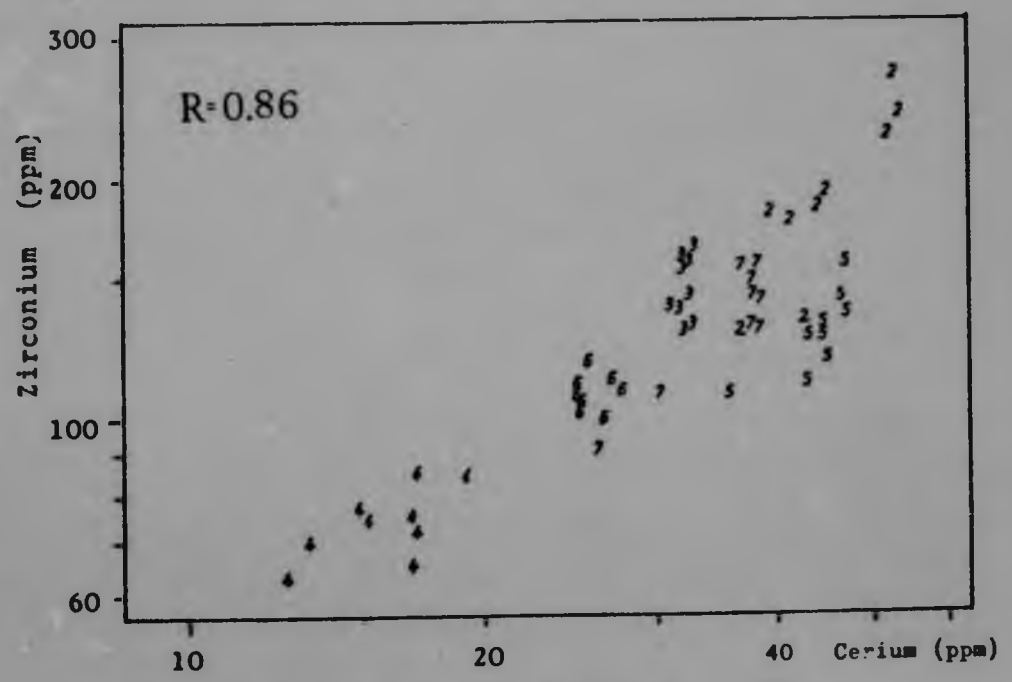


Figure 12.6 SCATTER DIAGRAM OF ZIRCONIUM AND CERIUM

Other granitophile elements such as Zr and Ta, see Figure 12.7, are also strongly correlated, but there appears to be no correlation between the granitophile elements and other elements with probable basaltic host minerals. This fact is emphasised by the poor correlation of Zr and Cr, see Figure 12.8.

Hence one could postulate a predominantly granitic provenance for the Kimberley Reef Conglomerates, with the possibility of a basic source during some ages.

(c) Sulphides

The sulphide phases in the conglomerates are represented by a number of minerals containing elements such as Fe, Co, Ni, As and Sb, which are markedly chalcophile in the Witwatersrand conglomerates. The correlation between these elements is as follows:

	Fe	Co	Ni	As	Sb
Fe	1	0.97	0.73	0.74	0.85
Co	0.97	1	0.68	0.85	0.86
Ni	0.73	0.68	1	0.44	0.66
As	0.74	0.85	0.44	1	0.85
Sb	0.85	0.86	0.66	0.85	1

The poor correlations with nickel are probably due to analytical errors (Chapter 10), but there is a very good overall correlation between these chalcophile elements.

The origin of the sulphides in the Witwatersrand sediments is subject to dispute. Some of the sulphides may be of detrital origin but others are undoubtably products of hydrothermal solutions.

A possible detrital origin can be concluded from the correlation coefficients of the chalcophile elements and elements from detrital host minerals.

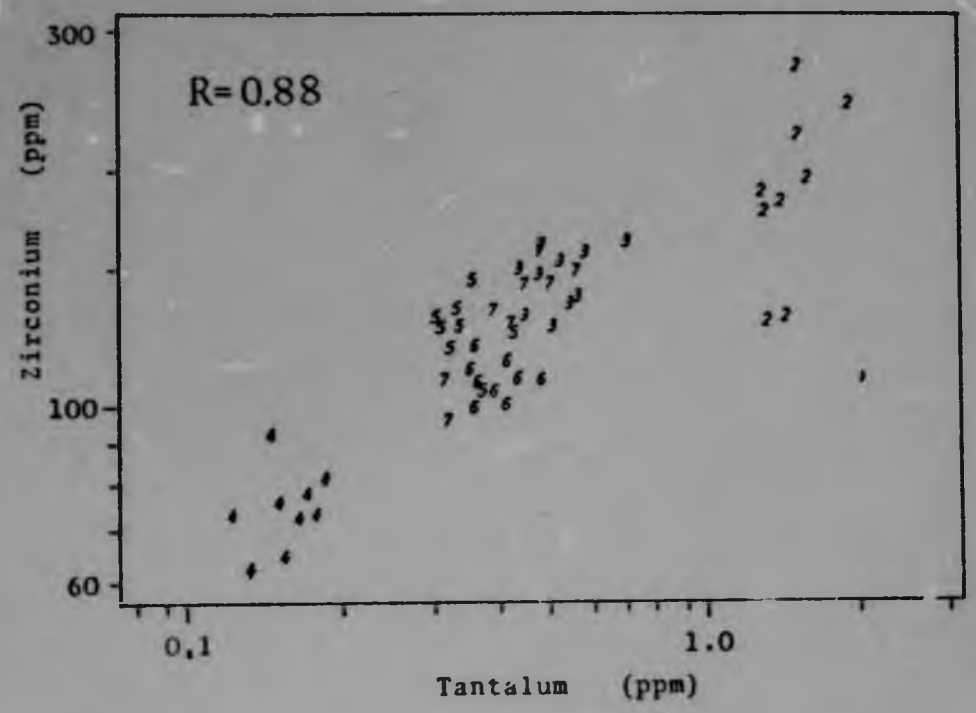


Figure 12.7 SCATTER DIAGRAM OF ZIRCONIUM AND TANTALUM

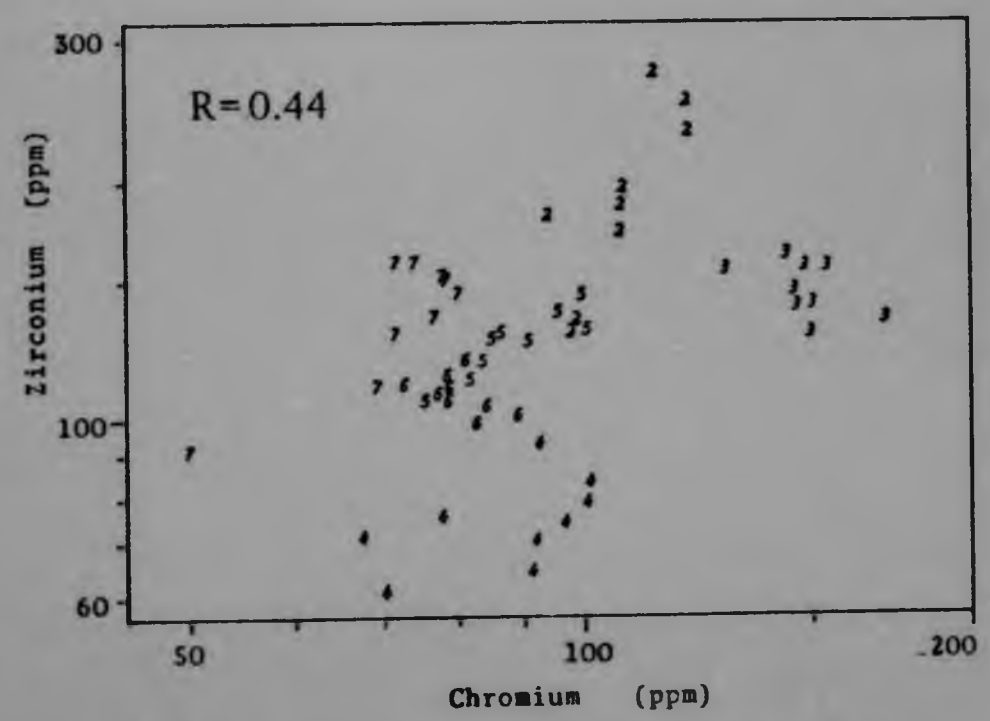


Figure 12.8 SCATTER DIAGRAM OF ZIRCONIUM AND CHROMIUM

	Ce	Yb	Th	Zr	Ta	Ti	Cr
Fe	0.37	0.57	0.49	0.63	0.78	0.60	0.21
Co	0.41	0.55	0.54	0.69	0.84	0.55	0.27
Ni	0.41	0.59	0.46	0.50	0.58	0.55	0.35
As	0.51	0.53	0.67	0.76	0.92	0.43	0.47
Sb	0.40	0.52	0.55	0.72	0.82	0.49	0.55

The chalcophile elements are seen to correlate well with Zr and Ta. The relatively poor correlation of Fe with Zr and Ta is due to the fact that iron is also a constituent of minerals which are neither sulphides nor from a granitic source. Arsenic appears to correlate better with Zr and Ta than with Sb, Co and Fe, which suggests a possible detrital origin for some of the arsenopyrite.

In fact some of the sulphides, e.g. the 'buckshot pyrite', are of detrital origin. (Hi68b) This detrital pyrite could well have acted as nuclei for the growth of later sulphides which would account for the good correlation of the apparently hydrothermal sulphides with the detrital minerals.

12.3 Uranium

The uranium in the Witwatersrand conglomerates is primarily contained in uraninite and the alteration products of this mineral. (Hi68a) The correlation of uranium with elements contained in the detrital minerals is as follows.

	Ce	Yb	Th	Zr	Ta	Ti	Cr
U	0.54	0.56	0.68	0.74	0.92	0.44	0.25

Uranium shows strong correlation with Zr and Ta, see Figure 12.9, but considerably poorer correlation with the other elements. This suggests that the uraninite is of detrital origin, and is from a predominantly granitic source.

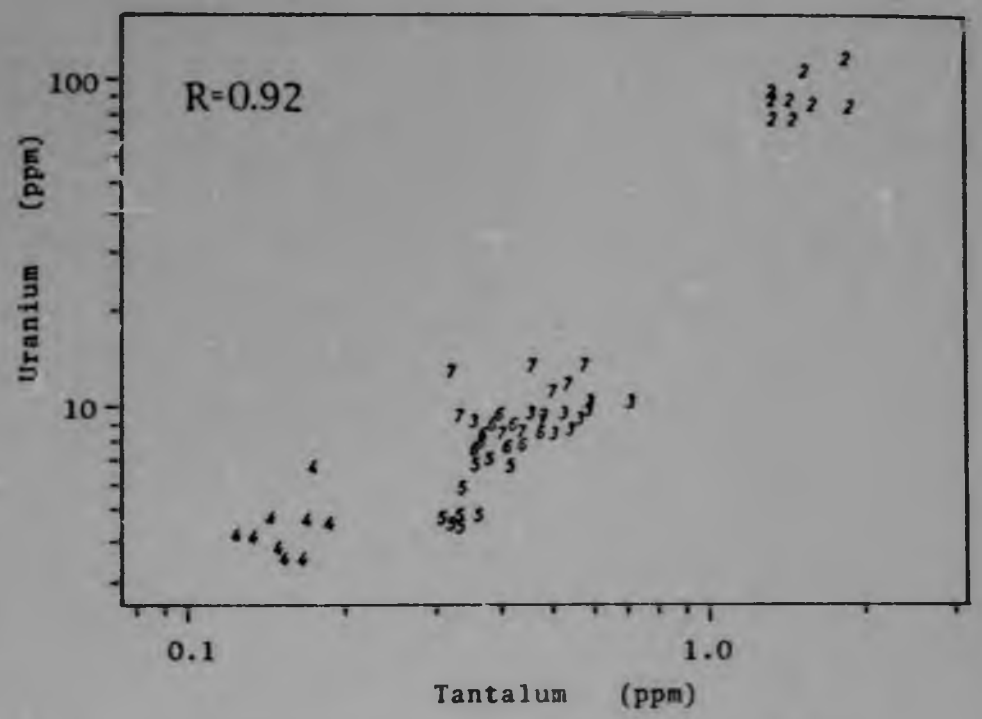


Figure 12.9 SCATTER DIAGRAM OF URANIUM AND TANTALUM

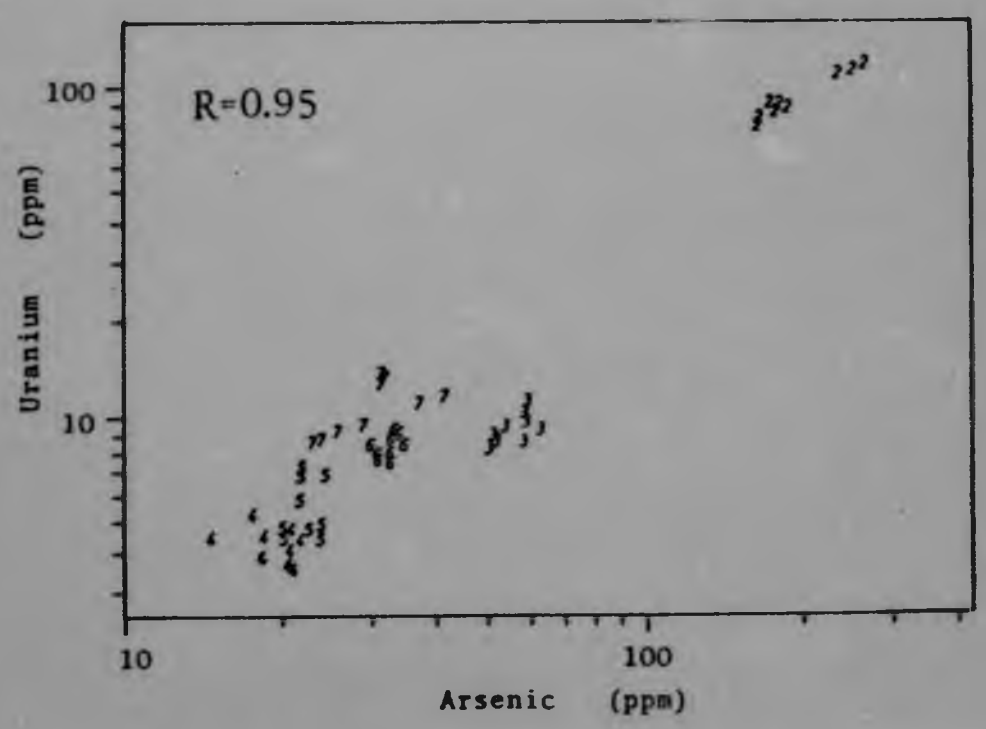


Figure 12.10 SCATTER DIAGRAM OF URANIUM AND ARSENIC

The correlation with the chalcophile elements is also highly significant.

	Fe	Co	Ni	As	Sb
U	0.74	0.83	0.37	0.95	0.74

The good correlation with As, see Figure 12.10, suggests that uraninite and arsenopyrite are highly correlated, and may in fact be of similar origin.

The extreme mobility of the uranyl complex implies that uranium must at some time have suffered some redistribution. The evidence of the good correlations of uranium with the sulphides suggests that the uranium was redistributed to a limited extent at the same time at which the later sulphide minerals were formed.

A stepwise multiple regression analysis of uranium with the other 27 elements determined showed that arsenic is the most important indicator, out that elements such as chromium and caesium are necessary to explain the residual variance. The results of the first three regression steps are as follows:

STEP	REGRESSION	MULTIPLE CORRELATION COEFFICIENT
1	1.23 As	0.950
2	1.39 As - 1.02 Cr	0.977
3	1.25 As - 0.97 Cr + 0.38 Cs	0.981

A locally stable regression of 23 elements gave a multiple correlation coefficient = 0.994.

Since the regression was of log concentrations, the absolute uranium value can be predicted by:

$$[U] = \frac{[As]^{1.25} \quad [Cs]^{0.38}}{[Cr]^{0.97}}$$

Detailed mineralogical investigations of Witwatersrand conglomerates have not shown consistent results as to the correlation of uranium and gold. In the Kimberley Reef Conglomerates sampled in this investigation, the correlation of gold and uranium, see Figure 12.11, is 0.68, which is significant at about the 85 % confidence level.

12.4 Gold

There are two schools of thought as to the origin of gold in the sediments of the Witwatersrand System. The 'hydrothermalists' claim that the presence of the gold is the result of post-depositional hydrothermal activity. The 'placerists' on the other hand assert that the gold was deposited in the basin from the rivers eroding the archean granite basin rim. Nevertheless, they do not deny that, after primary transport of the heavy minerals into the basin, there was probably some minor redistribution of the detrital gold.

The correlation of gold with elements with probable detrital host minerals is as follows:

	Ce	Yb	Th	Zr	Ta	Ti	Cr
Au	0.28	0.51	0.39	0.48	0.65	0.66	-0.11

Gold does not correlate very well with any of these elements, but shows a limited correlation with Ta and Ti, which could suggest a relationship between the metallic gold and ilmenite, a mineral of generally basic origin. The poor correlation of Au with particularly the REE and Zr does not support a granitic origin for the gold as originally postulated.

The correlation of gold with the chalcophile elements is as follows:

	Fe	Co	Ni	As	Sb
Au	0.88	0.84	0.55	0.61	0.65

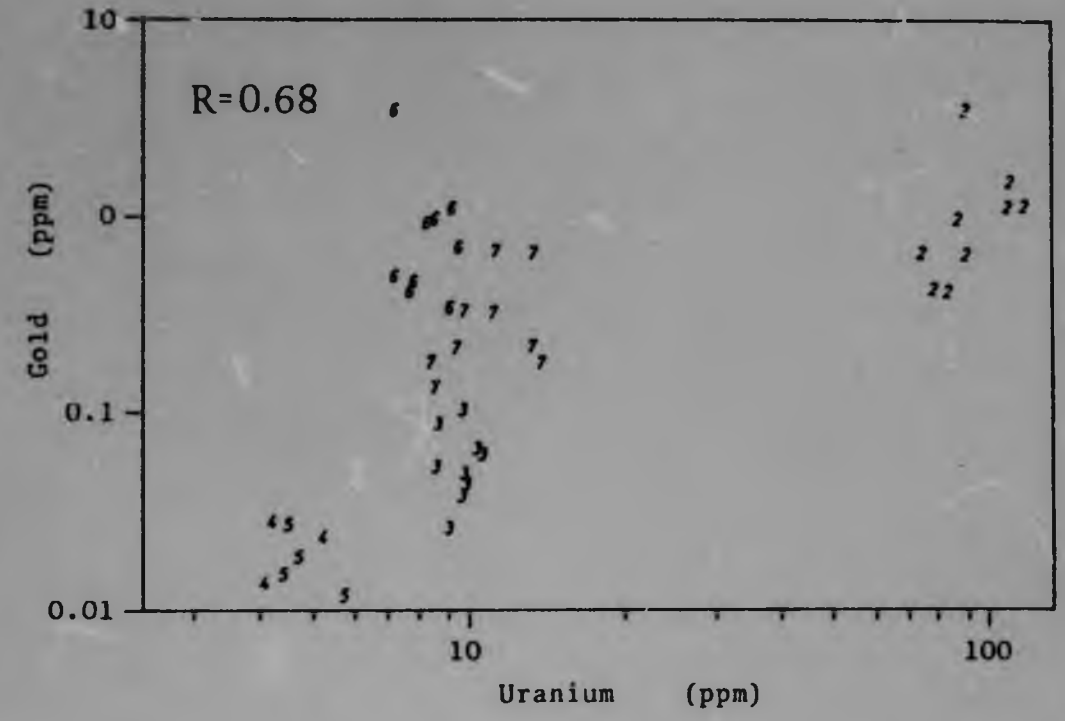


Figure 12.11 SCATTER DIAGRAM OF GOLD AND URANIUM

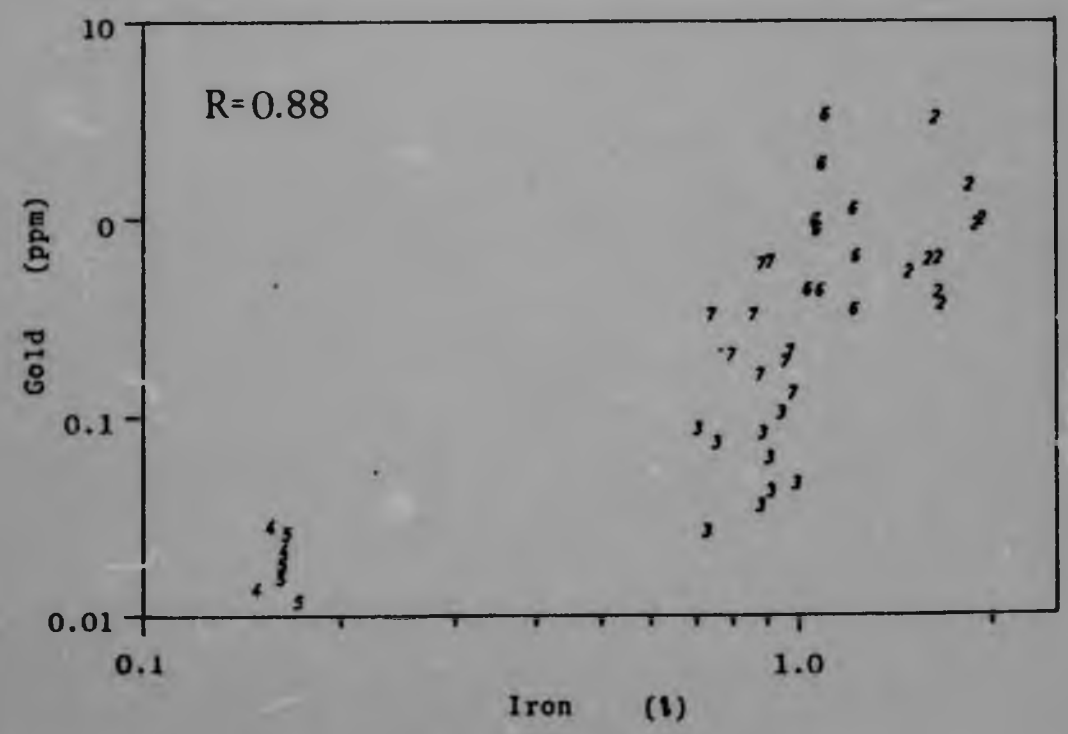


Figure 12.12 SCATTER DIAGRAM OF GOLD AND IRON

Thus Au correlates very well with Co and Fe, see Figure 12.12, but not as well with As (arsenopyrite) for which a possible detrital origin has been postulated, see Section 12.2 (c).

Consideration of the generally poor correlation of gold with elements from detrital host minerals, and the superior correlation with the hydrothermal sulphides suggests that the originally detrital gold has suffered redistribution by hydrothermal solutions at the stage of formation of the later sulphides.

The results for the first four steps of a stepwise regression of gold against the other 27 elements determined are as follows.

STEP	REGRESSION	MULTIPLE CORRELATION COEFFICIENT
1	1.67 Fe	0.876
2	1.80 Fe - 2.10 Cr	0.927
3	1.67 Fe - 2.00 Cr - 0.64 K	0.940
4	1.50 Fe - 1.94 Cr - 0.59 K + 0.54 Ti	0.948

A locally stable regression of 24 elements gave a multiple correlation coefficient of 0.985.

The absolute gold content can therefore be estimated from the following equation.

$$[Au] = \frac{[Fe]^{1.50} \quad [Ti]^{0.54}}{[Cr]^{1.94} \quad [K]^{0.59}}$$

As for the uranium prediction, it is necessary to include elements poorly correlated with gold, such as Cr, to reduce the overprediction obtained from highly correlated elements, in this case Fe and Ti.

12.5 Summary

Investigations of the rare earth element pattern has suggested monazite as the probable REE host mineral. Further analysis has shown that the monazite is probably from a granite pegmatite source.

The elements present in detrital minerals correlate well except for Ti and Cr which are probably contained in minerals of basic or ultramafic origin. These facts suggest a predominantly granitic provenance for the Kimberley Conglomerates, but the possibility of a mixed acidic-basic source cannot be excluded.

Consideration of the correlations of the chalcophile elements with the elements from detrital host minerals suggests that the hydrothermal sulphide formed around detrital sulphide, perhaps arsenopyrite, nuclei.

The good correlations of As, Fe, Co and Zr and Ta with U, suggest a granitic source for the detrital uraninite with a limited amount of hydrothermal redistribution.

Although gold does not correlate very well with elements from detrital host minerals, there is a limited correlation with Ta and Ti. This could suggest a basic rather than granitic source for the gold. The better correlation of gold with the sulphides suggests that the originally detrital gold was redistributed by hydrothermal solutions, at the time of formation of the later sulphides.

13 SUMMARY AND CONCLUSIONS

The objective of this investigation was to set up and develop the technique of instrumental neutron activation analysis and apply it to the analysis of geological material in order to determine trace element patterns which could be used to distinguish sedimentary strata. The aim of the technical developments has been to obtain precise and accurate analyses whilst exploiting the multi-element capability of the technique to the full.

Investigation of the neutron flux gradients in the reactor Safari I has shown that the neutron dosages received by a suite of samples irradiated within a single container can vary by 10 to 20 %. The use of iron foil to monitor both the thermal and fast neutron flux received by individual samples has shown that the errors due to neutron flux variations can be reduced to less than 1 %. In addition, methods have been proposed to correct for the residual error due to the contribution of epithermal neutrons to (n, γ) reaction cross sections.

The optimisation of irradiation and decay times has been approached via an empirical method. Computer programmes have been developed to analyse data obtained from the irradiation and counting of representative sample types. This analysis calculates the decay time at which any particular element can be determined with minimum error. A graphical method of determining optimum decay times for the analysis of multi-element samples is presented.

An attempt has been made to analyse the errors associated with each phase of the technique of I.N.A.A. For example, sample preparation methods have had to be altered to reduce possible contamination. The effect of count rate on the determination of peak areas in gamma spectroscopy has been investigated and methods have been developed to correct for pulse losses. In this respect, the positioning of samples has been shown to be critical.

An important but often neglected aspect of I.N.A.A. is that of peak and reaction interferences. Both of these have been investigated and suitable corrections applied as necessary. A knowledge of the geochemistry of the samples can often be useful as an indicator of unexpected interferences, for example uranium fission products. Neglect of possible interferences can lead to results which are very precise but completely inaccurate.

The precision of the technique developed has been estimated from 23 replicate analyses of a powdered quartzite for 28 elements. The element concentrations ranged from gold at 0.045 ppm to iron at 7100 ppm, with a median value of 10 ppm. The corresponding errors on these determinations had a median value of 6 %.

The accuracy of the technique has been measured by analysing a series of standard reference materials. A comparison of measured and reference values for 23 elements determined in four U.S.G.S. multi-element rock standards has shown that the median accuracy is about 6 % for element concentrations ranging from less than 1 ppm to about 10 %.

The technique has been applied to the analysis of gold bearing sediments from the Kimberley Reef Conglomerates, Witwatersrand System, at the Durban Roodepoort Deep Mine. A series of three conglomerate and three quartzite zones have been sampled by drilling three borehole cores through the region of interest. Initially the first core was sampled using a small diamond core drill to produce 'chip' samples. These chip samples were then analysed without any further sample preparation. In addition, homogenised powdered samples were prepared for each zone from each of the three borehole cores. These samples were analysed in triplicate for 28 elements.

Simple visual inspection of the results from the analysis of the chip samples showed no distinct between-zone differences. Inspection

of the powdered sample analyses indicated that a trace element pattern could be developed to distinguish zones. However, statistical methods have been used to accurately define these differences.

The statistical method applied was that of discriminant analysis, which is capable of the simultaneous analysis of all the data produced by a multi-element technique such as I.N.A.A. The technique was by calculating the Mahalanobis Distance between samples and the mean of each zone, and by classifying samples by a distance-from-the-mean criterion. A 100 % accurate classification of quartzite chip samples was obtained and an 87 % correct classification of conglomerate chip samples. Application of this technique to the powdered samples indicated that both quartzite and conglomerate samples could be classified with 100 % confidence.

This present investigation has been limited to three closely spaced borehole cores intersecting six sedimentary strata. The next phase of this investigation should be to investigate large scale within-zone variations. If the within-zone variations are too large they could mask any between-zone variations which might exist. Only when this phase has been successfully completed should any further sedimentary strata be included in the analysis.

In the course of this investig n some 4000 determinations of trace and minor elements in conglomerates and quartzites have been made. In particular the two elements of economic importance in these sediments, namely gold and uranium, have been determined. An investigation of the geochemical relationships between the elements determined is therefore of interest to obtain some indication as to the origin of the gold and uranium and of the sediments themselves. Inspection of the correlations between elements contained in detrital minerals suggests a predominantly granitic provenance for the Kimberley Reef Conglomerates, although a mixed source cannot be excluded. The gold, uranium and some of the

sulphides appear to be of detrital origin, but both the uranium and the gold may have suffered redistribution by hydrothermal solutions at the time of formation of the epig .etic sulphides.

In conclusion it can be stated that a precise and accurate analytical technique has been developed which has been applied successfully to the analysis of geological material. Statistical analysis of the data obtained has shown that it is possible to use trace element patterns to distinguish sedimentary strata.

APPENDIX 1 STANDARDS

CONTENTS

Table A 1.1 OPTIMUM DECAY PERIODS AND ERRORS FOR THE ANALYSIS OF STANDARDS

Table A 1.2 REFERENCE AND MEASURED VALUES FOR THE MULTI-ELEMENT ROCK STANDARDS

Table A 1.3 REFERENCE AND MEASURED VALUES FOR SINGLE ELEMENT ROCK STANDARDS AND PREPARED SOLUTIONS

Table A 1.4 REFERENCES USED FOR COMPILING STANDARD VALUES

Table A 1.1 OPTIMUM DECAY PERIODS AND ERRORS FOR THE ANALYSIS OF STANDARDS

		G - 2		GSP - 1		BCR - 1		BTS - 1		NIM - G		NIM - S		NIM - L		NIM - N		NIM - P		NIM - D	
ISOTOPE	ENERGY	DECAY	ERROR	DECAY	ERROR	DECAY	ERROR	DECAY	ERROR	DECAY	ERROR	DECAY	ERROR	DECAY	ERROR	DECAY	ERROR	DECAY	ERROR	DECAY	ERROR
^{46}Sc	1121	< 2	2 %	< 2	4 %	< 5	10 %			< 5	5 %	1 - 6	1 %								
^{24}Na	1368	1 - 6	0.5 %	2 - 6	0.5 %	2 - 6	0.5 %	1 - 6	0.5 %	1 - 6	1 %	1 - 6	0.5 %	1 - 7	1 %	1 - 6	0.5 %	1 - 6	1 %	1 - 6	0.5 %
	2753	2 - 6	1 %	2 - 6	1 %	2 - 6	1 %	1 - 7	1 %	1 - 6	1 %	1 - 6	1 %	1 - 7	1 %	1 - 6	1 %	1 - 6	1 %	1 - 6	1 %
^{99}La	559									6 - 20	6 %										
^{165}Dy	293			6 - 8	10 %					6 - 7	10 %										
^{140}La	329	9 - 12	1 %	9 - 15	1 %	9 - 11	4 %			8 - 13	1 %	8 - 20	4 %	4 - 10	2 %	9 - 11	15 %				
	1596	9 - 9	1 %	9 - 8	2 %	4 - 10	2 %	2 - 8	10 %	4 - 8	2 %	8 - 12	2 %			9 - 9	14 %			9 - 9	20 %
^{175}Yb	396	8 - 12	0 %	8 - 12	12 %	8 - 12	12 %			8 - 11	2 %	8 - 10	16 %	9 - 6	4 %						
	470	8 - 12	0 %	8 - 12	12 %	9 - 10	16 %			8 - 11	2 %	8 - 10	12 %	6 - 10	0 %						
^{177}Yb	396	8 - 10	0 %	4 8	8 %	9 - 11	8 %			8 - 15	1 %			10 - 12	8 %	8 - 12	24 %				
^{177}La	208	8 - 16	10 %	8 - 12	8 %	7 - 14	4 %			10 - 20	1 %					8 - 16	16 %				
^{131}Ba	496	10 - 16	2 %	10 - 20	3 %	10 - 20	8 %			< 10	0 %	9 - 20	2 %	10 - 20	8 %						
^{147}Nd	531	8 - 12	12 %	10 - 25	6 %					16 - 20	5 %			8 - 14	16 %						
^{85}Sr	1090	< 10	4 %	< 10	4 %	10 - 30	12 %			< 10	1.5 %	< 10	1 %	< 17	4 %						
^{233}Pa	300	< 10	1 %	< 10	1 %	< 10	4 %			< 15	1 %	< 20	13 %	< 20	2 %						
	312	< 10	1 %	< 10	0.5 %	< 10	1 %			< 10	0.5 %	< 20	14 %	< 15	0.4 %						
^{51}Cr	320	< 10	10 %	< 10	8 %	< 20	24 %	4 %	0.8 %	< 20	4 %	< 20	8 %			< 30	12 %	< 15	0.2 %	< 30	0.3 %
^{169}Yb	177	< 20	20 %	< 20	15 %	< 15	12 %			< 20	1 %			< 20	3 %	< 15	10 %				
	198	< 25	14 %	< 10	8 %	< 15	8 %			< 15	1 %			< 15	4 %	< 10	15 %				
^{141}Ce	145	< 10	1 %	< 15	1 %	< 12	2 %	< 20	2 %	< 15	0.5 %	< 20	4 %	< 15	0.5 %	< 20	5 %			< 20	2 %
^{181}Hf	133	< 12	3 %	< 10	2 %	< 15	4 %			< 15	1 %			< 15	0.2 %						
	482	< 20	1 %	< 10	2 %	< 20	8 %			< 15	1.2 %	< 30	10 %	< 20	0.3 %						
^{75}Se	1099	< 20	1.2 %	< 10	1 %	< 10	1 %	< 15	0.8 %	< 20	1 %	< 10	1 %	< 17	0.8 %	< 10	0.5 %	< 10	1 %	< 10	0.4 %
	1202	< 20	1 %	< 15	1 %	< 10	1 %	< 15	0.6 %	< 15	1 %	< 10	1 %	< 17	0.8 %	< 10	0.5 %	< 10	0.8 %	< 10	0.3 %
^{124}Sb	1691	< 15	15 %	< 20	6 %	< 20	10 %	< 10	20 %	< 15	4 %	< 20	10 %	< 30	20 %			< 10	20 %		
^{95}Zr	724	< 10	24 %	< 20	12 %					< 20	8 %			< 17	2 %						
	757	< 30	12 %	< 20	15 %					< 20	10 %			< 17	2 %						
^{51}Cr	319							< 15	1.6 %							< 30	20 %	< 10	8 %	< 20	2 %
^{198}Au	899	< 30	10 %	< 15	12 %	< 20	10 %			< 15	2 %			< 20	20 %						
	1170									< 20	2 %										
^{46}Sc	889	< 10	1 %	< 10	1 %	< 10	0.4 %	< 15	1.2 %	< 20	2 %	< 10	0.5 %	< 10	12 %	< 8	0.3 %	< 10	0.8 %	< 10	1.5 %
	1120	< 10	1 %	< 10	1 %	< 10	0.8 %	< 15	1.2 %			< 10	0.8 %			< 8	0.3 %	< 10	0.4 %	< 10	0.8 %
^{182}Ta	1121									< 20	1 %			< 15	1 %						
	1222	< 30	6 %	< 20	10 %	< 15	15 %			< 20	1 %			< 15	1 %						
														< 20	4 %						
^{85}Sr	1115																				
^{51}Cr	834	< 10	7 %	< 20	3 %	< 10	4 %	< 12	1 %	< 20	4 %	< 24	6 %	< 15	3 %	< 20	4 %	< 10	9 %	< 10	2 %
^{139}Ce	661	< 10	10 %	< 20	3 %	< 15	15 %			< 20	3 %			< 20	4 %						
	796	< 12	12 %	< 15	20 %	< 20	16 %			< 20	10 %	< 10	2 %	< 25	10 %						
^{46}Sc	1173	< 20	4 %	< 15	4 %	< 15	2 %	< 12	0.4 %			< 14	4 %	< 20	8 %	< 10	1 %	< 10	1 %	< 10	0.4 %
	1338	< 20	4 %	< 15	4 %	< 10	2 %	< 12	0.4 %	< 30	8 %	< 30	3 %	< 20	8 %	< 10	1 %	< 20	2 %	< 10	0.4 %
						< 20	4 %			< 30	4 %	< 30	10 %	< 30	8.6 %	< 15	12 %				
^{152}Eu	344	< 20	8 %			< 10	8 %			< 20	5 %	< 20	5 %	< 20	5 %	< 15	15 %				
	1407	< 20	4 %	< 20	4 %																

NOTES

(1) Standards were irradiated for 1.0 hour at a flux of 5×10^{13} n/cm^2/sec.

(2) Decay period is given in days.

(3) Errors are given for a 1 hour counting period.

(4) Isotopes are listed in order of increasing halflife.

(5) Samples were only counted after 2 days decay and up to 60 days. Therefore < 2 days implies that the minimum optimum decay time is less than 2 days, but the actual decay period for optimum determination is unknown.

Table A 1.2 REFERENCE AND MEASURED VALUES FOR THE MULTI-ELEMENT ROCK STANDARDS

Reference Standard	URANIUM ppm			THORIUM ppm			SODIUM %			POTASSIUM %			BARIUM ppm			RUBIDIUM ppm			CAESIUM ppm		
	REF.	MEASURED	DIFF.	REF.	MEASURED	DIFF.	REF.	MEASURED	DIFF.	REF.	MEASURED	DIFF.	REF.	MEASURED	DIFF.	REF.	MEASURED	DIFF.	REF.	MEASURED	DIFF.
U.S.G.S.																					
G-2	2.1	2.0 ± 0.1	- 4.8 %	21.1	21 ± 1	- 0.4 %	2.861	2.88 ± 0.1	- 0.1 %	3.7	3.8 ± 0.4	+ 2.7 %	1920	1930 ± 50	0 %	174	174 ± 4	0 %	1.15	1.4 ± 0.1	+22 %
GSP-1	3.2	3.3 ± 0.3	+ 3 %	106	104 ± 5	0 %	2.157	2.06 ± 0.1	- 3.7 %	4.39	4.4 ± 0.4	+ 0.2 %	1375	1340 ± 40	- 0.4 %	240	240 ± 10	0 %	0.92	1.4 ± 0.1	+52 %
BCR-1	1.8	1.3 ± 0.3	- 6.1 %	6.1	7.2 ± 0.3	+21 %	2.498	2.52 ± 0.1	+ 2.3 %	1.40	1.1 ± 0.2	-30 %	721	700 ± 30	- 3.4 %	50	82 ± 10	+ 24 %	0.97	1.1 ± 0.3	+20 %
BIR-1		-			-		0.007			0.017	-						-			-	
U.S.N.																					
NIM G	13	11 ± 3	-15 %	51.5	51 ± 3	- 0.8 %	2.49	2.46 ± 0.1	- 0.8 %	4.23	5.2 ± 0.4	+24 %	130	N.D.		340	335 ± 15	- 1.5 %	1.1	1.09 ± 0.1	- 0.9 %
NIM S	0.6	0.7 ± 0.1	+17 %	0.6	1.0 ± 0.1	+67 %	0.119	0.177 ± 0.01	+ 15 %	12.8	18.0 ± 0.8	+41 %	1830	1160 ± 100	-39 %	543	690 ± 20	+ 27 %	6.6	7.4 ± 0.3	+12 %
NIM L	13	11 ± 3	- 8.3 %	44.3	41 ± 3	- 8.5 %	0.72	0.77 ± 0.2	- 0.8 %	4.38	-		840	300 ± 30	-13 %	274	218 ± 8	- 6.8 %	3.75	3.2 ± 0.1	+18 %
NIM P	0.2	-		0.2	0.37 ± 0.02	+18 %	1.91	1.91 ± 0.1	+ 4.9 %	0.212	-		105	-		2.1	-			-	
NIM T	0.4	-		1.1	-		0.766	0.723 ± 0.01	+ 2.8 %	0.076	-		82	-		3.1	-			-	
NIM D	0.2	-			-		0.02	0.001 ± 0.003	- 35 %	0.0161	-		13	-		41.2	-			-	
U.S.T.																					
MH 237	0.4			3.0	1.8 ± 0.2	-40 %	0.91	0.93 ± 0.04	+ 0 %	0.437	0.4 ± 0.3	- 7.3 %	139	185 ± 20	+32 %	19.3	42 ± 10	+118 %	2.05	2.4 ± 0.3	+17 %

Reference Standard	LANTHANUM ppm			CERIUM ppm			NEODYMIUM ppm			EUROPIUM ppm			TERBIUM ppm			YTTERBIUM ppm			LUTETIUM ppm		
	REF.	MEASURED	DIFF.	REF.	MEASURED	DIFF.	REF.	MEASURED	DIFF.	REF.	MEASURED	DIFF.	REF.	MEASURED	DIFF.	REF.	MEASURED	DIFF.	REF.	MEASURED	DIFF.
U.S.G.S.																					
G-2	81	84 ± 3	+ 3.7 %	150	138 ± 6	-10 %	31	31 ± 3	0 %	1.4	1.4 ± 0.1	0 %	0.52	0.56 ± 0.04	+7.8 %	0.85	0.93 ± 0.1	+11.7 %	0.14	0.14 ± 0.02	0 %
GSP-1	171	172 ± 5	+ 0.6 %	320	320 ± 20	0 %	140	140 ± 10	0 %	2.2	2.2 ± 0.1	0 %	1.3	1.3 ± 0.1	0 %	2.0	2.0 ± 0.2	0 %	0.17	+0.27	
BCR-1	25.7	31 ± 1	+21 %	53	50 ± 8	- 5.7 %	32	N.D.		1.98	2.01 ± 0.1	+ 1.5 %	0.96	0.97 ± 0.17	+1.0 %	3.2	3.25 ± 0.1	+ 1.6 %	0.34	0.34 ± 0.02	0 %
BIR-1	≈0.3	0.17 ± 0.05			-			-			-			-			-			-	
U.S.N.																					
NIM G	107.7	108 ± 8	+ 0.3 %	194	150 ± 10	-23 %	42	43 ± 5	+2.5 %	1.85	0.36 ± 0.1	-80 %	3.3	3.3 ± 0.2	≈0.0 %	8.0	14.0 ± 0.5	+75 %	2.1	1.7 ± 0.1	-43 %
NIM S	71.4	56 ± 4	-27 %	11.6	11.3 ± 1	≈ 0.0 %	10	-		0.43	0.39 ± 0.03	-23 %		-		≈3	-		0.05	-	
NIM L	236	192 ± 8	-19 %	290	220 ± 20	-24 %	17	30 ± 3	+66 %	2.0	1.03 ± 0.1	-48 %	0.77	0.76 ± 0.1	-1.3 %	3.3	5.8 ± 0.5	+82 %	1.0	+0.5	
NIM P	3.4	2.7 ± 0.5	-20 %	12	≈5		7.3	-		0.61	0.61 ± 0.05	+ 1.0 %		-		≈3	0.6 ± 0.1		0.39	0.2 ± 0.1	0 %
NIM T	2.6	1.9 ± 0.2	-27 %	80	-		40	-		0.23	0.22 ± 0.03	+12 %		-		≈3	0.6 ± 0.2		-	-	
NIM D	0.4	0.12 ± 0.05	-70 %	≈10	-		16	-		0.09	-			-		≈3	-		-	-	
U.S.T.																					
MH 237	9.3	9.4 ± 0.4	+ 1.: %	19.6	20 ± 10	+2 %	11	-		0.74	0.8 ± 0.07	+ 5.0 %	0.58	-		+0.8	1.0 ± 0.1		0.19	0.17 ± 0.01	-10 %

Table A 1.2 (cont.) REFERENCE AND MEASURED VALUES FOR THE MULTI-ELEMENT ROCK STANDARDS

Reference Standard	IRON %			SCANDIUM ppm			CHROMIUM ppm			COBALT ppm			NICKEL ppm			ANTIMONY ppm		
	REF.	MEASURED	DIFF.	REF.	MEASURED	DIFF.	REF.	MEASURED	DIFF.	REF.	MEASURED	DIFF.	REF.	MEASURED	DIFF.	REF.	MEASURED	DIFF.
U.S.G.S.																		
G-2	1.82	1.76 ± 0.03	-4.0 %	3.3	3.3 ± 0.2	0 %	8.4	12 ± 1	+43 %	4.9	4.9 ± 0.3	0 %	8.4	-		0.33	0.37 ± 0.7	+49 %
GSP-1	5.00	5.0 ± 0.1	-0.7 %	9.9	9.7 ± 0.2	-3.6 %	11	14 ± 2	+27 %	7.5	7.5 ± 0.3	0 %	7	-		1.38	1.7 ± 0.2	+23 %
MON-1	9.28	9.27 ± 0.3	+0.1 %	31.9	32 ± 1	+0.2 %	16	16 ± 1	+16 %	38.2	38 ± 2	- 0.5 %	13	-		0.61	0.61 ± 0.1	0 %
MRG-1	8.06	8.7 ± 0.1	+1.0 %	5.33	5.4 ± 0.2	+1.3 %	4165	4160 ± 100	0 %	340	340 ± 1	0 %	1440	1480 ± 100	+6.4 %	0.1	0.1 ± 0.7	0 %
W.G.H.																		
DTS-1	1.1	1.08 ± 0.05	-7.4 %	0.37	0.37 ± 0.04	+0.4 %	10	10 ± 1	7 %	3.3	4.0 ± 0.2	+27 %	20	-		0.41	0.33 ± 0.05	+19 %
DTS-2	8.98	-	+7.3 %	4.3	4.4 ± 0.2	+2.3 %	10	12 ± 1	+20 %	5.6	3.4 ± 0.3	- 3.6 %	15	-		0.68	0.17 ± 0.01	+11 %
DTS-3	8.9	8.83 ± 0.3	+0.7 %	0.37	0.36 ± 0.04	-1.7 %	11	-		3.3	3.3 ± 0.2	- 0 %	20	-		0.29	0.19 ± 0.01	-34 %
DTS-4	9.26	8.93 ± 0.1	-0.1 %	39.3	41 ± 2	+4.3 %	20	20 ± 2	+12 %	60	58 ± 2	- 3.3 %	125	115 ± 3	-8.4 %	0.21	-	
DTS-5	8.78	8.8 ± 0.2	+0.2 %	35.3	35.3 ± 2	-3.3 %	34360	35200 ±2000	+ 4.8 %	112	111 ± 2	- 0.8 %	600	600 ± 20	0 %	0.77	0.74 ± 0.04	-48 %
DTS-6	11.0	11.0 ± 0.3	-0.3 %	3.4	4.7 ± 0.3	+4.9 %	3000	3500 ± 100	+ 0.6 %	370	338 ± 5	- 5 %	2040	1920 ± 100	-7.7 %	0.65	-	
U.S.T.																		
NK 227	8.22	8.47 ± 0.3	+1.2 %	35.5	38 ± 1	+7.7 %	1730	1780 ± 90	+ 1.7 %	84.3	84 ± 2	- 0.3 %	863	850 ± 50	-1.7 %	1.1	1.3 ± 0.05	0 %

Reference Standard	TITANIUM %			ZIRCONIUM ppm			HAFNIUM ppm			TANTALUM ppm		
	REF.	FOUND	DIFF.	REF.	MEASURED	DIFF.	REF.	MEASURED	DIFF.	REF.	MEASURED	DIFF.
U.S.G.S.												
G-2	0.318	0.337	+ 6.0 %	271	330 ± 47	+ %	7.8	7.7 ± 0.3	1.3 %	0.9	0.87 ± 0.05	- 3.3 %
GSP-1	0.414	0.418	+ 1.0 %	340	337 ± 7	- 1	14.8	14 ± 0.3	5	1.1	0.92 ± 0.07	-21 %
MON-1	1.339	1.20	-10 %	191	-		6.8	3.7 ± 0.4	19 %	0.5	0.46 ± 0.04	- 8.7 %
DTS-1		-			-			-			-	
W.G.H.												
DTS-2	0.054	-		300	304 ± 40	0 %	11.7	11.3 ± 1	11 %	3.0	-	
DTS-3	0.03	N.D.		40	-		-	0.09 ± 0.04	+11 %		-	
DTS-4	0.30	-		11600	83	-	272	N.D.		11	11 ± 2 %	- 8.3 %
DTS-5	0.13	N.D.		23	-		5	-			-	
DTS-6	0.13	N.D.		23	-			-			-	
NIM-D	0.912	-		4100	-			-			-	
U.S.T.												
NK 227	0.422	N.D.			-			2.0 ± 0.2			1.30 ± 0.07	

Table A 1.3 REFERENCE AND MEASURED VALUES FOR SINGLE ELEMENT ROCK STANDARDS AND PREPARED SOLUTIONS

STANDARD	ELEMENT	REF. VALUE	MEASURED	DIFFERENCE
(1) U.C.T. SHALES				
M38	Cs ppm	12.1	11.3 ± 0.5	-6.4 %
M39	Cs ppm	5.92	5.8 ± 0.2	-2.0 %
M60	Cs ppm	17.0	18.4 ± 0.4	+8.2 %
M38	Rb ppm	206	218 ± 10	+5.9 %
M39	Rb ppm	100	98 ± 5	-2.0 %
M60	Rb ppm	298	360 ± 15	+20 %
M63	Rb ppm	273	340 ± 10	+22 %
(2) NIM STANDARDS				
5/67	U ppm	68.0	68.0	0 %
61/67	W ppm	5950	5950	0 %
18/68	Cs ppm	392	315 ± 20	-20 %
18/68	Rb ppm	3700	3850 ± 50	+0.4 %
64/69	Ti %	5812	5812	0 %
107/69	Ta ppm	4013	4013	0 %
214/69	Ta ppm	44	44 ± 1	+0 %
(3) OTHERS				
Au-A	Au ppm	90.8	90.8	0 %
SG-95	Au ppm	0.11	-	-

Table A 1.3 (cont.) REFERENCE AND MEASURED VALUES FOR SINGLE ELEMENT ROCK STANDARDS AND PREPARED SOLUTIONS

(4) PREPARED SOLUTIONS

ELEMENT	WEIGHT (ug)	MEASURED WT	COMMENT
As	52.9	52.9	Used as standard
Au	5.56	8.7	Based on Au-A
Ba	52.5	112 ± 10	Based on G-2
Ca	462		No comparison
Lu	2.08	1.82 ± 0.2	Based on BCR-1
Mo	52.0		No comparison
Nd	56.8	34 ± 3	Based on GSP-1
Sb	5.71	2.18 ± 0.5	Based on BCR-1
Tb	2.08	2.7 ± 0.2	Based on GSP-1
U	5.24	4.2 ± 0.2	Based on 5/67
Yb	2.10	2.0 ± 0.1	Based on BCR-1
Zn	104		No comparison

Table A 1.4 REFERENCES USED FOR COMPILING STANDARD VALUES

Ab70 ABBEY S., U.S. Geological survey standards - a critical study of published data, Can. Spectrosc.; 15, 10-16, 1970

Br71 BRUNFELDT A.O., STEINNES E., Determination of 42 elements in lunar material, Talanta; 18, 1197-1208, 1971

Ch70 CHERRY R.D., HOBBS J.B.M., ERLANK A.J., WILLIS J.P., Thorium, uranium, potassium, lead, strontium and rubidium in silicate rocks by gamma-spectroscopy and/or X-ray fluorescence, Can. Spectrosc.; 15, 1-8, 1970

Er72 ERLANK A.J., Private communication

Fe72 FESQ H.W., Private communication

Fl69 FLANAGAN F.J., U.S. Geological survey standards - II. First compilation of data for the new U.S.G.S. rocks, Geochim. Cosmochim. Acta; 33, 81-120, 1969

Ho72 HOFMEYER P.K., Some emission spectrographic trace element data for reference silicate material, Chem. Geol.; 9, 23-28, 1972

Ru72 RUSSEL B.G., GOUDVIS R.G., DOMEL G., LEVIN J., Preliminary report on the analysis of the six NIMROC geochemical standard samples, Natn. Inst. Metall.; Report 1351, 74p, 1972

Wi69 WILLIS J.P., FESQ H.W., KABLE E.J.D., BERG G.W., The determination of barium in rocks of X-ray fluorescence spectrometry, Can. Spectrosc.; 14, 3-11, 1969

APPENDIX 2 RESULTS FOR 19 ELEMENTS DETERMINED IN CHIP SAMPLES

CONTENTS

Table A 2.1 ANALYSIS OF CONGLOMERATE SAMPLES FROM ZONE 2

Table A 2.2 ANALYSIS OF QUARTZITE SAMPLES FROM ZONE 3, ZONE 4 AND ZONE 5

Table A 2.3 ANALYSIS OF CONGLOMERATE SAMPLES FROM ZONE 6

Table A 2.4 ANALYSIS OF CONGLOMERATE SAMPLES FROM ZONE 7

Table A 2.1 ANALYSIS OF CONGLOMERATE SAMPLES FROM ZONE 2

SAMPLE NO	Au ppm	Th ppm	Ba ppm	Rb ppm	Ce ppm	La ppm	Ce ppm	Nd ppm	Eu ppm	Tb ppm	Yb ppm	Lu ppm	Hf ppm	Ta ppm	Fe %	Sc ppm	Cr ppm	Co ppm	Sb ppm
1	0.015	9.4	410	-	0.93	110	ND	ND	1.5	-	2.7	0.92	3.8	1.4	1.1	0.67	88	37	0.29
2	0.16	10.5	-	-	0.41	63	62	25	1.5	0.58	2.9	0.33	3.8	3.1	3.2	4.5	130	80	0.34
3	0.10	8.8	-	-	-	120	220	55	2.3	0.47	1.6	0.17	0.85	0.53	1.4	3.5	81	37	0.17
4	0.048	4.8	-	-	0.39	81	7[illegible]	30	1.3	0.45	1.3	0.35	1.3	0.45	0.89	3.8	69	25	0.08
5	0.011	1.4	-	9.2	0.50	62	60	25	1.2	0.34	1.5	0.13	1.1	0.38	0.30	4.6	64	4.1	-
6	0.26	5.6	-	-	-	26	30	-	0.32	0.31	1.8	0.33	4.0	0.65	2.2	5.1	115	42	0.27
7	0.32	7.0	130	-	-	37	37	-	0.34	-	2.1	0.39	4.4	1.1	2.7	9.1	150	50	0.30
8	0.93	16.	300	-	0.19	99	ND	ND	0.58	-	3.5	0.80	3.6	2.1	4.2	11.	290	110	0.58
9	1.07	3.7	43	-	-	61	65	32	0.62	-	0.52	0.055	0.68	0.23	0.66	1.9	17	2.8	0.08
10	0.088	47.	74	-	-	31	30	14	0.30	-	0.74	0.16	1.6	0.39	0.75	2.4	52	8.9	-
11	0.037	2.1	38	7.3	0.28	14	15	-	0.21	0.21	0.84	0.11	2.0	0.22	0.44	2.9	40	3.5	0.07
12	0.19	4.1	120	-	-	20	21	11	0.39	-	1.3	0.21	4.0	0.95	1.6	4.9	140	28	0.26
13	0.15	4.3	170	-	-	23	ND	ND	0.41	-	1.8	0.25	4.5	0.73	1.1	6.2	98	18	-
14	0.066	3.6	96	8.5	0.31	18	19.	8.3	0.32	0.33	0.14	0.22	3.8	0.55	0.80	3.8	94	14	0.12
15	0.014	1.9	71	11.1	0.43	10	11	-	0.19	-	0.68	0.083	1.5	0.29	0.51	2.8	31	3.0	0.07
16	0.15	3.4	87	-	0.23	1.6	17	-	0.15	-	0.56	0.17	1.5	0.63	1.2	1.5	44	27	0.18
17	0.16	3.2	190	6.8	0.57	27	28	11	0.22	-	0.67	0.28	0.88	0.29	0.94	2.5	35	15	0.12
18	0.46	5.6	310	-	1.12	47	ND	ND	0.22	-	0.63	0.50	0.98	0.49	1.1	3.6	31	21	0.24
19	1.24	15	910	-	2.3	110	38	32	0.49	-	2.7	2.2	3.4	5.7	3.5	8.4	110	89	0.60
20	0.76	8.3	250	-	0.92	43	41	15	0.48	-	1.5	0.50	4.1	6.6	2.6	5.7	100	48	0.35
21	1.67	62	3500	-	8.2	480	170	130	2.8	2.7	7.4	4.8	1.7	21.	3.2	6.1	59	230	0.99
22	0.65	42.	1600	-	5.0	280	130	96	1.7	1.9	3.9	2.4	1.1	13.	2.2	4.4	90	140	0.57
23	1.12	45.	1700	-	4.6	290	140	82	1.5	1.2	4.8	2.5	0.97	33.	3.8	4.7	160	200	0.68
24	1.11	67.	1700	-	6.0	420	320	140	3.7	-	7.6	2.7	38.	24.	5.6	13.	820	230	1.5
25	0.58	24.	400	-	2.9	170	ND	ND	1.3	-	1.1	0.86	14.	4.2	4.0	9.9	350	91	0.67

Table A 2.2 ANALYSIS OF QUARTZITE SAMPLES FROM ZONE 3, ZONE 4, AND ZONE 5

	SAMPLE NO	Au ppm	Th ppm	Ba ppm	Rb ppm	Cs ppm	La ppm	Eu ppm	Tb ppm	Lu ppm	Hf ppm	Ta ppm	Fe %	Sc ppm	Cr ppm	Co ppm	Sb ppm
	26	0.077	4.5	140	27.	0.72	41	0.74	1.0	0.10	2.8	0.30	0.61	0.70	8.3	7.5	0.17
	27	-	2.4	110	9.3	-	18	0.38	0.81	0.089	2.6	0.24	0.19	2.3	43.	5.0	0.09
ZONE 3	28	-	3.4	-	-	-	21	0.44	0.65	0.097	1.7	0.33	0.10	1.6	31.	3.8	-
	29	-	3.3	-	-	0.32	26	0.50	0.84	0.082	3.0	0.38	0.20	3.1	55.	4.1	-
	30	0.062	5.9	510	-	1.1	80	0.80	1.5	0.68	2.5	0.61	0.43	3.4	83.	27.	0.07
	31	-	5.0	71	12.	0.29	23	0.57	0.45	0.089	2.2	0.29	0.17	2.4	87.	7.6	0.06
	32	-	2.0	75	13.	0.35	19	0.48	0.66	0.075	2.4	0.32	0.15	1.9	77.	5.5	0.07
ZONE 4	33	0.058	4.1	-	-	0.56	26	0.62	1.2	0.15	6.4	0.40	1.1	2.0	290.	39.	0.14
	34	0.98	1.3	77	11.	0.42	17	0.51	0.38	0.061	1.2	0.12	0.03	1.9	22.	2.6	0.08
	35	-	2.6	100	12.	0.64	28	0.68	0.83	0.13	3.9	0.42	0.20	4.0	180.	5.9	0.12
	36	-	3.1	110	15.	0.47	38	0.61	0.64	0.11	2.3	0.43	0.28	4.4	130.	9.9	-
	37	-	4.0	-	-	0.65	55	0.79	1.4	0.15	2.2	0.64	0.13	5.6	46.	4.4	-
ZONE 5	38	-	7.1	160	29.	0.98	55	0.91	1.4	0.19	3.6	1.9	0.10	9.6	160.	2.2	0.23
	39	-	5.1	130	16.	1.1	49	0.70	0.97	0.12	2.8	0.46	0.10	8.2	58.	2.0	0.09
	40	-	6.1	-	11.	0.60	51	0.70	0.83	0.14	3.4	0.83	0.15	8.4	100.	1.0	0.12

Table A 2.3 ANALYSIS OF CONGLOMERATE SAMPLES FROM ZONE 6

SAMPLE NO	Au ppm	Th ppm	Ba ppm	Rb ppm	Cs ppm	La ppm	Ce ppm	Nd ppm	Sm ppm	Tb ppm	Yb ppm	Lu ppm	Hf ppm	Ta ppm	Fe %	Sc ppm	Cr ppm	Co ppm	Sb ppm
41	3.1	38.	1800	-	-	470	ND	ND	2.0	-	7.7	2.8	1.2	5.7	3.8	11.	54	120.	-
42	0.92	47.	1300	-	-	290	200	97	2.9	3.3	8.5	2.5	9.1	8.9	34.	13.	280	410.	1.3
43	0.48	36.	1660	-	1.13	340	280	110	3.3	3.3	10.	3.4	8.0	5.1	5.1	17.	250	250.	0.87
44	0.11	40.	1360	28.	1.60	290	240	890	3.1	3.0	9.4	2.9	14.	7.9	3.3	18.	250	83.	0.63
45	0.14	55.	1400	46.	1.08	310	260	97	3.4	3.6	9.3	2.8	1.1	13.	4.4	16.	380	120.	0.86
46	0.57	15.	-	-	1.30	82	94	-	1.8	-	4.3	0.53	6.4	1.2	9.3	22.	340	110.	1.5
47	16.	30.	-	-	-	220	250	-	6.0	-	17.	0.22	15.	43.	63.	14.	760	1050.	4.5
48	0.21	0.92	-	-	-	11	ND	ND	0.31	-	0.17	0.04	0.29	0.24	0.63	1.7	12	12.	0.066
49	1.3	9.9	-	34.	0.94	68	73	-	1.0	-	4.0	0.70	6.1	1.7	4.7	15.	170	59.	0.63
50	5.9	14.	440	-	-	81	100	-	1.9	-	0.53	0.70	6.4	3.6	16.	17.	310	200.	1.70
51	0.068	7.1	-	9.8	0.49	41	40	20	0.79	0.62	1.8	0.19	4.1	0.54	0.57	4.4	34	5.6	0.13
52	0.085	0.86	-	15.	0.53	44	46	23	1.1	0.64	2.0	0.23	4.2	3.6	0.62	4.8	51	6.9	-
53	0.065	3.8	-	-	-	18	ND	ND	0.68	-	2.5	0.34	3.4	0.36	0.56	4.2	56	10.	0.13
54	0.12	19.	-	-	1.3	81	84	43	2.9	5.5	15.	1.8	18.	2.4	2.1	17.	130	44.	0.40
55	0.02	9.7	71	13.	0.55	53	54	26	1.2	0.94	2.9	0.37	6.3	0.60	0.62	5.1	55	8.7	0.16
56	0.25	18.	-	73.	1.8	130	130	-	2.8	-	6.3	0.80	2.4	2.2	2.7	20.	225	39.	-
57	0.14	22.	-	58.	1.7	160	160	75	3.3	-	7.3	0.84	12.	2.5	2.3	22.	340	34.	-
58	0.13	5.9	-	-	-	40	ND	ND	0.65	-	1.9	0.26	4.5	0.76	0.89	8.4	130	31.	0.27
59	0.63	36.	510	-	-	130	140	-	2.7	-	8.5	0.11	2.0	3.2	8.8	22.	620	190.	1.17
60	0.21	28.	-	49.	1.8	160	160	-	2.9	-	6.0	0.71	14.	3.9	2.4	24.	410	31.	0.63
61	3.7	28.	-	-	-	320	330	156	5.1	-	9.8	1.5	1.7	2.9	20.	44.	510	360.	1.3
62	7.8	16.	350	-	-	140	130	51	2.5	1.4	6.1	1.0	9.0	1.9	12.	18.	270	240.	0.83
63	0.55	4.3	85	-	-	48	52	25	1.1	0.50	2.0	0.24	2.1	0.58	3.1	7.3	87	48.	0.15
64	0.27	9.7	-	-	-	140	140	83	2.3	0.87	3.2	0.38	2.0	0.88	1.7	9.0	110	14.	0.19
65	0.34	5.8	-	-	-	80	ND	ND	1.8	-	2.7	0.38	3.4	0.31	4.3	17.	110	44.	0.19

Table A 2.4 ANALYSIS OF CONGLOMERATE SAMPLES FROM ZONE 7

SAMPLE NO	Au ppm	Th ppm	Ba ppm	Rb ppm	Ce ppm	La ppm	Cr ppm	Ni ppm	Eu ppm	Tb ppm	Yb ppm	Lu ppm	Hf ppm	Ta ppm	Fe %	Sc ppm	Cr ppm	Co ppm	Sb ppm
66	0.38	4.0	-	-	-	36	ND	ND	0.73	-	0.94	0.16	12.	1.1	3.8	8.6	78	48.	0.28
67	2.1	2.0	-	-	0.32	21	23.	15	0.45	-	0.63	0.08	0.91	0.13	1.7	5.2	25	5.1	0.10
68	0.32	1.7	-	-	-	30	36.	14	0.60	0.35	0.92	0.12	1.1	0.30	2.8	4.9	45	35.	0.11
69	0.96	3.5	51	-	-	49	51.	29	0.88	0.25	0.75	0.11	0.51	0.57	1.2	4.2	41	8.7	0.095
70	0.30	6.2	-	-	-	44	47.	18	1.6	0.64	3.1	0.42	8.6	120.	3.4	9.7	57	40.	0.11
71	0.06	5.3	67	8.4	0.66	33	32.	12	0.58	0.30	1.2	0.16	3.9	0.20	0.62	2.6	63	13.	0.17
72	0.034	3.7	49	8.6	0.48	25	24.	12	0.35	0.19	0.80	0.11	3.2	0.46	0.25	2.5	46	7.1	0.071
73	0.026	3.4	-	-	0.12	35	ND	ND	0.59	-	0.84	0.12	2.2	0.22	0.087	2.4	24	1.4	0.052
74	0.007	3.3	54	7.3	0.34	29	29.	14	0.42	0.18	0.68	0.089	2.0	0.79	0.10	2.2	24	1.5	0.044
75	0.22	5.6	58	-	0.37	32	32.	16	0.55	0.40	1.3	0.15	4.4	0.62	1.4	2.3	73	38.	0.18
76	0.017	7.4	-	-	1.6	55	53.	22	0.90	0.36	2.3	0.28	4.9	1.2	0.89	9.1	160	6.6	-
77	0.011	5.3	-	8.4	1.3	52	5.4	29	0.85	0.40	1.7	0.20	3.1	0.81	0.38	7.5	110	2.6	-
78	0.11	5.0	-	-	1.5	38	ND	ND	0.50	-	1.9	0.15	32.	1.0	0.25	7.7	110	2.9	0.10
79	0.015	6.8	-	9.2	1.3	45	44.	23	0.77	0.35	2.1	0.23	5.0	1.0	0.40	6.9	150	4.8	0.22
80	0.066	6.6	-	11.	17.	53	54.	24	0.90	0.30	1.8	0.24	4.3	1.1	0.33	6.5	140	6.2	0.14
81	0.006	3.2	45	6.7	0.42	39	37.	15	0.54	0.30	0.78	0.082	2.4	0.62	0.20	3.1	44	3.8	0.060
82	1.1	3.4	-	3.5	0.35	37	34.	13	0.48	0.23	0.86	0.88	2.4	0.30	0.28	3.2	41	3.4	-
83	0.54	3.2	-	-	0.36	29	ND	ND	0.44	-	0.88	0.092	2.9	0.56	0.23	4.2	34	3.1	0.047
84	0.039	3.4	60	7.9	0.36	31	40.	21	0.58	0.21	0.83	0.092	2.0	0.45	0.18	3.7	42	1.5	0.067
85	0.039	4.0	-	9.3	0.34	39	37.	15	0.53	-	1.0	0.12	2.5	0.51	0.20	3.5	57	3.0	0.064
86	0.14	16.	-	-	-	75	68.	24	0.84	0.39	1.8	0.19	14.	0.55	1.0	2.6	140	35.	-
87	0.40	59.	340	-	-	310	300.	73	2.7	1.3	5.8	1.2	36.	2.7	4.8	4.8	420	160.	0.48
88	0.037	24.	260	-	-	150	150.	50	1.4	1.2	3.5	0.63	19.	1.1	2.7	3.8	240	72.	0.27
89	0.031	22.	110	-	1.6	180	165.	64	2.2	0.75	2.8	0.33	20.	1.4	2.0	3.5	190	65.	0.19
90	0.18	40.	-	-	-	240	ND	ND	2.4	-	5.2	0.62	52.	0.93	1.9	6.9	260	87.	0.19

APPENDIX 3 RESULTS FOR 28 ELEMENTS DETERMINED IN POWDERED SAMPLES

CONTENTS

Table A 3.1 RESULTS FOR Au, U, Th, Na, K, Ba, Rb and Cs

Table A 3.2 RESULTS FOR La, Ce, Nd, Eu, Tb, Yb and Lu

Table A 3.3 RESULTS FOR Ti, Zr, Hf, Ta, W and Ga

Table A 3.4 RESULTS FOR Fe, Sc, Cr, Co, Ni, As and Sb

Figures: Histograms of the data presented in Tables A 3.1, A 3.2, A 3.3 and A 3.4

Notes: Samples are referred to by a sample code, ABC, as follows:

A = Zone Number

B = Borehole Core Number

C = Replicate Number

TABLE A 3.1 Results for Au, U, Th, Na, K, Ba, Rb and Cs

SAMPLE	GOLD PPM	URANIUM PPM	THORIUM PPM	SODIUM %	POTASSIUM %	BARIUM PPM	RUBIDIUM PPM	CAESIUM PPM
211	.51 ± .07	75. ± 5.	8.7 ± .28	.0196 ± .0006	.029 ± .006	21. ± 35.	<8.	.61 ± .06
212	.39 ± .05	82. ± 5.	10.3 ± .28	.0224 ± .0007	.036 ± .010	130. ± 42.	<8.	.85 ± .08
213	.41 ± .05	79. ± 5.	9.4 ± .26	.0210 ± .0007	.030 ± .009	36. ± 44.	<8.	.70 ± .08
221	3.3 ± .4	86. ± 5.	11.0 ± .29	.0238 ± .0007	.029 ± .007	130. ± 46.	<8.	.68 ± .08
222	.98 ± .13	86. ± 6.	11.1 ± .76	.0236 ± .0008	.035 ± .008	140. ± 47.	<8.	.88 ± .10
223	.62 ± .08	87. ± 6.	9.7 ± .26	.0240 ± .0007	.030 ± .009	44. ± 46.	<8.	.73 ± .09
231	1.09 ± .15	112. ± 7.	11.4 ± .31	.0276 ± .0009	.022 ± .008	167. ± 54.	<8.	1.3 ± .10
232	1.0 ± .14	120. ± 8.	12.5 ± .33	.0249 ± .0010	.048 ± .014	225. ± 63.	<8.	1.3 ± .09
233	1.5 ± .2	115. ± 8.	11.0 ± .30	.0265 ± .0009	.040 ± .013	69. ± 52.	<8.	1.2 ± .10
311	.024 ± .008	9.2 ± .7	5.0 ± .17	.0575 ± .0017	.120 ± .017	67. ± 12.	8.2 ± 2.9	.46 ± .05
312	.068 ± .011	10.1 ± .8	5.8 ± .18	.0595 ± .0017	.121 ± .018	75. ± 13.	8.8 ± 3.3	.58 ± .06
313	.082 ± .013	8.3 ± .6	5.6 ± .17	.0559 ± .0017	.115 ± .018	77. ± 17.	<2.5	.46 ± .05
321	.065 ± .012	10.8 ± .8	5.5 ± .19	.0679 ± .0020	.120 ± .018	87. ± 14.	9.6 ± 2.7	.49 ± .06
322	.038 ± .008	9.9 ± .7	5.5 ± .19	.0669 ± .0019	.137 ± .021	74. ± 19.	<2.5	.60 ± .07
323	.096 ± .010	8.6 ± .7	5.2 ± .19	.0671 ± .0019	.132 ± .022	68. ± 17.	<2.5	.49 ± .06
331	.041 ± .009	9.9 ± .7	5.7 ± .18	.0529 ± .0015	.105 ± .015	71. ± 13.	9.2 ± 4.2	.54 ± .05
332	.11 ± .016	9.5 ± .7	5.5 ± .17	.0539 ± .0015	.107 ± .014	65. ± 14.	<2.5	.48 ± .05
333	.044 ± .029	9.9 ± .7	6.1 ± .19	.0592 ± .0016	.103 ± .018	72. ± 17.	15. ± 4.4	.58 ± .06
411	.022 ± .006	5.1 ± .4	1.5 ± .07	.0566 ± .0016	.098 ± .017	50. ± 8.	3.2 ± .9	.43 ± .03
412	<.015	4.6 ± .4	2.1 ± .08	.0549 ± .0016	.097 ± .014	40. ± 13.	5.7 ± 1.0	.33 ± .03
413	<.015	4.5 ± .3	2.2 ± .08	.0554 ± .0016	.095 ± .013	53. ± 10.	9.3 ± 2.5	.42 ± .04
421	.027 ± .006	4.1 ± .3	1.2 ± .06	.0531 ± .0015	.086 ± .013	48. ± 8.	3.0 ± .8	.29 ± .03
422	<.015	3.5 ± .3	2.0 ± .08	.0537 ± .0016	.089 ± .014	38. ± 10.	4.6 ± 1.5	.24 ± .03
423	<.015	4.7 ± .4	2.1 ± .08	.0536 ± .0016	.087 ± .012	50. ± 9.	5.1 ± 1.3	.29 ± .03
431	.014 ± .005	4.0 ± .3	1.2 ± .05	.0567 ± .0016	.116 ± .015	43. ± 8.	3.2 ± .8	.25 ± .03
432	<.015	3.9 ± .3	1.8 ± .07	.0552 ± .0016	.098 ± .012	54. ± 14.	5.0 ± 1.9	.28 ± .04
433	<.015	3.5 ± .3	1.9 ± .08	.0546 ± .0016	.112 ± .018	50. ± 10.	6.2 ± 1.9	.31 ± .03
511	<.015	8.9 ± .5	5.8 ± .17	.0347 ± .0011	.099 ± .017	48. ± 11.	2.8 ± 1.0	.52 ± .06
512	<.015	8.9 ± .5	7.4 ± .22	.0355 ± .0011	.095 ± .013	50. ± 15.	6.5 ± 2.1	.62 ± .06
513	<.015	8.7 ± .5	8.6 ± .22	.0356 ± .0011	.108 ± .016	56. ± 11.	8.2 ± 2.1	.55 ± .06
521	.015 ± .006	4.3 ± .4	7.6 ± .21	.0283 ± .0008	.074 ± .012	46. ± 12.	<2.5	.49 ± .05
522	<.015	4.8 ± .4	7.5 ± .21	.0279 ± .0008	.071 ± .011	<40.	<2.5	.62 ± .07
523	.019 ± .007	4.7 ± .4	7.7 ± .21	.0281 ± .0009	.079 ± .014	<40.	<2.5	.56 ± .06
531	.026 ± .007	4.4 ± .4	7.8 ± .21	.0277 ± .0008	.056 ± .010	<40.	<2.5	.47 ± .06
532	<.015	4.8 ± .4	7.7 ± .23	.0282 ± .0008	.071 ± .012	<40.	5.1 ± 1.8	.48 ± .05
533	.012 ± .005	5.9 ± .5	7.5 ± .21	.0291 ± .0008	.053 ± .011	<40.	5.8 ± 1.7	.41 ± .04
611	.65 ± .08	8.0 ± .7	4.1 ± .13	.0277 ± .0008	.067 ± .010	61. ± 13.	<8.	.36 ± .06
612	.33 ± .04	8.8 ± .7	3.8 ± .13	.0273 ± .0008	.064 ± .011	47. ± 16.	<8.	.31 ± .05
613	1.3 ± .17	9.1 ± .7	4.0 ± .13	.0284 ± .0008	.079 ± .011	43. ± 18.	<8.	.39 ± .06
621	3.5 ± .4	7.0 ± .6	4.0 ± .12	.0283 ± .0009	.070 ± .012	107. ± 17.	<8.	.33 ± .05
622	.4 ± .06	7.8 ± .6	4.3 ± .13	.0304 ± .0009	.077 ± .013	65. ± 19.	<8.	.37 ± .07
623	.48 ± .06	7.3 ± .6	4.5 ± .14	.0292 ± .0009	.070 ± .013	73. ± 23.	8.1 ± 3.1	.45 ± .09
631	.87 ± .11	9.2 ± .8	3.7 ± .13	.0333 ± .0010	.062 ± .011	31. ± 11.	<8.	.38 ± .06
632	.40 ± .05	7.7 ± .6	3.6 ± .14	.0333 ± .0010	.060 ± .009	<50.	<8.	.43 ± .09
633	.46 ± .13	8.3 ± .6	4.2 ± .14	.0338 ± .0010	.067 ± .011	58. ± 16.	12. ± 3.9	.31 ± .04
711	.19 ± .02	8.5 ± .7	5.3 ± .14	.0370 ± .0011	.078 ± .011	<50.	<8.	.60 ± .07
712	.14 ± .02	8.8 ± .7	5.0 ± .15	.0376 ± .0011	.091 ± .014	54. ± 14.	<8.	.64 ± .09
713	.21 ± .03	9.4 ± .7	5.5 ± .16	.0374 ± .0011	.076 ± .012	44. ± 14.	13. ± 4.1	.56 ± .05
721	.33 ± .04	9.7 ± .7	4.2 ± .14	.0419 ± .0012	.105 ± .014	62. ± 15.	<8.	.47 ± .06
722	.32 ± .04	11.7 ± .9	6.0 ± .17	.0511 ± .0015	.119 ± .015	74. ± 11.	<8.	.65 ± .06
723	.63 ± .08	12.0 ± .9	5.9 ± .18	.0515 ± .0015	.139 ± .019	62. ± 16.	<8.	.66 ± .08
731	.62 ± .08	13.1 ± 1.0	5.8 ± .16	.0543 ± .0016	.117 ± .016	76. ± 20.	8.5 ± 2.5	.57 ± .06
732	.70 ± .02	12.8 ± .9	4.1 ± .12	.0529 ± .0016	.116 ± .015	66. ± 14.	11. ± 3.8	.54 ± .06
733	.18 ± .02	13.9 ± 1.0	6.2 ± .18	.0560 ± .0016	.127 ± .021	110. ± 24.	10. ± 3.5	.58 ± .06

TABLE A 3.2 Results for La, Ce, Nd, Eu, Tb, Yb, and Lu

SAMPLE	LANTHANUM PPM	CERIUM PPM	NEODYMIUM PPM	EUROPIUM PPM	TERBIUM PPM	YTTERBIUM PPM	LUTETIUM PPM
211	15.0 ± .4	36. ± 1.5	<12.	.40 ± .031	.19 ± .036	1.19 ± .08	.12 ± .20
212	15.9 ± .4	44. ± 1.5	18. ± 5.	.41 ± .028	.29 ± .040	1.32 ± .07	.02 ± .20
213	16.0 ± .4	41. ± 1.6	23. ± 7.	.41 ± .025	.21 ± .044	1.32 ± .08	.14 ± .21
221	14.1 ± .4	41. ± 1.7	18. ± 5.	.41 ± .027	.28 ± .083	1.30 ± .08	.16 ± .22
222	13.7 ± .4	39. ± 1.6	18. ± 5.	.41 ± .026	.26 ± .087	1.32 ± .07	.09 ± .24
223	14.1 ± .4	41. ± 1.7	27. ± 5.	.44 ± .028	.20 ± .043	1.45 ± .08	.19 ± .22
231	17.0 ± .5	52. ± 2.0	26. ± 6.	.55 ± .034	.26 ± .043	1.47 ± .09	.11 ± .29
232	17.4 ± .5	52. ± 2.3	25. ± 6.	.47 ± .028	.76 ± .046	1.50 ± .09	.07 ± .33
233	17.1 ± .5	51. ± 2.2	16. ± 5.	.53 ± .039	.27 ± .046	1.41 ± .08	.11 ± .29
311	15.3 ± .4	31.7 ± .4	13. ± 4.	.51 ± .025	.24 ± .035	.93 ± .06	.14 ± .028
312	15.6 ± .4	32.9 ± .4	14. ± 4.	.52 ± .022	.25 ± .037	1.15 ± .06	.13 ± .033
313	14.9 ± .4	32.2 ± .4	14. ± 5.	.54 ± .028	.19 ± .031	.96 ± .06	.14 ± .025
321	15.5 ± .4	32.1 ± .4	< 7.	.52 ± .024	.26 ± .044	1.08 ± .06	.16 ± .032
322	15.4 ± .4	31.8 ± .4	14. ± 4.	.49 ± .022	.29 ± .038	1.07 ± .06	.15 ± .030
323	14.9 ± .4	31.0 ± .5	13. ± 6.	.50 ± .026	.27 ± .048	.91 ± .05	.14 ± .028
331	15.3 ± .4	30.9 ± .4	15. ± 4.	.51 ± .022	.28 ± .037	1.19 ± .07	.16 ± .032
332	15.1 ± .4	32.6 ± .4	14. ± 5.	.55 ± .025	.21 ± .033	.96 ± .05	.14 ± .028
333	15.8 ± .4	32.4 ± .5	14. ± 3.	.52 ± .023	.23 ± .042	1.10 ± .06	.15 ± .030
411	9.0 ± .3	15.2 ± .2	7. ± 2.	.45 ± .016	.20 ± .022	.51 ± .03	.09 ± .017
412	8.6 ± .2	14.9 ± .2	8. ± 2.	.40 ± .017	.14 ± .021	.47 ± .04	.08 ± .016
413	8.6 ± .3	14.2 ± .2	9. ± 3.	.42 ± .016	.18 ± .020	.55 ± .03	.08 ± .015
421	8.0 ± .2	13.3 ± .2	7. ± 2.	.35 ± .016	.17 ± .019	.45 ± .03	.07 ± .014
422	7.8 ± .2	13.3 ± .2	6. ± 2.	.35 ± .016	.15 ± .020	.51 ± .03	.07 ± .012
423	7.8 ± .2	13.0 ± .2	8. ± 3.	.35 ± .015	.17 ± .019	.52 ± .04	.06 ± .015
431	8.0 ± .2	12.5 ± .2	7. ± 3.	.32 ± .014	.15 ± .020	.44 ± .03	.07 ± .014
432	7.5 ± .2	14.7 ± .2	13. ± 4.	.36 ± .016	.16 ± .020	.52 ± .03	.08 ± .014
433	7.6 ± .2	14.9 ± .2	< 7.	.38 ± .017	.19 ± .025	.52 ± .03	.07 ± .013
511	22.3 ± .6	35.7 ± .4	19. ± 5.	.66 ± .029	.26 ± .027	1.21 ± .06	.1 ± .025
512	22.6 ± .6	46.1 ± .6	17. ± 5.	.63 ± .025	.33 ± .037	1.31 ± .07	.17 ± .021
513	22.7 ± .6	47.4 ± .6	21. ± 5.	.65 ± .027	.25 ± .033	1.37 ± .08	.19 ± .024
521	21.8 ± .6	43.9 ± .5	17. ± 4.	.65 ± .027	.22 ± .027	.19 ± .06	.16 ± .018
522	21.2 ± .6	41.9 ± .5	14. ± 4.	.66 ± .027	.22 ± .034	.18 ± .06	.18 ± .019
523	21.8 ± .6	42.6 ± .5	12. ± 4.	.66 ± .028	.24 ± .031	.23 ± .07	.17 ± .020
531	21.8 ± .6	45.5 ± .5	20. ± 6.	.65 ± .027	.22 ± .030	1.22 ± .06	.19 ± .020
532	21.7 ± .6	46.8 ± .6	18. ± 5.	.70 ± .027	.30 ± .037	1.36 ± .07	.17 ± .017
533	21.8 ± .6	42.7 ± .5	< 7.	.64 ± .027	.27 ± .030	1.24 ± .07	.15 ± .023
611	12.8 ± .4	25.3 ± .4	<12.	.50 ± .024	.18 ± .029	1.13 ± .06	.18 ± .026
612	12.7 ± .4	25.4 ± .4	<12.	.54 ± .026	.24 ± .033	1.13 ± .06	.17 ± .026
613	12.9 ± .4	25.3 ± .4	16. ± 7.	.48 ± .021	.23 ± .033	1.07 ± .06	.15 ± .030
621	12.7 ± .4	26.8 ± .4	14. ± 5.	.51 ± .023	.16 ± .028	1.04 ± .06	.14 ± .024
622	13.3 ± .4	27.6 ± .4	<12.	.52 ± .023	.21 ± .041	1.06 ± .06	.16 ± .024
623	12.4 ± .4	26.6 ± .4	<12.	.52 ± .024	.18 ± .033	1.13 ± .06	.15 ± .025
631	11.9 ± .3	24.6 ± .4	<12.	.48 ± .022	.22 ± .033	1.15 ± .07	.16 ± .025
632	12.0 ± .3	25.6 ± .4	<12.	.52 ± .027	.26 ± .042	1.22 ± .07	.19 ± .025
633	12.1 ± .3	24.8 ± .3	<12.	.50 ± .024	.23 ± .034	1.15 ± .06	.16 ± .028
711	18.7 ± .5	37.8 ± .5	<12.	.49 ± .023	.15 ± .036	1.11 ± .06	.17 ± .026
712	19.2 ± .5	37.6 ± .5	14. ± 5.	.51 ± .022	.17 ± .028	1.09 ± .06	.14 ± .025
713	18.8 ± .5	37.4 ± .5	<12.	.48 ± .022	.19 ± .031	1.07 ± .06	.13 ± .030
721	15.1 ± .4	30.6 ± .4	16. ± 6.	.40 ± .020	.18 ± .033	.42 ± .06	.13 ± .029
722	19.9 ± .5	36.9 ± .5	23. ± 8.	.51 ± .022	.19 ± .029	1.19 ± .07	.15 ± .034
723	19.5 ± .5	37.4 ± .5	<12.	.49 ± .027	.20 ± .032	1.22 ± .07	.15 ± .037
731	18.8 ± .5	37.3 ± .5	<12.	.51 ± .024	.29 ± .039	1.16 ± .06	.17 ± .037
732	18.4 ± .5	36.1 ± .4	<12.	.46 ± .026	.16 ± .022	1.01 ± .05	.16 ± .038
733	19.4 ± .5	37.4 ± .5	21. ± 5.	.51 ± .023	.19 ± .032	1.22 ± .07	.17 ± .040

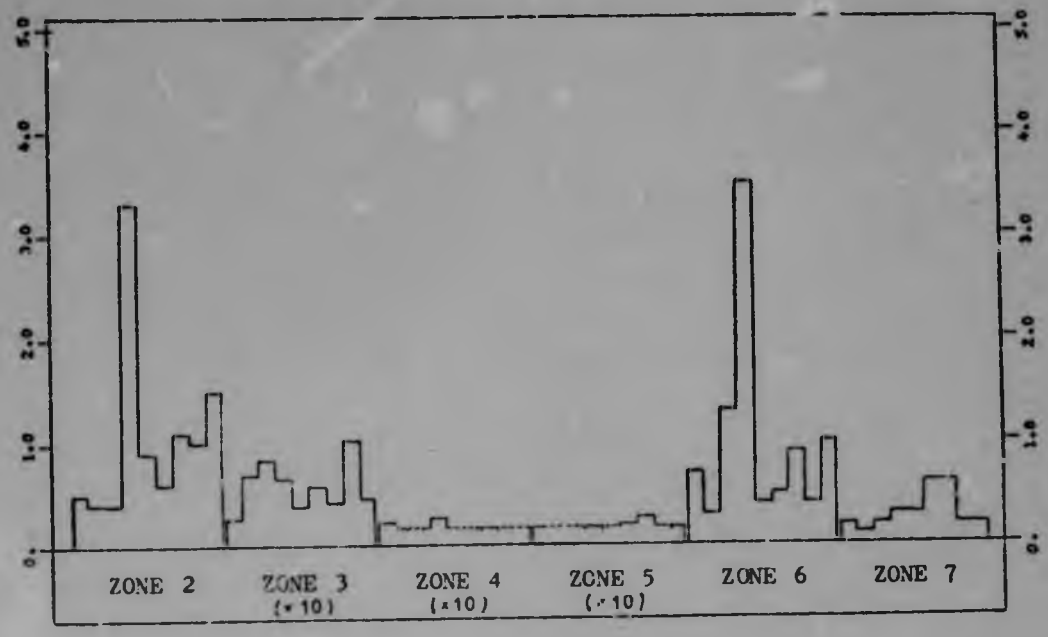
TABLE A 3.3 Results for Ti, Zr, Hf, Ta, W and Ga

SAMPLE	TITANIUM %	ZIRCONIUM PPM	HAFNIUM PPM	TANTALUM PPM	TUNGSTEN PPM	GALLIUM PPM
21*	.20 ± .034	136. ± 39.	2.08 ± .10	1.28 ± .050	<.45	2.7 ± 1.0
212	.17 ± .026	200. ± 38.	3.14 ± .11	1.58 ± .049	<.45	1.6 ± 1.2
213	.20 ± .042	130. ± 37.	2.63 ± .09	1.43 ± .051	<.45	2.3 ± 1.2
221	.44 ± .066	180. ± 41.	2.01 ± .07	1.27 ± .045	<.45	1.7 ± 1.4
222	.20 ± .029	190. ± 41.	2.41 ± .08	1.43 ± .047	<.45	5.7 ± 1.5
223	.07 ± .019	180. ± 44.	2.75 ± .10	1.24 ± .041	<.45	3.0 ± 1.1
231	.10 ± .022	280. ± 52.	2.86 ± .10	1.52 ± .050	<.45	2.2 ± 1.2
232	.21 ± .034	240. ± 53.	2.54 ± .09	1.86 ± .058	<.45	7.0 ± 2.1
233	.07 ± .022	240. ± 51.	2.60 ± .09	1.55 ± .053	<.45	6.1 ± 1.6
311	.12 ± .022	160. ± 16.	3.79 ± .13	.44 ± .021	.81 ± .29	4.8 ± 1.1
312	.12 ± .018	160. ± 16.	3.95 ± .13	.68 ± .025	1.13 ± .35	6.7 ± 1.6
313	.09 ± .022	145. ± 15.	4.17 ± .14	.47 ± .022	.43 ± .19	5.5 ± 1.3
321	.15 ± .026	198. ± 19.	4.06 ± .14	.58 ± .024	.49 ± .16	4.9 ± 1.4
322	.13 ± .017	140. ± 14.	4.22 ± .14	.57 ± .026	.89 ± .35	7.4 ± 2.0
323	.42 ± .022	131. ± 14.	3.87 ± .13	.51 ± .025	.57 ± .21	6.2 ± 1.3
331	.13 ± .016	138. ± 14.	4.05 ± .13	.57 ± .024	<.45	7.6 ± 1.8
332	.10 ± .021	133. ± 14.	3.85 ± .13	.44 ± .023	.56 ± .22	5.7 ± 1.4
333	.12 ± .019	156. ± 17.	4.26 ± .14	.53 ± .024	.79 ± .30	6.3 ± 1.4
411	.06 ± .011	75. ± 8.	1.85 ± .06	.17 ± .011	.78 ± .26	7.0 ± 1.4
412	.05 ± .015	78. ± 10.	1.68 ± .06	.16 ± .012	<.45	3.6 ± 1.1
413	.056 ± .009	83. ± 8.	2.23 ± .07	.18 ± .011	.88 ± .29	4.2 ± 1.0
421	.05 ± .011	71. ± 8.	1.64 ± .06	.12 ± .010	<.45	4.3 ± 1.0
422	.05 ± .012	72. ± 8.	1.89 ± .07	.16 ± .012	<.45	4.7 ± .8
423	.05 ± .010	91. ± 9.	2.27 ± .08	.14 ± .010	<.45	3.7 ± 1.4
431	.048 ± .007	62. ± 8.	1.78 ± .06	.13 ± .010	<.45	2.9 ± 1.0
432	.05 ± .012	66 ± 8.	1.95 ± .07	.15 ± .012	<.45	3.9 ± 1.2
433	.040 ± .008	76. ± 8.	1.98 ± .07	.15 ± .011	<.45	4.2 ± 1.0
511	.13 ± .018	107. ± 11.	3.26 ± .11	.38 ± .017	1.07 ± .27	18.0 ± 2.1
512	.11 ± .020	145. ± 17.	3.88 ± .13	.35 ± .017	.95 ± .27	16.1 ± 1.8
513	.12 ± .017	132. ± 13.	4.14 ± .14	.40 ± .019	.74 ± .25	16.5 ± 2.3
521	.12 ± .021	120. ± 14.	3.70 ± .11	.32 ± .017	.77 ± .33	13.9 ± 1.7
522	.12 ± .020	130. ± 14.	4.02 ± .13	.30 ± .016	<.45	13.3 ± 1.5
523	.10 ± .014	111. ± 12.	3.91 ± .13	.35 ± .017	<.45	14.3 ± 1.7
531	.11 ± .016	128. ± 15.	3.47 ± .13	.31 ± .017	<.45	15.0 ± 1.8
532	.09 ± .015	136. ± 14.	4.23 ± .14	.34 ± .017	<.45	13.3 ± 1.5
533	.09 ± .013	131. ± 14.	3.65 ± .12	.33 ± .016	<.45	16.6 ± 2.0
611	.16 ± .029	106. ± 15.	2.80 ± .13	.38 ± .019	.55 ± .21	5.5 ± 1.0
612	.13 ± .028	100. ± 13.	2.80 ± .10	.41 ± .022	.69 ± .22	5.4 ± 1.0
613	.19 ± .027	107. ± 14.	2.68 ± .10	.38 ± .021	.65 ± .25	4.6 ± 1.1
621	.57 ± .073	98. ± 14.	2.90 ± .10	.35 ± .021	<.45	5.3 ± 1.0
622	.15 ± .029	111. ± 16.	2.78 ± .13	.42 ± .021	<.45	5.3 ± 1.4
623	.10 ± .017	114. ± 16.	2.73 ± .13	.41 ± .023	<.45	4.2 ± 1.1
631	.15 ± .034	109. ± 13.	2.91 ± .13	.36 ± .021	<.45	5.8 ± 1.3
632	.10 ± .024	121. ± 15.	2.59 ± .09	.35 ± .023	.48 ± .18	5.3 ± 1.2
633	.14 ± .021	111. ± 14.	2.55 ± .09	.49 ± .023	<.45	5.5 ± 1.4
711	.13 ± .022	133. ± 17.	4.09 ± .14	.39 ± .023	<.45	8.1 ± 1.6
712	.11 ± .021	151. ± 19.	3.98 ± .13	.42 ± .022	<.45	8.9 ± 1.8
713	.11 ± .018	159. ± 19.	4.13 ± .14	.47 ± .022	<.45	8.3 ± 1.9
721	.15 ± .028	111. ± 13.	3.53 ± .12	.32 ± .018	.85 ± .26	6.9 ± 1.2
722	.13 ± .025	160. ± 18.	4.30 ± .14	.49 ± .023	.52 ± .21	7.8 ± 1.5
723	.13 ± .022	140. ± 16.	3.98 ± .14	.52 ± .025	.60 ± .23	7.1 ± 1.6
731	.19 ± .042	148. ± 18.	3.73 ± .12	.44 ± .022	<.45	10.5 ± 1.2
732	.08 ± .015	92. ± 12.	2.79 ± .09	.32 ± .018	.47 ± .18	7.5 ± 1.7
733	.11 ± .016	153. ± 14.	4.94 ± .16	.58 ± .026	<.45	8.0 ± 1.6

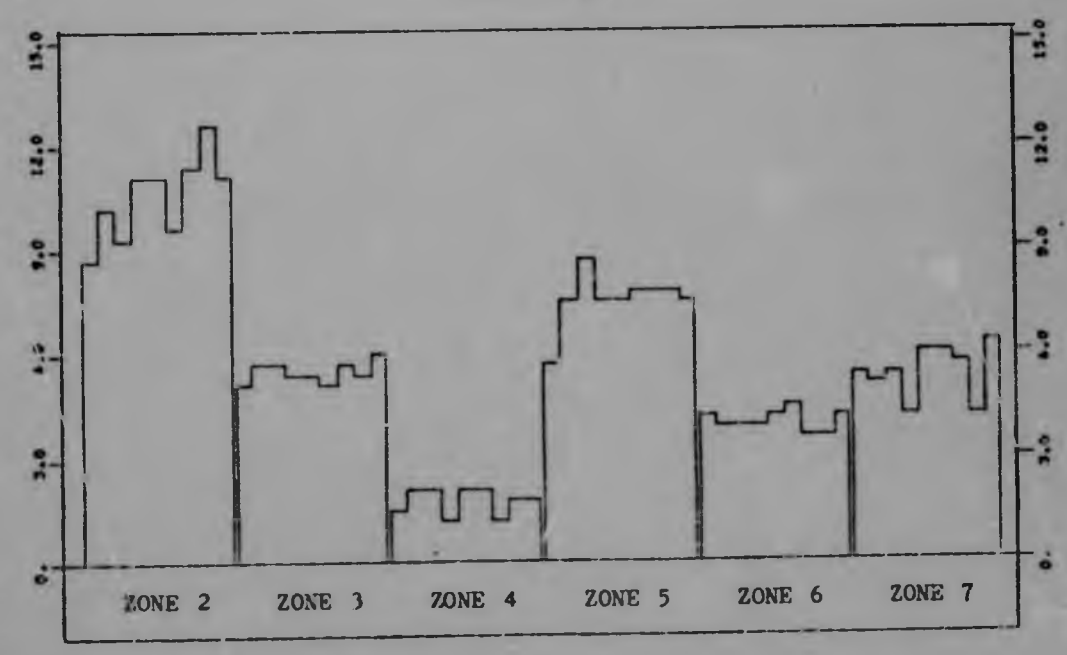
TABLE A 3.4 Results for Fe, Sc, Cr, Co, Ni, As and Sb

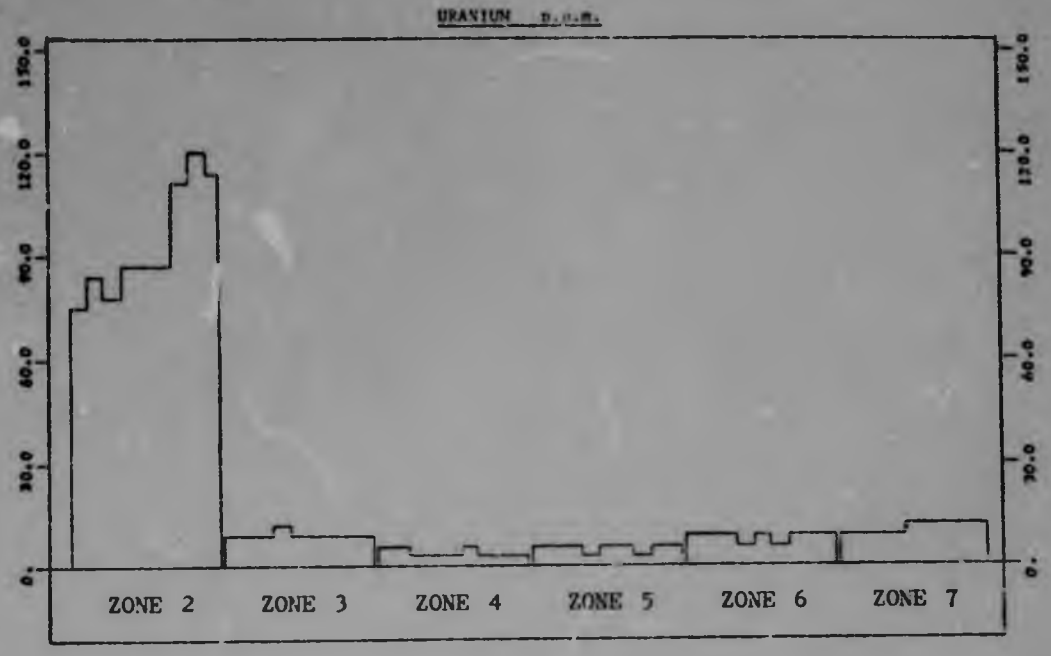
SAMPLE	IRON %	SCANDIUM PPM	CHROMIUM PPM	COBALT PPM	NICKEL PPM	ARSENIC PPM	ANTIMONY PPM
211	1.51 ± .036	3.45 ± .10	98. ± 5.	37.6 ± .75	47. ± 8.	159. ± 2.9	.33 ± .061
212	1.65 ± .024	3.84 ± .08	104. ± 4.	41.4 ± .54	57. ± 9.	171. ± 2.9	.43 ± .043
213	1.63 ± .029	3.79 ± .08	99. ± 4.	38.9 ± .51	48. ± 9.	158. ± 2.7	.39 ± .046
221	1.59 ± .029	4.06 ± .08	108. ± 4.	37.8 ± .49	21. ± 8.	170. ± 2.9	.56 ± .039
222	1.61 ± .027	4.18 ± .09	94. ± 4.	41.4 ± .54	38. ± 8.	183. ± 3.3	.41 ± .039
223	1.61 ± .031	4.09 ± .08	109. ± 4.	38.3 ± .54	38. ± 11.	168. ± 2.9	.36 ± .052
231	1.87 ± .034	3.71 ± .07	114. ± 4.	48.9 ± .64	<30.	236. ± 4.0	.46 ± .049
232	1.90 ± .032	3.78 ± .08	119. ± 5.	51.0 ± .66	45. ± 6.	267. ± 4.6	.52 ± .049
233	1.85 ± .035	3.82 ± .07	121. ± 5.	48.7 ± .63	44. ± 10.	249. ± 4.2	.53 ± .057
311	.710 ± .016	2.74 ± .05	129. ± 5.	17.7 ± .25	53. ± 11.	51. ± 1.0	.34 ± .030
312	.737 ± .014	2.81 ± .05	143. ± 5.	19.4 ± .27	42. ± 9.	58. ± 1.1	.37 ± .013
313	.702 ± .015	2.74 ± .05	145. ± 6.	18.4 ± .26	30. ± 7.	50. ± 1.0	.29 ± .029
321	.881 ± .018	3.04 ± .05	148. ± 5.	20.5 ± .29	59. ± 10.	58. ± 1.1	.37 ± .030
322	.874 ± .018	2.99 ± .05	151. ± 6.	20.6 ± .29	49. ± 6.	61. ± 1.2	.38 ± .035
323	.900 ± .018	3.04 ± .05	155. ± 6.	21.2 ± .30	50. ± 10.	58. ± 1.2	.39 ± .032
331	.905 ± .015	2.80 ± .05	148. ± 6.	22.0 ± .29	42. ± 4.	59. ± 1.2	.38 ± .034
332	.951 ± .019	2.92 ± .05	172. ± 7.	23.3 ± .33	59. ± 12.	54. ± 1.0	.35 ± .034
333	.948 ± .019	2.94 ± .05	53. ± 6.	23.1 ± .32	46. ± 6.	59. ± 1.1	.40 ± .034
411	.169 ± .004	1.32 ± .02	77. ± 3.	5.4 ± .08	15. ± 2.	17.3 ± .4	.157 ± .015
412	.173 ± .005	1.38 ± .02	102. ± 4.	5.1 ± .08	23. ± 4.	16.7 ± .4	.158 ± .016
413	.192 ± .004	1.41 ± .03	102. ± 4.	6.2 ± .09	21. ± 4.	18.0 ± .4	.158 ± .016
421	.155 ± .004	1.08 ± .02	64. ± 3.	6.5 ± .10	12. ± 3.	21.6 ± .5	.198 ± .017
422	.180 ± .005	1.16 ± .02	92. ± 4.	5.7 ± .09	20. ± 6.	20.6 ± .5	.212 ± .018
423	.176 ± .004	1.15 ± .02	92. ± 4.	5.2 ± .08	11. ± 2.	19.9 ± .5	.224 ± .019
431	.148 ± .004	1.12 ± .02	70. ± 3.	6.0 ± .09	16. ± 3.	20.2 ± .5	.119 ± .012
432	.193 ± .005	1.23 ± .02	93. ± 4.	5.6 ± .08	19. ± 6.	18.0 ± .4	.153 ± .014
433	.223 ± .005	1.25 ± .02	98. ± 4.	6.1 ± .09	17. ± 2.	20.0 ± .4	.184 ± .016
511	.158 ± .004	4.10 ± .07	76. ± 3.	5.3 ± .09	25. ± 5.	22.3 ± .5	.185 ± .021
512	.167 ± .006	4.40 ± .07	101. ± 4.	5.5 ± .09	24. ± 6.	22.2 ± .5	.155 ± .019
513	.211 ± .006	4.40 ± .07	102. ± 4.	5.4 ± .09	30. ± 7.	21.4 ± .6	.213 ± .027
521	.160 ± .005	3.94 ± .07	84. ± 3.	5.1 ± .08	21. ± 7.	20.2 ± .5	.159 ± .020
522	.160 ± .005	3.97 ± .07	83. ± 3.	5.0 ± .08	25. ± 7.	19.8 ± .5	.160 ± .022
523	.159 ± .005	3.85 ± .07	82. ± 3.	5.1 ± .08	21. ± 3.	22.8 ± .5	.192 ± .022
531	.165 ± .005	4.18 ± .07	91. ± 4.	6.3 ± .09	29. ± 7.	23.7 ± .5	.172 ± .023
532	.180 ± .005	4.21 ± .07	96. ± 4.	5.8 ± .09	25. ± 9.	21.5 ± .5	.160 ± .021
533	.167 ± .005	3.85 ± .07	86. ± 3.	5.1 ± .08	20. ± 5.	22.1 ± .5	.163 ± .019
611	1.19 ± .023	4.02 ± .07	84. ± 3.	20.1 ± .28	41. ± 9.	32.4 ± .7	.276 ± .031
612	1.20 ± .022	4.18 ± .07	89. ± 4.	19.5 ± .27	39. ± 8.	33.1 ± .7	.289 ± .030
613	1.20 ± .020	3.99 ± .07	79. ± 3.	20.2 ± .28	48. ± 6.	34.6 ± .7	.311 ± .030
621	1.10 ± .021	3.98 ± .07	83. ± 3.	18.4 ± .26	38. ± 9.	29.5 ± .6	.263 ± .027
622	1.08 ± .021	3.88 ± .07	78. ± 3.	18.5 ± .26	38. ± 9.	31.9 ± .6	.261 ± .023
623	1.09 ± .020	3.81 ± .06	78. ± 3.	18.7 ± .26	40. ± 6.	33.6 ± .7	.313 ± .030
631	1.06 ± .020	3.86 ± .06	76. ± 3.	16.7 ± .23	53. ± 13.	29.4 ± .6	.291 ± .026
632	1.05 ± .020	3.64 ± .06	81. ± 3.	17.5 ± .24	45. ± 10.	30.2 ± .6	.283 ± .027
633	1.06 ± .018	3.60 ± .06	74. ± 3.	17.8 ± .25	41. ± 6.	36.2 ± .7	.358 ± .033
711	.967 ± .018	3.55 ± .06	76. ± 3.	17.0 ± .24	27. ± 10.	23.3 ± .5	.232 ± .025
712	.957 ± .018	3.49 ± .06	72. ± 3.	16.7 ± .23	30. ± 8.	24.5 ± .6	.222 ± .028
713	.943 ± .017	3.38 ± .06	72. ± 3.	16.5 ± .23	42. ± 6.	26.0 ± .6	.279 ± .027
721	.716 ± .015	2.86 ± .05	70. ± 3.	19.3 ± .27	44. ± 13.	30.0 ± .6	.162 ± .021
722	.840 ± .016	3.46 ± .06	74. ± 3.	23.9 ± .34	46. ± 12.	35.0 ± .7	.249 ± .028
723	.865 ± .016	3.53 ± .06	81. ± 3.	24.3 ± .34	46. ± 7.	39.8 ± .8	.255 ± .029
731	1.14 ± .022	3.42 ± .04	81. ± 3.	23.8 ± .33	32. ± 12.	31.1 ± .7	.224 ± .026
732	.754 ± .013	2.30 ± .04	50. ± 2.	22.8 ± .46	23. ± 4.	31.1 ± .7	.177 ± .017
733	1.15 ± .020	3.33 ± .04	79. ± 3.	24.2 ± .34	40. ± 8.	31.4 ± .6	.283 ± .027

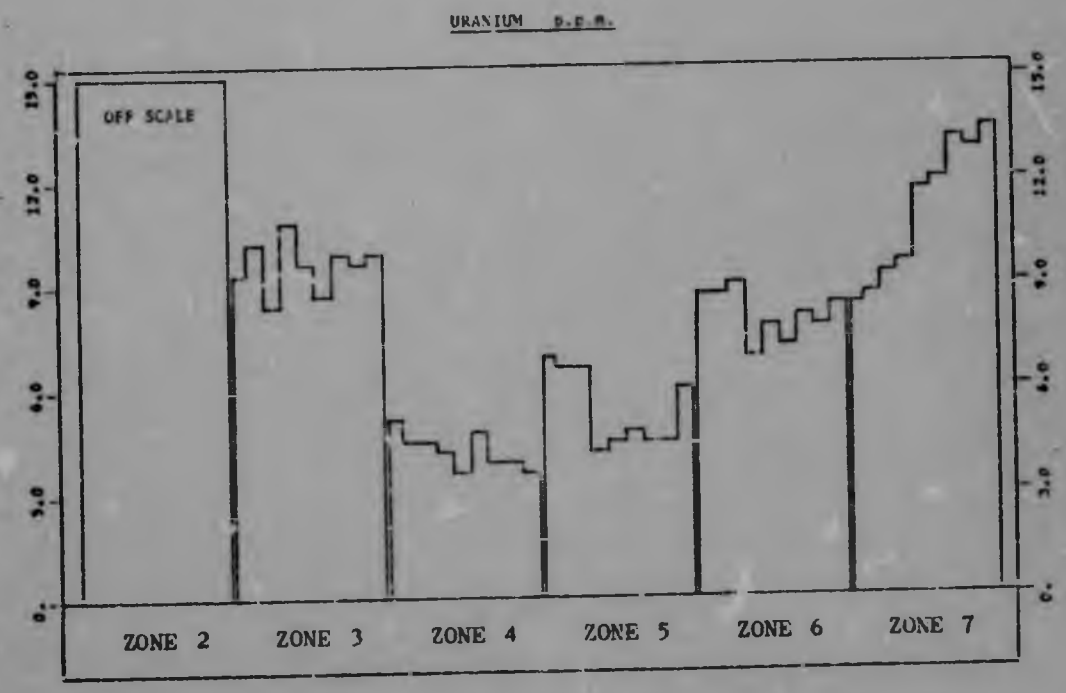
GOLD p.p.m.



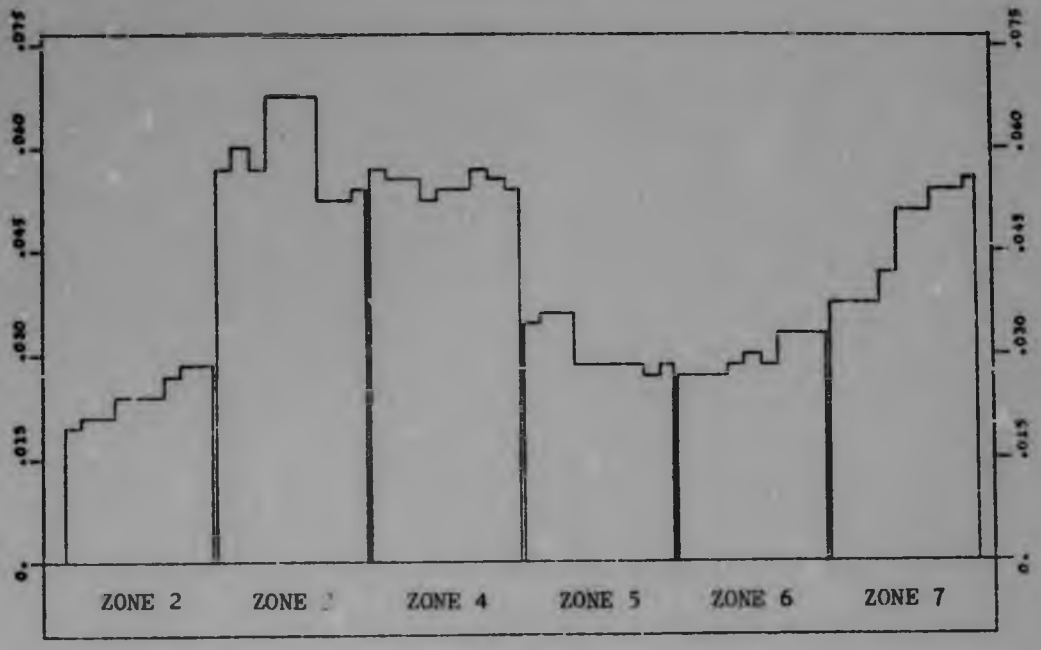
THORIUM p.p.m.



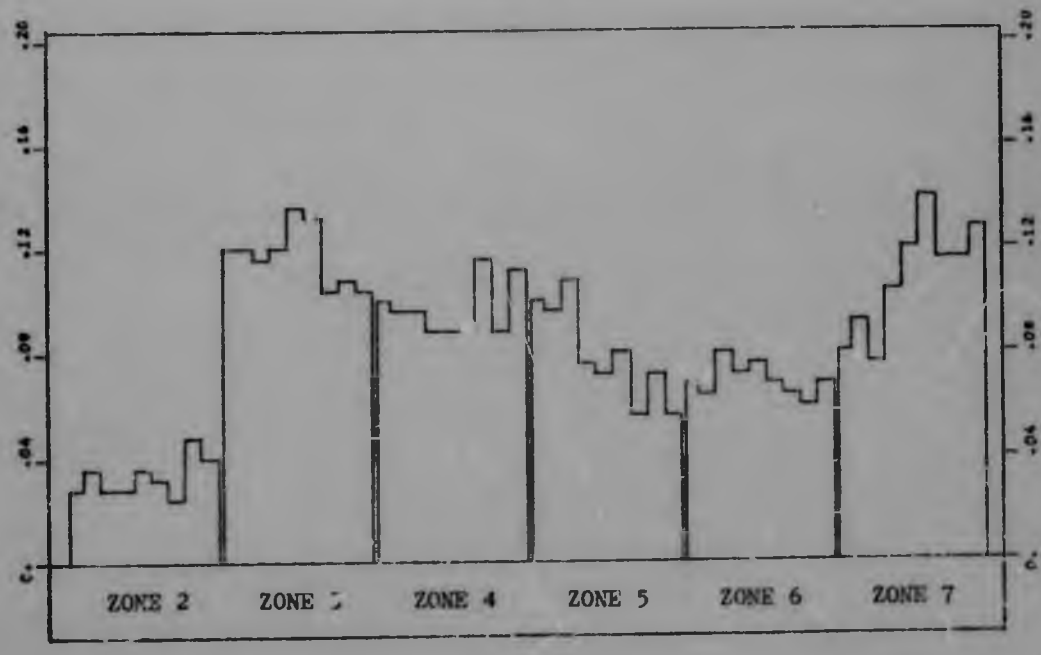

URANIUM
150.0
120.0
90.0
60.0
30.0
0.
ZONE 2
ZONE 3
ZONE 4
ZONE 5
ZONE 6
ZONE 7


URANIUM
15.0
12.0
9.0
6.0
3.0
0.
OFF SCALE
ZONE 2
ZONE 3
ZONE 4
ZONE 5
ZONE 6
ZONE 7

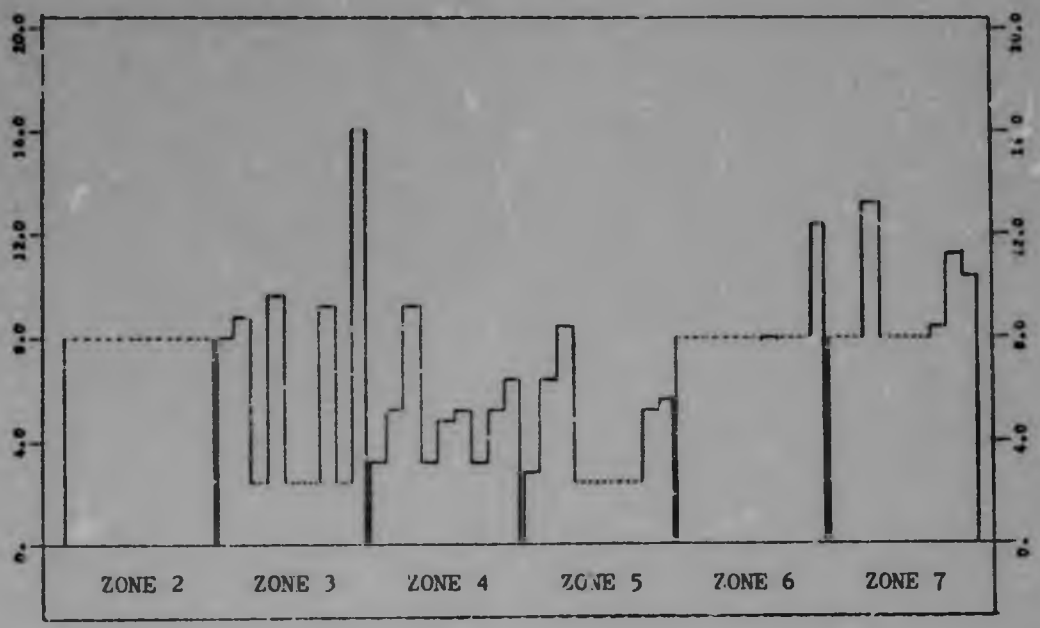
SODIUM 1



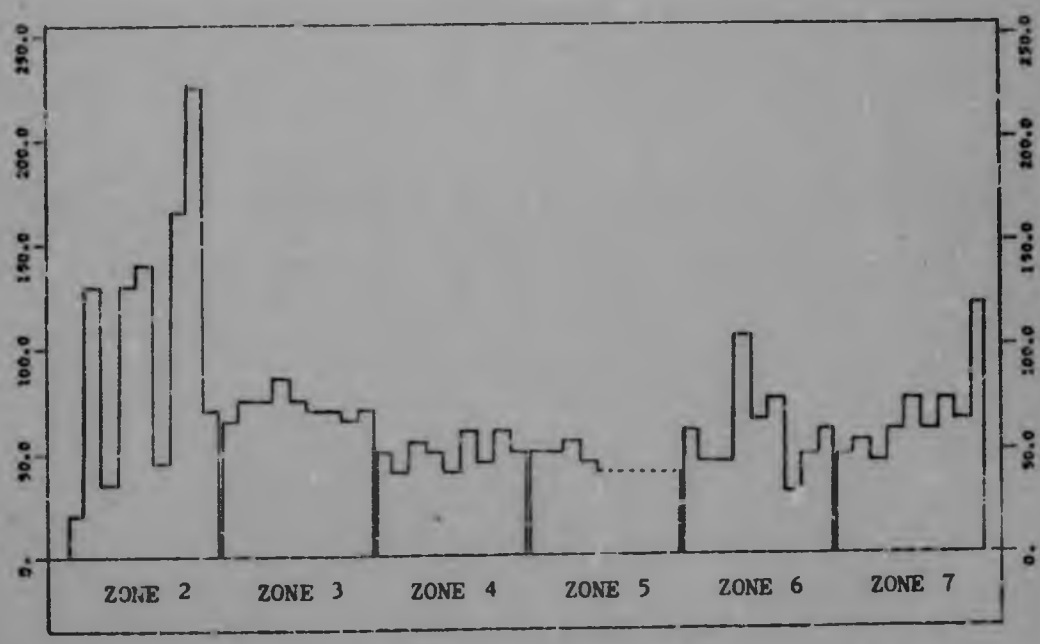
POTASSIUM 1



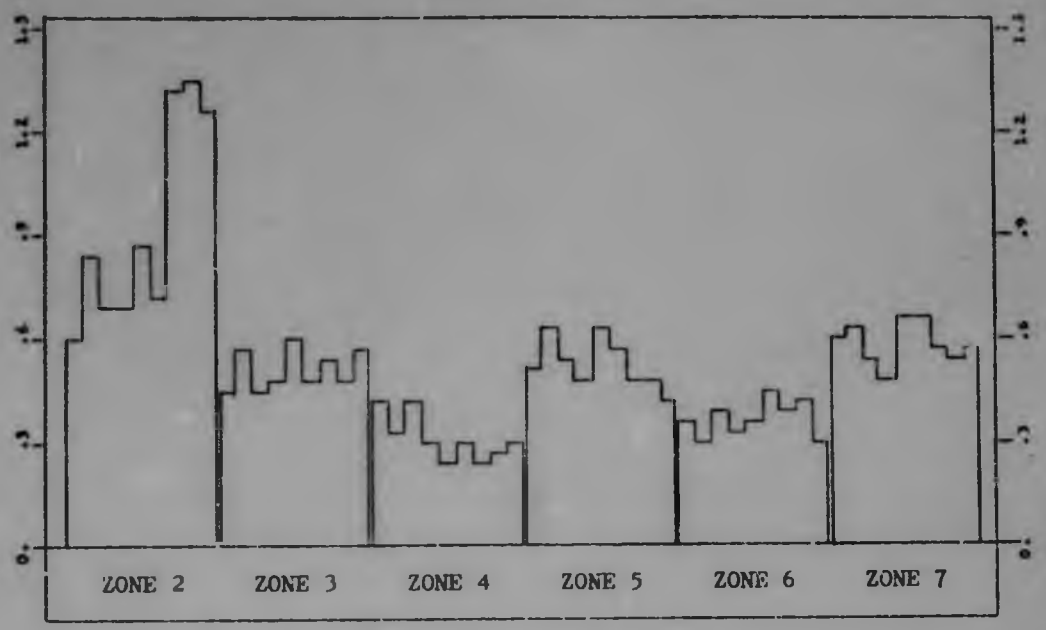
RUBIDIUM p.p.m.



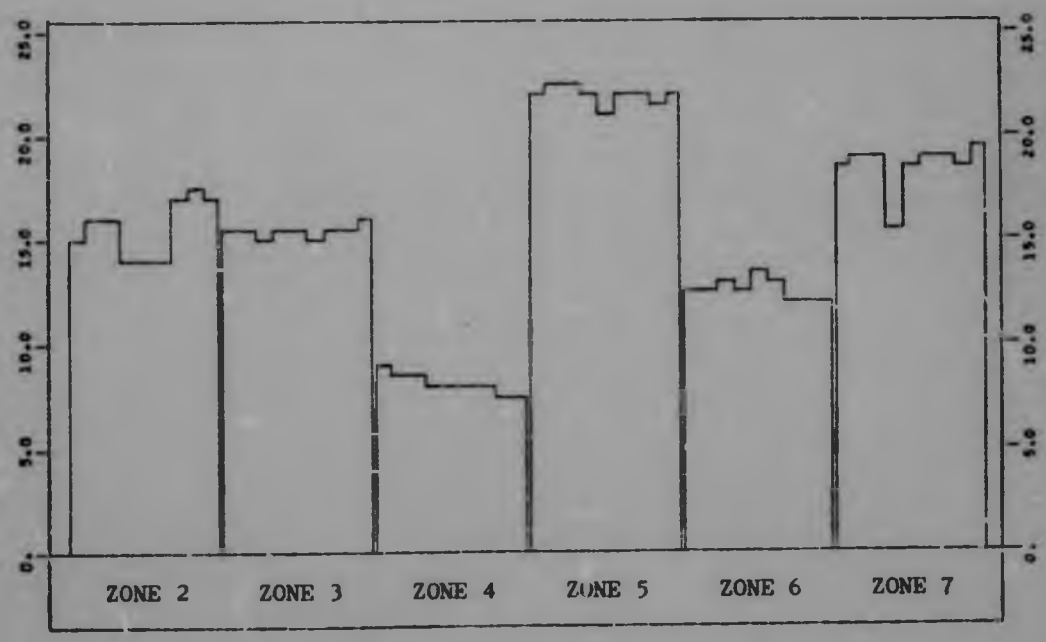
BARIUM p.p.m.



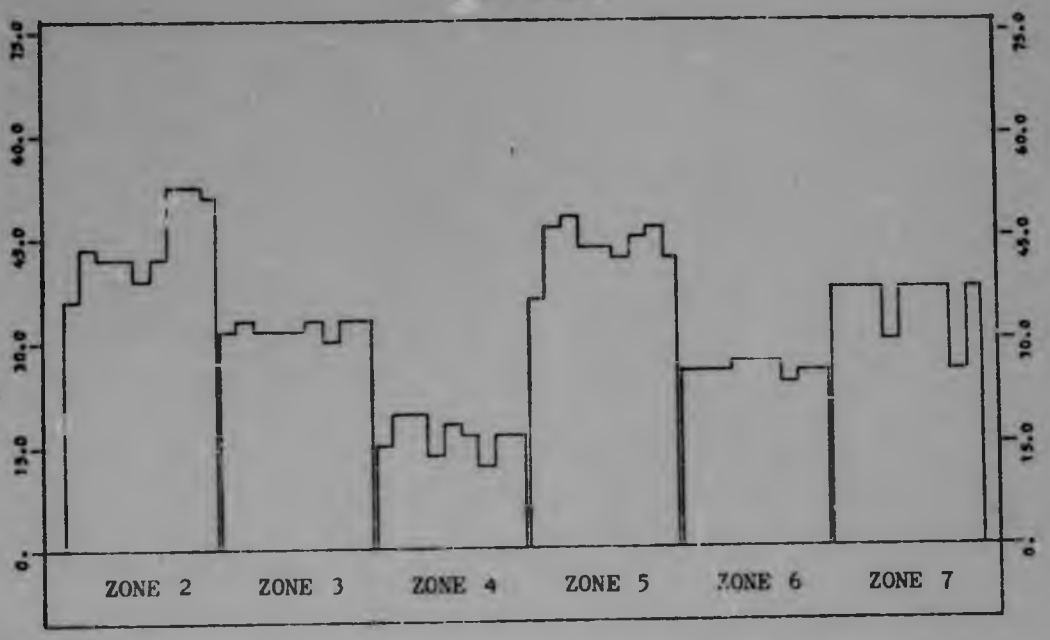
CAESIUM p.p.m.



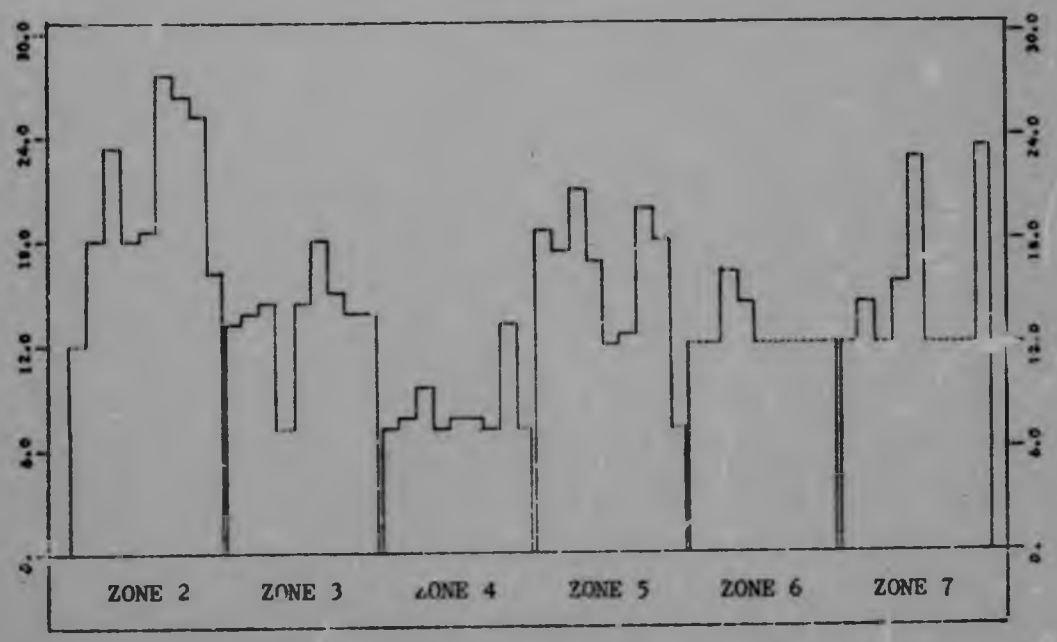
LANTHANUM p.p.m.



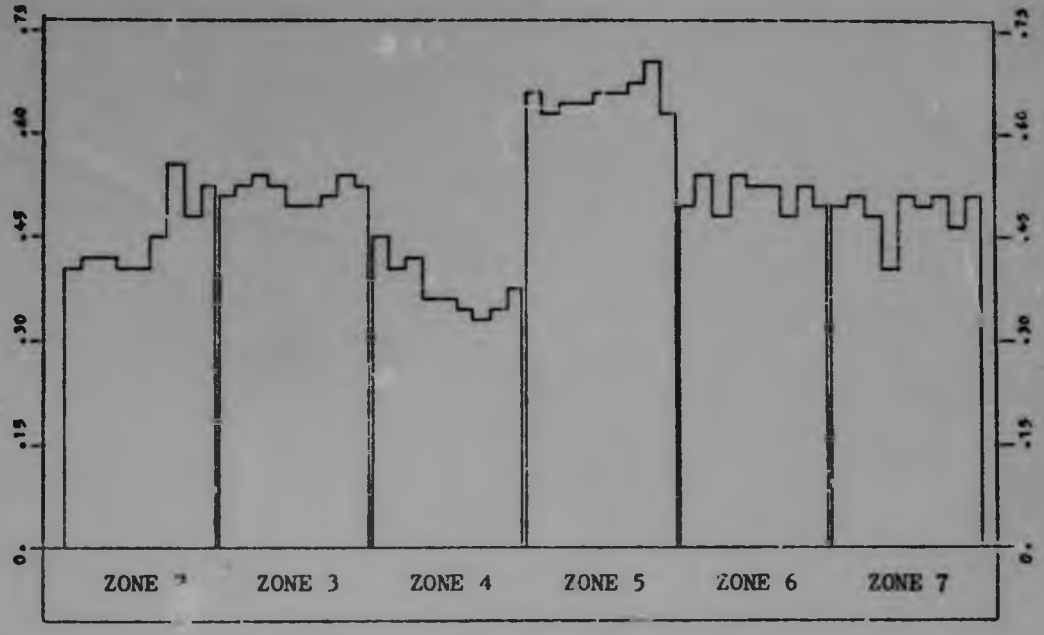
CERIUM p.p.m.



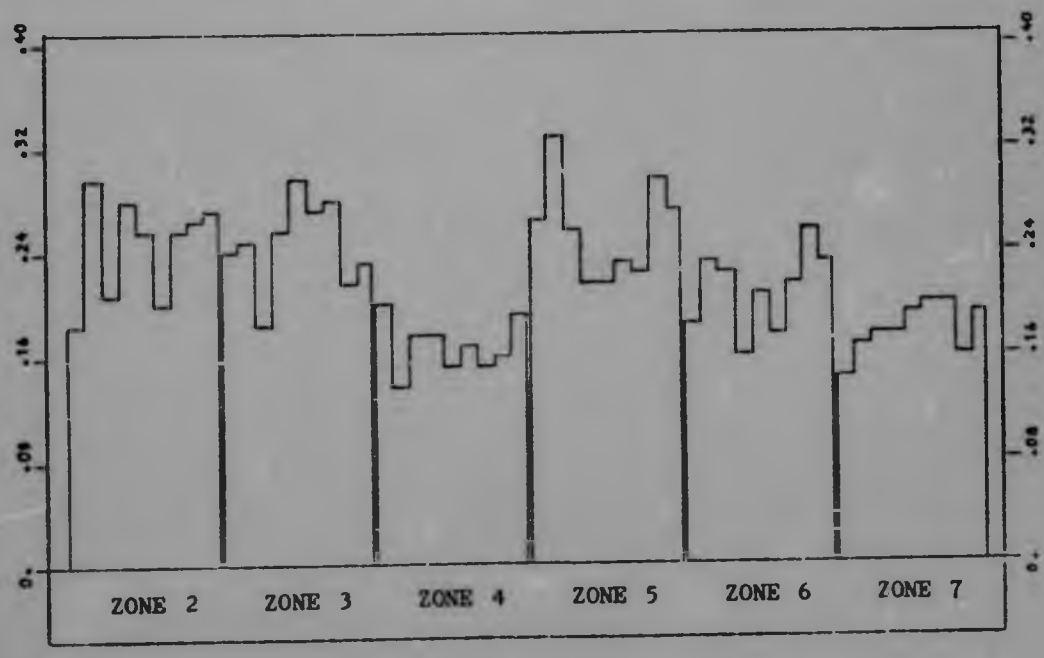
NEODYMIUM p.p.m.

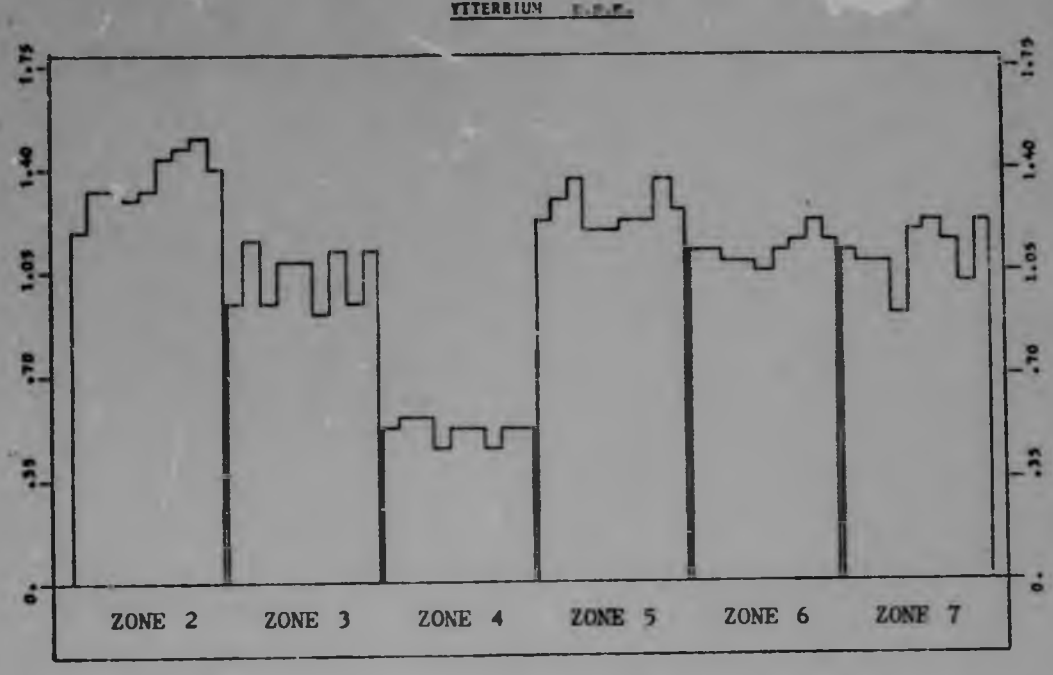


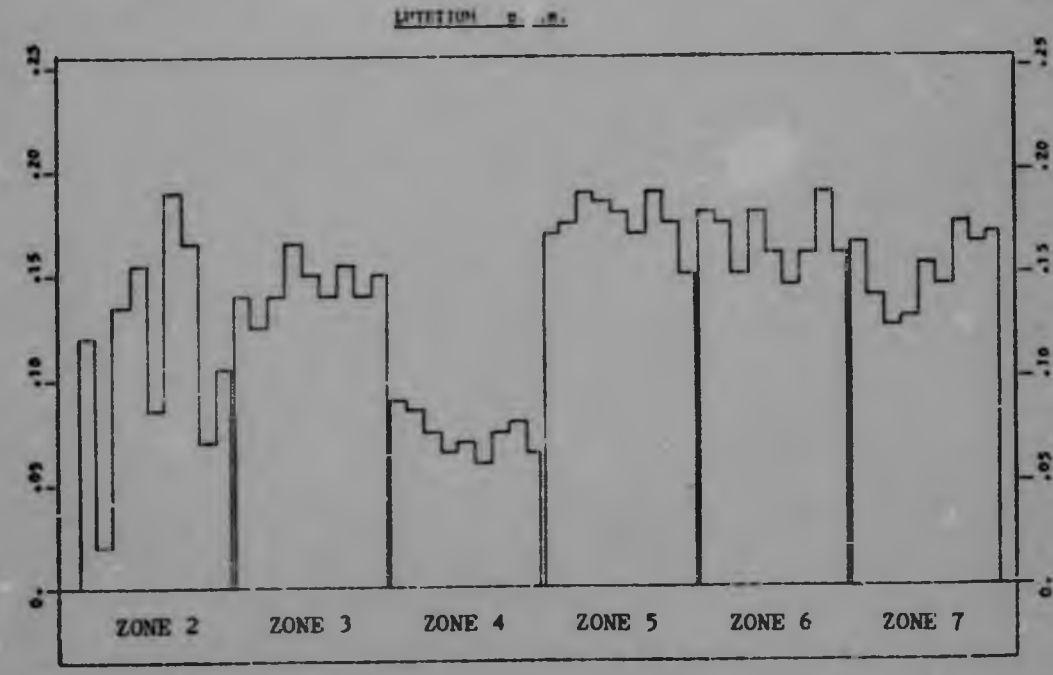
EUROPIUM p.p.m.



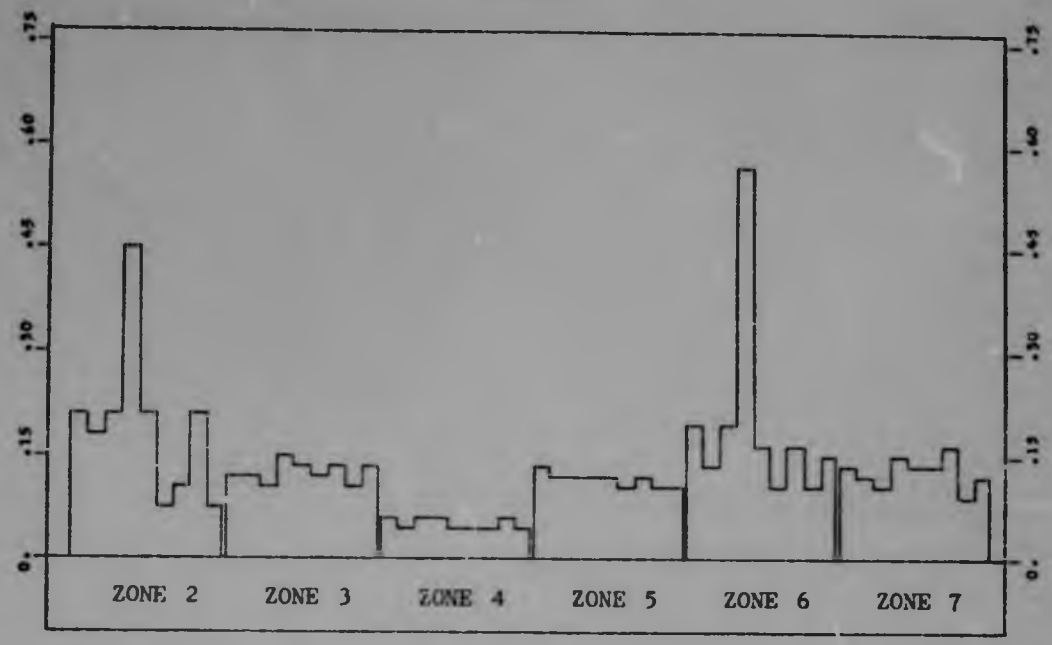
TERBIUM p.p.m.



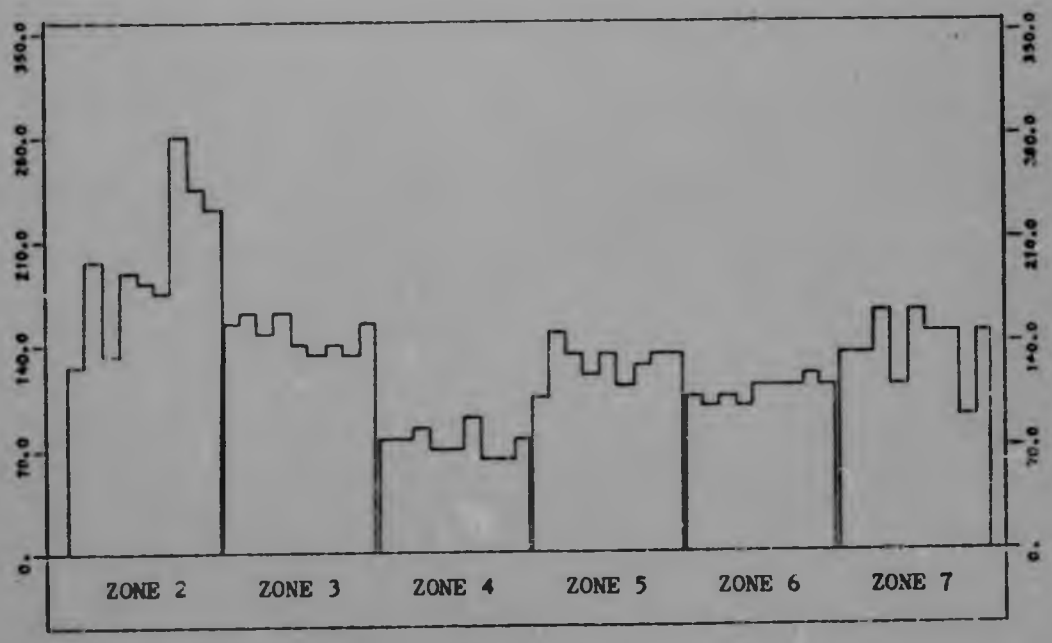

ZONE 2
ZONE 3
ZONE 4
ZONE 5
ZONE 6
ZONE 7


ZONE 2
ZONE 3
ZONE 4
ZONE 5
ZONE 6
ZONE 7

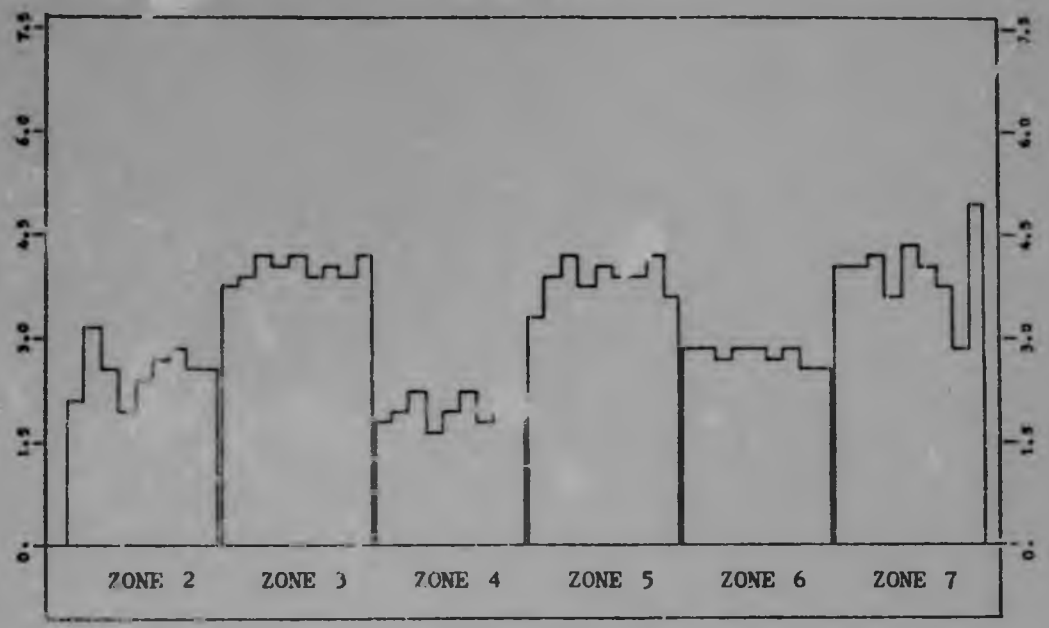
TITANIUM



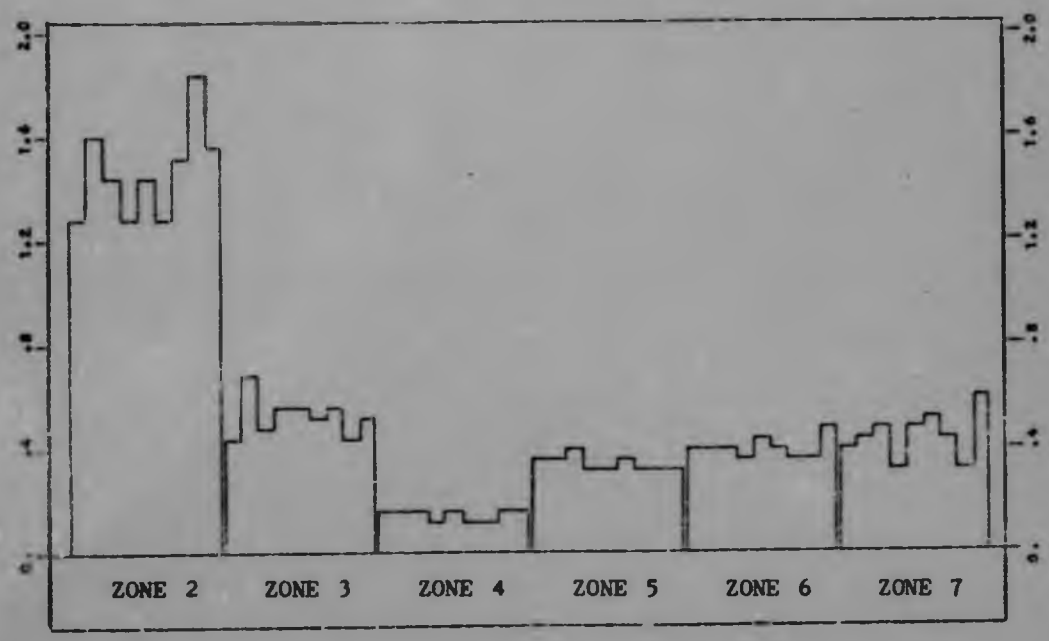
ZIRCONIUM S.P.E.



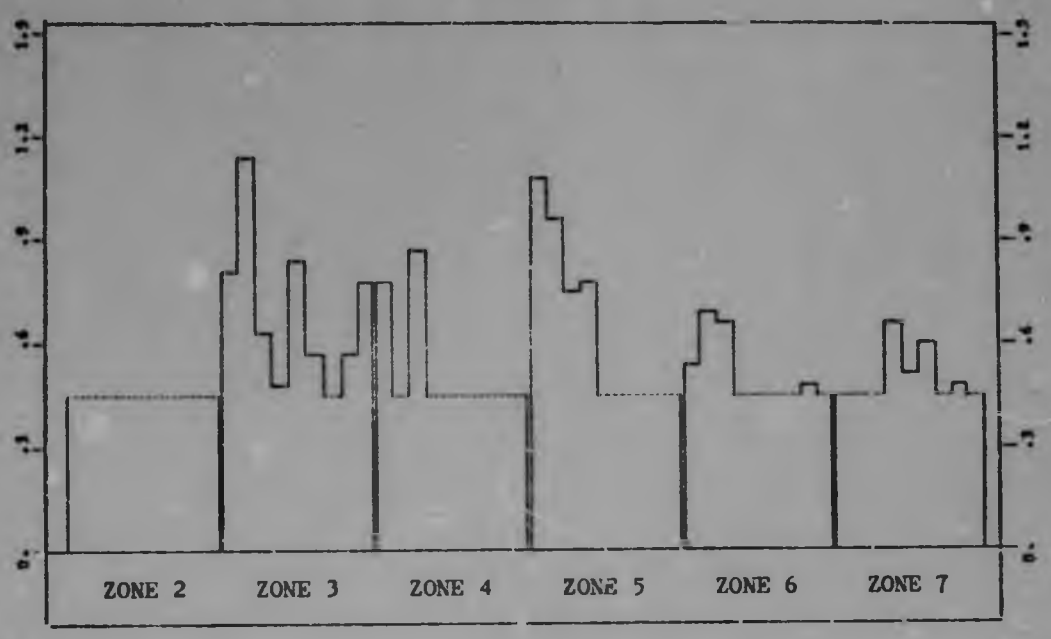
HAFNIUM p.p.m.



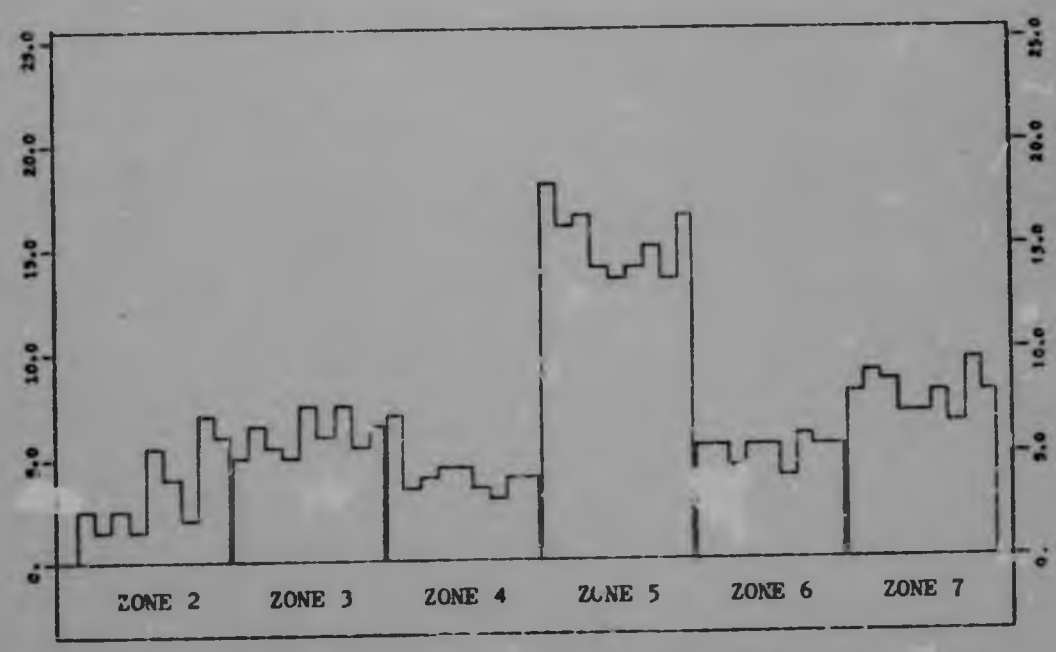
TANTALUM p.p.m.



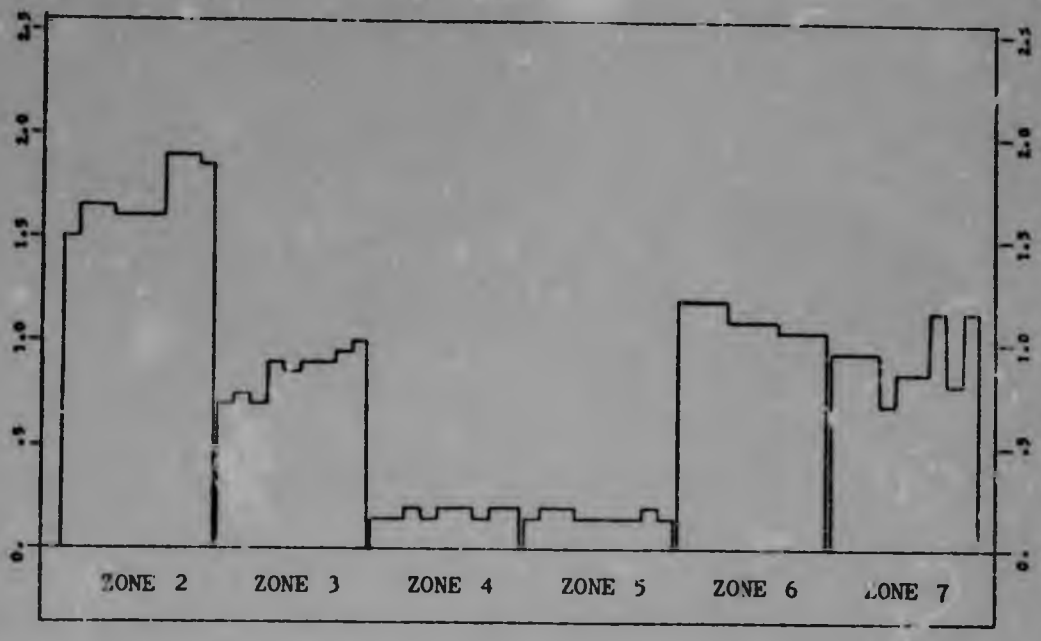
TUNGSTEN p.p.m.



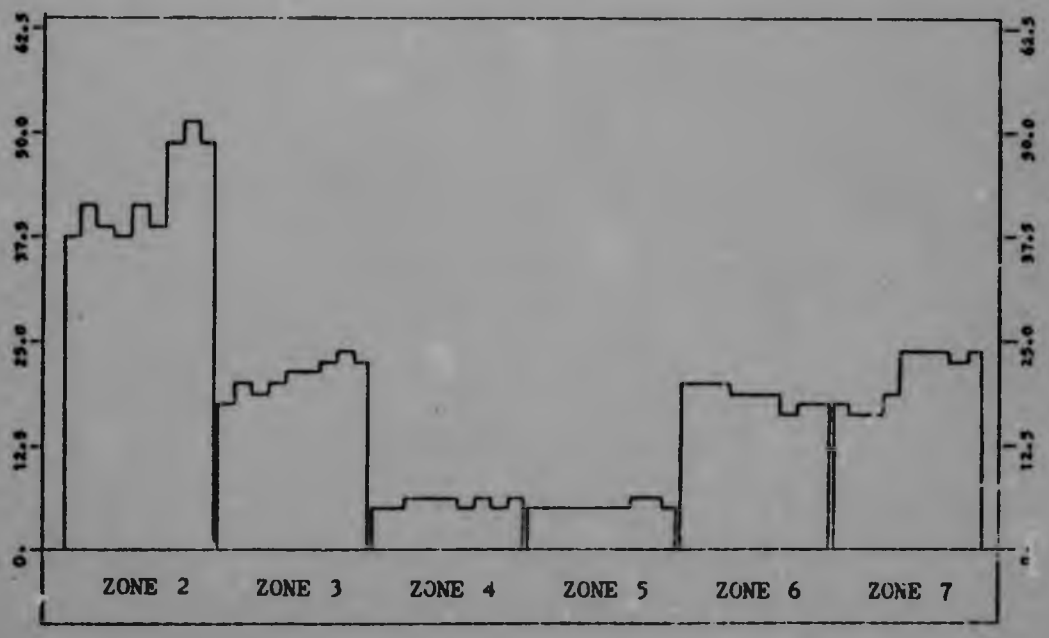
GALLIUM p.p.m.



IRON



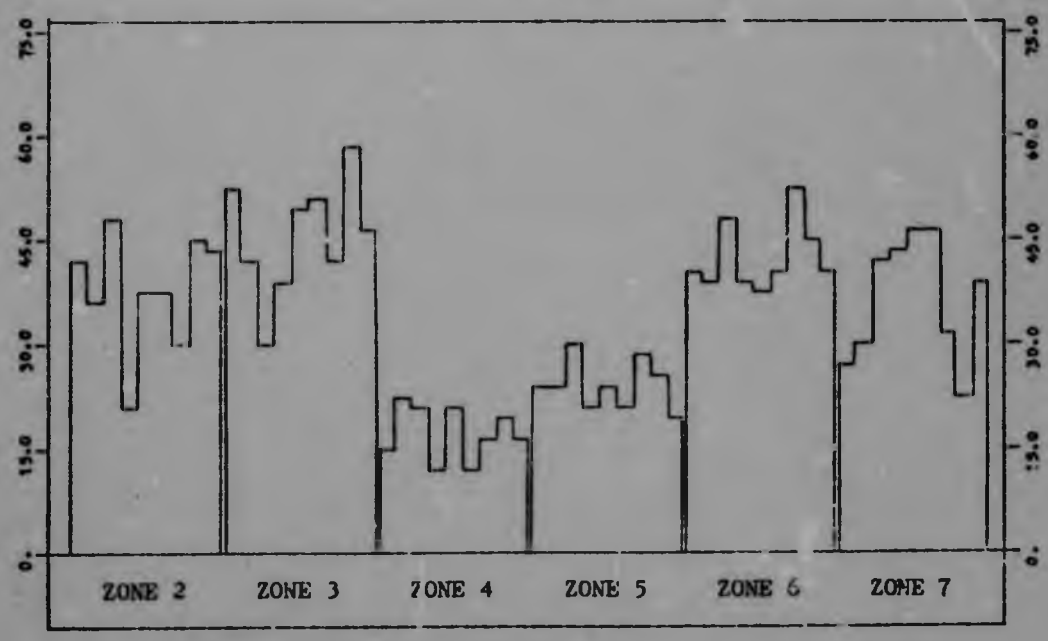
COBALT p.p.m.



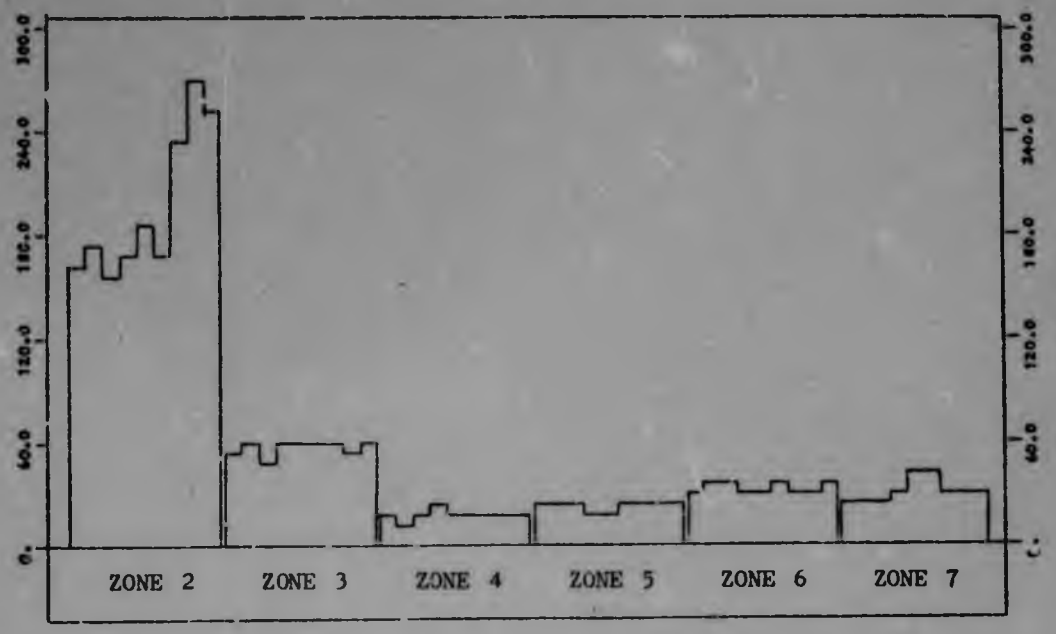
SCANDIUM p.p.m.



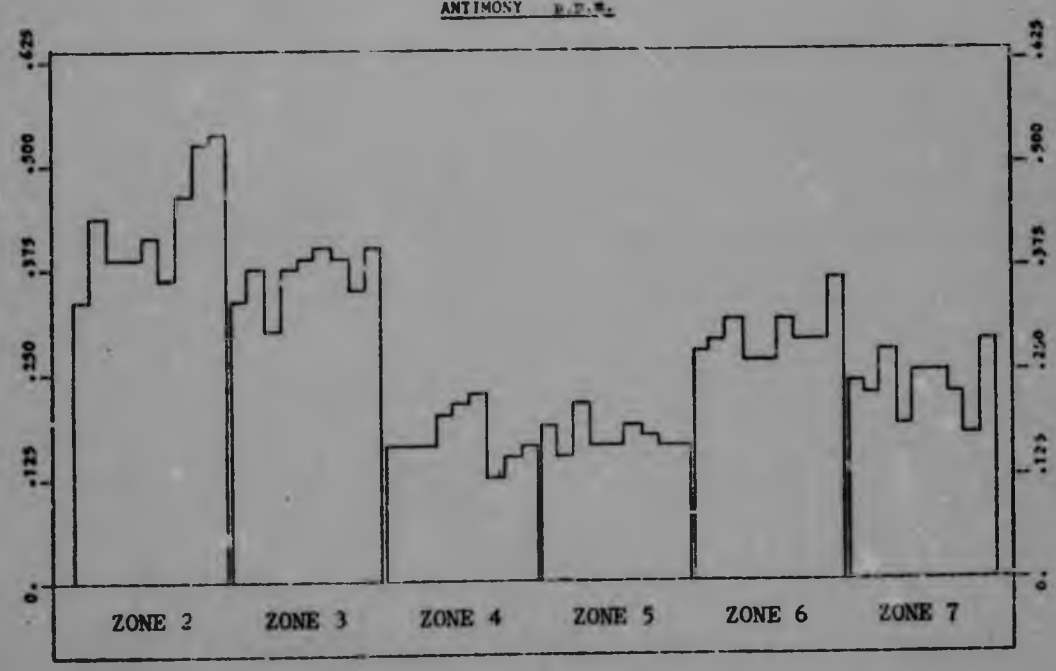
NICKEL p.p.m.

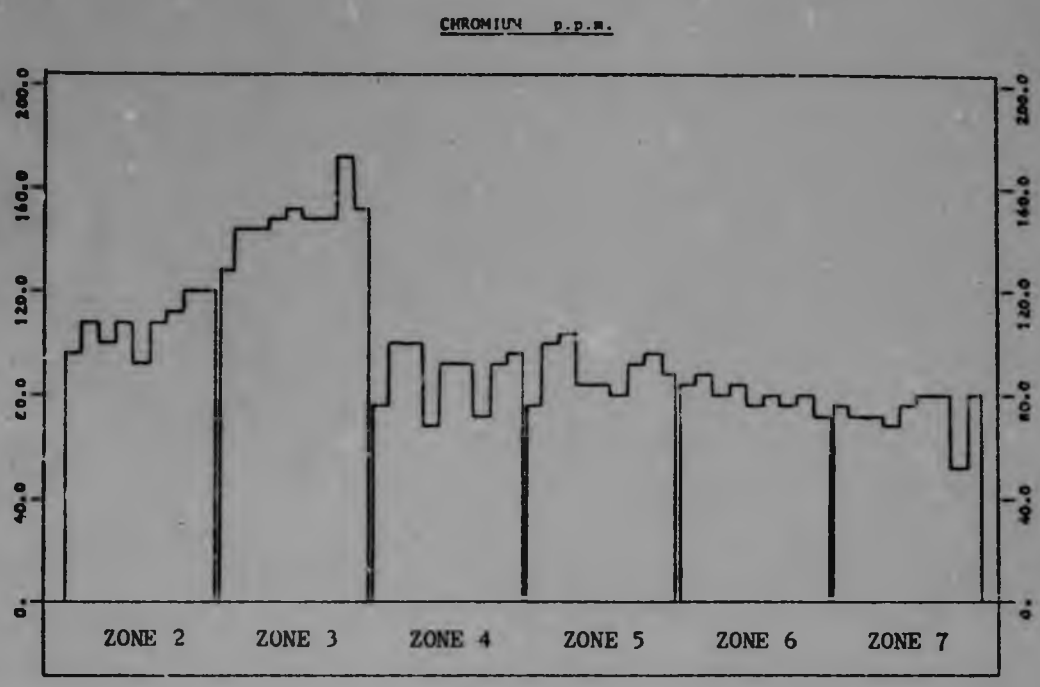


ARSENIC p.p.m.



ANTIMONY p.p.m.




CHROMIUM p.p.m.
200.0
160.0
120.0
80.0
40.0
0.
ZONE 2
ZONE 3
ZONE 4
ZONE 5
ZONE 6
ZONE 7

APPENDIX 4 FORMULATION OF THE STATISTICAL ANALYSIS

This appendix consists of a paper entitled:

"An Investigation into the use of discriminant analysis
for the classification of strata in a sedimentary succession"

by

Douglas M. Hawkins and Stephen E. Rasmussen

Journal of the International Association for Mathematical Geology
Volume 5 : No 2, pp 163 - 177, 1973

The paper develops the mathematics used in the classification of the chip samples, and corresponds to 'run 5' as described in the text.

An Investigation into the use of discriminant analysis for the classification of strata in a sedimentary succession

Douglas M. Hawkins

Mathematical Institute
University of the Witwatersrand
Johannesburg
Republic of South Africa

and

Stephen E. Rasmussen

Activation Analysis Research Group
Nuclear Physics Research Unit
University of the Witwatersrand
Johannesburg
Republic of South Africa

ABSTRACTS

The technique of instrumental neutron activation analysis has been used to analyse chip samples of geological material for 12 elements down to trace levels. Statistical discriminant analysis has been used to classify the unknown chip samples to the correct stratum in a sedimentary succession. The results are reported.

KEYWORDS

Instrumental Neutron Activation Analysis (INAA)

Chip sampling,

Discriminant analysis,

Classification.

1. Introduction

In the Witwatersrand system, the gold bearing reefs of economic importance form only a very small part of the total sedimentary sequence. A gold reef - pay band - can vary greatly in thickness from zero to a metre or more within a short distance of a few metres along strike. At the same time, the problem of following the pay band is acute, and complicated by the presence of extensive folding and faulting of the strata.

When opening up a new area of a mine, or on crossing a fault zone, it is often very difficult to locate the pay band. The method used at present is based on the identification of "marker horizons" whose position relative to the pay band is believed to be known. This method is limited in application by the fact that there are few distinctive marker horizons.

An alternative method of identification would be a study of the geochemistry of the strata. If it is found that the strata have characteristic geochemical "signatures", then these signatures could be used to solve the problems of location in the same way as the visual marker. The geochemistry of a sample of the unknown reef would then be compared with the signatures of the known strata. If the unknown resembles one stratum rather than the others, then it is reasonable to suppose that it came from that stratum.

The geochemical signature of a stratum will consist of measures of concentration and variability of each of a set of elements, and of the interrelationships between the amounts of these different elements. This information is contained in a multivariate statistical distribution of the concentrations of the set of elements.

2. Sampling Technique

The strata sampled and analysed in this study formed a section of the Kimberley reef of the Kimberley-Elsburg series in the Witwatersrand system. A single core was taken through the reef. This core intersected three quartzite strata which were very difficult or impossible to distinguish visually, and three equally indistinguishable conglomerate layers. The strata were sampled in the following way. Within each of the quartzites, five samples were taken at regular intervals, giving fifteen quartzite samples. Within each of the conglomerates five samples were taken at each of five sampling points, at regular intervals, giving seventy-five conglomerate samples. These samples were taken by cutting a 7mm slice through the core and then removing the centre of the core with a diamond drill to give a 17mm diameter tablet weighing approximately 5 g.

This 'chip' sampling technique has the advantage of being very rapid. It was also appreciated that this method gives information of element variations present within a stratum that is lost if a homogenised sample is prepared from the stratum.

3. Analytical Technique

The technique used to analyse these chip samples should ideally be insensitive to matrix effects and the physical form of the sample. The method used was instrumental neutron activation analysis.

The technique of instrumental neutron activation analysis, as opposed to neutron activation analysis using radiochemical separation techniques, has become feasible since the advent of improved equipment, in particular the development of Ge(Li) gamma detectors. The scope of the technique has been surveyed by Randle and Goles (1968). An outline of the metnod is given below. Details will be published elsewhere.

The chip samples were irradiated in a thermal neutron flux in the reactor Safari I, an Oak Ridge type reactor of the Atomic Energy Board at Pelindaba. The presence of an element is determined from the characteristics of the gamma ray spectrum emitted by the isotopes produced by the neutron irradiation. The activity of the samples was measured after a decay period of ten days using a Ge(Li) detector system. The spectra were then processed by a computer programme and the various elements present were identified and quantitatively determined.

This technique has the advantage that a number of elements can be determined simultaneously, and generally at very low levels of concentration.

The following eleven elements were determined in all the samples; La, Eu, Co, Fe, Ta, Sc, Hf, Yb, Cs, Th and Lu. In addition Au was determined in the conglomerate samples.

4. Statistical Analysis

The statistical technique developed for handling the data is discussed only with reference to the conglomerate samples for two main reasons:

1) There are seventy-five analyses available on the conglomerate samples, as compared with fifteen on the quartzite samples. Thus results on the conglomerate samples are statistically more reliable.

2) The classification of conglomerates, using a chip sampling technique, should be very much more difficult than that of quartzites. This is because the quartzites are fine grained whereas the conglomerates are coarse grained and can be very inhomogeneous.

The concentration of the elements in the conglomerate chips was indeed found to vary enormously from one chip to another, even for adjacent samples. The reason for this is not hard to find. The elements analysed were predominantly contained in the matrix, the pebbles of the conglomerate being practically pure quartz. Thus, the concentration of the elements will vary widely due to the dilution effect of varying amounts of quartz included in each chip. This fact effectively precludes any possibility of identification simply from the concentration of any single element.

The next attack on the problem was to examine the ratios of concentrations of pairs of elements. This approach was suggested by the fact that the dilution effect reduces the concentrations of all elements by the same factor. Thus the ratios of concentration of elements would be independent of the dilution, and might provide more constant signatures. We may note that taking ratios of the concentrations of different elements is equivalent to transforming to log concentrations, and then finding the difference between the log concentrations of these elements. We return to this point shortly. The results of this analysis were encouraging, though not adequate for any accurate identification.

Extending the concept of the ratio of concentrations, we were led to consider whether, if we measure the concentrations of a number of elements 1, 2, . . n, there might exist a set of powers, a_i, such that

$$\prod_{i=1}^{n} \{\text{concentration of element } i\}^{a_i}$$

has low variability within a stratum, and large variability between strata. We note that this generalised ratio is equivalent to

$$\sum_{i=1}^{n} a_i \{\log \text{ concentration of element } i\}$$

In subsequent statistical analyses, the concentrations were therefore transformed to a natural log scale. This transformation was also motivated by two further considerations:

1) The argument above suggests that it is likely on the basis of physical reasoning that identifiable signatures will be based on weighted sums of the log transformed concentrations. The statistical technique of discriminant analysis that was used deals with precisely this type of weighted sum. Thus it is reasonable for the input to the discriminant analysis to be in terms of log concentrations.
2) It is likely from experience in geological systems, that the concentrations will follow a distribution similar to the log-normal. The log-normal distribution is well established in case of gold (Link, 1971), and may, therefore, apply to some of the other elements analysed, as well.

The nature of the chip sampling scheme is such that the analyses will contain information on the following aspects of variation in the characteristics of the reef:

1) The small scale local variation in element concentration: this variation is termed the "nugget effect" (David,1969). Since the five chips taken from each sampling point were closely spaced, the nugget effect may be assessed by a study of the variation from chip to chip at each sampling point.
2) The larger scale variation in composition within a stratum: if we compare the average composition of each sampling point within a stratum with that of other points within the same stratum, we can assess the variability within the stratum. This information is valuable as it gives a

measure of the homogeneity of a single stratum.

3) The variation between the strata, as measured by comparison of the average elemental composition of the strata.

The assessment of the variability arising from each of these sources is vital in the identification of chip samples. Hopefully, one would find that the first variation mentioned above would be small, indicating that the characteristics of the rock are fairly constant in the small scale. The second variation should preferably be small, and the third large, indicating that the differences between strata are greater than those between different sampling points in the same stratum. These aspects can be quantified and assessed by means of a statistical nested multivariate analysis of variance.

The analysis of variance model is as follows: on each of the chip samples, we have a set of twelve values reflecting the log concentrations of the twelve elements determined. Let these twelve values be set out in a vector, identified as follows:

x_{ijk} is the vector of log concentrations in chip sample number k from sampling point number j in stratum number i:

η_{ij} is the adjusted true average vector of log concentrations at sampling point j of stratum i:

ξ_i is the true average log concentration vector in stratum i.

Then $x_{ijk} = \xi_i + \eta_{ij} + e_{ijk}$

for i=1 to 3; j=1 to 5; and k=1 to 5.
The term e_{ijk} is a "vector of deviations" between the model and the actual analysis vector observed. Statistically, we assume that the vector e_{ijk} follows a multivariate normal distribution with a zero mean vector and a covariance matrix Σ.

The statistical characteristics of the ξ_i and η_{ij} terms are of interest. They are clearly dependent on where we happen to sample our core, and so it is reasonable to think of them too, as being random realisations of some statistical process. As such, they will have covariance matrices which can be estimated, and which will cast some light on the variation between the characteristics of different strata as such, or of different sampling points as such, without specific reference to the present data.

Thus the nested multivariate analysis of variance model is:

For given ξ_i and η_{ij}: $x_{ijk} \sim N(\xi_i + \eta_{ij}, \Sigma)$

For given ξ_i : $\eta_{ij} \sim N(O, \Sigma_p)$

and $\xi_i \sim N(\mu, \Sigma_h)$

The analysis of variance is then:

Source	S.S.	d.f.
Between strata	$\sum_{i=1}^{3} 25(x_{i..} - x_{...})(x_{i..} - x_{...})'$	2
Points within strata	$\sum_{i=1}^{3}\sum_{j=1}^{5} 5(x_{ij.} - x_{i..})(x_{ij.} - x_{i..})'$	12
Error	$\sum_{i=1}^{3}\sum_{j=1}^{5}\sum_{k=1}^{5} (x_{ijk} - x_{ij.})(x_{ijk} - x_{ij.})'$	60
Total	$\sum_{i=1}^{3}\sum_{j=1}^{5}\sum_{k=1}^{5} (x_{ijk} - x_{...})(x_{ijk} - x_{...})'$	74

where substitution of a point for an index denotes averaging over that index.

The mean square and cross product terms have expectations as follows:

Source	MS	E(MS)
Between strata	S_h	$\Sigma + 5\Sigma_p + 25\Sigma_h$
Points within strata	S_p	$\Sigma + 5\Sigma_p$
Error	S	Σ

The hypothesis $\Sigma_p = 0$ may be tested by reducing $S_p S^{-1}$ to canonical form. On these data, this yielded a leading eigenvalue of 22.6, which is significant at the 1% level. Thus we conclude that there is significant variation between sampling points within strata.

To test $\Sigma_h = 0$ a similar analysis could be applied to $S_h S_p^{-1}$. Using all 12 elements yields insufficient degrees of freedom, but analysis with fewer than 12 elements indicated significance at the 5% level.

The covariance matrices may be estimated from the components of the analysis.

$$\hat{\Sigma} = S$$
$$\hat{\Sigma}_p = (S_p - S)/5$$
$$\hat{\Sigma}_h = (S_h - S_p)/25$$

In table 1 we display the covariance matrix $\hat{\Sigma}$. We note that the different elements have positive, and fairly large covariances between their concentrations. This may be due to some extent to cogeneticism, but is largely due to the dilution effect. The presence of a large quartz pebble in a chip sample will depress the concentration of all elements, thus there will be a tendency for high values of any element to be associated with high values of any other.

The standard deviations in table 1 are interpretable as follows:
The standard deviation of, for example, gold is 1.23. In other words, in about two-thirds of cases (assuming a log-normal model) the chips will have a log concentration of gold within plus or minus 1.23 of the mean gold concentration at the sampling point. Transposing this statement, in about a third of cases, the chip will have a gold content which differs from the mean at that sampling point by a factor of

more than 3.4 (=antilog 1.23). Some of the other elements - for example Europium, Scandium - have much lower standard deviations. Since the dilution effect affects all elements equally, this fact suggests that these elements are more uniformly distributed in the matrix. It is known that gold occurs in small particles in the matrix rather than in some more continuous form. This result suggests that the same applies to, for example, Tantalum, but not to Europium or Scandium.

Table 2 displays the covariance matrix $\hat{\Sigma}_p$. We see that the standard deviations are of very much the same size as those in table 1. This means that the variation between sampling points is of the same order as the nugget effect.

In table 3, we give the estimated standard deviations of the ξ_i. Due to the small number of strata studied (3), the covariance matrix was subject to large sampling variations, and is not given. These standard deviations are generally much lower than those in the preceding two tables. This result suggests that overall, the strata show less variability from one another than from point to point within a stratum.

5. Canonical Variate Analysis

Although 12 elements were available for separating the samples from the strata, it is not to be expected that all elements will be relevant. To determine which elements are of value in separating strata, a multivariate analysis of variance was carried out on the matrices S_h and S. This produced the canonical variates (Rao, 1952) y_1 and y_2 having the following properties:

a) y_1 and y_2 are weighted sums of the log concentrations of the elements. In vector notation

$$y_1 = \beta_1 x$$

$$y_2 = \beta_2 x$$

where β_1 and β_2 are coefficient vectors, whose i th component is the weight attached to the i th element.

b) y_1 and y_2 are statistically independent, and have unit variance between replicates.

c) y_1 and y_2 vary maximally between strata, having variances v_1 and v_2 between strata.

If an element does not have a large weight in these coefficient vectors, then it does not contribute markedly to the classification, and so may be omitted.

The values of v_1, v_2 and of the coefficient vectors are listed in table 4a. On the basis of the weights, it was concluded that the major part of the discrimination was due to the elements La, Eu, Fe, Sc, Cr, and Th. The canonical variate analysis was repeated using only these elements. The results are given in table 4b. From this we see that these six elements account for 71% of the trace v_1 and v_2.

The subsequent analysis was therefore carried out using these six elements only. Parallel computation using the full set of elements yielded very similar conclusions.

6. Discriminant Analysis

It has already been suggested that linear functions of the log concentration vector could be expected to provide signatures of sampling points. Our problem is to find weights to attach to each element that will provide optimal discrimination. This formulation leads us at once to the statistical theory of discriminant analysis (Anderson, 1961).

Briefly, this technique is as follows: Suppose there are k groups to one of which an unknown sample belongs. Suppose also that we observe vectors of p observations on the objects under study. The vector of observations on the unknown is x, and in the i th group, the vector of observations follows a multivariate normal distribution with mean vector μ_i, and covariance matrix Σ.

The problem of discrimination can then be approached as follows:

The Mahalanobis distance D_i^2 between the unknown and the i th group is defined as (Sokal and Sneath, 1963)

$$D_i = (x - \mu_i)' \Sigma^{-1} (x - \mu_i)$$

and is a measure of the dissimilarity between the unknown and the group. It is zero if the two are identical, and increases the more dissimilar the two are.

We note that the matrix Σ^{-1} performs the function of the weights that attach to the difference in the concentration of any given element. Theory shows that the weights implied by Σ^{-1} are optimal.

Suppose that q_i is the a priori probability that the unknown came from the i th group. Then the classification rule is:- compute $-D_i^2 \log q_i$ for all values of i from 1 to k. Assign the unknown to that group for which this measure is smallest. If in ignorance about the true values of the q_i, then assume that they are all equal. The classification rule is then: assign the unknown to that group for which D_i^2 is a minimum.

The success of this technique depends on the degree of dissimilarity between the groups. This can be measured by means of the Mahalanobis distance between the groups. This is defined as:

$$d_{ij} = (\mu_i - \mu_j)' \Sigma^{-1} (\mu_i - \mu_j)$$

Suppose an observation vector x comes from group i. Its distances D_i^2 and D_j^2 from groups i and j follow respectively a central chisquared distribution with p degrees of freedom and a noncentral chisquared distribution with p degrees of freedom and noncentrality d_{ij}. The expected values of these are:

$$E(D_i^2) = p$$

$$E(D_j^2) = p + d_{ij}$$

If d_{ij} is large, then it is likely that D_j^2 will exceed D_i^2, and that a correct classification will result.

In the absence of knowledge of the values of the μ_i and of Σ, we must estimate them from data. The standard estimates for the μ_i are the mean vectors of the data in the i th group, and for Σ the matrix S of pooled within groups

covariances (Anderson).

In table 5, we show the estimated Mahalanobis distances between every pair of the 15 sampling points. Since each mean is based on 5 replicates, and the pooled within groups covariance matrix has 60 degrees of freedom, it follows that on data vectors having 6 components $F = .382\ D^2$ has an F distribution with 6 and 55 degrees of freedom if the difference between two sampling points is due entirely to random variation.

From tables of the F distribution the significance levels for D^2 can be derived. These are 5.94 (5% level) and 8.27 (1% level).

Comparing the entries in table 5 with these values, we find that all but 8 are significant at the 5% level, the majority being significant beyond the 1% level. The size of the distances suggests that it should be possible to classify the chip samples to a high degree of accuracy.

Finally, an attempt was made to use the classification procedure to classify the given data to their known sampling points. Often over-optimistic results emerge when the classification procedure is used on the data from which it was derived. To avoid this difficulty, the analysis was carried out as follows: each sample was excluded in turn from the set of samples. The mean of each sampling point was then estimated from the remaining samples. The Mahalanobis distance between the excluded sample and the estimated means was then computed, and the assignment carried out. The accuracy of this classification was noted, and the next sample omitted in its turn.

The results of this test are summarised in table 6. It is clear from this table that a remarkably high proportion of the samples were classified correctly. It should be pointed out that these results are probably conservative since means at each sampling point were estimated from small samples, and so would contribute variability to the distances.

It is possible to attain any arbitrary accuracy in classification by means of analysing more samples of the unknown rock sample. The technique of neutron activation analysis allows such multiple analyses to be carried out at relatively little extra cost. The composition of the unknown is estimated from the average of the individual analyses.

The theory of discriminant analysis shows that the use of n samples in this way is equivalent to increasing the Mahalanobis distances between sampling points by a factor of $\sqrt{n}$ i.e. it magnifies the apparent separation between the levels by this factor. Thus use of large n values will, in principle, allow arbitrarily high accuracy. Another point is that the theory of discriminant analysis allows us to determine how many such replicate analyses should be carried out to secure a given correct-classification percentage.

7. Conclusion

At first sight, the classification of chip samples would seem to be a hopeless task. The variability between adjacent chips is so large as to seem to obscure the

differences between sampling points. However, we have shown that by using a multidimensional approach, looking at a number of elements simultaneously, fairly large differences between strata are apparent. On the basis of these differences, it is possible to attain a remarkably high level of accuracy in the classification.

For the conglomerate samples 88% were classified to the correct stratum, although of these 23% were to the incorrect sampling point within the stratum.

A similar analysis for the quartzite samples resulted in 100% successful classification. This must still be confirmed when more than 5 analyses from each stratum are available.

This initial study leaves several questions unanswered, among which is the large-scale horizontal variability of the strata. Should the results of further investigations substantiate this initial success, we will apply this technique in a number of problems associated with mining exploration.

Acknowledgements

The sampling was made possible through the active co-operation of Mr. A. Kriek, Mr. V. Werdmuller and others of Rand Mines Ltd.

The analyses were carried out at the Activation Analysis Research Group, a joint group of the University of the Witwatersrand and the National Institute for Metallurgy, Johannesburg. Dr. R.E.Robinson, Director of the National Institute for Metallurgy and Professor J.P.F.Sellschop, Director of the Nuclear Physics Research Unit are thanked for their encouragement and assistance during this research programme and permission to publish the results.

We would also like to thank our colleagues, in particular Mr.H.W.Fesq and Mr. P.Fatti, for their helpful discussion and criticism.

Financial support from Rand Mines Ltd., the Atomic Energy Board, the National Institute for Metallurgy and the University of the Witwatersrand is gratefully acknowledged.

REFERENCES

Anderson, T.W., Introduction to multivariate analysis (J.Wiley, New York, 1961).

David, M., "The notion of extension variance and its application to the grade estimation of stratiform deposits" in A Decade of digital computing in the mineral industry, American Institute of Mining Metallurgical and Petroleum Engineer (1969).

Link, R., Koch, G., Schuenemeyer, J., U.S.Department of Interior, Bureau of Mines Report RI 7495 (1971).

Randle, K. and Goles, G., Ge(Li) detectors in the Activation Analysis of Geological Samples. Proceedings Modern Trends in Activation Analysis, Vol.II (1968) 347.

Rao, C.R. Advanced Statistical Methods in Biometric Research (J.Wiley, New York, 1952).

Sokal, A.H., and Sneath, R.R., Principles of numerical taxonomy (W.H.Freeman & Co., San Francisco, 1963).

TABLE 1: Covariance matrix S of the error term e

	La	Eu	Co	Fe	Ta	Sc	Hf	Yb	Cr	Th	Lu	Au
La	0.410	0.255	0.268	0.256	0.366	0.203	0.175	0.300	0.229	0.285	0.288	0.303
Eu	0.255	0.244	0.269	0.259	0.373	0.173	0.226	0.273	0.249	0.249	0.211	0.216
Co	0.268	0.269	0.979	0.734	0.655	0.290	0.492	0.495	0.544	0.439	0.475	0.658
Fe	0.256	0.259	0.734	0.636	0.528	0.270	0.432	0.400	0.478	0.376	0.360	0.554
Ta	0.366	0.373	0.655	0.528	1.242	0.285	0.517	0.555	0.469	0.433	0.442	0.394
Sc	0.203	0.173	0.290	0.270	0.285	0.301	0.274	0.247	0.310	0.231	0.240	0.219
Hf	0.175	0.226	0.492	0.432	0.517	0.274	0.782	0.360	0.431	0.310	0.318	0.245
Yb	0.300	0.273	0.495	0.400	0.555	0.247	0.360	0.507	0.366	0.369	0.370	0.313
Cr	0.229	0.249	0.544	0.478	0.469	0.310	0.431	0.366	0.610	0.334	0.329	0.286
Th	0.285	0.249	0.439	0.376	0.433	0.231	0.310	0.369	0.334	0.408	0.348	0.326
Lu	0.288	0.211	0.475	0.360	0.442	0.240	0.318	0.370	0.329	0.348	0.556	0.365
Au	0.303	0.216	0.658	0.554	0.394	0.219	0.245	0.313	0.286	0.326	0.365	1.508
STANDARD DEVIATIONS	0.641	0.494	0.990	0.738	1.114	0.548	0.885	0.712	0.781	0.639	0.746	1.228

TABLE 2: Covariance matrix $\hat{\Sigma}_p$ of the true average vector of log concentration n

	La	Eu	Co	Fe	Ta	Sc	Hf	Yb	Cr	Th	Lu	Au
La	0.726	0.495	0.745	0.393	0.616	C.121	0.251	0.404	0.391	0.714	0.611	0.267
Eu	0.495	0.385	0.480	0.257	0.363	0.067	0.134	0.257	0.252	0.428	0.351	0.113
Co	0.745	0.480	1.136	0.820	0.709	0.144	0.193	0.304	0.372	0.749	0.592	0.886
Fe	0.393	0.257	0.820	0.707	0.425	0.149	0.016	0.118	0.219	0.381	0.284	0.864
Ta	0.616	0.363	0.709	0.425	0.738	0.172	0.063	0.276	0.268	0.641	0.640	0.555
Sc	0.121	0.067	0.144	0.149	0.172	0.111	-0.040	0.062	0.129	0.122	0.110	0.215
Hf	0.251	0.134	0.193	0.016	0.063	-0.040	0.330	0.178	0.238	0.340	0.182	-0.216
Yb	0.404	0.257	0.304	0.118	0.276	0.062	0.178	0.228	0.224	0.399	0.344	-0.481
Cr	0.391	0.252	0.372	0.219	0.268	0.129	0.238	0.224	0.361	0.430	0.271	0.092
Th	0.714	0.428	0.749	0.381	0.641	0.122	0.340	0.399	0.430	0.751	0.641	0.264
Lu	0.611	0.351	0.592	0.284	0.640	0.110	0.182	0.344	0.271	0.641	0.601	0.247
Au	0.267	0.113	0,886	0.864	0.55?	0.215	-0.216	-0.481	0.092	0.264	0.247	1.350
STANDARD DEVIATIONS	0.852	0.621	1.066	0.841	0.859	0.333	0.575	0.477	0.601	0.867	0.775	1.162

TABLE 3

Estimated Standard deviations of the true average log concentration

Element	Standard Deviation
La	0.056
Eu	0.507
Co	0.723
Fe	0.703
Ta	0.226
Sc	0.580
Hf	0.153
Yb	0.526
Cr	0.336
Th	0.118
Lu	0.484
Au	0.530

Table 4

Canonical variates: variances and coefficient vectors

	4a - 12 elements		4b - 6 elements	
	1	2	1	2
Variances	104.4	43.8	31.9	23.6
Coefficients				
La	- .835	- .044	- .693	- .385
Eu	1.706	.835	1.524	.941
Co	.160	.433	-	-
Fe	.433	-1.588	.371	-1.494
Ta	- .448	- .423	-	-
Sc	.786	.011	.855	- .053
Hf	- .387	.756	-	-
Yb	.191	.211	-	-
Cr	- .665	.263	- .743	.584
Th	- .879	- .080	- .789	- .106
Lu	.328	- .657	-	-
Au	- .048	.164	-	-

TABLE 5: Estimated Mahalanobis distance between every pair of the 15 sampling points

Stratum		1					2					3				
	Point	1	2	3	4	5	6	7	8	9	10	11	12	13	14	15
1	1	0.	26.96	26.93	37.19	20.52	18.21	23.87	11.38	17.86	21.87	27.40	10.67	18.61	13.68	13.96
	2		0.	4.57	2.21	18.86	20.42	24.08	28.37	25.77	30.79	26.82	14.25	20.73	16.92	23.18
	3			0.	6.21	32.81	30.18	22.78	20.75	21.71	29.45	22.38	11.12	14.47	12.12	32.04
	4				0.	25.60	28.06	28.68	35.43	36.32	39.32	30.70	19.82	29.95	24.78	31.27
	5					0.	7.15	40.43	34.89	25.84	40.62	51.95	19.66	27.76	25.39	4.50
2	6						0.	21.05	18.81	14.93	17.56	30.12	22.45	23.42	23.47	16.01
	7							0.	14.49	23.28	3.04	3.53	34.82	36.34	35.15	46.15
	8								0.	11.12	10.44	13.53	13.90	13.03	11.62	34.13
	9									0.	18.17	31.67	17.07	6.57	13.78	23.87
	10										0.	5.70	35.24	31.71	31.90	47.31
3	11											0.	34.84	38.27	33.16	58.26
	12												0.	6.39	2.00	14.21
	13													0.	2.77	23.29
	14														0.	21.45
	15															0.

TABLE 6

Accuracy of Sample Classification

Classification class	Number	Fraction of total
Incorrect level	9	12%
Correct level	66	88%
CORRECT LEVEL		
i)correct sampling point	49	65%
ii)incorrect sampling point	17	23%

APPENDIX 5 STATISTICAL ANALYSIS OF CHIP SAMPLES

The statistical analysis of the chip samples has been carried out using a number of permutations of the data. The results obtained for each 'run' are given in this appendix under separate sections. A summary of the analyses is given in the text.

The permutation of the data for each run is as follows:

RUN	SAMPLES	PARENT POPULATIONS	ELEMENTS INCLUDED IN THE ANALYSIS
1	Quartzites & Conglomerates	6	only 11
2	Quartzites	3	only 11
3	Conglomerates	3	all 12
4	Conglomerates	15	all 12
5	Conglomerates	15	best 6

The elements referred to are as follows:

only 11 : Th, La, Eu, Yb, Lu, Hf, Ta, Fe, Sc, Cr, Co

all 12 : Au, Th, La, Eu, Yb, Lu, Hf, Ta, Fe, Sc, Cr, Co

best 6 : Th, La, Eu, Fe, Sc, Cr

The following data is presented for each run:

Table 1 : VALUES OF D^2 BETWEEN POPULATION MEANS

The value of the Mahalanobis distance, D^2, for each individual sample to the parent population mean are approximately equal to the number of observations (elements) included in the analysis. Thus for good separation, the value of D^2 between populations should be at least four times the average distance of each sample to the mean of the parent population.

Table 2 : CLASSIFICATION OF SAMPLES

The value of D^2 is calculated for each sample to the mean of each population. The sample is then assigned to the nearest population. The accuracy of classification is calculated from the number of correctly assigned samples.

Table 3 : CANONICAL VARIANT VECTORS

The variance or eigen value (λ_i) of each canonical vector (Y_i) is given. The relative magnitudes of the eigen values reflect the degree of discrimination of each canonical variate. The coefficients (β_{ij}) of each element are given for the first two vectors.

Table 4 : RELATIVE IMPORTANCE OF ELEMENTS

The relative importance of each element is given on an arbitrary scale. The most important element has been assigned a value of 10. These values are obtained from the variances and coefficients given in Table 3.

Figure 1 : TWO DIMENSIONAL REPRESENTATION

This is a representation of the plane in multidimensional space which shows the largest discrimination between populations. The percentage discrimination of each axis is given, and of the overall representation of the population means. The representation is based on the data given in Table 3.

Section A 5.1 RUN 1 - CLASSIFICATION OF CONGLOMERATES AND QUARTZITES TO 6 ZONES

Table A 5.1.1 VALUES OF D^2 BETWEEN POPULATION MEANS

ZONE	2	3	4	5	6	7
2	0	6.9	20	17	9.5	3.8
3	6.9	0	7.8	9.9	15	3.6
4	20	7.8	0	12	27	15
5	17	9.9	12	0	19	8.4
6	9.5	15	27	19	0	7.7
7	3.8	3.6	15	8.4	7.7	0

Table A 5.1.2 CLASSIFICATION OF SAMPLES

PARENT ZONE	NUMBER OF SAMPLES CLASSIFIED TO ZONE					
	2	3	4	5	6	7
2	17	3			1	4
3					5	
4		1			4	
5					4	1
6		5		1	12	7
7	1	7	6	4		7

Accuracy of classification:

Correct : 36 - 40%

Incorrect : 54 - 60%

Table A 5.1.3 CANONICAL VARIATE VECTORS

VECTOR	VARIANCE	ELEMENT	COEFFICIENTS FOR Y_1	COEFFICIENTS FOR Y_2
Y_1	35.1	Th	-0.035	0.326
Y_2	20.1	La	-0.825	0.636
Y_3	7.68	Eu	0.685	-1.494
Y_4	3.46	Yb	0.599	0.276
Y_5	0.93	Hf	-0.180	-0.301
		Ta	-0.421	0.315
		Fe	1.413	1.574
		Sc	0.462	-0.931
		Cr	-0.638	0.251
		Co	-0.986	-1.235

Table A 5.1.4 RELATIVE IMPORTANCE OF ELEMENTS

ELEMENT	ARBITRARY SCALE
Fe	10
Co	8.2
Eu	6.7
La	4.8
Sc	4.2
Lu	4.1
Cr	3.7
Yb	3.1
Ta	2.6
Hf	1.8
Th	1.7

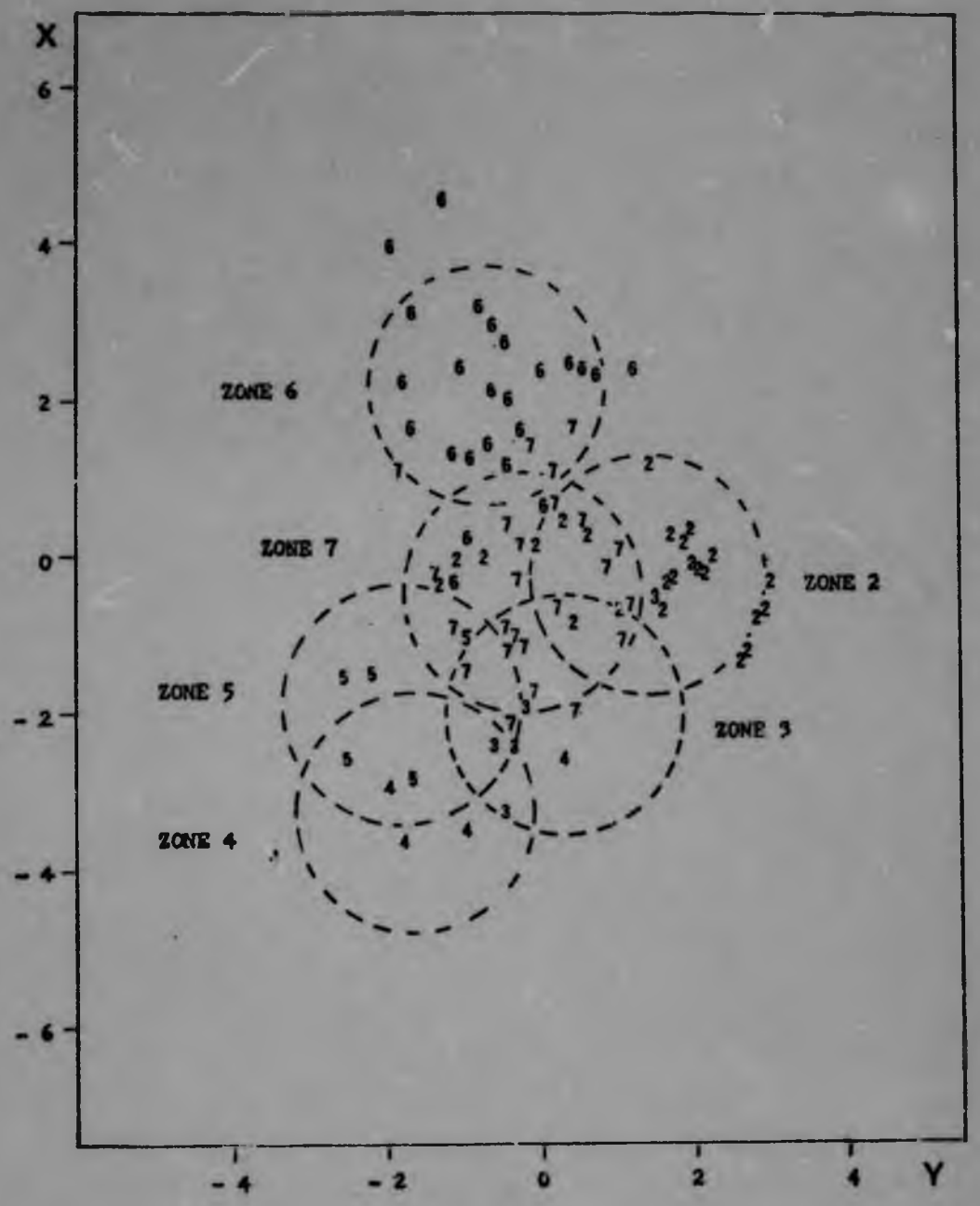


Figure A 5.1 TWO DIMENSIONAL REPRESENTATION

X-AXIS : Based on Y_1 : 52.5 % Representation

Y-AXIS : Based on Y_2 : 29.9 % Representation

Accuracy of representation : 82 %

Section A 5.2 RUN 2 - CLASSIFICATION OF QUARTZITES TO 3 ZONES

Table A 5.2.1 VALUES OF D^2 BETWEEN POPULATION MEANS

ZONE	3	4	5
3	0	461	101
4	461	0	239
5	101	239	0

Table A 5.2.2 CLASSIFICATION OF SAMPLES

PARENT ZONE	NUMBER OF SAMPLES CLASSIFIED TO ZONE		
	3	4	5
3	5	0	0
4	0	5	0
5	0	0	5

Accuracy of classification:

Correct: 15 - 100%

Incorrect: 0 - 0%

Table A 5.2.3 CANONICAL VARIANT VECTORS

VECTOR	VARIANCE	ELEMENT	COEFFICIENTS FOR Y_1	COEFFICIENTS FOR Y_2
Y_1	594.5	Th	9.732	-1.725
Y_2	71.4	La	-8.694	-2.288
		Eu	13.378	-0.807
		Yb	16.498	-2.862
		Lu	-3.875	4.525
		Hf	-23.581	4.411
		Ta	-18.776	2.070
		Fe	5.706	-0.715
		Sc	-11.971	0.586
		Cr	32.682	-5.010
		Co	-19.725	2.014

Table A 5.2.4 RELATIVE IMPORTANCE OF ELEMENTS

ELEMENT	ARBITRARY SCALE
Cr	10
Hf	7.3
Co	5.9
Ta	5.7
Yb	5.1
Eu	4.0
Sc	3.6
Th	3.0
La	2.6
Fe	1.7
Lu	1.5

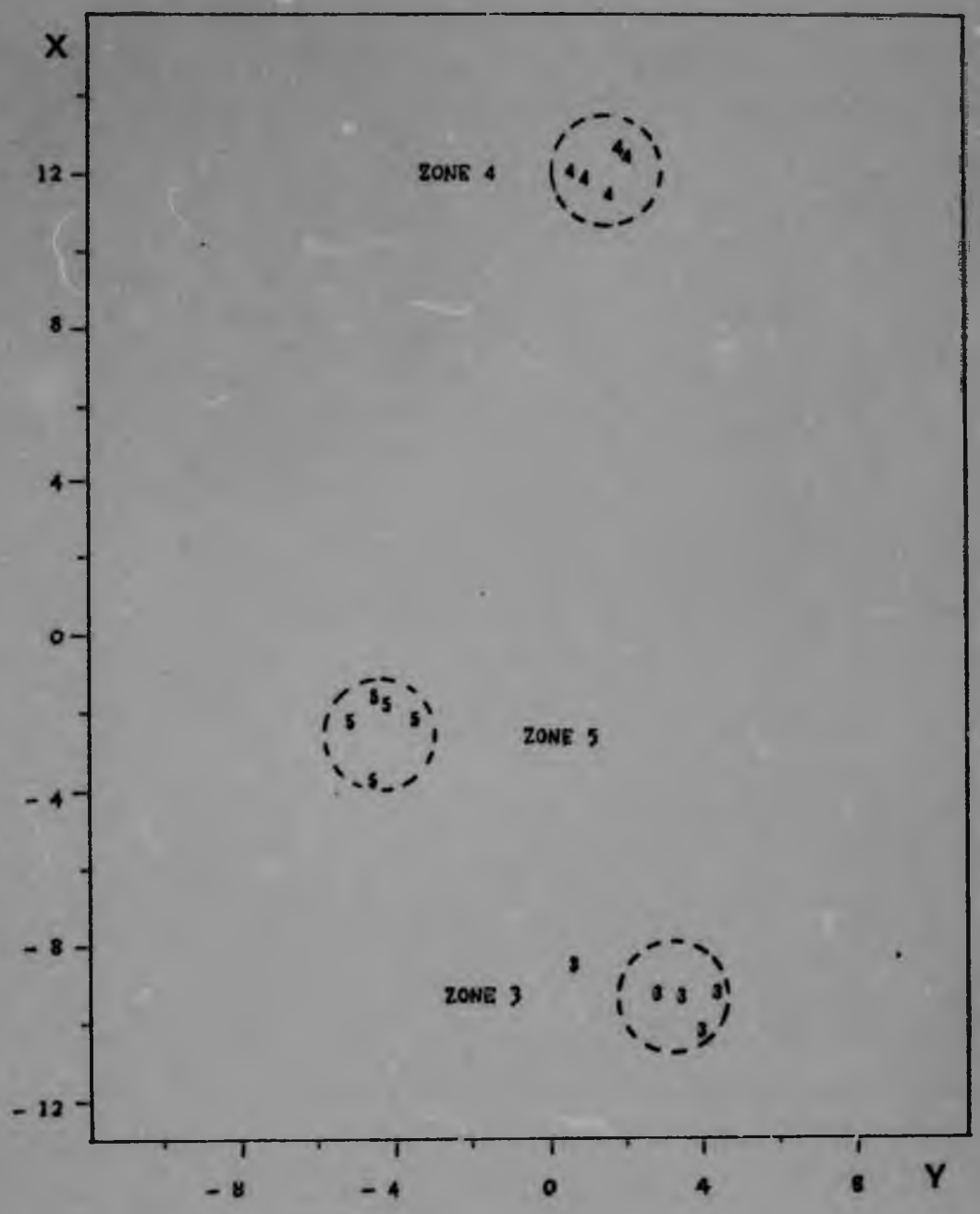


Figure A 5.2 TWO DIMENSIONAL REPRESENTATION

X-AXIS : Based on Y_1 : 89.3 % Representation

Y-AXIS : Based on Y_2 : 10.7 % Representation

Accuracy of representation : 100 %

Section A 5.3 RUN 3 - CLASSIFICATION OF CONGLOMERATES TO 3 ZONES

Table A 5.3.1 VALUES OF D^2 BETWEEN POPULATION MEANS

ZONE	2	6	7
2	0	8.8	3.8
6	8.8	0	6.9
7	3.8	6.9	0

Table A 5.3.2 CLASSIFICATION OF SAMPLES

PARENT ZONE	NUMBER OF SAMPLES CLASSIFIED TO ZONE 2	6	7
2	19	1	5
6	1	2	3
7	3	4	18

Accuracy of classification:

Correct: 58 - 77.3%

Incorrect: 17 - 22.7%

Table A 5.3.3 CANONICAL VARIANT VECTORS

VECTOR	VARIANCE	ELEMENT	COEFFICIENTS FOR	
			Y_1	Y_2
Y_1	58.6	Au	0.120	0.348
Y_2	22.5	Th	-0.355	0.353
		La	-1.162	0.227
		Eu	1.592	0.612
		Yb	0.355	-0.337
		Lu	0.274	-1.034
		Hf	0.029	0.757
		Ta	-0.597	0.017
		Fe	-0.257	-1.081
		Sc	0.922	0.336
		Cr	-0.650	-0.311
		Co	0.364	0.063

Table A 5.3.4 RELATIVE IMPORTANCE OF ELEMENTS

ELEMENT	ARBITRARY SCALE
Eu	10
La	6.8
Sc	5.8
Cr	4.2
Fe	3.7
Lu	3.7
Ta	3.3
Th	2.7
Yb	2.7
Co	2.1
Hf	1.8
Au	1.4

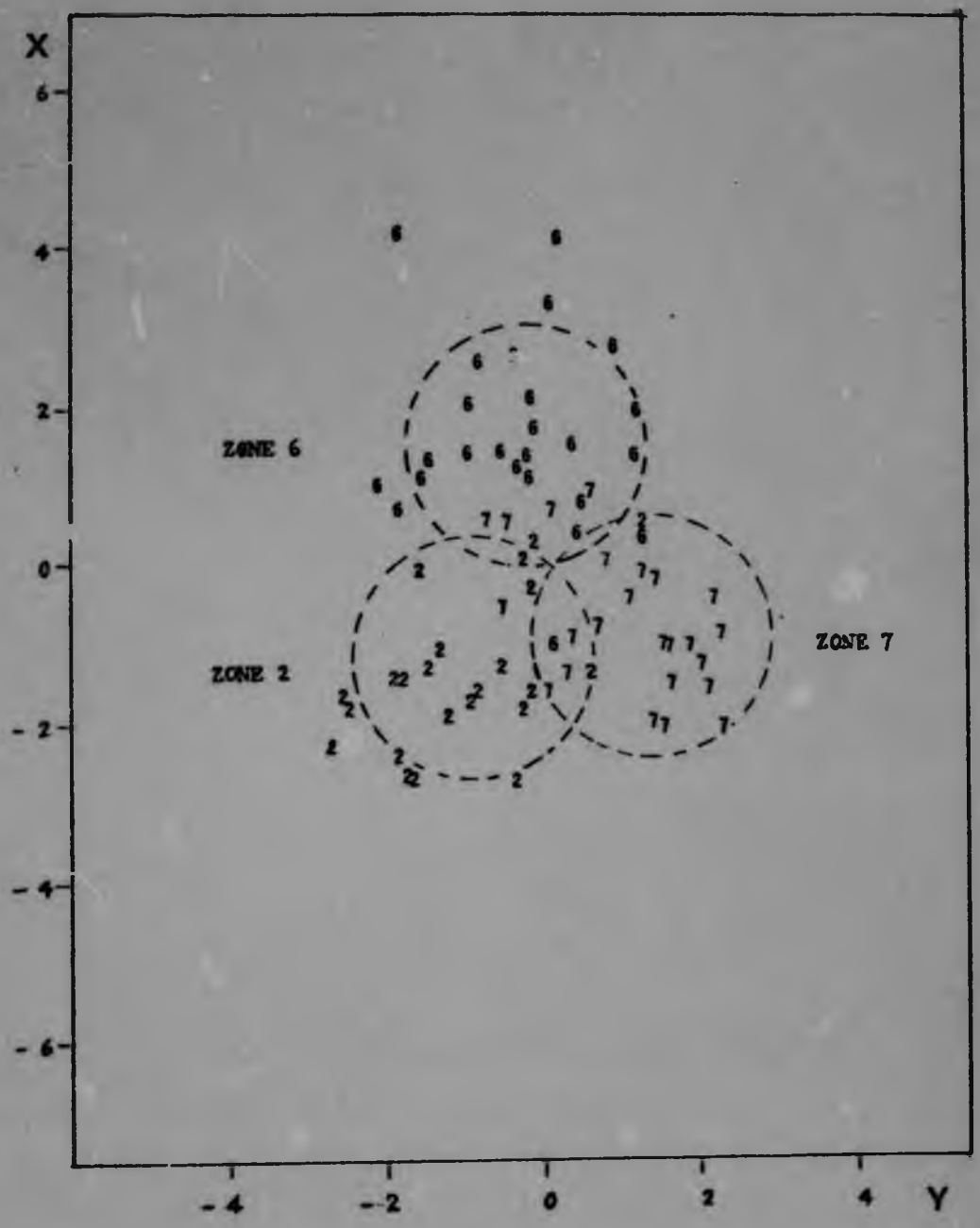


Figure A 5.3 TWO DIMENSIONAL REPRESENTATION

X-AXIS : Based on Y_1 : 73 % Representation

Y-AXIS : Based on Y_2 : 27 % Representation

Accuracy of representation : 100 %

Section A 5.4 RUN 4 - CLASSIFICATION OF CONGLOMERATES TO 15 LEVELS

Table A 5.4.1 VALUES OF D^2 BETWEEN POPULATION MEANS

ZONE		2					6					7				
	LEVEL	1	2	3	4	5	21	22	23	24	25	26	27	28	29	30
	1	0	48	51	60	35	22	36	24	23	31	47	21	35	29	31
	2	48	0	7	8	43	37	30	40	33	44	30	24	22	21	55
2	3	51	7	0	13	64	49	36	29	32	46	29	24	16	19	67
	4	60	8	13	0	40	40	36	50	48	57	34	36	36	33	74
	5	35	43	64	40	0	17	54	64	41	67	72	36	50	42	36
	21	22	37	49	40	17	0	30	30	21	26	42	36	37	37	46
	22	36	30	36	36	54	30	0	32	28	10	6	47	44	44	76
6	23	24	40	29	50	64	30	32	0	19	22	29	24	20	20	61
	24	23	33	32	48	41	21	28	19	0	22	39	22	12	19	44
	25	31	44	46	57	67	26	10	22	22	0	15	53	45	47	82
	26	47	30	29	34	72	42	6	29	39	15	0	52	44	43	100
	27	21	24	24	36	36	36	47	24	22	53	52	0	13	5	23
7	28	35	22	16	36	50	37	44	20	12	45	44	13	0	5	48
	29	29	21	19	33	42	37	44	20	19	47	43	5	5	0	40
	30	31	55	67	74	36	46	76	61	44	52	100	23	48	40	0

Table A 5.4.2 CLASSIFICATION OF SAMPLES

PARENT ZONE	LEVEL	NUMBER OF SAMPLES CLASSIFIED TO														
		ZONE 2					ZONE 6							ZONE 7		
		1	2	3	4	5	21	22	23	24	25	26	27	28	29	30
	1	3								1						1
	2		3	3								1				
2	3			5												
	4		1	1	3											
	5					5										
	21						5									
	22							1			2	2				
6	23								3			1			1	
	24									4				1		
	25										5					
	26						2					3				
	27												4		1	
7	28													3	2	
	29												1	1	3	
	30															5

Accuracy of classification:

Correct Zone : 65 - 87 %

Incorrect Zone : 10 - 13 %

Correct Zone:

(i) Correct Level : 55 - 74 %

(ii) Incorrect Level : 10 - 13 %

Table A 5.4.3 CANONICAL VARIANT VECTORS

VECTOR	VARIANCE	ELEMENT	COEFFICIENTS FOR	
			Y_1	Y_2
Y_1	32.27	Au	0.12	0.20
Y_2	23.17	Th	-0.98	-0 54
Y_3	17.24	La	-0.71	-0.36
Y_4	6.67	Eu	0.15	2.04
Y_5	4.50	Yb	0.41	-0.42
Y_6	3.29	Lu	0.27	0.20
Y_7	1.75	Hf	-0.55	-0.25
Y_8	1.08	Ta	0.15	-0.54
Y_9	0.72	Fe	2.22	-0.59
Y_{10}	0.28	Sc	0.77	0.18
Y_{11}	0.12	Cr	-0.65	-0.49
Y_{12}	0.02	Co	-1.43	1.29

Table A 5.4.4 RELATIVE IMPORTANCE OF ELEMENTS

ELEMENT	ARBITRARY SCALE
Fe	10
Co	8.9
Eu	6.1
Th	5.2
Cr	3.8
La	3.7
Sc	3.4
Hf	2.8
Yb	2.7
Ta	2,0
Lu	1.6
Au	1.0

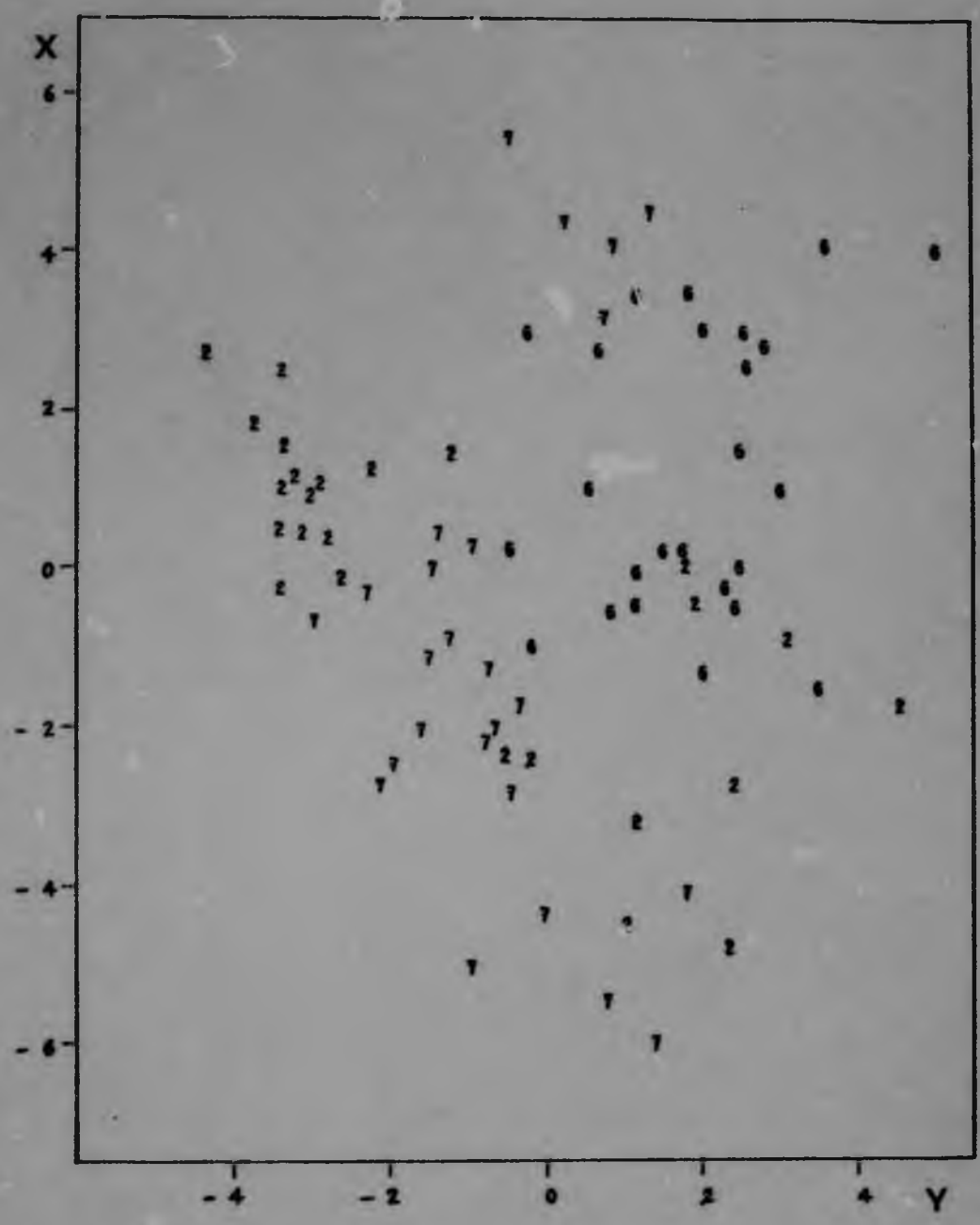


Figure A 5.4 TWO DIMENSIONAL REPRESENTATION

X-AXIS : Based on Y_1 : 35.4 % Representation

Y-AXIS : Based on Y_2 : 25.4 % Representation

Accuracy of representation : 61 %

Section A 5.5 RUN 5 - CLASSIFICATION OF CONGLOMERATES TO 15 LEVELS

Table A 5.5.1 VALUES OF D^2 BETWEEN POPULATION MEANS

ZONE		2					6					7				
	LEVEL	1	2	3	4	5	21	22	23	24	25	26	27	28	29	30
	1	0	27	27	37	21	18	24	11	18	22	27	11	19	14	14
	2	27	0	5	2	19	20	24	28	26	31	27	14	21	17	23
1	3	27	5	0	6	33	30	23	21	22	29	22	11	14	12	32
	4	37	2	6	0	26	28	29	35	36	39	31	20	30	25	31
	5	21	19	33	26	0	7	40	35	26	41	52	20	28	25	5
	21	18	20	30	28	7	0	21	19	15	18	30	22	23	23	16
	22	24	24	23	29	40	21	0	14	23	3	4	35	36	35	46
6	23	11	28	21	35	35	19	14	0	11	10	14	14	13	12	34
	24	18	26	22	36	26	15	23	11	0	18	32	17	7	14	24
	25	22	31	29	39	41	18	3	10	18	0	6	35	32	32	47
	26	27	27	22	31	52	30	4	14	32	6	0	35	38	33	58
	27	11	14	11	20	20	22	35	14	17	35	35	0	6	2	14
7	28	19	21	14	30	28	23	36	13	7	32	38	6	0	3	23
	29	14	17	12	25	25	23	35	12	14	32	33	2	3	0	21
	30	14	23	32	31	5	16	46	34	24	47	58	14	21	21	0

Table A 5.5.2 CLASSIFICATION OF SAMPLES

PARENT ZONE	LEVEL	NUMBER OF SAMPLES CLASSIFIED TO														
		ZONE 2					ZONE 6						ZONE 7			
		1	2	3	4	5	21	22	23	24	25	26	27	28	29	30
	1	4							1							
	2	1	2		2											
2	3			5												
	4		4	1												
	5		1			2	1									
	21						5									
	22							1			3	1				
6	23								3		1		1			
	24									3				2		
	25							2	1		2					
	26										1	4				
	27		1									2		2		
7	28													5		
	29														5	
	30															5

Accuracy of classification:

Correct Zone	:	66 -	88 %
Incorrect Zone	:	9 -	12 %
Correct Zone:			
(i) Correct Level	:	49 -	65 %
(ii) Incorrect Level	:	17 -	23 %

Table A 5.5.3 CANONICAL VARIANT VECTORS

VECTOR	VARIANCE	ELEMENT	COEFFICIENTS FOR	
			Y_1	Y_2
Y_1	23.3	Th	-1.27	-0.17
Y_2	14.5	La	-0.62	-0.28
Y_3	11.9	Eu	0.94	1.64
Y_4	4.7	Fe	1.11	-0.72
Y_5	1.9	Sc	0.86	-0.12
Y_6	0.7	Cr	-1.00	0.10

Table A 5.5.4 RELATIVE IMPORTANCE OF ELEMENTS

ELEMENTS	ARBITRARY SCALE
La	10
Eu	9.0
Fe	7.2
Th	6.3
Cr	4.9
Sc	4.3

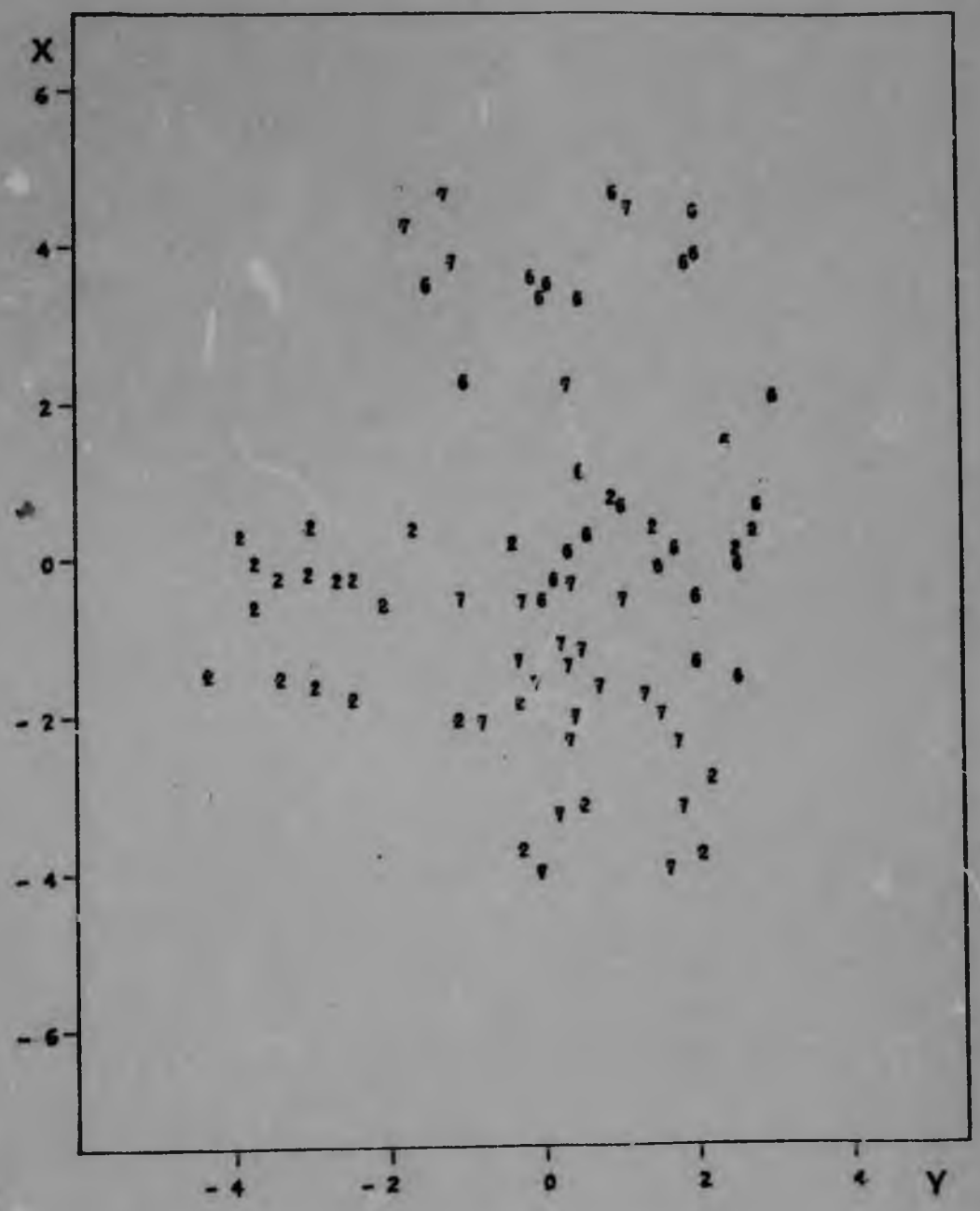


Figure A 5.5 TWO DIMENSIONAL REPRESENTATION

X-AXIS : Based on Y_1 : 40.9 % Representation

Y-AXIS : Based on Y_2 : 25.1 % Representation

Accuracy of representation : 65 %

APPENDIX 6 STATISTICAL ANALYSIS OF POWDERED SAMPLES

The statistical analysis of the powdered samples follows an analogous method to that of the chip samples. The results show 100% accuracy of classification for all permutations of the data attempted.

Results are presented for an analysis using all 28 elements, and for an analysis using the 11 elements used for the statistical analysis of the chip samples. In addition, the quartzite zones have been treated separately to obtain some indication of the relative importance of the various elements in discriminating quartzite zones. A similar analysis has been undertaken for the conglomerate zones.

The permutation of the data for each run is as follows:

RUN	SAMPLES	PARENT POPULATIONS	ELEMENTS INCLUDED IN THE ANALYSIS
1	Quartzites & Conglomerates	6	all 28
2	Quartzites & Conglomerates	6	'chip 11'
3	Quartzites	3	all 28
4	Conglomerates	3	all 28

Note: 'chip 11' refers to the 11 elements used in the analysis of chip samples; Th, La, Eu, Yb, Lu, Hf, Ta, Fe, Sc, Cr and Co

The following data is presented for each run:

Table 1 : VALUES OF D^2 BETWEEN POPULATION MEANS

The values of the Mahalanobis distance, D^2, for each individual sample to the parent population mean are approximately equal to the number of observations (elements) included in the analysis. Thus for good separation, the value of D^2 between populations should be at least four times the average distance of each sample to the mean of the parent population.

Table 2 : CANONICAL VARIANT VECTORS

The variance or eigen value (λ_i) of each canonical vector (Y_i) is given. The relative magnitudes of the eigen values reflect the degree of discrimination of each canonical variate. The coefficients (β_{ij}) of each element are given for the first two vectors.

Table 3 : RELATIVE IMPORTANCE OF ELEMENTS

The relative importance of each element is given on an arbitrary scale. The most important element has been assigned a value of 10. These values are obtained from the variances and coefficients given in Table 3.

Figure 1 : TWO DIMENSIONAL REPRESENTATION

This is a representation of the plane in multidimensional space which shows the largest discrimination between populations. The percentage discrimination of each axis is given, and of the overall representation of the population means. The representation is based on the data given in Table 2.

Section A 6.1 RUN 1 - CLASSIFICATION OF CONGLOMERATES AND QUARTZITES TO 6 ZONES

Table A 6.1.1 VALUES OF D^2 BETWEEN POPULATION MEANS

ZONE	2	3	4	5	6	7
2	0	6980	10200	11700	4100	5110
3	6980	0	1240	2550	1590	1570
4	10200	1240	0	4110	4210	4330
5	11700	2550	4110	0	4610	3820
6	4100	1590	4210	4610	0	478
7	5110	1570	4330	3820	478	0

Table A 6.1.2 CANONICAL VARIANT VECTORS

VECTOR	Y_1	Y_2	Y_3	Y_4	Y_5
VARIANCE	12931	4005	2407	326	317

ELEMENT	COEFFICIENT FOR Y_1	COEFFICIENT FOR Y_2	ELEMENT	COEFFICIENT FOR Y_1	COEFFICIENT FOR Y_2
Au	0.130	-0.886	Lu	-0.294	-0.344
U	1.909	0.294	Ti	0.035	0.875
Th	-0.728	-0.977	Zr	-0.088	0.882
Na	-1.076	0.296	Hf	-0.356	-0.552
K	-0.068	0.020	Ta	1.098	1.657
Ba	-0.410	-0.975	W	0.122	-0.394
Rb	-0.785	0.364	Ga	-0.556	-0.062
Cs	0.072	1.111	Fe	1.710	-0.277
La	-2.083	-1.790	Sc	-0.063	-0.736
Ce	3.276	-0.572	Cr	-3.001	2.057
Nd	-0.279	0.365	Co	0.243	0.850
Eu	-0.011	0.688	Ni	0.095	-0.774
Tb	-0.691	-0.779	As	0.337	-0.635
Yb	0.190	-1.331	Sb	-0.676	0.288

Table A 6.1.3 RELATIVE IMPORTANCE OF ELEMENTS

ELEMENT	ARBITRARY SCALE	ELEMENT	ARBITRARY SCALE
Cr	10	As	1.5
Ce	9.5	Hf	1.5
La	7.3	Co	1.4
U	5.5	Cs	1.2
Fe	4.9	Au	1.1
Ta	4.4	Lu	1.1
Na	3.2	Nd	1.1
Th	2.8	Zr	1.0
Tb	2.6	Ni	0.92
Rb	2.5	Ti	0.85
Sb	2.1	Sc	0.80
Ba	2.0	V	0.67
Yb	1.7	Eu	0.62
Ga	1.6	K	0.20

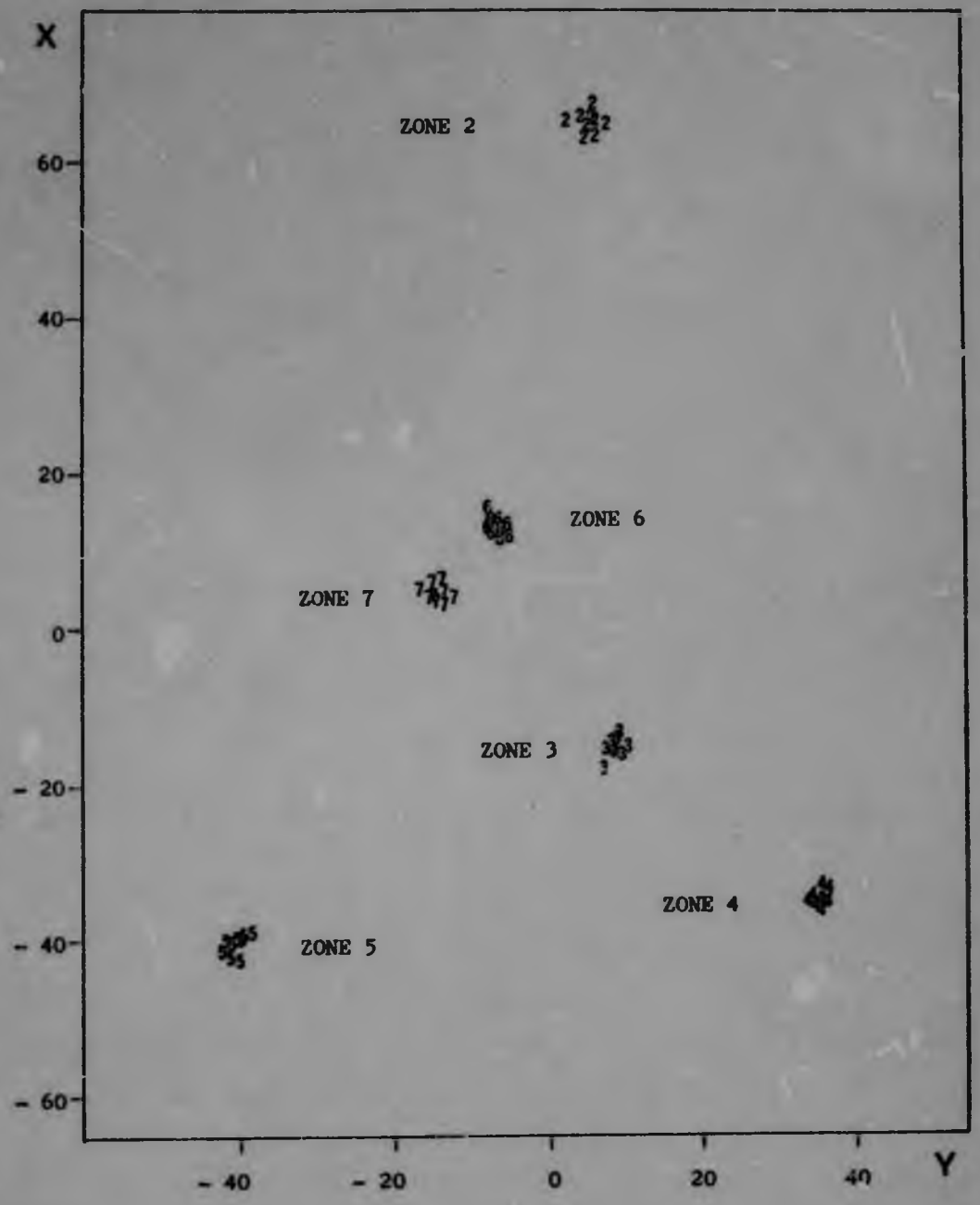


Figure A 6.1 TWO DIMENSIONAL REPRESENTATION

X-AXIS : Based on Y_1 : 64.8 % Representation

Y-AXIS : Based on Y_2 : 20.0 % Representation

Accuracy of representation : 85 %

Section A 6.2 RUN 2 - CLASSIFICATION OF CONGLOMERATES __ UARTZITES TO 6 ZONES USING 11 ELEMENTS

Table A 6.2.1 VALUES OF D^2 BETWEEN POPULATION MEANS

ZONE	2	3	4	5	6	7
2	0	403	1500	1630	290	379
3	403	0	565	1030	358	319
4	1500	565	0	1780	1190	1460
5	1630	1030	1780	0	1290	762
6	290	358	1190	1290	0	237
7	379	319	1460	762	237	0

Table A 6.2.2 CANONICAL VARIANT VECTORS

VECTOR	VARIANCE	ELEMENT	COEFFICIENTS FOR	
			Y_1	Y_2
Y_1	1809	Th	-0.6	-0.089
Y_2	1698	La	-1.015	-0.751
Y_3	259	Eu	0.729	0.170
Y_4	157	Tb	-0.724	-0.264
Y_5	36	Lu	-0.044	-0.064
		Hf	-0.026	-0.163
		Ta	1.101	0.588
		Fe	0.084	1.167
		Sc	-1.062	0.034
		Cr	1.314	-0.700
		Co	-0.284	0.314

Table A 6.2.3 RELATIVE IMPORTANCE OF ELEMENTS

ELEMENT	ARBITRARY SCALE
Cr	10
La	8.7
Ta	8.4
Fe	6.0
Sc	5.6
Tb	4.9
Th	4.7
Eu	4.5
Co	2.9
Hf	0.91
Lu	0.53

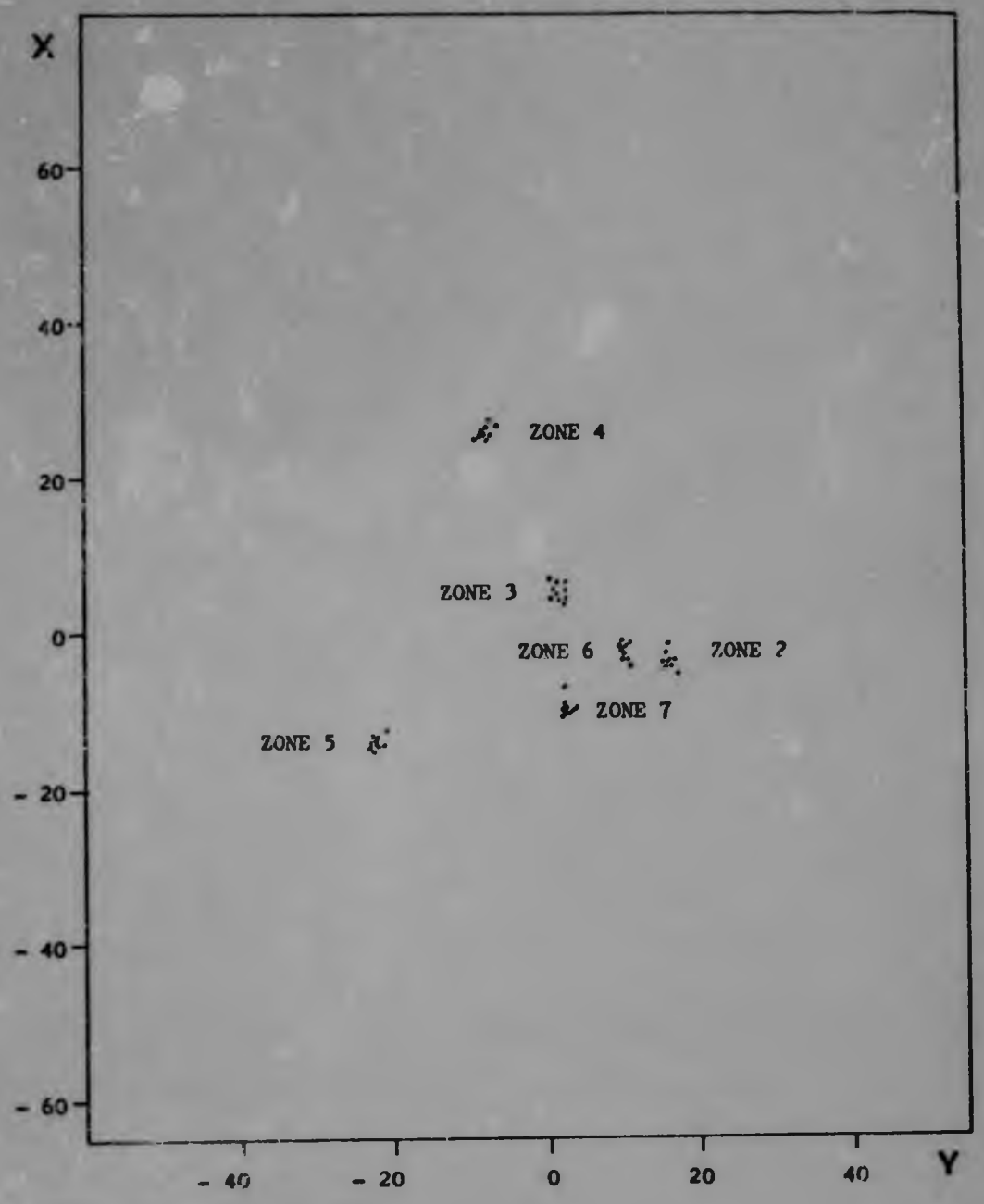


Figure A 6.2 TWO DIMENSIONAL REPRESENTATION

X-AXIS : Based cn Y_1 : 45.7 % Representation

Y-AXIS : Based on Y_2 : 42.8 % Representation

Accuracy of representation : 89 %

Section A 6.3 RUN 3 - CLASSIFICATION OF QUARTZITES TO 3 ZONES

Table A 6.3.1 VALUES OF D^2 BETWEEN POPULATION MEANS

ZONE	3	4	5
3	0	2300	3200
4	2300	0	5600
5	3200	5600	0

Table A 6.3.2 CANONICAL VARIANT VECTORS

VECTOR	Y_1	Y_2
VARIANCE	13100	4050

ELEMENT	COEFFICIENT FOR		ELEMENT	COEFFICIENT FOR	
	Y_1	Y_2		Y_1	Y_2
Au	0.14	-0.56	Lu	-0.92	0.23
U	-0.37	0.74	Ti	0.57	-0.02
Th	0.48	-0.03	Zr	-0.48	1.03
Na	-1.29	-0.24	Hf	-0.05	-0.38
K	0.65	-0.14	Ta	-0.80	1.38
Ba	0.52	0.14	W	-0.57	-0.13
Rb	-0.20	-1.54	Ga	0.45	-0.71
Cs	-0.60	-0.16	Fe	-0.31	1.44
La	1.40	0.28	Sc	2.09	-0.83
Ce	0.44	0.73	Cr	-0.97	-0.91
Nd	0.03	0.23	Co	-0.62	0.56
Eu	-0.92	0.17	Ni	0.00	-0.08
Tb	-0.17	-0.48	As	0.76	0.44
Yb	0.52	-0.36	Sb	-0.41	-0.46

Table A 6.3.3 RELATIVE IMPORTANCE OF ELEMENTS

ELEMENT	ARBITRARY SCALE	ELEMENT	ARBITRARY SCALE
Sc	10	Ce	2.8
La	6.3	Cs	2.8
Na	5.8	Yb	2.7
Cr	5.3	V	2.6
Ta	5.3	U	2.5
Lu	4.2	Ti	2.5
Eu	4.1	Ba	2.4
As	3.8	Sb	2.4
Zr	3.4	Th	2.1
Co	3.4	Tb	1.4
Fe	3.2	Au	1.3
K	2.9	Hf	0.7
Rb	2.9	Nd	0.4
Ga	2.8	Ni	0.1

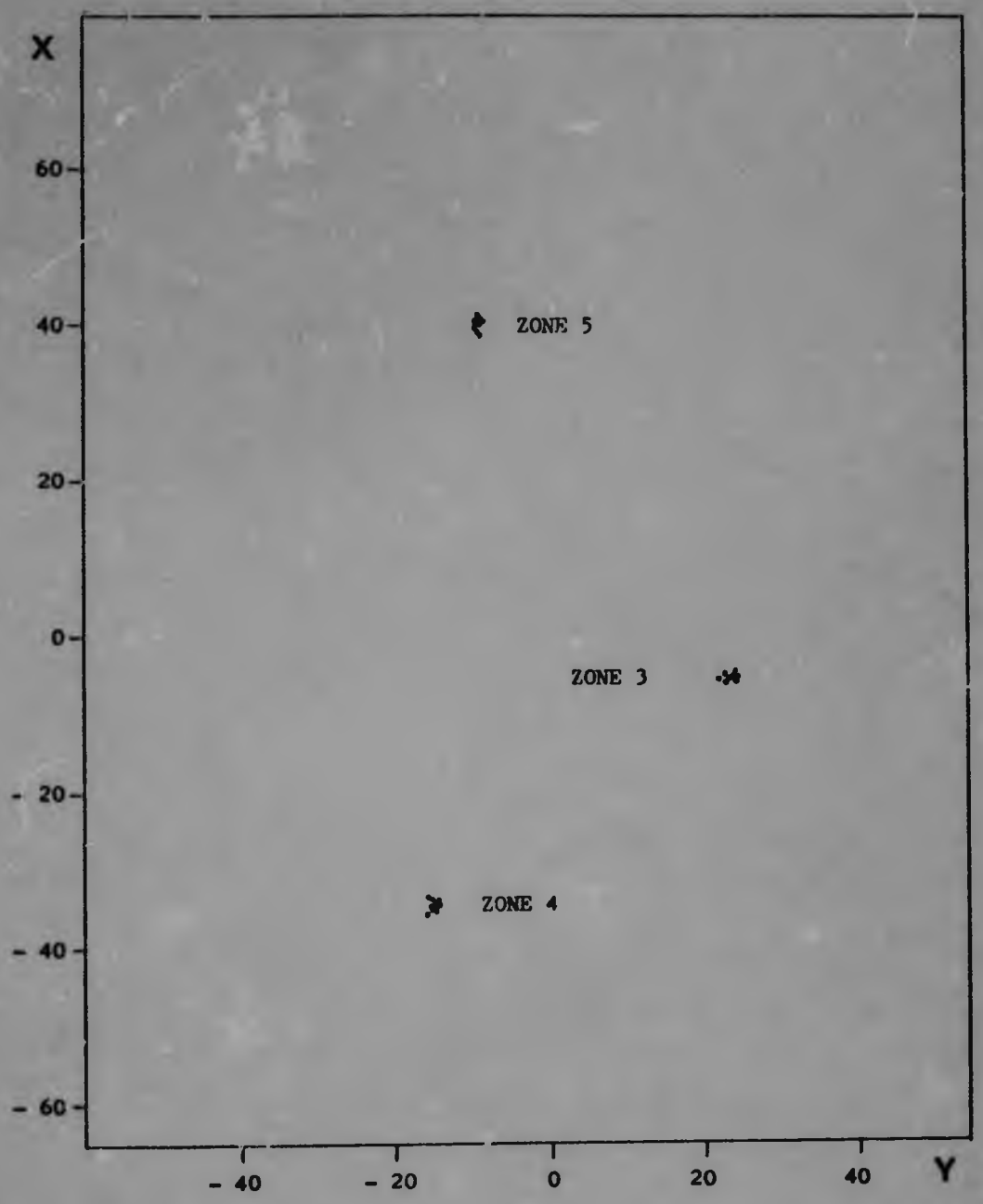


Figure A 6.3 TWO DIMENSIONAL REPRESENTATION

X-AXIS : Based on Y_1 : 76 % Representation

Y-AXIS : Based on Y_2 : 24 % Representation

Accuracy of representation : 100 %

Section A 6.4 RUN 4 - CLASSIFIACTION OF CONGLOMERATES TO 3 ZONES

Table A 6.4.1 VALUES OF D^2 BETWEEN POPULATION MEANS

ZONE	2	6	7
2	0	3400	4400
6	3400	0	560
7	4400	560	0

Table A 6.4.2 CANONICAL VARIANT VECTORS

VECTOR	Y_1	Y_2
VARIANCE	11527	1164

ELEMENT	COEFFICIENT FOR Y_1	COEFFICIENT FOR Y_2	ELEMENT	COEFFICIENT FOR Y_1	COEFFICIENT FOR Y_2
Au	0.06	0.01	Lu	-0.55	-0.18
U	2.02	1.09	Ti	-0.28	0.24
Th	0.27	1.15	Zr	-1.20	0.08
Na	-1.53	0.68	Hf	-0.63	0.58
K	-1.03	-0.26	Ta	0.71	0.03
Ba	-0.12	-0.81	W	-1.37	0.64
Rb	-0.55	0.61	Ga	-0.14	0.53
Cs	0.25	0.31	Fe	0.03	-1.34
La	-1.05	0.99	Sc	-0.06	-0.12
Ce	0.44	0.73	Cr	0.43	0.17
Nd	0.34	0.18	Co	0.03	-0.31
Eu	-0.25	-0.88	Ni	0.07	-0.48
Tb	-0.08	-0.02	As	0.98	-1.12
Yb	0.15	-0.08	Sb	-0.39	-1.04

Table A 6.4.3 RELATIVE IMPORTANCE OF ELEMENTS

ELEMENT	ARBITRARY SCALE	ELEMENT	ARBITRARY SCALE
U	10	Cr	2.1
Na	7.5	Th	1.8
W	6.7	Nd	1.7
Zr	.7	Eu	1.6
La	5.4	Ti	1.4
As	5.1	Cs	1.3
K	5.0	Ba	0.96
Ta	3.4	Ga	0.91
Hf	3.2	Fe	0.75
Rb	2.9	Yb	0.72
Au	2.7	Ni	0.58
Lu	2.7	Tb	0.36
Ce	2.4	Sc	0.34
Sb	2.3	Co	0.31

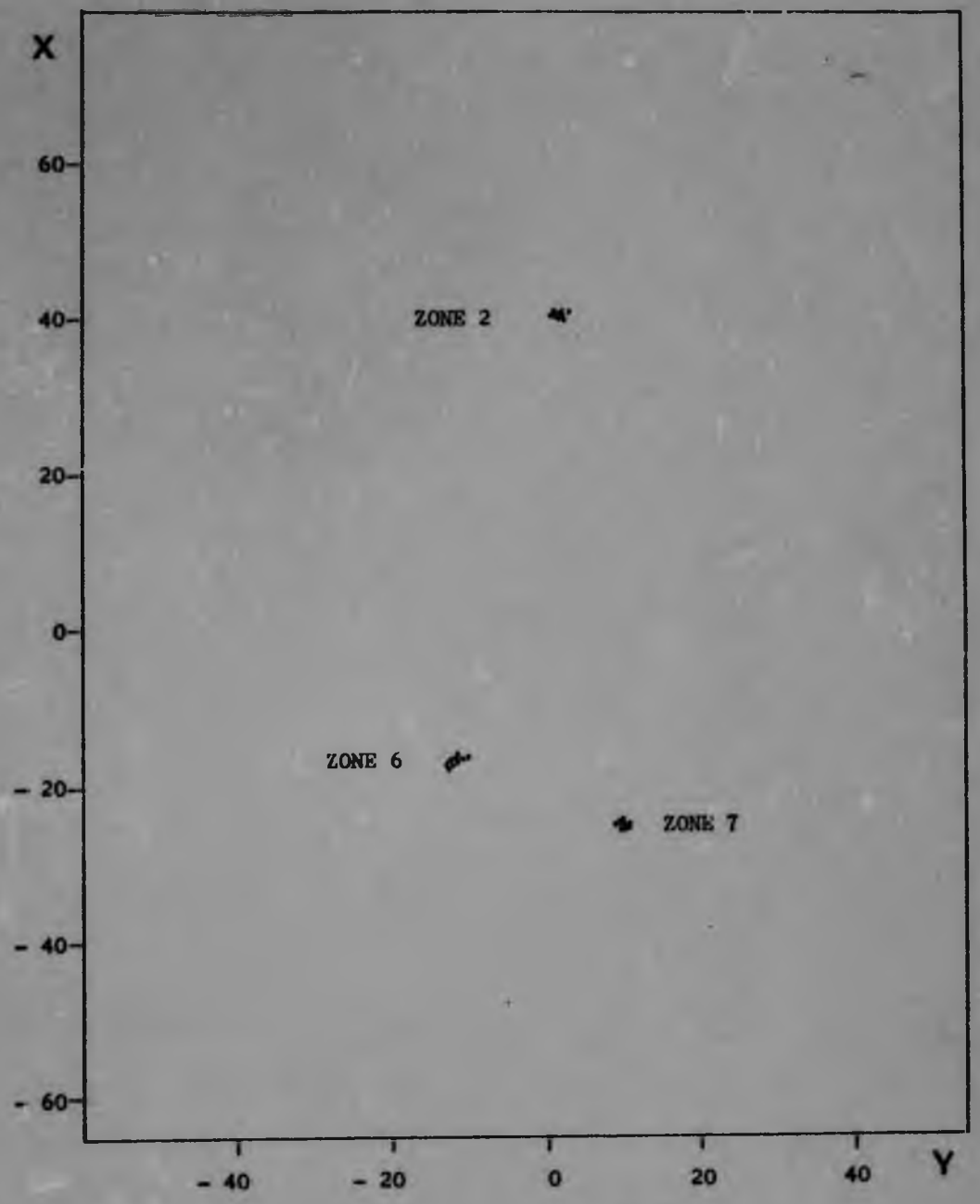


Figure A 6.4 TWO DIMENSIONAL REPRESENTATION

X-AXIS : Based on Y_1 : 91 % Representation

Y-AXIS : Based on Y_2 : 9 % Representation

Accuracy of representation : 100 %

REFERENCES

Ab70 ABBEY S., U.S. Geological Survey Standards - A critical study of published analytical data, Can. Spectrosc.; 10 - 16, 1970

Ah54 AHRENS L.H., The lognormal distribution of the elements - a fundamental law of geochemistry and its subsidiary, Geochim. Cosmochim. Acta; 5, 49 - 73, 1954

Al70 ALLEN R.O., HASKIN L.A., ANDERSON M.R., MULLER O., Neutron Activation Analysis for 39 elements in small or precious geologic samples, J. Radioanal. Chem.; 6, 115-137, 1970

An69 ANDERS O.U., Experiences with the Ge(Li) detector for high-resolution gamma ray spectrometry and a practical approach to the pileup problem, Nucl. Instrum. Methods; 68, 205-208, 1969

Ba68 BARNES V., GASPAN - An advanced computer code for the analysis of high resolution gamma-ray spectra, IEEE Trans. Nucl. Sci.; NS-15, 437-449, 1968

Bi72 BIBBY D.M., RASMUSSEN S.E., Reactor neutron flux monitoring with iron foils, Radiochem. Radioanal. Lett.; 9, 1-8, 1972

Bi73 BIBBY D.M., RASMUSSEN S.E., Performance of a counting head for an automatic sample changer, Radiochem. Radioanal. Lett.; 13, 1973 (to be published)

Bl65 BLACKBURN J.A., Computer program for multicomponent spectrum analysis using least-squares method, Anal. Chem.; 37, 1000-1003, 1965

Bo70 BOLOTIN H.H., STRAUSS M.G., McCLURE D.A., Simple technique for precise determinations for counting losses in nuclear pulse processing systems, Nucl. Instrum. Methods; 83, 1-12, 1970

Bn71 BRUNFELDT A.O., STEINNES E., A neutron-activation scheme developed for the determination of 42 elements in lunar material, Talanta, 18, 1197-1208, 1971

Br64 BROCK B.B., PRETORIUS D.A., Rand basin sedimentation and tectonics, in Some ore deposits of Southern Africa, (ed. Haughton S.H.), Geol. Soc. S. Afr.; 1, 549-599 1964

Bx72 BRUNINX E., The evaluation of errors caused by flux inhomogeneities in thermal neutron activation analysis, Anal. Chim. Acta; 60, 207-217, 1972

Ca64 CASETTI E., Classificatory and regional analysis by discriminant iterations, Office of Naval Research, Geog. Br.; Tech. Rept. No12, ONR Task No 389-135, 95p, 1964

Ch68 CHARYULA V., HORN M.K., Geochemical and loggi - applications of a computer simulated neutron activation system, Kansas Geol. Surv.; Computer Contr. 22, 35-42, 1968

Co59 COVELL D.F., Determination of gamma ray abundance directly from the total absorption peak, Anal. Chem.; 31, 1785-1790, 1959

Cr71 CRISLER D.F., JARMER J.J., ELDRIDGE H.B., A method for absolute calibration of Ge(Li) detectors using effective interaction depth, Nucl. Instrum. Methods; 94, 285-288, 1971

Da68 DAMS R., ADAMS F., Gamma ray energies of radionuclides formed by neutron capture determined by Ge(Li) spectrometry, Radiochim. Acta; 10, 1-11, 1968

Dv66 DAVIS J.C., SAMPSON R.J., Fortran II program for multivariate discriminant analysis using an IBM 1620 computer, Kansas Geol. Surv.; Computer Contr. 4, 8p, 1966

DC69 De CORTE F., SPEECKE A., HOSTE J., Reactor neutron activation analysis by a triple comparator method, J. Radioanal. Chem.; 3, 205-215, 1969

DS72 De SOETE D., GIJBELS R., HOSTE J., Neutron activation analysis, London, Wiley-Interscience; 836p, 1972

Em54 EMERY J.R., GRIFFITHS J.C., Differentiation of oil-bearing from barren sediments by quantitative petrographic analysis, Producers Monthly; 19, 33-37, 1954

Er72 ERDTMAN G., Interference in neutron activation analytical determinations by uranium fission, J. Radioanal. Chem.; 10, 137-138, 1972

Fl68 FLANAGAN F.J., U.S. Geological survey standards - II. First compilation of data for the new U.S.G.S. rocks, Geochim. Cosmochim. Acta; 33, 81-120, 1969

Gi65 GIRARDI F., GUZZI G., PAULY J., Reactor neutron activation analysis by the single comparator method, Anal. Chem.; 37, 1085-1092, 1965

Gr66 GRIFFITHS J.C., Application of discriminant functions as a classification tool in the geosciences, Kansas Geol. Surv.; Computer Contr. 7, 48-52, 1966

Gr71 GRIFFITHS J.C., Problems of sampling in geoscience, Inst. of Min. and Metall.; 80 : Bull 780, B346-B356, 1971

Gu72 GUINN V.P., Neutron activation analysis, in Physical methods of chemistry Vol 1, Part III D, Ch VII, (ed. Weissberger A., and Rossildt B.W.) New York, John Wiley; 448-500, 1972

Ha67 HARMS J., Automatic dead-time correction for multichannel pulse-height analyzers at variable counting rates, Nucl. Instrum. Methods; 53, 192-196, 1967

Hw72 HAWKINS D.M., Personal communication

He70 HERMANN A.G., Yttrium and the lanthanides, in Handbook of geochemistry (ed. Wedepohl K.H.) Heidelberg, Springer-Verlag, 1970

Hi68a HIEMSTRA S.A., The mineralogy and petrology of the uraniferous conglomerate of the Dominion Reefs Mine, Klerksdorp area, Trans. Geol. Soc. S.Afr.; 71, 1-65, 1968

Hi68b HIEMSTRA S.A., The geochemistry of the uraniferous conglomerate of the Dominion Reefs Mine, Klerksdorp area, Trans. Geol. Soc. S.Afr.; 71, 67-100, 1968

Is64 ISENHOUR T.L., MORRISON G.H., A computer program to optimise times of irradiation and decay in activation analysis, Anal. Chem.; 36, 1089-1092, 1964

Kl67 KLOVAN J.E., BILLINGS G.K., Classification of geological samples by discriminant-function analysis, Bull. Can. Petroleum Geol.; 15, 313-330, 1967

Ma71 MAENHAUT W., ADAMS F., HOSTE J., Determination of thermal and epithermal neutron fluxes with a single flux monitor, J. Radioanal. Chem.; 9, 325-328, 1971

Mh49 MAHALANOBIS P.C., An historical note on D^2 statistic, Sankhyā; 9, 237-240, 1949

Mn72 MANTEL MARIANNA, AMIEL S., Application of high resolution X-ray spectrometry to activation analysis, Anal. Chem.; 44, 548-553, 1972

Ni71 NICHOLLS G.D., Geochemical sampling problems in the analytical laboratory, Inst. of Min. and Metall.; 80 : Bull 780, B299-B304, 1971

Op72 OP DE BEECK J.P., A program for complete quantitative neutron activation analysis using Ge(Li) detector gamma spectrometry and a small computer, J. Radioanal. Chem.; 11, 283-303, 1972

Pa68 PARKER R.B., BRUNFELDT A.O., Precision and accuracy of sodium determination by neutron activation, Chem. Geol.; 3, 213-217, 1968

Pi69 PILLAY K.K.S., MILLER W.W., Characteristic X-rays from (n, γ) products and their utilisation in activation analysis, J. Radioanal. Chem.; 2, 97-107, 1969

Qu69 QUITTNER P., Precise peak area determinations for Ge(Li) detectors, Anal. Chem.; 41, 1504-1506, 1969

Re63 REYMENT R.A., Studies on Nigerian upper cretaceous and lower tertiary ostracoda, Pt 2. Stockholm Contr. Geol.; 10, 286p, 1963

Re69 REYMENT R.A., RAMDEN H-A., WAHLSTEDT W.J., Fortran IV program for the generalised statistical distance and analysis of covariance matrices for the CDC 3600 computer, Kansas Geol. Surv.; Computer Contr. 39, 42p, 1969

Ro69 ROUTTI J.T., PRÜSSIN S.G., Photopeak method for the computer analysis of gamma ray spectra from semiconductor detectors, Nucl. Instrum. Methods; 72, 125-142, 1969

Sa71 SABBAH B., KLEIN I., ARBEL A., Pile up rejection by comparison of the shaped pulse with its second derivative, Nucl. Instrum. Methods; 95, 163-171, 1971

Sm71 SMALES A.A., The place of activation analysis in geochemistry and cosmochemistry, in Activation analysis in geochemistry and cosmochemistry (ed. Brunfeldt A.O. and Steinnes E.) Oslo, Universitetsforlaget; 17-24 1971

St64 STEHN J.R., GOLDBERG M.D., MAGURNO B.A., WIENER-CHASMAN R., Neutron cross sections, Brookhaven National Laboratory, BNL 325; 2nd Ed., Suppl. No 2, 1964

To72 TOMINAGA H., DOYO M., TANAKA M., Effect of spectrum smoothing on peak a determinations, Nucl. Instrum. Methods; 98, 69-76, 1972

Uk69 UKEN E.A., Aspects of neutron activation analysis, Unpublished PhD thesis, University of the Witwatersrand, 1969

Wi71 WIERNIK M., Normal and random pulse generators for the correction of dead-time losses in nuclear spectrometry, Nucl. Instrum. Methods; 96, 325-329, 1971

Wi68 WOLLEBEN J.A., PAUKEN R.J., DEARIEN J.A., Fortran IV program for multivariate paleontologic analysis using an IBM system/360 model 40 computer, Kansas Geol.Surv.; Computer Contr. 20, 1-12, 1968

Wo61 WOOD G.V., Discriminating between refractory and nonrefractory quartzite by quantitative petrography, J. Sediment. Petrol.; 31, 530-533, 1961

Yu67 YULE H.P., Mathematical smoothing of gamma ray spectra, Nucl. Instrum. Methods; 54, 61-65, 1967

Yu68 YULE H.P., Computation of lithium-drifted germanium detector peak areas for activation analysis and gamma ray spectrometry, Anal. Chem.; 40, 1480-1486, 1968

Yu71 YULE H.P., Computer data reduction in activation analysis, in Activation analysis in geochemistry and cosmochemistry, (ed. Brunfeldt A.O. and Steinnes E.) Oslo, Universitetsforlaget, 145-166, 1971

Yu72 YULE H.P., Study of gamma-ray spectrum distortion by mathematical smoothing, Anal. Chem.; 44, 1245-1249, 1972

Za73 ZANDERS J., BIBBY D.M., RASMUSSEN S.E., A simple automatic sample changer for gamma-ray counting of reactor-irradiated samples, J. Phys. E., Sci. Instr.; to be published

Zi61 ZIMMERMAN W., Evaluation of photopeaks in scintillation gamma-ray spectroscopy, Rev. Sci. Instrum.; 31, 1063-1065, 1961

Author Rasmussen S E
Name of thesis Neutron activation analysis of samples from the Kimberley Reef Conglomerate 1973

PUBLISHER:
University of the Witwatersrand, Johannesburg
©2013

LEGAL NOTICES:

Copyright Notice: All materials on the University of the Witwatersrand, Johannesburg Library website are protected by South African copyright law and may not be distributed, transmitted, displayed, or otherwise published in any format, without the prior written permission of the copyright owner.

Disclaimer and Terms of Use: Provided that you maintain all copyright and other notices contained therein, you may download material (one machine readable copy and one print copy per page) for your personal and/or educational non-commercial use only.

The University of the Witwatersrand, Johannesburg, is not responsible for any errors or omissions and excludes any and all liability for any errors in or omissions from the information on the Library website.